

FINAL REPORT

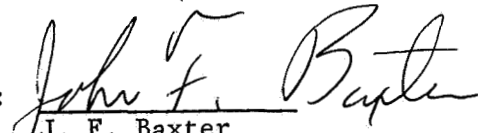
BUOYANT VENUS STATION MISSION FEASIBILITY STUDY
FOR 1972 - 1973 LAUNCH OPPORTUNITIES

VOLUME III: CONFIGURATION DEFINITION
PART II: APPENDIXES

Allan R. Barger, H. Edward Sparhawk, John R. Mellin,
Ronald E. Frank, Jack D. Pettus, Patrick C. Carroll,
Robert W. Stoffel, James E. Cole, Ted H. Tucker,
James W. Berry, and Walter F. Hane

Distribution of this report is provided
in the interest of information exchange.
Responsibility for the contents resides
in the author or organization that pre-
pared it.

Submitted by:


J. F. Baxter
BVS Study Manager

Approved by:


S. R. Sadin
Program Director,
Venus and Deep Space Programs

Prepared under Contract No. NAS1-7590 by
MARTIN MARIETTA CORPORATION
Denver, Colorado 80201

for

NATIONAL AERONAUTICS AND SPACE ADMINISTRATION

FOREWORD

The use of a buoyant station to explore the atmosphere of Venus has shown great promise in previous studies.* The high temperatures and pressures likely to be encountered and the unknown surface characteristics tend to make the in situ exploration of this planet difficult. The buoyant station concept permits the mission's instruments to be floated in the atmosphere in a moderate environment, localizing the environment problem to relatively compact drop sondes, and avoiding the problem of landing, deployment, and survival on the surface. Relatively simple missions can thus be defined that have the advantages of long duration and mobility over the surface, depending on the existing wind patterns. From such a station, measurements relating both to the atmosphere and the surface can be made. The surface measurements can be obtained either indirectly or by sondes dropped from the parent buoyant station.

This final report on the Buoyant Venus Station Mission Feasibility Study for 1972 - 1973 Launch Opportunities is submitted by the Martin Marietta Corporation, Denver Division, in accordance with Contract NAS1-7590.

This report is submitted in three volumes as follows:

- Volume I - Mission Summary Definition and Comparison;
- Volume II - Trajectory Analysis for 1972 and 1973 Missions;
- Volume III - Configuration Definition.

*J. F. Baxter: Final Report, Buoyant Venus Station Feasibility Study, Volume I, Summary and Problem Identification.

CONTENTS

	<u>Page</u>
FOREWORD	ii
CONTENTS	iii thru vi
APPENDIX	
A VENUS MODEL ATMOSPHERES	1
Model Used for BVS Study	1
Revised Models	2
References	27
B HEAT SHIELD ANALYSIS	29
Heat Shield Requirements	29
Heat Shield Development Requirements	48
References	51
C SPACECRAFT MODIFICATIONS	53
Lunar Orbiter	53
Mariner '69	72
Mariner, Venus/Mercury	85
D TV DROP SONDE	93
Symbols	97
Mission Profile	97
Science Subsystem	99
Telecommunications	103
Effect on BVS and Spacecraft Design for Orbital Mission	105
Effect on BVS Design with a Direct Earth Link	110
Structure and Thermal Control	110
E DUAL-ALTITUDE BALLOON	113
Dual-Altitude Mission Design Criteria	114
Configuration Description and Operation	115
Concept Description and Operation	120
F STERILIZATION	127
Sterilization Criteria	127
Sterilization Impact on Systems and Components	128
BVS Sterilizable Equipment Survey Results	129
BVS Study Summary	131
References	131
G MULTIPATH ANALYSIS	133
Symbols	133
Surface Model	134

	Communications Geometry	141
	Summary	141
	References	141
H	DOPPLER AND RANGING OPTIONS FOR BVS POSITION	
	DETERMINATION	145
	Symbols	146
	Changes to Baseline System	148
	One-Way Doppler from Spacecraft to BVS	148
	One-Way Doppler from BVS to Spacecraft	153
	Two-Way Doppler, Spacecraft to BVS to Spacecraft	153
	Two-Way Doppler and Ranging	156
	References	160
		and
		161

Figure

A1	Venus Pressure and Temperature Profile Models Used in Study	21
A2	Venus Pressure vs Temperature on H ₂ O Phase Diagram	22
A3	Venus Lower Atmosphere	23
A4	Mariner and Venera Pressure Profiles	24
A5	Venus Temperature Profiles	25
A6	Venus Atmosphere	26
B1	Ablation Material Required vs Velocity	30
B2	BVS Heat Shield Requirement Summary	36
B3	Heat Shield Ablation Summary	37
B4	Structure Temperature Histories	38
B5	Stagnation Point Ablator Sensitivity to Radiation Heating	41
B6	Ultimate Tensile Strength of AXF-5Q POCO Graphite	42
B7	Carbon Phenolic Ablation Sensitivity, V/M Swingby	44
B8	ESA-5500 and ESA-5500(M) Ablation Sensitivity, Direct Entry	45
B9	Carbon Vapor Pressure	46
B10	Effect of Carbon Vapor Properties on Carbon Phenolic Ablation	47
C1	Orbiter Spacecraft with BVS Capsule	55
C2	Performance Capability, Capsule System Weight in Orbit vs Orbit	59
C3	Unmodified Telecommunication System, Mars/ Venus Orbiter	62
C4	Spacecraft Science Equipment Showing Additions	63
C5	Orbital Power Requirement for Spacecraft	67

C6	BVS/Entry Vehicle	69
C7	Lunar Orbiter/Capsule Electrical Interface . .	71
C8	Flyby Spacecraft Configuration with BVS Capsule	73
C9	Spacecraft Support Equipment	78
C10	Mariner/Capsule Electrical Interface	84
C11	Venus/Mercury Spacecraft Configuration with BVS Capsule	87
D1	TV Drop Sonde	95
D2	Altitude/Time History of TV Drop Sonde	98
D3	Surface Imaging	100
D4	Smear due to Roll and Pitch	102
D5	Sonde Telecommunications	104
D6	Bit Rate Required vs Number of Images to be Transmitted for Various Transmission Periods	107
D7	Transmitter Power Antenna Gain Products vs Bit Rate for Various Communications Ranges Using Frequency Shift Key Modulation	108
D8	Transmitter Power Antenna Gain Product vs Bit Rate for Various Communications Ranges Using Coherent Phase Shift Key Modulation . .	109
E1	Effect of Allowable Balloon Stress on Balloon Size	116
E2	Effect of Allowable Balloon Stress on Balloon Weight	117
E3	Balloon Temperature	119
E4	Gas Mixtures Required for Equilibrium Float . .	121
E5	Gondola Arrangement Showing Pump Installation, Dual-Altitude Mission	122
E6	BVS Altitude with Time for a Slowly Inflated Balloon	124
G1	Angle Convention	136
G2	Reflection Coefficient for Venus Surface . . .	138
G3	Fading Margin vs Fading Parameter	140
G4	Communications Geometry	142
G5	Incidence Angle Variation and Fading Margin . .	143
H1	Spacecraft Transmitter for Doppler and Command	150
H2	One-Way Doppler Receiver and Demodulator . . .	152
H3	BVS Receiver and Demodulator for Doppler, Ranging and Command	154
H4	BVS Transmitter for Ranging, Doppler, and Data	155
H5	Spacecraft Doppler Frequency Measurement . . .	157
H6	Spacecraft Transmitters for Ranging, Doppler, and Command	159

Table

A1	Radio Refractivity of Gases at 293°K, 1 atm . .	1
A2	Venus Model Atmospheres, Extrapolation of Mariner 5 Data to Surface, Adiabatic Lapse Rate (CO ₂ = 95%, Mean Molecular Weight = 43.21)	3
A3	Venus Model Atmospheres, Extrapolation of Mariner 5 Data to Surface, Adiabatic Lapse Rate (CO ₂ = 90%, Mean Molecular Weight = 42.41)	9
A4	Venus Model Atmospheres, Extrapolation of Mariner 5 Data to Surface, Adiabatic Lapse Rate (CO ₂ = 85%, Mean Molecular Weight = 41.61)	15
B1	Heat Shield Material Environmental Sensitivity	31
B2	ESA-5500 and ESA-5500(M) Recession Rates . . .	34
C1	Spacecraft Modifications	54
C2	Summary Weight Statement	57
C3	Spacecraft Modifications Affecting Weight . . .	58
C4	BVS and Subsonic Probe Functions to be Supported by Orbiter Spacecraft	61
C5	Orbiter Spacecraft Experiment Characteristics .	65
C6	Spacecraft Modifications	75
C7	BVS and Subsonic Probe Functions to be Supported by Mariner Spacecraft	77
C8	Spacecraft Support Equipment Power and Weight Summary	79
C9	Scientific Objectives and Instruments for Flyby Spacecraft	80
C10	Flyby Spacecraft Experiment Characteristics . .	81
C11	Spacecraft Modifications	86
C12	Spacecraft Experiments	89
D1	TV Sonde Weight Statement	93
D2	Drop Sonde Link Calculations, FSK Modulation (1024 bps)	105
E1	Comparison of Dual-Altitude Configuration . . .	126
F1	BVS Sterilization Hardware	130
H1	Performance Data Doppler and Ranging Measure- ment Systems	147
H2	Equipment Weight, Power, and Volume Summary . .	149
H3	Acquisition Time Ranging Code	161

APPENDIX A

VENUS MODEL ATMOSPHERES

by Allan R. Barger
Martin Marietta Corporation

APPENDIX A

The model atmospheres used in this study were based on the preliminary Mariner V and Venera IV data (refs A1 and A2). The radius reference for the Mariner V data has since been revised (ref. A3). However, this revision merely shifts the profiles given in reference A1 downward by 8.85 km. (The model profiles used in the BVS study were based on a radius scale that was shifted 6.74 km downward from that given in ref. A1.) The only effect of this new revision is to slightly change the radius (by ~ 2 km) at which significant deployment events occur.

This appendix summarizes both the model atmospheres used in the study and a model based on the more recent analyses of the Mariner V data.

MODELS USED FOR BVS STUDY

The three models used in the study were developed from the Mariner V and Regulus occultation data and the Venera IV measurements. First, the Mariner V refractivity profile (shifted downward by 6.74 km from that of ref. A1) was used to establish the radius reference and the pressures and temperatures calculated for compositions of $90 \pm 5\% \text{CO}_2$ and $10 \pm 5\% \text{N}_2$ over the range 6091 to 6118 km radius. The refractivities used for the calculations are given in table A1 (from ref. A4).

TABLE A1.- RADIO REFRACTIVITY OF GASES AT 293 °K, 1 ATM

CO_2	$N = 461 \pm 1 \times 10^6$
N_2	$N = 274.0 \pm .5$
Ar	$N = 258.6 \pm .4$
He	$N = 32.5 \pm .2$
O_2	$N = 247.4 \pm .2$

Next, the profiles were extended upwards from 6118 and made to pass through the Regulus data. To match the Mariner pressures to those of the Regulus data by extrapolating between them with an isothermal region and a constant temperature lapse rate, the Regulus occultation level had to be shifted upward by 7 to 10 km.

APPENDIX A

Below 6091 km, the atmospheric properties were extrapolated downward to 6050 km radius assuming a pressure- and temperature-dependent dry adiabatic lapse rate.

The properties for the three models are tabulated in tables A2 thru A4. Figure A1 shows the pressure and temperature profiles and the location of the clouds.

The cloud top radius is 6121 ± 8 km. If it is assumed that the clouds are composed of H_2O , in either liquid or solid form, the thickness of the cloud layer can be estimated. Anduevskiy (ref. A2) finds that any water clouds formed would be composed of ice or supercooled water droplets with the bottom of the layer being 35.5 to 34.3 km above the point where Venera IV ceased transmission (assuming a water vapor content of 0.5 to 1.0% by volume). Similar results are obtained using the Mariner V P-T curve (see fig. A2). The cloud layer is then about 6 to 10 km thick.

Fortunately, confidence in the models is greatest in the regions where the BVS is to float (i.e., below 6120 and above 6090 km radius) since most of the measurements refer to that region. Above the cloud tops and below the last Venera IV measurements of pressure and temperature, the confidence level decreases with distance.

REVISED MODELS

These models are based on more recent analyses (e.g., refs. A3 and A5).

As above, the Mariner V refractivity profile (revised as in ref. A3) was used to establish the radius reference and the lower atmosphere properties obtained by extrapolating down to 6050 ± 5 km with a pressure- and temperature-dependent adiabatic lapse rate. This is shown in fig. A3; figures A4 and A5 compare the Mariner and Venera data.

Work is still in progress on making a model for the upper atmosphere consistent with the Mariner and Regulus data because there is still some uncertainty concerning the lapse rate above the clouds. However, fig. A6 shows that approximate agreement can be obtained merely by matching McElroy's model (ref. A5) to the Mariner pressure profile; the temperature profiles do not quite match up but this is not significant.

APPENDIX A

TABLE A2.- VENUS MODEL ATMOSPHERES; EXTRAPOLATION OF MARINER 5 DATA TO SURFACE; ADIABATIC LAPSE RATE,
(CO₂ = 95%, MEAN MOLECULAR WEIGHT = 43.21)

18 MARCH 68

RADIUS KM	ALTITUDE KM	PRESSURE		TEMPERATURE		MASS DENSITY		PRESSURE SCALE HT		TEMPERATURE SPECIF	
		MILLIBARS	LBS/SQIN	KELVIN	FAHRENHEIT	GM/CUCM	LBS/CUFT	SCALE HT.	GRADIENT	LAPSE RATE	HEAT
								KM	KM/KM	DEG K/KM	(CP/R)
6091.0	41.0	134514.4 (5.07 ATM)	0.5145E 04	0.7460E 02	455.52	360.26	0.5870E-02	0.3664E 00	10.009	-0.1936	-8.8127 5.1638
6090.0	40.0	131233.6 (5.60 ATM)	0.5680E 04	0.8236E 02	464.33	376.13	0.6357E-02	0.3969E 00	10.203	-0.1923	-8.7570 5.1983
6089.0	39.0	127952.7 (6.17 ATM)	0.6259E 04	0.9075E 02	473.09	391.90	0.6876E-02	0.4292E 00	10.395	-0.1911	-8.7033 5.2321
6088.0	38.0	124671.9 (6.79 ATM)	0.6885E 04	0.9983E 02	481.80	407.57	0.7427E-02	0.4636E 00	10.586	-0.1899	-8.6508 5.2656
6087.0	37.0	121391.0 (7.46 ATM)	0.7560E 04	0.1096E 03	490.45	423.14	0.8012E-02	0.5001E 00	10.776	-0.1887	-8.6000 5.2985
6086.0	36.0	118110.2 (8.18 ATM)	0.8289E 04	0.1201E 03	499.05	438.63	0.8632E-02	0.5389E 00	10.965	-0.1875	-8.5504 5.3309
6085.0	35.0	114829.4 (8.95 ATM)	0.9073E 04	0.1315E 03	507.61	454.03	0.9230E-02	0.5799E 00	11.153	-0.1864	-8.5034 5.3622
6084.0	34.0	111548.5 (9.78 ATM)	0.9917E 04	0.1438E 03	516.11	469.34	0.9986E-02	0.6234E 00	11.339	-0.1854	-8.4573 5.3931
6083.0	33.0	108267.7 (10.68 ATM)	0.1082E 05	0.1569E 03	524.57	484.56	0.1072E-01	0.6694E 00	11.525	-0.1843	-8.4120 5.4240
6082.0	32.0	104986.8 (11.64 ATM)	0.1179E 05	0.1710E 03	532.99	499.71	0.1150E-01	0.7181E 00	11.709	-0.1833	-8.3678 5.4544
6081.0	31.0	101706.0 (12.67 ATM)	0.1284E 05	0.1861E 03	541.36	514.78	0.1232E-01	0.7695E 00	11.892	-0.1823	-8.3246 5.4845
6080.0	30.0	98425.2 (13.77 ATM)	0.1395E 05	0.2023E 03	549.69	529.77	0.1319E-01	0.8238E 00	12.075	-0.1813	-8.2832 5.5138
6079.0	29.0	95144.3 (14.95 ATM)	0.1515E 05	0.2197E 03	557.97	544.68	0.1411E-01	0.8811E 00	12.256	-0.1804	-8.2426 5.5427
6078.0	28.0	91863.5 (16.21 ATM)	0.1643E 05	0.2382E 03	566.22	559.52	0.1508E-01	0.9416E 00	12.436	-0.1794	-8.2035 5.5710
6077.0	27.0	88582.6 (17.56 ATM)	0.1779E 05	0.2580E 03	574.42	574.29	0.1610E-01	0.1005E 01	12.616	-0.1786	-8.1653 5.5989
6076.0	26.0	85301.8 (19.00 ATM)	0.1925E 05	0.2792E 03	582.59	589.00	0.1717E-01	0.1072E 01	12.794	-0.1777	-8.1280 5.6264
6075.0	25.0	82021.0 (20.53 ATM)	0.2080E 05	0.3017E 03	590.72	603.63	0.1830E-01	0.1142E 01	12.972	-0.1768	-8.0918 5.6535
6074.0	24.0	78740.1 (22.17 ATM)	0.2246E 05	0.3257E 03	598.82	618.20	0.1949E-01	0.1217E 01	13.149	-0.1760	-8.0562 5.6803
6073.0	23.0	75459.3 (23.91 ATM)	0.2422E 05	0.3513E 03	606.87	632.71	0.2074E-01	0.1295E 01	13.325	-0.1752	-8.0211 5.7071
6072.0	22.0	72178.4 (25.76 ATM)	0.2610E 05	0.3784E 03	614.90	647.15	0.2206E-01	0.1377E 01	13.500	-0.1744	-7.9865 5.7337
6071.0	21.0	68897.6 (27.72 ATM)	0.2809E 05	0.4074E 03	622.89	661.53	0.2344E-01	0.1463E 01	13.675	-0.1736	-7.9529 5.7598
6070.0	20.0	65616.8 (29.81 ATM)	0.3021E 05	0.4381E 03	630.84	675.85	0.2489E-01	0.1553E 01	13.848	-0.1728	-7.9205 5.7853
6069.0	19.0	62335.9 (32.03 ATM)	0.3246E 05	0.4707E 03	638.77	690.11	0.2641E-01	0.1648E 01	14.021	-0.1720	-7.8886 5.8106

TABLE A2.- VENUS MODEL ATMOSPHERES, EXTRAPOLATION OF MARINER 5 DATA TO SURFACE, ADIABATIC LAPSE RATE,
(CO₂ = 95%, MEAN MOLECULAR WEIGHT = 43.21) - Continued

VENUS MODEL ATMOSPHERES, EXTRAPOLATION OF MARINER 5 DATA TO SURFACE, ADIABATIC LAPSE RATE.												18 MARCH 68	
PERCENT CO2 = 95.00, MEAN MOLECULAR WT = 43.21													
RADIUS		ALTITUDE		PRESSURE		TEMPERATURE		MASS DENSITY		PRESSURE SCALE		HT TEMPERATURE SPECIF	
KM	KM	FEET	MILLIBARS	LBS/SQIN	KELVIN	FAHRENHEIT	GM/CUCM	LBS/CUFT	KM	KM/KM	DEG K/KM	CP/R	HEAT
6068.0	18.0	59055.1	0.3484E 05	0.5052E 03	646.66	704.32	0.2800E-01	0.1748E 01	14.193	-0.1713	-7.8572	5.8357	
		(34.39 ATM)											
6067.0	17.0	55774.2	0.3737E 05	0.5419E 03	654.52	718.46	0.2967E-01	0.1852E 01	14.365	-0.1706	-7.8265	5.8606	
		(36.88 ATM)											
6066.0	16.0	52493.4	0.4005E 05	0.5807E 03	662.35	732.56	0.3142E-01	0.1962E 01	14.535	-0.1699	-7.7962	5.8853	
		(39.52 ATM)											
6065.0	15.0	49212.6	0.4288E 05	0.6218E 03	670.14	746.59	0.3326E-01	0.2076E 01	14.705	-0.1691	-7.7659	5.9102	
		(42.32 ATM)											
6064.0	14.0	45931.7	0.4588E 05	0.6653E 03	677.91	760.58	0.3517E-01	0.2196E 01	14.874	-0.1684	-7.7360	5.9350	
		(45.28 ATM)											
6063.0	13.0	42650.9	0.4906E 05	0.7113E 03	685.65	774.51	0.3718E-01	0.2321E 01	15.043	-0.1678	-7.7068	5.9594	
		(48.41 ATM)											
6062.0	12.0	39370.0	0.5241E 05	0.7599E 03	693.36	788.38	0.3928E-01	0.2452E 01	15.211	-0.1671	-7.6782	5.9836	
		(51.72 ATM)											
6061.0	11.0	36089.2	0.5595E 05	0.8113E 03	701.04	802.21	0.4148E-01	0.2589E 01	15.378	-0.1664	-7.6500	6.0077	
		(55.22 ATM)											
6060.0	10.0	32808.4	0.5969E 05	0.8655E 03	708.69	815.98	0.4377E-01	0.2732E 01	15.544	-0.1658	-7.6226	6.0312	
		(58.91 ATM)											
6059.0	9.0	29527.5	0.6363E 05	0.9227E 03	716.32	829.71	0.4617E-01	0.2882E 01	15.710	-0.1651	-7.5957	6.0546	
		(62.80 ATM)											
6058.0	8.0	26246.7	0.6779E 05	0.9830E 03	723.92	843.39	0.4867E-01	0.3038E 01	15.875	-0.1645	-7.5691	6.0778	
		(66.91 ATM)											
6057.0	7.0	22965.8	0.7218E 05	0.1046E 04	731.49	857.01	0.5128E-01	0.3201E 01	16.040	-0.1639	-7.5426	6.1012	
		(71.23 ATM)											
6056.0	6.0	19685.0	0.7680E 05	0.1113E 04	739.03	870.60	0.5400E-01	0.3371E 01	16.204	-0.1632	-7.5164	6.1245	
		(75.79 ATM)											
6055.0	5.0	16404.2	0.8166E 05	0.1184E 04	746.55	884.13	0.5684E-01	0.3549E 01	16.367	-0.1626	-7.4909	6.1474	
		(80.59 ATM)											
6054.0	4.0	13123.3	0.8678E 05	0.1258E 04	754.05	897.62	0.5981E-01	0.3734E 01	16.530	-0.1620	-7.4660	6.1699	
		(85.64 ATM)											
6053.0	3.0	9842.5	0.9216E 05	0.1336E 04	761.52	911.06	0.6290E-01	0.3928E 01	16.692	-0.1614	-7.4416	6.1922	
		(90.96 ATM)											
6052.0	2.0	6561.6	0.9782E 05	0.1418E 04	768.96	924.46	0.6611E-01	0.4127E 01	16.853	-0.1609	-7.4177	6.2142	
		(96.54 ATM)											
6051.0	1.0	3280.8	0.1037E 06	0.1504E 04	776.38	937.82	0.6947E-01	0.4337E 01	17.014				

TABLE A2.- VENUS MODEL ATMOSPHERES, EXTRAPOLATION OF MARINER 5 DATA TO SURFACE; ADIABATIC LAPSE RATE,
($\text{CO}_2 = 95\%$, MEAN MOLECULAR WEIGHT = 43.21) - Continued
VENUS MODEL ATMOSPHERES COMPUTED FROM DATA FROM THE OCCULTATIONS OF MARINER V AND REGULUS
MEAN MOLECULAR WGT = 43.21 (95.0 PERCENT CARBON DIOXIDE 5.0 PERCENT NITROGEN)

13 MARCH 1966

RADIUS	PRESSURE		TEMPERATURE		MASS DENSITY	REFRACTIVITY	PRESSURE SCALE HT	ALTITUDE ABOVE SURF
	MILLIBARS	LBS/SQIN	KELVIN	FAHRENHEIT				
KM					GM/CUCM	LBS/CUFT	N UNITS	FEET
6090.78	0.5260E 04	0.7627E 02	457.56	363.94	0.5974E-02	0.3730E 00	0.1500E 04	133790.3
6091.00	0.5145E 04	0.7461E 02	455.52	360.27	0.5870E-02	0.3664E 00	0.1473E 04	134514.4
6092.00	0.4651E 04	0.6745E 02	446.27	343.62	0.5415E-02	0.3380E 00	0.1359E 04	137795.2
6093.00	0.4196E 04	0.6085E 02	437.03	326.98	0.4986E-02	0.3113E 00	0.1251E 04	141076.1
6094.00	0.3777E 04	0.5477E 02	427.79	310.36	0.4584E-02	0.2862E 00	0.1150E 04	144356.9
6095.00	0.3392E 04	0.4919E 02	418.56	293.75	0.4207E-02	0.2626E 00	0.1056E 04	147637.8
6096.00	0.3040E 04	0.4440E 02	409.34	277.14	0.3853E-02	0.2405E 00	0.9674E 03	150918.6
6097.00	0.2717E 04	0.3940E 02	400.12	260.55	0.3522E-02	0.2199E 00	0.8843E 03	154199.5
6098.00	0.2422E 04	0.3512E 02	390.91	243.97	0.3213E-02	0.2006E 00	0.8067E 03	157480.3
6099.00	0.2154E 04	0.3123E 02	381.70	227.40	0.2924E-02	0.1826E 00	0.7343E 03	160761.1
6100.00	0.1909E 04	0.2769E 02	372.50	210.84	0.2656E-02	0.1658E 00	0.6609E 03	164042.0
6101.00	0.1688E 04	0.2447E 02	363.31	194.29	0.2406E-02	0.1502E 00	0.6042E 03	167322.8
6102.00	0.1487E 04	0.2157E 02	354.12	177.75	0.2175E-02	0.1358E 00	0.5461E 03	170603.6
6103.00	0.1306E 04	0.1894E 02	344.94	161.22	0.1960E-02	0.1224E 00	0.4923E 03	173884.5
6103.18	0.1276E 04	0.1850E 02	343.29	161.22	0.1924E-02	0.1201E 00	0.4830E 03	174744.0
6104.00	0.1143E 04	0.1658E 02	336.51	146.05	0.1759E-02	0.1098E 00	0.4416E 03	177165.3
6105.00	0.9981E 03	0.1447E 02	328.24	131.17	0.1573E-02	0.9820E-01	0.3949E 03	180446.2
6106.00	0.8680E 03	0.1258E 02	319.98	116.31	0.1402E-02	0.8757E-01	0.3521E 03	183727.0
6106.97	0.7553E 03	0.1095E 02	311.98	116.31	0.1251E-02	0.7814E-01	0.3142E 03	186908.5
6107.00	0.7520E 03	0.1090E 02	311.76	101.50	0.1247E-02	0.7785E-01	0.3120E 03	187007.8
6108.00	0.6493E 03	0.9415E 01	304.42	88.28	0.1102E-02	0.6881E-01	0.2767E 03	190288.7
6109.00	0.5586E 03	0.8100E 01	297.08	75.07	0.9714E-03	0.6064E-01	0.2438E 03	193565.5
6110.00	0.4788E 03	0.6942E 01	289.74	61.87	0.8534E-03	0.5327E-01	0.2142E 03	196850.4
6111.00	0.4088E 03	0.5927E 01	282.42	48.68	0.7473E-03	0.4665E-01	0.1876E 03	200131.2
6112.00	0.3476E 03	0.5040E 01	275.09	35.50	0.6521E-03	0.4071E-01	0.1637E 03	203412.0
6113.00	0.2942E 03	0.4267E 01	267.77	22.33	0.5670E-03	0.3540E-01	0.1423E 03	206692.9
6114.00	0.2480E 03	0.3596E 01	260.46	9.16	0.4911E-03	0.3066E-01	0.1233E 03	209973.7
6114.51	0.2269E 03	0.3290E 01	256.73	9.16	0.4557E-03	0.2845E-01	0.1144E 03	211646.2
6115.00	0.2081E 03	0.3018E 01	256.18	1.46	0.4189E-03	0.2615E-01	0.1051E 03	213254.5
6116.00	0.1744E 03	0.2529E 01	255.06	-0.55	0.3525E-03	0.2200E-01	0.8850E 02	216535.4
6117.00	0.1460E 03	0.2118E 01	253.93	-2.58	0.2964E-03	0.1850E-01	0.7442E 02	219816.2
6118.00	0.1222E 03	0.1772E 01	252.81	-4.60	0.2491E-03	0.1555E-01	0.6254E 02	223097.1
6118.21	0.1177E 03	0.1707E 01	252.57	-4.60	0.2401E-03	0.1499E-01	0.6029E 02	223785.9
6119.00	0.1022E 03	0.1482E 01	252.15	-5.78	0.2088E-03	0.1303E-01	0.5242E 02	226377.9
6120.00	0.8550E 02	0.1239E 01	251.62	-6.74	0.1749E-03	0.1092E-01	0.4391E 02	229658.8
6121.00	0.7146E 02	0.1036E 01	251.09	-7.70	0.1464E-03	0.9144E-02	0.3677E 02	232939.6
6122.00	0.5971E 02	0.8659E 00	250.55	-8.66	0.1226E-03	0.7654E-02	0.3078E 02	236220.5
6123.00	0.4988E 02	0.7233E 00	250.02	-9.62	0.1026E-03	0.6405E-02	0.2575E 02	239501.3
6124.00	0.4165E 02	0.6040E 00	249.49	-10.57	0.8583E-04	0.5358E-02	0.2154E 02	242782.1
6125.00	0.3477E 02	0.5042E 00	248.96	-11.53	0.7177E-04	0.4481E-02	0.1802E 02	246063.0
6126.00	0.2901E 02	0.4207E 00	248.43	-12.49	0.6000E-04	0.3746E-02	0.1506E 02	249343.8
6127.00	0.2420E 02	0.3510E 00	247.90	-13.44	0.5015E-04	0.3130E-02	0.1259E 02	252624.6
6128.00	0.2018E 02	0.2927E 00	247.37	-14.40	0.4189E-04	0.2615E-02	0.1051E 02	255905.5
6128.21	0.1943E 02	0.2817E 00	247.26	-14.40	0.4034E-04	0.2518E-02	0.1012E 02	256594.3
6129.00	0.1683E 02	0.2440E 00	247.55	-14.07	0.3490E-04	0.2178E-02	0.8762E 01	259186.3
6130.00	0.1404E 02	0.2035E 00	247.92	-13.41	0.2905E-04	0.1814E-02	0.7295E 01	262467.2

TABLE A2.- VENUS MODEL ATMOSPHERES, EXTRAPOLATION OF MARINER 5 DATA TO SURFACE, ADIABATIC LAPSE RATE, (CO₂ = 95%, MEAN MOLECULAR WEIGHT = 43.21) - ContinuedVENUS MODEL ATMOSPHERES COMPUTED FROM DATA FROM THE OCCULTATIONS OF MARINER V AND REGULUS
MEAN MOLECULAR WEIGHT = 43.21 (95.0 PERCENT CARBON DIOXIDE, 5.0 PERCENT NITROGEN)

RADIUS	PRESSURE	TEMPERATURE	MASS DENSITY	REFRACTIVITY	PRESSURE	ALTITUDE			
KM	MILLIBARS	KELVIN	GM/CM ³	N UNITS	SCALE HT	ABOVE-SURF			
		FAHRENHEIT	LBS/CM ³		KM	FEET			
6131.00	0.1171E-02	0.1698E+00	248.28	-12.75	0.2420E-04	0.1510E-02	0.6076E-01	5.5279	265748.0
6132.00	0.9778E-01	0.1417E-00	248.65	-12.08	0.2016E-04	0.1258E-02	0.5062E-01	5.5379	269028.8
6133.00	0.8164E-01	0.1183E-00	249.02	-11.42	0.1680E-04	0.1049E-02	0.4218E-01	5.5479	272309.7
6134.00	0.6818E-01	0.9888E-01	249.39	-10.76	0.1401E-04	0.8746E-03	0.3517E-01	5.5579	275590.5
6135.00	0.5696E-01	0.8260E-01	249.75	-10.10	0.1168E-04	0.7294E-03	0.2933E-01	5.5679	278871.4
6136.00	0.4761E-01	0.6903E-01	250.12	-9.44	0.9747E-05	0.6085E-03	0.2447E-01	5.5779	282152.2
6137.00	0.3980E-01	0.5771E-01	250.49	-8.78	0.8134E-05	0.5078E-03	0.2042E-01	5.5879	285433.1
6138.00	0.3328E-01	0.4826E-01	250.85	-8.12	0.6790E-05	0.4239E-03	0.1704E-01	5.5979	288713.9
6139.00	0.2784E-01	0.4037E-01	251.22	-7.46	0.5670E-05	0.3539E-03	0.1423E-01	5.6079	291994.7
6140.00	0.2330E-01	0.3378E-01	251.59	-6.80	0.4736E-05	0.2957E-03	0.1189E-01	5.6178	295275.6
6141.00	0.1950E-01	0.2828E-01	251.95	-6.14	0.3957E-05	0.2470E-03	0.9936E-02	5.6279	298556.4
6142.00	0.1633E-01	0.2368E-01	252.32	-5.48	0.3308E-05	0.2065E-03	0.8305E-02	5.6379	301837.3
6143.00	0.1367E-01	0.1983E-01	252.68	-4.83	0.2765E-05	0.1726E-03	0.6944E-02	5.6479	305118.1
6144.00	0.1146E-01	0.1662E-01	253.05	-4.17	0.2313E-05	0.1444E-03	0.5808E-02	5.6578	308399.0
6145.00	0.9606E-00	0.1392E-01	253.41	-3.51	0.1935E-05	0.1208E-03	0.4859E-02	5.6679	311679.8
6146.00	0.8054E-00	0.1167E-01	253.78	-2.86	0.1619E-05	0.1011E-03	0.4066E-02	5.6779	314960.6
6147.00	0.6754E-00	0.9794E-02	254.14	-2.20	0.1356E-05	0.8466E-04	0.3404E-02	5.6879	318241.5
6148.00	0.5666E-00	0.8216E-02	254.51	-1.55	0.1135E-05	0.7089E-04	0.2851E-02	5.6978	321522.3
6149.00	0.4754E-00	0.6894E-02	254.87	-0.89	0.9513E-06	0.5939E-04	0.2388E-02	5.7079	324803.1
6150.00	0.3991E-00	0.5787E-02	255.23	-0.24	0.7971E-06	0.4976E-04	0.2001E-02	5.7179	328084.0
6151.00	0.3351E-00	0.4859E-02	255.60	0.41	0.6681E-06	0.4171E-04	0.1677E-02	5.7279	331364.8
6152.00	0.2815E-00	0.4081E-02	255.96	1.06	0.5602E-06	0.3497E-04	0.1406E-02	5.7379	334645.6
6153.00	0.2365E-00	0.3429E-02	256.32	1.71	0.4699E-06	0.2933E-04	0.1179E-02	5.7479	337926.5
6154.00	0.1987E-00	0.2882E-02	256.68	2.37	0.3942E-06	0.2461E-04	0.9897E-03	5.7579	341207.3
6155.00	0.1671E-00	0.2423E-02	257.05	3.02	0.3308E-06	0.2065E-04	0.8306E-03	5.7679	344488.1
6156.00	0.1405E-00	0.2037E-02	257.41	3.67	0.2779E-06	0.1734E-04	0.6973E-03	5.7779	347769.0
6157.00	0.1182E-00	0.1714E-02	257.77	4.32	0.2332E-06	0.1456E-04	0.5855E-03	5.7878	351049.8
6158.00	0.9947E-01	0.1442E-02	258.13	4.97	0.1959E-06	0.1223E-04	0.4918E-03	5.7979	354330.7
6159.00	0.8372E-01	0.1214E-02	258.49	5.62	0.1646E-06	0.1027E-04	0.4133E-03	5.8079	357611.5
6160.00	0.7049E-01	0.1022E-02	258.85	6.27	0.1383E-06	0.8638E-05	0.3473E-03	5.8179	360892.4
6161.00	0.5937E-01	0.8608E-03	259.22	6.92	0.1163E-06	0.7262E-05	0.2920E-03	5.8278	364173.2
6162.00	0.5001E-01	0.7252E-03	259.58	7.57	0.9784E-07	0.6108E-05	0.2456E-03	5.8379	367454.1
6163.00	0.4214E-01	0.6111E-03	259.94	8.22	0.8230E-07	0.5138E-05	0.2066E-03	5.8479	370734.9
6164.00	0.3552E-01	0.5151E-03	260.30	8.87	0.6926E-07	0.4324E-05	0.1738E-03	5.8579	374015.7
6165.00	0.2995E-01	0.4343E-03	260.66	9.51	0.5830E-07	0.3639E-05	0.1463E-03	5.8679	377296.6
6166.00	0.2526E-01	0.3663E-03	261.02	10.16	0.4909E-07	0.3064E-05	0.1232E-03	5.8779	380577.4
6167.00	0.2131E-01	0.3091E-03	261.37	10.81	0.4134E-07	0.2581E-05	0.1038E-03	5.8879	383858.3
6167.38	0.1998E-01	0.2898E-03	261.51	10.81	0.3873E-07	0.2418E-05	0.9725E-02	5.8916	385104.6
6168.00	0.1800E-01	0.2611E-03	266.96	20.87	0.3418E-07	0.2134E-05	0.8582E-02	6.0157	387139.1
6169.00	0.1529E-01	0.2217E-03	275.75	36.68	0.2809E-07	0.1753E-05	0.7053E-02	6.2157	390420.0
6170.00	0.1305E-01	0.1892E-03	284.53	52.49	0.2323E-07	0.1450E-05	0.5832E-02	6.4157	393700.8
6171.00	0.1119E-01	0.1623E-03	293.30	68.28	0.1932E-07	0.1206E-05	0.4851E-02	6.6157	396981.6
6172.00	0.9646E-02	0.1398E-03	302.07	84.07	0.1616E-07	0.1009E-05	0.4057E-02	6.8157	400262.5
6173.00	0.8347E-02	0.1210E-03	310.84	99.84	0.1358E-07	0.8482E-06	0.3411E-02	7.0157	403543.3
6174.00	0.7253E-02	0.1051E-03	319.59	115.60	0.1147E-07	0.7166E-06	0.2881E-02	7.2157	406824.1

TABLE A2.- VENUS MODEL ATMOSPHERES, EXTRAPOLATION OF MARINER 5 DATA TO SURFACE, ADIABATIC LAPSE RATE,
(CO₂ = 95%, MEAN MOLECULAR WEIGHT = 43.21) - Continued

VENUS MODEL ATMOSPHERES COMPUTED FROM DATA FROM THE OCCULTATIONS OF MARINER V AND REGULUS
MEAN MOLECULAR WEIGHT = 43.21 (95.0 PERCENT CARBON DIOXIDE 5.0 PERCENT NITROGEN)

RADIUS KM	PRESSURE MILLIBARS	LBS/SQIN	KELVIN	FAHRENHEIT	MASS DENSITY GM/CCM	LBS/CUFT	REFRACTIVITY N UNITS	PRESSURE SCALE HT KM	ALTITUDE ABOVE SURF FEET
6175.00	0.6326E-02	0.9173E-04	328.35	131.36	0.9742E-08	0.6082E-06	0.2445E-02	7.4157	410105.0
6176.00	0.5538E-02	0.8030E-04	337.09	147.10	0.8304E-08	0.5184E-06	0.2084E-02	7.6157	413385.8
6177.00	0.4865E-02	0.7054E-04	345.83	162.83	0.7108E-08	0.4437E-06	0.1784E-02	7.8157	416666.6
6178.00	0.4287E-02	0.6217E-04	354.57	178.56	0.6108E-08	0.3813E-06	0.1533E-02	8.0157	419947.5
6179.00	0.3790E-02	0.5496E-04	363.30	194.27	0.5288E-08	0.3289E-06	0.1322E-02	8.2157	423228.3
6180.00	0.3361E-02	0.4873E-04	372.02	209.97	0.4560E-08	0.2847E-06	0.1145E-02	8.4157	426509.1
6180.55	0.3149E-02	0.4567E-04	376.82	209.97	0.4219E-08	0.2633E-06	0.1059E-02	8.5256	428313.0
6181.00	0.2988E-02	0.4333E-04	380.74	225.66	0.3961E-08	0.2473E-06	0.9545E-03	8.6157	429790.0
6182.00	0.2864E-02	0.3863E-04	389.45	241.35	0.3451E-08	0.2154E-06	0.8655E-03	8.8157	433070.8
6183.00	0.2381E-02	0.3453E-04	398.16	257.02	0.3017E-08	0.1883E-06	0.7574E-03	9.0157	436351.7
6184.00	0.2134E-02	0.3094E-04	406.86	272.68	0.2644E-08	0.1651E-06	0.6640E-03	9.2157	439632.5
6185.00	0.1917E-02	0.2779E-04	415.55	288.33	0.2325E-08	0.1451E-06	0.5837E-03	9.4157	442913.4
6186.00	0.1725E-02	0.2502E-04	424.24	303.97	0.2049E-08	0.1279E-06	0.5145E-03	9.6157	446194.2
6187.00	0.1557E-02	0.2257E-04	432.93	319.60	0.1811E-08	0.1130E-06	0.4548E-03	9.8157	449475.0
6188.00	0.1407E-02	0.2041E-04	441.61	335.23	0.1605E-08	0.1002E-06	0.4029E-03	10.0157	452755.9
6189.00	0.1275E-02	0.1849E-04	450.28	350.84	0.1425E-08	0.8999E-07	0.3578E-03	10.2157	456036.7
6190.00	0.1157E-02	0.1678E-04	458.95	366.44	0.1268E-08	0.7922E-07	0.3185E-03	10.4157	459317.6
6191.00	0.1052E-02	0.1526E-04	467.61	382.03	0.1132E-08	0.7067E-07	0.2842E-03	10.6157	462598.4
6192.00	0.9586E-03	0.1390E-04	476.26	397.61	0.1012E-08	0.6318E-07	0.2541E-03	10.8157	465879.3
6193.00	0.8747E-03	0.1268E-04	484.91	413.38	0.9067E-09	0.5661E-07	0.2276E-03	11.0157	469160.1
6194.00	0.7994E-03	0.1159E-04	493.56	428.74	0.8139E-09	0.5081E-07	0.2043E-03	11.2157	472441.0
6195.00	0.7318E-03	0.1061E-04	502.20	444.29	0.7320E-09	0.4570E-07	0.1837E-03	11.4157	475721.8
6196.00	0.6709E-03	0.9729E-05	510.83	459.83	0.6595E-09	0.4118E-07	0.1656E-03	11.6157	479002.6
6197.00	0.6160E-03	0.8933E-05	519.46	475.36	0.5954E-09	0.3717E-07	0.1494E-03	11.8157	482283.5
6198.00	0.5664E-03	0.8213E-05	528.08	490.88	0.5382E-09	0.3361E-07	0.1351E-03	12.0157	485564.3
6199.00	0.5216E-03	0.7563E-05	536.70	506.39	0.4876E-09	0.3044E-07	0.1224E-03	12.2157	488845.1
6200.00	0.4809E-03	0.6973E-05	545.31	521.89	0.4423E-09	0.2761E-07	0.1110E-03	12.4157	492126.0
6201.00	0.4439E-03	0.6437E-05	553.92	537.38	0.4018E-09	0.2509E-07	0.1008E-03	12.6157	495406.8
6202.00	0.4104E-03	0.5950E-05	562.52	552.86	0.3657E-09	0.2283E-07	0.9181E-04	12.8157	498687.6
6203.00	0.3798E-03	0.5507E-05	571.11	568.33	0.3332E-09	0.2080E-07	0.8366E-04	13.0157	501968.5
6204.00	0.3519E-03	0.5103E-05	579.70	583.79	0.3041E-09	0.1898E-07	0.7635E-04	13.2157	505249.3
6205.00	0.3264E-03	0.4734E-05	588.28	599.24	0.2779E-09	0.1734E-07	0.6977E-04	13.4157	508530.1
6206.00	0.3032E-03	0.4396E-05	596.86	614.68	0.2542E-09	0.1587E-07	0.6384E-04	13.6157	511811.0
6207.00	0.2818E-03	0.4087E-05	605.43	630.11	0.2329E-09	0.1454E-07	0.5849E-04	13.8157	515091.8
6208.00	0.2623E-03	0.3803E-05	614.00	645.53	0.2137E-09	0.1334E-07	0.5366E-04	14.0157	518372.7
6209.00	0.2443E-03	0.3543E-05	622.56	660.94	0.1963E-09	0.1225E-07	0.4928E-04	14.2157	521653.5
6210.00	0.2279E-03	0.3304E-05	631.12	676.34	0.1805E-09	0.1127E-07	0.4532E-04	14.4157	524934.5
6211.00	0.2127E-03	0.3084E-05	639.67	691.73	0.1662E-09	0.1037E-07	0.4172E-04	14.6157	528215.2
6212.00	0.1987E-03	0.2881E-05	648.21	707.11	0.1531E-09	0.9564E-08	0.3846E-04	14.8157	531496.1
6213.00	0.1858E-03	0.2695E-05	656.75	722.48	0.1413E-09	0.8824E-08	0.3548E-04	15.0157	534777.0
6214.00	0.1739E-03	0.2522E-05	665.28	737.84	0.1305E-09	0.8151E-08	0.3277E-04	15.2157	538057.7
6215.00	0.1629E-03	0.2363E-05	673.81	753.19	0.1207E-09	0.7536E-08	0.3030E-04	15.4157	541338.6
6216.00	0.1528E-03	0.2215E-05	682.33	768.53	0.1117E-09	0.6976E-08	0.2805E-04	15.6157	544619.5
6217.00	0.1433E-03	0.2079E-05	690.85	783.86	0.1035E-09	0.6463E-08	0.2599E-04	15.8157	547900.3
6218.00	0.1346E-03	0.1952E-05	699.36	799.18	0.9600E-10	0.5993E-08	0.2410E-04	16.0157	551181.1
6219.00	0.1265E-03	0.1834E-05	707.87	814.49	0.8911E-10	0.5563E-08	0.2237E-04	16.2157	554462.0

TABLE A2.- VENUS MODEL ATMOSPHERES, EXTRAPOLATION OF MARINER 5 DATA TO SURFACE, ADIABATIC LAPSE RATE,
(CO₂ = 95%, MEAN MOLECULAR WEIGHT = 43.21) - Concluded

VENUS MODEL ATMOSPHERES COMPUTED FROM DATA FROM THE OCCULTATIONS OF MARINER V AND REGULUS
MEAN MOLECULAR WGT = 43.21 (95.0 PERCENT CARBON DIOXIDE 5.0 PERCENT NITROGEN)

RADIUS KM	PRESSURE MILLIBARS	LBS/SQ IN	KELVIN	TEMPERATURE FAHRENHEIT	GM/CUCM	MASS DENSITY LBS/CUFT	REFRACTIVITY N UNITS	PRESSURE SCALE HT ABOVE SURF MM	ALTITUDE FEET
6220.00	0.1190E-03	0.1725E-05	716.37	829.79	0.8279E-10	0.45169E-08	0.2078E-04	16.4157	557742.8
6221.00	0.1120E-03	0.1624E-05	724.86	845.08	0.7699E-10	0.48006E-08	0.1933E-04	16.6157	561023.0
6222.00	0.1055E-03	0.1530E-05	733.35	860.36	0.7166E-10	0.44473E-08	0.1799E-04	16.8157	564304.5
6223.00	0.0994E-04	0.1442E-05	741.83	875.64	0.6675E-10	0.4167E-08	0.1675E-04	17.0157	567585.3
6224.00	0.0938E-04	0.1360E-05	750.31	890.90	0.6223E-10	0.3885E-08	0.1562E-04	17.2157	570866.2
6225.00	0.0885E-04	0.1284E-05	758.79	906.15	0.5806E-10	0.3625E-08	0.1457E-04	17.4157	574147.0
6226.00	0.0836E-04	0.1212E-05	767.25	921.39	0.5422E-10	0.3385E-08	0.1361E-04	17.6157	577427.8
6227.00	0.0790E-04	0.1146E-05	775.71	936.62	0.5067E-10	0.3163E-08	0.1272E-04	17.8157	580708.7
6228.00	0.0747E-04	0.1084E-05	784.17	951.84	0.4738E-10	0.2958E-08	0.1189E-04	18.0157	583989.5
6229.00	0.0707E-04	0.1025E-05	792.62	967.05	0.4435E-10	0.2768E-08	0.1113E-04	18.2157	587270.3
6230.00	0.0669E-04	0.9713E-06	801.07	982.26	0.4153E-10	0.2593E-08	0.1042E-04	18.4157	590551.2
6231.00	0.0634E-04	0.9202E-06	809.51	997.45	0.3893E-10	0.2430E-08	0.9774E-05	18.6157	593832.1
6232.00	0.0601E-04	0.8723E-06	817.94	1012.63	0.3651E-10	0.2279E-08	0.9167E-05	18.8157	597112.8
6233.00	0.0570E-04	0.8274E-06	826.37	1027.80	0.3426E-10	0.2139E-08	0.8603E-05	19.0157	600393.7
6234.00	0.0541E-04	0.7852E-06	834.79	1042.96	0.3218E-10	0.2009E-08	0.8030E-05	19.2157	603674.0
6235.00	0.0514E-04	0.7456E-06	843.21	1058.12	0.3024E-10	0.1888E-08	0.7593E-05	19.4157	606955.3
6236.00	0.0488E-04	0.7084E-06	851.63	1073.26	0.2844E-10	0.1775E-08	0.7140E-05	19.6157	610236.2
6237.00	0.0464E-04	0.6733E-06	860.03	1088.39	0.2676E-10	0.1670E-08	0.6718E-05	19.8157	613517.1
6238.00	0.0441E-04	0.6403E-06	868.43	1103.52	0.2519E-10	0.1573E-08	0.6326E-05	20.0157	616798.0
6239.00	0.0420E-04	0.6093E-06	876.83	1118.63	0.2373E-10	0.1481E-08	0.5959E-05	20.2157	620078.7
6240.00	0.0400E-04	0.5803E-06	885.22	1133.73	0.2237E-10	0.1396E-08	0.5617E-05	20.4157	623359.6
6241.00	0.03810E-04	0.5524E-06	893.61	1148.83	0.2110E-10	0.1317E-08	0.5298E-05	20.6157	626640.5
6242.00	0.03630E-04	0.5264E-06	901.99	1163.91	0.1991E-10	0.1243E-08	0.5000E-05	20.8157	629921.3
6243.00	0.03461E-04	0.5018E-06	910.36	1178.99	0.1880E-10	0.1174E-08	0.4721E-05	21.0157	633202.1
6244.00	0.03301E-04	0.4786E-06	918.73	1194.05	0.1776E-10	0.1109E-08	0.4460E-05	21.2157	636483.0
6245.00	0.03149E-04	0.4567E-06	927.10	1209.11	0.1679E-10	0.1048E-08	0.4216E-05	21.4157	639763.8
6246.00	0.03006E-04	0.4359E-06	935.45	1224.15	0.1583E-10	0.9916E-09	0.3987E-05	21.6157	643044.6
6247.00	0.02871E-04	0.4163E-06	943.81	1239.19	0.1503E-10	0.9383E-09	0.3773E-05	21.8157	646325.5
6248.00	0.02743E-04	0.3977E-06	952.16	1254.21	0.1422E-10	0.8883E-09	0.3572E-05	22.0157	649606.3
6249.00	0.02622E-04	0.3801E-06	960.50	1269.23	0.1347E-10	0.8414E-09	0.3383E-05	22.2157	652887.2
6250.00	0.02507E-04	0.3635E-06	968.83	1284.24	0.1277E-10	0.7973E-09	0.3206E-05	22.4157	656168.0
6251.00	0.02507E-04	0.3635E-06	968.83	1284.24	0.1277E-10	0.7973E-09	0.3206E-05	22.4157	656168.0

TABLE A3.- VENUS MODEL ATMOSPHERES, EXTRAPOLATION OF MARINER 5 DATA TO SURFACE, ADIABATIC LAPSE RATE
(CO₂ = 90%, MEAN MOLECULAR WEIGHT = 42.41)

18 MARCH 68

RADIUS KM	ALTITUDE KM	FEET	PRESSURE		TEMPERATURE		MASS DENSITY		PRESSURE SCALE HT		SCALE HT		TEMPERATURE SPECIF	
			MILLIBARS	LBS/SQIN	KELVIN	FAHRENHEIT	GM/CUCM	LBS/CUFT	KM	HT	KM/KM	DEG K/KM	HT	HEAT (CP/R)
6091.0	41.0	134514.4	0.4980E 04	0.7221E 02	442.62	337.04	0.5739E-02	0.3582E 00	9.909		-0.1986	-8.8714	5.0347	
		(4.91 ATM)												
6090.0	40.0	131233.6	0.5503E 04	0.7979E 02	451.49	353.01	0.6217E-02	0.3881E 00	10.108		-0.1972	-8.8147	5.0687	
		(5.43 ATM)												
6089.0	39.0	127952.7	0.6069E 04	0.8801E 02	460.31	368.89	0.6726E-02	0.4199E 00	10.305		-0.1959	-8.7597	5.1022	
		(5.99 ATM)												
6088.0	38.0	124671.9	0.6682E 04	0.9689E 02	469.07	384.66	0.7266E-02	0.4536E 00	10.501		-0.1947	-8.7072	5.1347	
		(6.59 ATM)												
6087.0	37.0	121391.0	0.7343E 04	0.1064E 03	477.78	400.34	0.7839E-02	0.4894E 00	10.696		-0.1935	-8.6556	5.1670	
		(7.24 ATM)												
6086.0	36.0	118110.2	0.8056E 04	0.1168E 03	486.44	415.92	0.8447E-02	0.5274E 00	10.889		-0.1923	-8.6055	5.1988	
		(7.95 ATM)												
6085.0	35.0	114829.4	0.8823E 04	0.1279E 03	495.05	431.42	0.9092E-02	0.5676E 00	11.082		-0.1912	-8.5569	5.2300	
		(8.70 ATM)												
6084.0	34.0	111548.5	0.9649E 04	0.1399E 03	503.61	446.83	0.9774E-02	0.6101E 00	11.273		-0.1900	-8.5102	5.2605	
		(9.52 ATM)												
6083.0	33.0	108267.7	0.1053E 05	0.1527E 03	512.12	462.15	0.1049E-01	0.6552E 00	11.463		-0.1890	-8.4647	5.2905	
		(10.39 ATM)												
6082.0	32.0	104986.8	0.1148E 05	0.1665E 03	520.59	477.39	0.1125E-01	0.7028E 00	11.652		-0.1879	-8.4197	5.3205	
		(11.33 ATM)												
6081.0	31.0	101706.0	0.1251E 05	0.1813E 03	529.01	492.55	0.1206E-01	0.7530E 00	11.840		-0.1869	-8.3761	5.3499	
		(12.34 ATM)												
6080.0	30.0	98425.2	0.1360E 05	0.1972E 03	537.39	507.63	0.1291E-01	0.8061E 00	12.027		-0.1859	-8.3334	5.3791	
		(13.42 ATM)												
6079.0	29.0	95144.3	0.1477E 05	0.2142E 03	545.72	522.64	0.1380E-01	0.8621E 00	12.213		-0.1849	-8.2923	5.4076	
		(14.58 ATM)												
6078.0	28.0	91863.5	0.1602E 05	0.2323E 03	554.02	537.57	0.1475E-01	0.9210E 00	12.398		-0.1839	-8.2522	5.4356	
		(15.81 ATM)												
6077.0	27.0	88582.6	0.1736E 05	0.2517E 03	562.27	552.43	0.1574E-01	0.9832E 00	12.582		-0.1830	-8.2132	5.4632	
		(17.13 ATM)												
6076.0	26.0	85301.8	0.1878E 05	0.2723E 03	570.49	567.22	0.1679E-01	0.1048E 01	12.765		-0.1821	-8.1755	5.4903	
		(18.53 ATM)												
6075.0	25.0	82021.0	0.2030E 05	0.2944E 03	578.67	581.94	0.1789E-01	0.1117E 01	12.947		-0.1812	-8.1385	5.5170	
		(20.03 ATM)												
6074.0	24.0	78740.1	0.2192E 05	0.3178E 03	586.81	596.59	0.1905E-01	0.1189E 01	13.128		-0.1803	-8.1026	5.5433	
		(21.63 ATM)												
6073.0	23.0	75459.3	0.2364E 05	0.3428E 03	594.91	611.18	0.2027E-01	0.1265E 01	13.309		-0.1795	-8.0673	5.5694	
		(23.33 ATM)												
6072.0	22.0	72178.4	0.2547E 05	0.3694E 03	602.98	625.71	0.2155E-01	0.1345E 01	13.488		-0.1787	-8.0326	5.5953	
		(25.14 ATM)												
6071.0	21.0	68897.6	0.2742E 05	0.3976E 03	611.02	640.17	0.2289E-01	0.1429E 01	13.667		-0.1779	-7.9984	5.6211	
		(27.06 ATM)												
6070.0	20.0	65616.8	0.2949E 05	0.4276E 03	619.02	654.57	0.2430E-01	0.1517E 01	13.845		-0.1770	-7.9647	5.6467	
		(29.10 ATM)												
6069.0	19.0	62335.9	0.3168E 05	0.4594E 03	626.99	668.91	0.2578E-01	0.1609E 01	14.022		-0.1763	-7.9324	5.6716	
		(31.27 ATM)												

TABLE A3.- VENUS MODEL ATMOSPHERES, EXTRAPOLATION OF MARINER 5 DATA TO SURFACE, ADIABATIC LAPSE RATE
(CO₂ = 90%, MEAN MOLECULAR WEIGHT = 42.41) - Continued

VENUS MODEL ATMOSPHERES, EXTRAPOLATION OF MARINER 5 DATA TO SURFACE, ADIABATIC LAPSE RATE. PERCENT CO2 = 90.00, MEAN MOLECULAR WT = 42.41													18 MARCH 68	
RADIUS		ALTITUDE		PRESSURE		TEMPERATURE		MASS DENSITY		PRESSURE SCALE HT		TEMPERATURE SPECIF		
KM	KM	FEET	MILLIBARS	LBS/SQIN	KELVIN	FAHRENHEIT	GM/CUCM	LBS/CUFT	KM	KM/KM	DEG K/KM	HEAT		
(CP/R)														
6068.0	18.0	59055.1	0.3401E 05	0.4932E 03	634.92	683.20	0.2732E-01	0.1706E 01	14.198	-0.1755	-7.9007	5.6962		
6067.0	17.0	55774.2	0.3648E 05	0.5289E 03	642.83	697.42	0.2894E-01	0.1807E 01	14.374	-0.1748	-7.8696	5.7206		
6066.0	16.0	52493.4	0.3909E 05	0.5668E 03	650.70	711.59	0.3064E-01	0.1913E 01	14.548	-0.1740	-7.8390	5.7449		
6065.0	15.0	49212.6	0.4185E 05	0.6069E 03	658.54	725.71	0.3242E-01	0.2024E 01	14.723	-0.1733	-7.8086	5.7691		
6064.0	14.0	45931.7	0.4478E 05	0.6493E 03	666.35	739.77	0.3428E-01	0.2140E 01	14.896	-0.1726	-7.7783	5.7935		
6063.0	13.0	42650.9	0.4787E 05	0.6941E 03	674.13	753.77	0.3622E-01	0.2261E 01	15.068	-0.1718	-7.7486	5.8176		
6062.0	12.0	39370.0	0.5113E 05	0.7415E 03	681.88	767.72	0.3825E-01	0.2388E 01	15.240	-0.1711	-7.7195	5.8415		
6061.0	11.0	36089.2	0.5458E 05	0.7915E 03	689.61	781.62	0.4037E-01	0.2520E 01	15.412	-0.1704	-7.6909	5.8651		
6060.0	10.0	32808.4	0.5822E 05	0.8442E 03	697.30	795.47	0.4259E-01	0.2659E 01	15.582	-0.1698	-7.6628	5.8886		
6059.0	9.0	29527.5	0.6206E 05	0.8999E 03	704.96	809.27	0.4490E-01	0.2803E 01	15.752	-0.1691	-7.6354	5.9117		
6058.0	8.0	26246.7	0.6610E 05	0.9585E 03	712.60	823.02	0.4732E-01	0.2954E 01	15.921	-0.1685	-7.6086	5.9344		
6057.0	7.0	22965.8	0.7037E 05	0.1020E 04	720.21	836.72	0.4983E-01	0.3111E 01	16.089	-0.1678	-7.5823	5.9570		
6056.0	6.0	19685.0	0.7485E 05	0.1085E 04	727.80	850.37	0.5246E-01	0.3275E 01	16.257	-0.1672	-7.5556	5.9800		
6055.0	5.0	16404.2	0.7958E 05	0.1153E 04	735.36	863.97	0.5520E-01	0.3446E 01	16.425	-0.1665	-7.5294	6.0028		
6054.0	4.0	13123.3	0.8455E 05	0.1225E 04	742.89	877.53	0.5805E-01	0.3624E 01	16.591	-0.1659	-7.5039	6.0252		
6053.0	3.0	9842.5	0.8977E 05	0.1301E 04	750.39	891.04	0.6102E-01	0.3809E 01	16.757	-0.1653	-7.4791	6.0472		
6052.0	2.0	6561.6	0.9526E 05	0.1381E 04	757.88	904.51	0.6412E-01	0.4003E 01	16.923	-0.1647	-7.4547	6.0689		
6051.0	1.0	3280.8	0.1010E 06	0.1465E 04	765.33	917.93	0.6734E-01	0.4204E 01	17.087	-0.1641	-7.4309	6.0904		
6050.0	0.0	0.0	0.1070E 06	0.1552E 04	772.77	931.31	0.7069E-01	0.4413E 01	17.251					

TABLE A3.- VENUS MODEL ATMOSPHERES, EXTRAPOLATION OF MARINER 5 DATA TO SURFACE, ADIABATIC LAPSE RATE
(CO₂ = 90%, MEAN MOLECULAR WEIGHT = 42.41) - Continued

18 MARCH 1968

VENUS MODEL ATMOSPHERES COMPUTED FROM DATA FROM THE OCCULTATIONS OF MARINER V AND REGULUS
MEAN MOLECULAR WGT = 42.41 (90.0 PERCENT CARBON DIOXIDE 10.0 PERCENT NITROGEN)

RADIUS	PRESSURE		TEMPERATURE		MASS DENSITY	REFRACTIVITY	PRESSURE SCALE HT	ALTITUDE	
	MILLIBARS	LBS/SQIN	KELVIN	FAHRENHEIT					GM/CUCM
6090.78	0.5092E 04	0.7384E 02	444.63	340.66	0.5842E-02	0.3647E 00	0.1463E 04	9.9540	133790.3
6091.00	0.4980E 04	0.7222E 02	442.62	337.05	0.5739E-02	0.3583E 00	0.1437E 04	9.9098	134514.4
6092.00	0.4498E 04	0.6522E 02	433.55	320.72	0.5290E-02	0.3302E 00	0.1325E 04	9.7098	137795.2
6093.00	0.4053E 04	0.5877E 02	424.48	304.39	0.4867E-02	0.3038E 00	0.1219E 04	9.5098	141076.1
6094.00	0.3644E 04	0.5285E 02	415.41	288.06	0.4470E-02	0.2791E 00	0.1119E 04	9.3098	144356.9
6095.00	0.3269E 04	0.4741E 02	406.36	271.78	0.4098E-02	0.2558E 00	0.1026E 04	9.1098	147637.8
6096.00	0.2926E 04	0.4243E 02	397.30	255.48	0.3750E-02	0.2341E 00	0.9395E 03	8.9098	150918.6
6097.00	0.2612E 04	0.3787E 02	388.26	239.20	0.3425E-02	0.2138E 00	0.8579E 03	8.7098	154199.5
6098.00	0.2325E 04	0.3372E 02	379.22	222.93	0.3121E-02	0.1948E 00	0.7818E 03	8.5098	157480.3
6099.00	0.2065E 04	0.2994E 02	370.19	206.67	0.2837E-02	0.1771E 00	0.7109E 03	8.3098	160761.1
6100.00	0.1828E 04	0.2654E 02	361.16	190.42	0.2574E-02	0.1607E 00	0.6448E 03	8.1098	164042.0
6101.00	0.1613E 04	0.2339E 02	352.13	174.18	0.2329E-02	0.1454E 00	0.5835E 03	7.9098	167322.8
6102.00	0.1419E 04	0.2058E 02	343.12	157.95	0.2102E-02	0.1312E 00	0.5267E 03	7.7098	170603.6
6103.00	0.1244E 04	0.1805E 02	334.11	141.73	0.1892E-02	0.1181E 00	0.4742E 03	7.5098	173884.5
6103.18	0.1215E 04	0.1762E 02	332.49	141.73	0.1866E-02	0.1159E 00	0.4651E 03	7.4739	174474.0
6104.00	0.1087E 04	0.1577E 02	325.83	126.83	0.1695E-02	0.1058E 00	0.4247E 03	7.3262	177165.3
6105.00	0.9474E 03	0.1373E 02	317.72	112.24	0.1513E-02	0.9451E-01	0.3752E 03	7.1462	180446.2
6106.00	0.8222E 03	0.1192E 02	309.62	97.65	0.1347E-02	0.8414E-01	0.3376E 03	6.9662	183727.0
6106.97	0.7141E 03	0.1035E 02	301.77	97.65	0.1200E-02	0.7496E-01	0.3007E 03	6.7917	186908.5
6107.00	0.7109E 03	0.1030E 02	301.55	83.12	0.1196E-02	0.7468E-01	0.2996E 03	6.7868	187007.8
6108.00	0.6124E 03	0.8880E 01	294.34	70.15	0.1055E-02	0.6588E-01	0.2643E 03	6.6268	190288.7
6109.00	0.5256E 03	0.7622E 01	287.14	57.19	0.9283E-03	0.5795E-01	0.2325E 03	6.4668	193569.5
6110.00	0.4495E 03	0.6517E 01	279.94	44.23	0.8138E-03	0.5081E-01	0.2038E 03	6.3068	196850.4
6111.00	0.3828E 03	0.5550E 01	272.75	31.29	0.7111E-03	0.4439E-01	0.1781E 03	6.1468	200131.2
6112.00	0.3246E 03	0.4707E 01	265.57	18.35	0.6192E-03	0.3865E-01	0.1551E 03	5.9868	203412.0
6113.00	0.2740E 03	0.3974E 01	258.38	5.93	0.5371E-03	0.3353E-01	0.1345E 03	5.8268	206692.9
6114.00	0.2302E 03	0.3339E 01	251.21	-7.98	0.4640E-03	0.2897E-01	0.1162E 03	5.6668	209973.7
6114.51	0.2103E 03	0.3050E 01	247.55	-7.48	0.4300E-03	0.2684E-01	0.1077E 03	5.5853	211646.2
6115.00	0.1926E 03	0.2793E 01	246.42	-16.09	0.3955E-03	0.2469E-01	0.9909E 02	5.5607	213254.5
6116.00	0.1607E 03	0.2331E 01	244.13	-20.22	0.3332E-03	0.2080E-01	0.8347E 02	5.5107	216535.4
6117.00	0.1340E 03	0.1943E 01	241.83	-24.35	0.2802E-03	0.1749E-01	0.7019E 02	5.4607	219816.2
6118.00	0.1114E 03	0.1616E 01	239.54	-28.58	0.2325E-03	0.1468E-01	0.5894E 02	5.4107	223097.1
6118.21	0.1072E 03	0.1554E 01	239.06	-28.48	0.2267E-03	0.1415E-01	0.5680E 02	5.4002	223782.9
6119.00	0.9263E 02	0.1343E 01	238.65	-30.09	0.1961E-03	0.1224E-01	0.4914E 02	5.3923	226377.9
6120.00	0.7694E 02	0.1115E 01	238.13	-31.02	0.1632E-03	0.1019E-01	0.4089E 02	5.3823	229658.6
6121.00	0.6388E 02	0.9263E 00	237.61	-31.96	0.1357E-03	0.8477E-02	0.3401E 02	5.3723	232939.6
6122.00	0.5302E 02	0.7688E 00	237.09	-32.00	0.1129E-03	0.7049E-02	0.2828E 02	5.3623	236220.5
6123.00	0.4399E 02	0.6379E 00	236.57	-33.83	0.9386E-04	0.5860E-02	0.2351E 02	5.3523	239501.3
6124.00	0.3649E 02	0.5291E 00	236.05	-34.77	0.7800E-04	0.4869E-02	0.1954E 02	5.3423	242782.1
6125.00	0.3025E 02	0.4387E 00	235.53	-35.70	0.6479E-04	0.4045E-02	0.1623E 02	5.3323	246063.0
6126.00	0.2507E 02	0.3636E 00	235.01	-36.63	0.5360E-04	0.3359E-02	0.1347E 02	5.3223	249343.8
6127.00	0.2077E 02	0.3012E 00	234.50	-37.56	0.4466E-04	0.2788E-02	0.1118E 02	5.3123	252624.6
6128.00	0.1721E 02	0.2495E 00	233.98	-38.50	0.3706E-04	0.2314E-02	0.9285E 01	5.3023	255903.5
6128.21	0.1654E 02	0.2398E 00	233.87	-38.50	0.3564E-04	0.2225E-02	0.8928E 01	5.3002	256594.3
6129.00	0.1425E 02	0.2066E 00	233.16	-38.17	0.3066E-04	0.1914E-02	0.7681E 01	5.3081	259186.3
6130.00	0.1180E 02	0.1712E 00	234.52	-37.52	0.2535E-04	0.1582E-02	0.6351E 01	5.3181	262467.2

TABLE A3.- VENUS MODEL ATMOSPHERES, EXTRAPOLATION OF MARINER 5 DATA TO SURFACE, ADIABATIC LAPSE RATE
(CO₂ = 90%, MEAN MOLECULAR WEIGHT = 42.41) - Continued

VENUS MODEL ATMOSPHERES COMPUTED FROM DATA FROM THE OCCULTATIONS OF MARINER V AND REGULUS MEAN MOLECULAR WGT = 42.41 {90.0 PERCENT CARBON DIOXIDE 10.0 PERCENT NITROGEN}									
RADIUS	PRESSURE	TEMPERATURE	MASS DENSITY	REFRACTIVITY	PRESSURE	ALTITUDE			
KM	MILLIBARS	LBS/SQIN	KELVIN	FAHRENHEIT	GM/CUCM	LBS/CUFT	N UNITS	SCALE HT	ABOVE SURF
								KM	FEET
6131.00	0.9785E 01	0.1418E 00	234.89	-36.86	0.2097E-04	0.1309E-02	0.5253E 01	5.3281	265748.0
6132.00	0.8112E 01	0.1176E 00	235.25	-36.21	0.1735E-04	0.1083E-02	0.4347E 01	5.3381	269028.8
6133.00	0.6727E 01	0.9755E-01	235.61	-35.55	0.1436E-04	0.8968E-03	0.3598E 01	5.3481	272309.7
6134.00	0.5581E 01	0.8093E-01	235.98	-34.90	0.1189E-04	0.7426E-03	0.2980E 01	5.3581	275590.5
6135.00	0.4632E 01	0.6716E-01	236.34	-34.24	0.9853E-05	0.6151E-03	0.2468E 01	5.3681	278871.4
6136.00	0.3845E 01	0.5576E-01	236.70	-33.59	0.8165E-05	0.5097E-03	0.2045E 01	5.3781	282152.2
6137.00	0.3193E 01	0.4630E-01	237.07	-32.94	0.6768E-05	0.4225E-03	0.1695E 01	5.3881	285433.1
6138.00	0.2653E 01	0.3847E-01	237.43	-32.28	0.5612E-05	0.3503E-03	0.1405E 01	5.3981	288713.9
6138.21	0.2551E 01	0.3700E-01	237.51	-32.28	0.5396E-05	0.3368E-03	0.1351E 01	5.4002	289402.8
6139.00	0.2204E 01	0.3197E-01	237.79	-31.63	0.4655E-05	0.2906E-03	0.1166E 01	5.4081	291994.7
6140.00	0.1833E 01	0.2657E-01	238.15	-30.98	0.3863E-05	0.2411E-03	0.9677E 00	5.4181	295275.6
6141.00	0.1524E 01	0.2210E-01	238.52	-30.33	0.3206E-05	0.2002E-03	0.8033E 00	5.4281	298556.4
6142.00	0.1268E 01	0.1838E-01	238.88	-29.68	0.2662E-05	0.1662E-03	0.6670E 00	5.4381	301837.3
6143.00	0.1055E 01	0.1530E-01	239.24	-29.03	0.2211E-05	0.1380E-03	0.5540E 00	5.4481	305118.1
6144.00	0.8784E 00	0.1273E-01	239.60	-28.38	0.1837E-05	0.1147E-03	0.4604E 00	5.4581	308399.0
6145.00	0.7315E 00	0.1060E-01	239.96	-27.73	0.1527E-05	0.9537E-04	0.3826E 00	5.4681	311679.8
6146.00	0.6093E 00	0.8835E-02	240.32	-27.08	0.1270E-05	0.7930E-04	0.3182E 00	5.4781	314960.6
6147.00	0.5077E 00	0.7362E-02	240.68	-26.43	0.1056E-05	0.6596E-04	0.2646E 00	5.4881	318241.5
6148.00	0.4232E 00	0.6137E-02	241.04	-25.78	0.8791E-06	0.5488E-04	0.2202E 00	5.4981	321522.3
6149.00	0.3529E 00	0.5117E-02	241.40	-25.13	0.7317E-06	0.4568E-04	0.1832E 00	5.5081	324803.1
6150.00	0.2943E 00	0.4268E-02	241.76	-24.49	0.6092E-06	0.3803E-04	0.1526E 00	5.5181	328084.0
6151.00	0.2456E 00	0.3561E-02	242.12	-23.84	0.5074E-06	0.3167E-04	0.1271E 00	5.5281	331364.8
6152.00	0.2050E 00	0.2972E-02	242.48	-23.19	0.4227E-06	0.2639E-04	0.1059E 00	5.5381	334645.6
6153.00	0.1711E 00	0.2482E-02	242.84	-22.55	0.3523E-06	0.2199E-04	0.8826E-01	5.5481	337926.5
6154.00	0.1429E 00	0.2073E-02	243.20	-21.90	0.2937E-06	0.1833E-04	0.7358E-01	5.5581	341207.3
6155.00	0.1194E 00	0.1732E-02	243.56	-21.26	0.2449E-06	0.1529E-04	0.6136E-01	5.5681	344488.1
6156.00	0.9982E-01	0.1447E-02	243.91	-20.61	0.2043E-06	0.1275E-04	0.5119E-01	5.5781	347769.0
6157.00	0.8346E-01	0.1210E-02	244.27	-19.97	0.1705E-06	0.1064E-04	0.4272E-01	5.5881	351049.8
6158.00	0.6979E-01	0.1012E-02	244.63	-19.32	0.1423E-06	0.8888E-05	0.3566E-01	5.5981	354330.7
6159.00	0.5838E-01	0.8466E-03	244.99	-18.68	0.1188E-06	0.7422E-05	0.2978E-01	5.6081	357611.5
6160.00	0.4885E-01	0.7084E-03	245.34	-18.04	0.9931E-07	0.6200E-05	0.2487E-01	5.6181	360892.4
6161.00	0.4089E-01	0.5930E-03	245.70	-17.39	0.8298E-07	0.5180E-05	0.2078E-01	5.6281	364173.2
6162.00	0.3424E-01	0.4965E-03	246.06	-16.75	0.6936E-07	0.4330E-05	0.1737E-01	5.6381	367454.1
6163.00	0.2868E-01	0.4159E-03	246.41	-16.11	0.5799E-07	0.3620E-05	0.1452E-01	5.6481	370734.9
6164.00	0.2403E-01	0.3484E-03	246.77	-15.47	0.4850E-07	0.3028E-05	0.1215E-01	5.6581	374015.7
6165.00	0.2014E-01	0.2920E-03	247.13	-14.83	0.4058E-07	0.2533E-05	0.1016E-01	5.6681	377296.6
6166.00	0.1688E-01	0.2448E-03	247.48	-14.19	0.3396E-07	0.2120E-05	0.8508E-02	5.6781	380577.4
6166.53	0.1538E-01	0.2231E-03	247.67	-14.19	0.3091E-07	0.1930E-05	0.7744E-02	5.6834	382314.0
6167.00	0.1417E-01	0.2054E-03	250.71	-8.38	0.2812E-07	0.1755E-05	0.7044E-02	5.7540	383858.3
6168.00	0.1193E-01	0.1730E-03	257.16	3.22	0.2308E-07	0.1441E-05	0.5783E-02	5.9040	387139.1
6169.00	0.1009E-01	0.1464E-03	263.61	14.83	0.1904E-07	0.1189E-05	0.4771E-02	6.0540	390420.0
6170.00	0.8577E-02	0.1243E-03	270.05	26.43	0.1578E-07	0.9856E-06	0.3955E-02	6.2040	393700.8
6171.00	0.7314E-02	0.1060E-03	276.49	38.02	0.1314E-07	0.8207E-06	0.3293E-02	6.3540	396981.6
6172.00	0.6261E-02	0.9078E-04	282.93	49.60	0.1099E-07	0.6862E-06	0.2753E-02	6.5040	400262.5
6173.00	0.5378E-02	0.7798E-04	289.36	61.18	0.9230E-08	0.5762E-06	0.2312E-02	6.6540	403543.3
6174.00	0.4635E-02	0.6721E-04	295.79	72.75	0.7779E-08	0.4857E-06	0.1948E-02	6.8040	406824.1

TABLE A3.- VENUS MODEL ATMOSPHERES, EXTRAPOLATION OF MARINER 5 DATA TO SURFACE, ADIABATIC LAPSE RATE
(CO₂ = 90%, MEAN MOLECULAR WEIGHT = 42.41) - Continued

VENUS MODEL ATMOSPHERES COMPUTED FROM DATA FROM THE OCCULTATIONS OF MARINER V AND REGULUS MEAN MOLECULAR WGT = 42.41 (90.0 PERCENT CARBON DIOXIDE 10.0 PERCENT NITROGEN)									
RADIUS	PRESSURE	TEMPERATURE	MASS DENSITY	REFRACTIVITY	PRESSURE	ALTITUDE			
KM	MILLIBARS	LBS/SQIN	KELVIN	FAHRENHEIT	CM/CUCM	LBS/CUFT	N UNITS	SCALE HT KM	ABOVE SURF FEET
6175.00	0.4008E-02	0.5812E-04	302.21	84.31	0.6582E-08	0.4109E-06	0.1648E-02	6.9540	410105.0
6176.00	0.3476E-02	0.5041E-04	308.63	95.86	0.5588E-08	0.3489E-06	0.1400E-02	7.1040	413385.8
6177.00	0.3024E-02	0.4385E-04	315.04	107.41	0.4761E-08	0.2972E-06	0.1192E-02	7.2540	416666.6
6178.00	0.2638E-02	0.3826E-04	321.45	118.95	0.4070E-08	0.2540E-06	0.1019E-02	7.4040	419947.5
6178.63	0.2424E-02	0.3516E-04	325.49	118.95	0.3692E-08	0.2305E-06	0.9251E-03	7.4985	422014.0
6179.00	0.2308E-02	0.3347E-04	327.86	130.48	0.3489E-08	0.2178E-06	0.8742E-03	7.5540	423228.3
6180.00	0.2024E-02	0.2936E-04	334.26	142.00	0.3001E-08	0.1873E-06	0.7519E-03	7.7040	428509.1
6181.00	0.1780E-02	0.2582E-04	340.66	153.52	0.2589E-08	0.1616E-06	0.6485E-03	7.8540	429790.8
6182.00	0.1569E-02	0.2276E-04	347.05	165.03	0.2239E-08	0.1398E-06	0.5610E-03	8.0040	433070.8
6183.00	0.1386E-02	0.2011E-04	353.44	176.53	0.1942E-08	0.1212E-06	0.4865E-03	8.1540	436351.7
6184.00	0.1228E-02	0.1780E-04	359.83	188.03	0.1689E-08	0.1054E-06	0.4231E-03	8.3040	439632.5
6185.00	0.1090E-02	0.1580E-04	366.21	199.51	0.1472E-08	0.9192E-07	0.3688E-03	8.4540	442913.4
6186.00	0.9694E-03	0.1405E-04	372.59	210.99	0.1286E-08	0.8032E-07	0.3223E-03	8.6040	446194.2
6187.00	0.8639E-03	0.1252E-04	378.96	222.46	0.1127E-08	0.7035E-07	0.2823E-03	8.7540	449475.0
6188.00	0.7714E-03	0.1118E-04	385.33	233.93	0.9893E-09	0.6176E-07	0.2478E-03	8.9040	452755.9
6189.00	0.6901E-03	0.1000E-04	391.69	245.38	0.8704E-09	0.5434E-07	0.2180E-03	9.0540	456036.7
6190.00	0.6185E-03	0.8968E-05	398.05	256.83	0.7674E-09	0.4790E-07	0.1922E-03	9.2040	459317.6
6191.00	0.5553E-03	0.8052E-05	404.41	268.27	0.6779E-09	0.4232E-07	0.1698E-03	9.3540	462598.4
6192.00	0.4994E-03	0.7242E-05	410.76	279.71	0.6001E-09	0.3746E-07	0.1503E-03	9.5040	465879.3
6193.00	0.4499E-03	0.6524E-05	417.11	291.14	0.5322E-09	0.3322E-07	0.1333E-03	9.6540	469160.1
6194.00	0.4059E-03	0.5886E-05	423.46	302.55	0.4728E-09	0.2952E-07	0.1184E-03	9.8040	472441.0
6195.00	0.3669E-03	0.5320E-05	429.80	313.97	0.4209E-09	0.2627E-07	0.1054E-03	9.9540	475721.8
6196.00	0.3320E-03	0.4815E-05	436.13	325.37	0.3753E-09	0.2343E-07	0.9402E-04	10.1040	479002.6
6197.00	0.3010E-03	0.4364E-05	442.46	336.77	0.3352E-09	0.2092E-07	0.8397E-04	10.2540	482283.5
6198.00	0.2732E-03	0.3961E-05	448.79	348.16	0.2999E-09	0.1872E-07	0.7512E-04	10.4040	485564.3
6199.00	0.2483E-03	0.3601E-05	455.12	359.54	0.2687E-09	0.1677E-07	0.6731E-04	10.5540	488845.1
6200.00	0.2260E-03	0.3277E-05	461.43	370.92	0.2411E-09	0.1505E-07	0.6041E-04	10.7040	492126.0
6201.00	0.2060E-03	0.2987E-05	467.75	382.28	0.2167E-09	0.1353E-07	0.5430E-04	10.8540	495406.8
6202.00	0.1869E-03	0.2726E-05	474.06	393.64	0.1951E-09	0.1218E-07	0.4887E-04	11.0040	498687.6
6203.00	0.1717E-03	0.2490E-05	480.37	405.00	0.1758E-09	0.1098E-07	0.4405E-04	11.1540	501968.5
6204.00	0.1571E-03	0.2278E-05	486.67	416.34	0.1587E-09	0.9911E-08	0.3977E-04	11.3040	505249.3
6205.00	0.1439E-03	0.2087E-05	492.97	427.68	0.1434E-09	0.8958E-08	0.3594E-04	11.4540	508530.1
6206.00	0.1319E-03	0.1913E-05	499.27	439.01	0.1298E-09	0.8108E-08	0.3253E-04	11.6040	511811.0
6207.00	0.1211E-03	0.1756E-05	505.56	450.34	0.1176E-09	0.7347E-08	0.2948E-04	11.7540	515091.8
6208.00	0.1113E-03	0.1614E-05	511.84	461.65	0.1067E-09	0.6667E-08	0.2675E-04	11.9040	518372.7
6209.00	0.1024E-03	0.1484E-05	518.13	472.96	0.9701E-10	0.6056E-08	0.2430E-04	12.0540	521653.5
6210.00	0.9430E-04	0.1367E-05	524.40	484.26	0.8824E-10	0.5508E-08	0.2210E-04	12.2040	524934.5
6211.00	0.8692E-04	0.1260E-05	530.68	495.56	0.8035E-10	0.5016E-08	0.2012E-04	12.3540	528215.2
6212.00	0.8020E-04	0.1163E-05	536.95	506.84	0.7325E-10	0.4573E-08	0.1834E-04	12.5040	531496.1
6213.00	0.7407E-04	0.1074E-05	543.22	518.12	0.6685E-10	0.4173E-08	0.1674E-04	12.6540	534777.0
6214.00	0.6848E-04	0.9929E-06	549.48	529.40	0.6107E-10	0.3813E-08	0.1530E-04	12.8040	538057.7
6215.00	0.6335E-04	0.9187E-06	555.74	540.66	0.5585E-10	0.3487E-08	0.1399E-04	12.9540	541338.6
6216.00	0.5868E-04	0.8509E-06	561.99	551.92	0.5114E-10	0.3192E-08	0.1281E-04	13.1040	544619.5
6217.00	0.5439E-04	0.7887E-06	568.24	563.17	0.4686E-10	0.2925E-08	0.1174E-04	13.2540	547900.3
6218.00	0.5046E-04	0.7317E-06	574.49	574.41	0.4299E-10	0.2684E-08	0.1076E-04	13.4040	551181.1
6219.00	0.4685E-04	0.6794E-06	580.73	585.65	0.3947E-10	0.2464E-08	0.9889E-05	13.5540	554462.0

TABLE A3.- VENUS MODEL ATMOSPHERES, EXTRAPOLATION OF MARINER 5 DATA TO SURFACE, ADIABATIC LAPSE RATE
(CO₂ = 90%, MEAN MOLECULAR WEIGHT = 42.41) - Concluded

VENUS MODEL ATMOSPHERES COMPUTED FROM DATA FROM THE OCCULTATIONS OF MARINER V AND REGULUS MEAN MOLECULAR WGT = 42.41 (90.0 PERCENT CARBON DIOXIDE 10.0 PERCENT NITROGEN)									
RADIUS	PRESSURE		TEMPERATURE		MASS DENSITY		REFRACTIVITY	PRESSURE	ALTITUDE
KM	MILLIBARS	LBS/SQIN	KELVIN	FAHRENHEIT	GM/CUCM	LBS/CUFT	N UNITS	SCALE HT	ABOVE SURF
								KM	FEET
6220.00	0.4354E-04	0.6313E-06	586.97	596.88	0.3628E-10	0.2265E-08	0.3089E-05	13.7040	557742.8
6221.00	0.4049E-04	0.5871E-06	593.20	608.10	0.3337E-10	0.2083E-08	0.3361E-05	13.8540	561023.6
6222.00	0.3768E-04	0.5464E-06	599.43	619.31	0.3073E-10	0.1918E-08	0.3698E-05	14.0040	564304.5
6223.00	0.3510E-04	0.5090E-06	605.66	630.52	0.2832E-10	0.1768E-08	0.4094E-05	14.1540	567585.3
6224.00	0.3272E-04	0.4744E-06	611.88	641.72	0.2612E-10	0.1630E-08	0.4543E-05	14.3040	570866.2
6225.00	0.3052E-04	0.4425E-06	618.10	652.91	0.2411E-10	0.1508E-08	0.5040E-05	14.4540	574147.0
6226.00	0.2849E-04	0.4131E-06	624.31	664.09	0.2227E-10	0.1390E-08	0.5581E-05	14.6040	577427.8
6227.00	0.2661E-04	0.3859E-06	630.52	675.27	0.2060E-10	0.1286E-08	0.6160E-05	14.7540	580708.7
6228.00	0.2488E-04	0.3607E-06	636.73	686.44	0.1906E-10	0.1190E-08	0.6775E-05	14.9040	583989.5
6229.00	0.2327E-04	0.3374E-06	642.93	697.61	0.1765E-10	0.1102E-08	0.7422E-05	15.0540	587270.3
6230.00	0.2178E-04	0.3158E-06	649.13	708.76	0.1636E-10	0.1021E-08	0.8098E-05	15.2040	590551.2
6231.00	0.2040E-04	0.2958E-06	655.32	719.91	0.1517E-10	0.9474E-09	0.8801E-05	15.3540	593832.1
6232.00	0.1912E-04	0.2773E-06	661.51	731.05	0.1408E-10	0.8794E-09	0.9528E-05	15.5040	597112.8
6233.00	0.1793E-04	0.2600E-06	667.70	742.19	0.1308E-10	0.8168E-09	0.1027E-05	15.6540	600393.7
6234.00	0.1683E-04	0.2440E-06	673.88	753.31	0.1216E-10	0.7592E-09	0.1104E-05	15.8040	603674.6
6235.00	0.1580E-04	0.2291E-06	680.06	764.43	0.1131E-10	0.7061E-09	0.1183E-05	15.9540	606955.3
6236.00	0.1484E-04	0.2152E-06	686.23	775.55	0.1052E-10	0.6573E-09	0.1263E-05	16.1040	610236.2
6237.00	0.1395E-04	0.2023E-06	692.40	786.65	0.9806E-11	0.6122E-09	0.1345E-05	16.2540	613517.1
6238.00	0.1312E-04	0.1903E-06	698.56	797.75	0.9139E-11	0.5708E-09	0.1428E-05	16.4040	616798.0
6239.00	0.1235E-04	0.1791E-06	704.73	808.84	0.8523E-11	0.5321E-09	0.1513E-05	16.5540	620078.7
6240.00	0.1163E-04	0.1686E-06	710.88	819.93	0.7953E-11	0.4965E-09	0.1599E-05	16.7040	623359.6
6241.00	0.1096E-04	0.1589E-06	717.04	831.00	0.7426E-11	0.4638E-09	0.1680E-05	16.8540	626640.5
6242.00	0.1033E-04	0.1498E-06	723.19	842.07	0.6939E-11	0.4332E-09	0.1738E-05	17.0040	629921.3
6243.00	0.9744E-05	0.1413E-06	729.33	853.14	0.6487E-11	0.4050E-09	0.1625E-05	17.1540	633202.1
6244.00	0.9195E-05	0.1333E-06	735.48	864.19	0.6068E-11	0.3783E-09	0.1520E-05	17.3040	636483.0
6245.00	0.8681E-05	0.1258E-06	741.61	875.24	0.5679E-11	0.3545E-09	0.1422E-05	17.4540	639763.8
6246.00	0.8199E-05	0.1188E-06	747.75	886.28	0.5319E-11	0.3320E-09	0.1332E-05	17.6040	643044.6
6247.00	0.7748E-05	0.1123E-06	753.88	897.31	0.4984E-11	0.3111E-09	0.1248E-05	17.7540	646325.5
6248.00	0.7326E-05	0.1062E-06	760.00	908.34	0.4672E-11	0.2917E-09	0.1170E-05	17.9040	649606.3
6249.00	0.6929E-05	0.1004E-06	766.13	919.36	0.4383E-11	0.2736E-09	0.1098E-05	18.0540	652887.2
6250.00	0.6558E-05	0.9509E-07	772.24	930.37	0.4113E-11	0.2568E-09	0.1030E-05	18.2040	656168.0
6250.00	0.6558E-05	0.9509E-07	772.24	930.37	0.4113E-11	0.2568E-09	0.1030E-05	18.2040	656168.0

APPENDIX A

TABLE A4.- VENUS MODEL ATMOSPHERES, EXTRAPOLATION OF MARINER 5 DATA TO SURFACE, ADIABATIC LAPSE RATE
(CO₂ = 85%, MEAN MOLECULAR WEIGHT = 41.61)

18 MARCH 68

RADIUS KM	ALTITUDE		PRESSURE		TEMPERATURE		MASS DENSITY		PRESSURE SCALE SCALE HT. KM	TEMPERATURE SCALE HT. KM/KM	SPECIFIC HEAT (CP/R)	
	FEET	KM	MILLIBARS	LBS/SQIN	KELVIN	FAHRENHEIT	GM/CUCM	LBS/CUFT				
6091.0	41.0	134514.4	0.4726E 04 (4.66 ATM)	0.6852E 02	429.90	314.14	0.5501E-02	0.3434E 00	9.809	-0.2037	-8.9280	4.9085
6090.0	40.0	131233.6	0.5227E 04 (5.15 ATM)	0.7580E 02	438.83	330.22	0.5962E-02	0.3722E 00	10.013	-0.2023	-8.8700	4.9422
6089.0	39.0	127952.7	0.5770E 04 (5.69 ATM)	0.8367E 02	447.70	346.19	0.6451E-02	0.4027E 00	10.215	-0.2010	-8.8147	4.9748
6088.0	38.0	124671.9	0.6358E 04 (6.27 ATM)	0.9219E 02	456.52	362.06	0.6970E-02	0.4351E 00	10.416	-0.1997	-8.7611	5.0069
6087.0	37.0	121391.0	0.6992E 04 (6.90 ATM)	0.1013E 03	465.28	377.84	0.7521E-02	0.4695E 00	10.616	-0.1984	-8.7096	5.0382
6086.0	36.0	118110.2	0.7676E 04 (7.57 ATM)	0.1113E 03	473.99	393.52	0.8105E-02	0.5060E 00	10.815	-0.1972	-8.6591	5.0692
6085.0	35.0	114829.4	0.8413E 04 (8.30 ATM)	0.1219E 03	482.65	409.11	0.8723E-02	0.5446E 00	11.012	-0.1960	-8.6099	5.0999
6084.0	34.0	111548.5	0.9205E 04 (9.08 ATM)	0.1334E 03	491.27	424.62	0.9378E-02	0.5854E 00	11.208	-0.1949	-8.5625	5.1298
6083.0	33.0	108267.7	0.1005E 05 (9.92 ATM)	0.1458E 03	499.83	440.03	0.1006E-01	0.6286E 00	11.403	-0.1938	-8.5165	5.1592
6082.0	32.0	104986.8	0.1097E 05 (10.82 ATM)	0.1590E 03	508.35	455.37	0.1080E-01	0.6742E 00	11.597	-0.1927	-8.4718	5.1881
6081.0	31.0	101706.0	0.1195E 05 (11.79 ATM)	0.1732E 03	516.83	470.62	0.1157E-01	0.7224E 00	11.789	-0.1916	-8.4277	5.2170
6080.0	30.0	98425.2	0.1299E 05 (12.82 ATM)	0.1884E 03	525.26	485.80	0.1238E-01	0.7732E 00	11.981	-0.1906	-8.3847	5.2455
6079.0	29.0	95144.3	0.1412E 05 (13.93 ATM)	0.2047E 03	533.64	500.89	0.1324E-01	0.8267E 00	12.172	-0.1896	-8.3428	5.2735
6078.0	28.0	91863.5	0.1532E 05 (15.12 ATM)	0.2221E 03	541.99	515.92	0.1414E-01	0.8832E 00	12.361	-0.1886	-8.3020	5.3012
6077.0	27.0	88582.6	0.1660E 05 (16.38 ATM)	0.2407E 03	550.29	530.86	0.1509E-01	0.9425E 00	12.550	-0.1876	-8.2626	5.3282
6076.0	26.0	85301.8	0.1796E 05 (17.73 ATM)	0.2605E 03	558.56	545.74	0.1609E-01	0.1005E 01	12.738	-0.1867	-8.2241	5.3549
6075.0	25.0	82021.0	0.1942E 05 (19.16 ATM)	0.2816E 03	566.79	560.55	0.1715E-01	0.1070E 01	12.924	-0.1858	-8.1869	5.3810
6074.0	24.0	78740.1	0.2097E 05 (20.70 ATM)	0.3041E 03	574.98	575.29	0.1825E-01	0.1139E 01	13.110	-0.1849	-8.1504	5.4069
6073.0	23.0	75459.3	0.2262E 05 (22.32 ATM)	0.3280E 03	583.13	589.97	0.1941E-01	0.1212E 01	13.295	-0.1840	-8.1148	5.4324
6072.0	22.0	72178.4	0.2437E 05 (24.06 ATM)	0.3535E 03	591.25	604.58	0.2063E-01	0.1288E 01	13.479	-0.1832	-8.0801	5.4575
6071.0	21.0	68897.6	0.2624E 05 (25.90 ATM)	0.3805E 03	599.33	619.13	0.2191E-01	0.1368E 01	13.663	-0.1823	-8.0460	5.4825
6070.0	20.0	65616.8	0.2822E 05 (27.85 ATM)	0.4092E 03	607.38	633.62	0.2325E-01	0.1451E 01	13.845	-0.1815	-8.0122	5.5074
6069.0	19.0	62335.9	0.3032E 05 (29.92 ATM)	0.4396E 03	615.39	648.04	0.2466E-01	0.1539E 01	14.027	-0.1807	-7.9790	5.5321

TABLE A4.- VENUS MODEL ATMOSPHERES, EXTRAPOLATION OF MARINER 5 DATA TO SURFACE, ADIABATIC LAPSE RATE
(CO₂ = 85%, MEAN MOLECULAR WEIGHT = 41.61) - Continued

VENUS MODEL ATMOSPHERES, EXTRAPOLATION OF MARINER 5 DATA TO SURFACE, ADIABATIC LAPSE RATE. PERCENT CO2 = 85.00, MEAN MOLECULAR WT = 41.61													18 MARCH 68
RADIUS	ALTITUDE	PRESSURE	TEMPERATURE	MASS DENSITY	PRESSURE	SCALE HT	TEMPERATURE	SPECIFIC					
KM	KM	FEET	MILLIBARS	LBS/SQIN	KELVIN	FAHRENHEIT	GM/CUCM	LBS/CUFT	KM	SCALE HT	DEG K/KM	HEAT	
6068.0	18.0	59055.1	0.3254E 05	0.4719E 03	623.38	662.41	0.2613E-01	0.1631E 01	14.207	-0.1799	-7.9467	5.5564	
		(32.12 ATM)											
6067.0	17.0	55774.2	0.3490E 05	0.5061E 03	631.32	676.72	0.2767E-01	0.1727E 01	14.387	-0.1792	-7.9154	5.5803	
		(34.45 ATM)											
6066.0	16.0	52493.4	0.3740E 05	0.5423E 03	639.24	690.97	0.2928E-01	0.1828E 01	14.566	-0.1784	-7.8846	5.6039	
		(36.91 ATM)											
6065.0	15.0	49212.6	0.4004E 05	0.5806E 03	647.13	705.17	0.3096E-01	0.1933E 01	14.745	-0.1777	-7.8544	5.6274	
		(39.52 ATM)											
6064.0	14.0	45931.7	0.4283E 05	0.6211E 03	654.99	719.31	0.3273E-01	0.2043E 01	14.923	-0.1769	-7.8241	5.6510	
		(42.27 ATM)											
6063.0	13.0	42650.9	0.4578E 05	0.6639E 03	662.81	733.40	0.3457E-01	0.2158E 01	15.100	-0.1762	-7.7942	5.6746	
		(45.18 ATM)											
6062.0	12.0	39370.0	0.4890E 05	0.7090E 03	670.61	747.43	0.3649E-01	0.2278E 01	15.276	-0.1755	-7.7648	5.6979	
		(48.26 ATM)											
6061.0	11.0	36089.2	0.5219E 05	0.7567E 03	678.38	761.41	0.3850E-01	0.2403E 01	15.451	-0.1747	-7.7359	5.7211	
		(51.50 ATM)											
6060.0	10.0	32808.4	0.5566E 05	0.8070E 03	686.12	775.34	0.4060E-01	0.2534E 01	15.626	-0.1740	-7.7076	5.7439	
		(54.93 ATM)											
6059.0	9.0	29527.5	0.5931E 05	0.8601E 03	693.83	789.22	0.4278E-01	0.2671E 01	15.800	-0.1734	-7.6798	5.7667	
		(58.54 ATM)											
6058.0	8.0	26246.7	0.6317E 05	0.9159E 03	701.51	803.05	0.4506E-01	0.2813E 01	15.974	-0.1727	-7.6525	5.7892	
		(62.34 ATM)											
6057.0	7.0	22965.8	0.6723E 05	0.9748E 03	709.16	816.83	0.4744E-01	0.2962E 01	16.146	-0.1720	-7.6259	5.8112	
		(66.35 ATM)											
6056.0	6.0	19685.0	0.7150E 05	0.1036E 04	716.79	830.56	0.4992E-01	0.3116E 01	16.318	-0.1714	-7.5998	5.8331	
		(70.56 ATM)											
6055.0	5.0	16404.2	0.7599E 05	0.1101E 04	724.39	844.24	0.5250E-01	0.3277E 01	16.490	-0.1707	-7.5735	5.8553	
		(75.00 ATM)											
6054.0	4.0	13123.3	0.8072E 05	0.1170E 04	731.97	857.88	0.5519E-01	0.3445E 01	16.661	-0.1701	-7.5476	5.8774	
		(79.66 ATM)											
6053.0	3.0	9842.5	0.8568E 05	0.1242E 04	739.52	871.47	0.5799E-01	0.3620E 01	16.831	-0.1695	-7.5222	5.8991	
		(84.56 ATM)											
6052.0	2.0	6561.6	0.9090E 05	0.1318E 04	747.04	885.01	0.6090E-01	0.3802E 01	17.000	-0.1689	-7.4976	5.9205	
		(89.71 ATM)											
6051.0	1.0	3280.8	0.9638E 05	0.1397E 04	754.54	898.51	0.6393E-01	0.3991E 01	17.169	-0.1683	-7.4734	5.9416	
		(95.12 ATM)											
6050.0	0.0	0.0	0.1021E 06	0.1481E 04	762.02	911.97	0.6708E-01	0.4187E 01	17.337				

TABLE A4.- VENUS MODEL ATMOSPHERES, EXTRAPOLATION OF MARINER 5 DATA TO SURFACE, ADIABATIC LAPSE RATE
(CO₂ = 85%, MEAN MOLECULAR WEIGHT = 41.61) - Continued

18 MARCH 1968

VENUS MODEL ATMOSPHERES COMPUTED FROM DATA FROM THE OCCULTATIONS OF MARINER V AND REGULUS
MEAN MOLECULAR WEIGHT = 41.61 (85.0 PERCENT CARBON DIOXIDE 15.0 PERCENT NITROGEN)

RADIUS KM	PRESSURE		TEMPERATURE		MASS DENSITY		REFRACTIVITY N UNITS	PRESSURE SCALE HT KM	ALTITUDE ABOVE SURF FEET
	MILLIBARS	LBS/SQIN	KELVIN	FAHRENHEIT	GM/CM ³	LBS/CUFT			
6090.78	0.4833E 04	0.7008E 02	431.86	317.69	0.5601E-02	0.3496E 00	0.1400E 04	9.8540	133790.3
6091.00	0.4726E 04	0.6853E 02	429.90	314.15	0.5501E-02	0.3434E 00	0.1375E 04	9.8098	134514.4
6092.00	0.4263E 04	0.6182E 02	420.99	298.12	0.5066E-02	0.3163E 00	0.1266E 04	9.6098	137795.2
6093.00	0.3838E 04	0.5565E 02	412.10	282.11	0.4657E-02	0.2907E 00	0.1164E 04	9.4098	141076.1
6094.00	0.3447E 04	0.4998E 02	403.20	266.10	0.4274E-02	0.2668E 00	0.1068E 04	9.2098	144356.9
6095.00	0.3088E 04	0.4478E 02	394.32	250.11	0.3914E-02	0.2444E 00	0.9784E 03	9.0098	147637.8
6096.00	0.2760E 04	0.4003E 02	385.44	234.13	0.3578E-02	0.2234E 00	0.8944E 03	8.8098	150918.6
6097.00	0.2461E 04	0.3569E 02	376.57	218.15	0.3264E-02	0.2038E 00	0.8159E 03	8.6098	154199.5
6098.00	0.2188E 04	0.3173E 02	367.70	202.19	0.2971E-02	0.1855E 00	0.7427E 03	8.4098	157480.3
6099.00	0.1940E 04	0.2813E 02	358.84	186.24	0.2698E-02	0.1684E 00	0.6745E 03	8.2098	160761.1
6100.00	0.1715E 04	0.2487E 02	349.98	170.30	0.2445E-02	0.1526E 00	0.6111E 03	8.0098	164042.0
6101.00	0.1511E 04	0.2191E 02	341.13	154.37	0.2210E-02	0.1379E 00	0.5523E 03	7.8098	167322.8
6102.00	0.1327E 04	0.1925E 02	332.28	138.44	0.1992E-02	0.1243E 00	0.4979E 03	7.6098	170603.6
6103.00	0.1162E 04	0.1685E 02	323.44	122.53	0.1790E-02	0.1118E 00	0.4476E 03	7.4098	173884.5
6103.18	0.1134E 04	0.1644E 02	321.86	122.53	0.1756E-02	0.1096E 00	0.4390E 03	7.3739	174474.0
6104.00	0.1013E 04	0.1469E 02	315.33	107.92	0.1601E-02	0.1000E 00	0.4003E 03	7.2262	177165.3
6105.00	0.8811E 03	0.1277E 02	307.37	93.60	0.1427E-02	0.8914E-01	0.3568E 03	7.0462	180446.2
6106.00	0.7631E 03	0.1106E 02	299.42	79.29	0.1269E-02	0.7923E-01	0.3172E 03	6.8662	183727.0
6106.97	0.6614E 03	0.9593E 01	291.72	79.29	0.1128E-02	0.7046E-01	0.2821E 03	6.6917	186908.5
6108.00	0.5884E 03	0.8205E 01	284.43	65.04	0.1124E-02	0.7019E-01	0.2810E 03	6.6868	187007.8
6108.00	0.5659E 03	0.8205E 01	284.43	52.32	0.9901E-03	0.6181E-01	0.2474E 03	6.5268	190288.7
6109.00	0.4846E 03	0.7026E 01	277.37	39.60	0.8691E-03	0.5426E-01	0.2172E 03	6.3668	193589.5
6110.00	0.4133E 03	0.5993E 01	270.51	26.90	0.7604E-03	0.4747E-01	0.1900E 03	6.2068	196850.4
6111.00	0.3510E 03	0.5090E 01	263.26	14.20	0.6630E-03	0.4139E-01	0.1657E 03	6.0468	200131.2
6112.00	0.2969E 03	0.4305E 01	256.21	1.51	0.5759E-03	0.3595E-01	0.1439E 03	5.8868	203412.0
6113.00	0.2499E 03	0.3624E 01	249.16	-11.16	0.4983E-03	0.3111E-01	0.1245E 03	5.7268	206692.9
6114.00	0.2093E 03	0.3035E 01	242.12	-23.84	0.4295E-03	0.2681E-01	0.1073E 03	5.5668	209973.7
6114.51	0.1909E 03	0.2768E 01	238.53	-23.84	0.3974E-03	0.2481E-01	0.9934E 02	5.4853	211646.2
6115.00	0.1745E 03	0.2530E 01	236.85	-33.32	0.3659E-03	0.2284E-01	0.9145E 02	5.4475	213254.5
6116.00	0.1450E 03	0.2103E 01	233.42	-39.49	0.3085E-03	0.1926E-01	0.7710E 02	5.3703	216535.4
6117.00	0.1202E 03	0.1743E 01	230.00	-45.66	0.2594E-03	0.1619E-01	0.6485E 02	5.2932	219816.2
6118.00	0.9942E 02	0.1441E 01	226.57	-51.83	0.2176E-03	0.1358E-01	0.5440E 02	5.2161	223097.1
6118.21	0.9550E 02	0.1384E 01	225.85	-51.83	0.2097E-03	0.1309E-01	0.5409E 02	5.1999	223785.9
6119.00	0.8202E 02	0.1189E 01	225.45	-53.84	0.1804E-03	0.1126E-01	0.4509E 02	5.1920	226377.9
6120.00	0.6764E 02	0.9808E 00	224.94	-54.76	0.1490E-03	0.9306E-02	0.3725E 02	5.1820	229658.8
6121.00	0.5576E 02	0.8085E 00	224.44	-55.67	0.1231E-03	0.7686E-02	0.3077E 02	5.1720	232939.6
6122.00	0.4595E 02	0.6663E 00	223.93	-56.58	0.1016E-03	0.6346E-02	0.2540E 02	5.1620	236220.5
6123.00	0.3785E 02	0.5488E 00	223.42	-57.49	0.8389E-04	0.5237E-02	0.2096E 02	5.1520	239501.3
6124.00	0.3116E 02	0.4519E 00	222.92	-58.41	0.6921E-04	0.4321E-02	0.1730E 02	5.1420	242782.1
6125.00	0.2565E 02	0.3719E 00	222.41	-59.32	0.5708E-04	0.3563E-02	0.1426E 02	5.1320	246063.0
6126.00	0.2110E 02	0.3060E 00	221.90	-60.23	0.4706E-04	0.2938E-02	0.1176E 02	5.1220	249343.8
6127.00	0.1736E 02	0.2517E 00	221.40	-61.14	0.3878E-04	0.2421E-02	0.9893E 01	5.1120	252624.6
6128.00	0.1427E 02	0.2069E 00	220.89	-62.05	0.3194E-04	0.1994E-02	0.7585E 01	5.1020	255905.5
6128.21	0.1369E 02	0.1986E 00	220.79	-62.05	0.3067E-04	0.1914E-02	0.7666E 01	5.0999	256594.3
6129.00	0.1173E 02	0.1701E 00	221.07	-61.72	0.2623E-04	0.1637E-02	0.6556E 01	5.1078	259186.3
6130.00	0.9650E 01	0.1399E 00	221.43	-61.08	0.2153E-04	0.1344E-02	0.5381E 01	5.1178	262467.2

TABLE A4.- VENUS MODEL ATMOSPHERES, EXTRAPOLATION OF MARINER 5 DATA TO SURFACE, ADIABATIC LAPSE RATE
(CO₂ = 85%, MEAN MOLECULAR WEIGHT = 41.61) - Continued

VENUS MODEL ATMOSPHERES COMPUTED FROM DATA FROM THE OCCULTATIONS OF MARINER V AND REGULUS MEAN MOLECULAR WGT = 41.61 (85.0 PERCENT CARBON DIOXIDE 15.0 PERCENT NITROGEN)									
RADIUS	PRESSURE		TEMPERATURE		MASS DENSITY		REFRACTIVITY	PRESSURE	ALTITUDE
KM	MILLIBARS	LBS/SQIN	KELVIN	FAHRENHEIT	GM/CUCM	LBS/CUFT	N UNITS	SCALE HT	ABOVE SURF
								KM	FEET
6131.00	0.7938E-01	0.1151E-00	221.79	-60.43	0.1767E-04	0.1103E-02	0.4418E-01	5.1278	265748.0
6132.00	0.6533E-01	0.9473E-01	222.15	-59.78	0.1452E-04	0.9065E-03	0.3629E-01	5.1378	269028.8
6133.00	0.5378E-01	0.7799E-01	222.51	-59.13	0.1193E-04	0.7449E-03	0.2982E-01	5.1478	272309.7
6134.00	0.4430E-01	0.6423E-01	222.87	-58.48	0.9808E-05	0.6123E-03	0.2451E-01	5.1578	275590.5
6135.00	0.3650E-01	0.5292E-01	223.23	-57.84	0.8055E-05	0.5035E-03	0.2015E-01	5.1678	278871.4
6136.00	0.3008E-01	0.4362E-01	223.59	-57.19	0.6634E-05	0.4142E-03	0.1658E-01	5.1778	282152.2
6137.00	0.2480E-01	0.3596E-01	223.95	-56.55	0.5480E-05	0.3408E-03	0.1384E-01	5.1878	285433.1
6138.00	0.2046E-01	0.2966E-01	224.31	-55.90	0.4495E-05	0.2806E-03	0.1123E-01	5.1978	288713.9
6138.21	0.1965E-01	0.2849E-01	224.38	-55.90	0.4315E-05	0.2694E-03	0.1078E-01	5.1999	289402.8
6139.00	0.1688E-01	0.2448E-01	224.67	-55.25	0.3702E-05	0.2311E-03	0.9252E-02	5.2078	291994.7
6140.00	0.1393E-01	0.2020E-01	225.03	-54.61	0.3050E-05	0.1904E-03	0.7623E-02	5.2178	295275.6
6141.00	0.1150E-01	0.1668E-01	225.38	-53.97	0.2513E-05	0.1569E-03	0.6282E-02	5.2278	298556.4
6142.00	0.9505E-02	0.1378E-01	225.74	-53.32	0.2072E-05	0.1293E-03	0.5179E-02	5.2378	301837.3
6143.00	0.7855E-02	0.1139E-01	226.10	-52.68	0.1709E-05	0.1067E-03	0.4272E-02	5.2478	305118.1
6144.00	0.6493E-02	0.9415E-02	226.46	-52.04	0.1410E-05	0.8804E-04	0.3524E-02	5.2578	308399.0
6145.00	0.5369E-02	0.7786E-02	226.81	-51.39	0.1164E-05	0.7267E-04	0.2909E-02	5.2678	311679.8
6146.00	0.4442E-02	0.6441E-02	227.17	-50.75	0.9611E-06	0.6000E-04	0.2402E-02	5.2778	314960.6
6147.00	0.3676E-02	0.5330E-02	227.53	-50.11	0.7938E-06	0.4956E-04	0.1984E-02	5.2878	318241.5
6148.00	0.3043E-02	0.4441E-02	227.88	-49.47	0.6559E-06	0.4095E-04	0.1639E-02	5.2978	321522.3
6149.00	0.2520E-02	0.3654E-02	228.24	-48.83	0.5422E-06	0.3385E-04	0.1355E-02	5.3078	324803.1
6150.00	0.2087E-02	0.3027E-02	228.59	-48.19	0.4483E-06	0.2799E-04	0.1120E-02	5.3178	328084.0
6151.00	0.1730E-02	0.2508E-02	228.95	-47.55	0.3708E-06	0.2315E-04	0.9268E-03	5.3278	331364.8
6152.00	0.1434E-02	0.2079E-02	229.30	-46.91	0.3068E-06	0.1915E-04	0.7669E-03	5.3378	334645.6
6153.00	0.1189E-02	0.1724E-02	229.66	-46.27	0.2540E-06	0.1585E-04	0.6308E-03	5.3478	337926.5
6154.00	0.9868E-03	0.1430E-02	230.01	-45.63	0.2103E-06	0.1313E-04	0.5257E-03	5.3578	341207.3
6155.00	0.8189E-03	0.1187E-02	230.37	-44.99	0.1742E-06	0.1087E-04	0.4354E-03	5.3678	344488.1
6156.00	0.6798E-03	0.9858E-03	230.72	-44.36	0.1443E-06	0.9012E-05	0.3608E-03	5.3778	347769.0
6157.00	0.5646E-03	0.8187E-03	231.08	-43.72	0.1196E-06	0.7471E-05	0.2991E-03	5.3878	351049.8
6158.00	0.4690E-03	0.6801E-03	231.43	-43.08	0.9923E-07	0.6195E-05	0.2480E-03	5.3978	354330.7
6159.00	0.3898E-03	0.5652E-03	231.78	-42.45	0.8231E-07	0.5138E-05	0.2057E-03	5.4078	357611.5
6160.00	0.3240E-03	0.4698E-03	232.14	-41.81	0.6830E-07	0.4264E-05	0.1707E-03	5.4178	360892.4
6161.00	0.2694E-03	0.3907E-03	232.49	-41.18	0.5659E-07	0.3539E-05	0.1417E-03	5.4278	364173.2
6162.00	0.2241E-03	0.3250E-03	232.84	-40.54	0.4707E-07	0.2939E-05	0.1176E-03	5.4378	367454.1
6163.00	0.1865E-03	0.2705E-03	233.19	-39.91	0.3910E-07	0.2441E-05	0.9773E-04	5.4478	370734.9
6164.00	0.1552E-03	0.2251E-03	233.55	-39.27	0.3249E-07	0.2028E-05	0.8120E-04	5.4578	374015.7
6165.00	0.1293E-03	0.1875E-03	233.90	-38.64	0.2700E-07	0.1686E-05	0.6750E-04	5.4678	377296.6
6166.00	0.1077E-03	0.1561E-03	234.25	-38.01	0.2245E-07	0.1401E-05	0.5612E-04	5.4778	380577.4
6166.13	0.1051E-03	0.1525E-03	234.30	-38.01	0.2192E-07	0.1368E-05	0.5479E-04	5.4791	381003.5
6167.00	0.8986E-02	0.1303E-03	237.95	-31.35	0.1843E-07	0.1150E-05	0.4607E-04	5.5661	383858.3
6168.00	0.7520E-02	0.1090E-03	242.15	-23.79	0.1515E-07	0.9462E-06	0.3788E-04	5.6661	387139.1
6169.00	0.6313E-02	0.9154E-04	246.34	-16.24	0.1250E-07	0.7805E-06	0.3125E-04	5.7661	390420.0
6170.00	0.5316E-02	0.7708E-04	250.53	-8.70	0.1034E-07	0.6460E-06	0.2586E-04	5.8661	393700.8
6171.00	0.4489E-02	0.6509E-04	254.72	-1.16	0.8592E-08	0.5364E-06	0.2147E-04	5.9661	396981.6
6172.00	0.3801E-02	0.5512E-04	258.90	6.36	0.7157E-08	0.4468E-06	0.1788E-04	6.0661	400262.5
6173.00	0.3228E-02	0.4681E-04	263.09	13.89	0.5978E-08	0.3732E-06	0.1494E-04	6.1661	403543.3
6174.00	0.2748E-02	0.3985E-04	267.27	21.42	0.5009E-08	0.3127E-06	0.1251E-04	6.2661	406824.1

TABLE A4.- VENUS MODEL ATMOSPHERES, EXTRAPOLATION OF MARINER 5 DATA TO SURFACE, ADIABATIC LAPSE RATE
(CO₂ = 85%, MEAN MOLECULAR WEIGHT = 41.61) - Continued

VENUS MODEL ATMOSPHERES COMPUTED FROM DATA FROM THE OCCULTATIONS OF MARINER V AND REGULUS
MEAN MOLECULAR WGT = 41.61 (85.0 PERCENT CARBON DIOXIDE 15.0 PERCENT NITROGEN)

RADIUS	PRESSURE	TEMPERATURE	MASS DENSITY	REFRACTIVITY	PRESSURE	ALTITUDE
KM	MILLIBARS	KELVIN	GRAMS/CUBIC CM	N UNITS	SCALE HT KM	ABOVE SURF FEET
6175.00	0.2346E-02	271.44	0.4208E-08	0.1051E-02	6.3661	410105.0
6176.00	0.2200E-02	275.62	0.3545E-08	0.8861E-03	6.4661	413385.8
6176.34	0.1905E-02	277.04	0.3346E-08	0.8364E-03	6.5001	414500.8
6177.00	0.1721E-02	279.79	0.2994E-08	0.7484E-03	6.5661	416666.6
6178.00	0.1480E-02	283.96	0.2536E-08	0.6538E-03	6.6661	419947.5
6179.00	0.1275E-02	288.13	0.2152E-08	0.5380E-03	6.7661	423228.3
6180.00	0.1101E-02	292.29	0.1832E-08	0.4578E-03	6.8661	426509.1
6181.00	0.9532E-03	296.45	0.1562E-08	0.3905E-03	6.9661	429790.0
6182.00	0.8266E-03	300.61	0.1335E-08	0.3338E-03	7.0661	433070.8
6183.00	0.7182E-03	304.77	0.1144E-08	0.2860E-03	7.1661	436351.7
6184.00	0.6253E-03	308.92	0.9827E-09	0.2456E-03	7.2661	439632.5
6185.00	0.5454E-03	313.07	0.8455E-09	0.2113E-03	7.3661	442913.4
6186.00	0.4766E-03	317.22	0.7289E-09	0.1822E-03	7.4661	446194.2
6187.00	0.4172E-03	321.36	0.6297E-09	0.1573E-03	7.5661	449475.0
6188.00	0.3659E-03	325.50	0.5450E-09	0.1362E-03	7.6661	452755.9
6189.00	0.3214E-03	329.64	0.4726E-09	0.1181E-03	7.7661	456036.7
6190.00	0.2828E-03	333.78	0.4105E-09	0.1026E-03	7.8661	459317.6
6191.00	0.2492E-03	337.91	0.3573E-09	0.8930E-04	7.9661	462598.4
6192.00	0.2200E-03	342.05	0.3115E-09	0.7785E-04	8.0661	465879.3
6193.00	0.1945E-03	346.17	0.2720E-09	0.6798E-04	8.1661	469160.1
6194.00	0.1722E-03	350.30	0.2379E-09	0.5946E-04	8.2661	472441.0
6195.00	0.1527E-03	354.42	0.2084E-09	0.5209E-04	8.3661	475721.8
6196.00	0.1356E-03	358.54	0.1829E-09	0.4571E-04	8.4661	479002.6
6197.00	0.1205E-03	362.66	0.1607E-09	0.4017E-04	8.5661	482283.5
6198.00	0.1073E-03	366.78	0.1414E-09	0.3536E-04	8.6661	485564.3
6199.00	0.9573E-04	370.89	0.1247E-09	0.3116E-04	8.7661	488845.1
6200.00	0.8546E-04	375.00	0.1100E-09	0.2751E-04	8.8661	492126.0
6201.00	0.7639E-04	379.11	0.9730E-10	0.2431E-04	8.9661	495406.8
6202.00	0.6837E-04	383.21	0.8612E-10	0.2152E-04	9.0661	498687.6
6203.00	0.6127E-04	387.31	0.7633E-10	0.1907E-04	9.1661	501968.5
6204.00	0.5497E-04	391.41	0.6774E-10	0.1693E-04	9.2661	505249.3
6205.00	0.4937E-04	395.51	0.6020E-10	0.1504E-04	9.3661	508530.1
6206.00	0.4440E-04	399.60	0.5356E-10	0.1338E-04	9.4661	511811.0
6207.00	0.3997E-04	403.70	0.4771E-10	0.1192E-04	9.5661	515091.8
6208.00	0.3602E-04	407.78	0.4256E-10	0.1063E-04	9.6661	518372.7
6209.00	0.3250E-04	411.87	0.3800E-10	0.9498E-05	9.7661	521653.5
6210.00	0.2935E-04	415.95	0.3397E-10	0.8491E-05	9.8661	524934.5
6211.00	0.2653E-04	420.03	0.3040E-10	0.7600E-05	9.9661	528215.2
6212.00	0.2401E-04	424.11	0.2724E-10	0.6809E-05	10.0661	531496.1
6213.00	0.2175E-04	428.19	0.2443E-10	0.6108E-05	10.1661	534777.0
6214.00	0.1972E-04	432.26	0.2194E-10	0.5484E-05	10.2661	538057.7
6215.00	0.1790E-04	436.33	0.1972E-10	0.4929E-05	10.3661	541338.6
6216.00	0.1626E-04	440.40	0.1774E-10	0.4435E-05	10.4661	544619.5
6217.00	0.1479E-04	444.46	0.1598E-10	0.3995E-05	10.5661	547900.3
6218.00	0.1346E-04	448.52	0.1441E-10	0.3601E-05	10.6661	551181.1
6219.00	0.1226E-04	452.58	0.1300E-10	0.3250E-05	10.7661	554462.0

TABLE A4.- VENUS MODEL ATMOSPHERES, EXTRAPOLATION OF MARINER 5 DATA TO SURFACE, ADIABATIC LAPSE RATE
(CO₂ = 85%, MEAN MOLECULAR WEIGHT = 41.61) - Concluded

VENUS MODEL ATMOSPHERES COMPUTED FROM DATA FROM THE OCCULTATIONS OF MARINER V AND REGULUS MEAN MOLECULAR WGT = 41.61 (85.0 PERCENT CARBON DIOXIDE 15.0 PERCENT NITROGEN)									
RADIUS	PRESSURE		TEMPERATURE		MASS DENSITY		REFRACTIVITY	PRESSURE	ALTITUDE
KM	MILLIBARS	LBS/SQIN	KELVIN	FAHRENHEIT	GM/CUCM	LBS/CUFT	N UNITS	SCALE HT KM	ABOVE SURF FEET
6220.00	0.1117E-04	0.1620E-06	456.64	362.29	0.1174E-10	0.7334E-09	0.2936E-05	10.8661	557742.8
6221.00	0.1020E-04	0.1479E-06	460.70	369.59	0.1062E-10	0.6631E-09	0.2654E-05	10.9661	561023.6
6222.00	0.9315E-05	0.1350E-06	464.75	376.88	0.9612E-11	0.6001E-09	0.2402E-05	11.0661	564304.5
6223.00	0.8513E-05	0.1234E-06	468.80	384.17	0.8706E-11	0.5433E-09	0.2176E-05	11.1661	567585.3
6224.00	0.7787E-05	0.1129E-06	472.84	391.45	0.7893E-11	0.4927E-09	0.1972E-05	11.2661	570866.2
6225.00	0.7128E-05	0.1033E-06	476.89	398.73	0.7162E-11	0.4471E-09	0.1790E-05	11.3661	574147.0
6226.00	0.6530E-05	0.9469E-07	480.93	406.00	0.6504E-11	0.4060E-09	0.1625E-05	11.4661	577427.8
6227.00	0.5987E-05	0.8682E-07	484.97	413.27	0.5911E-11	0.3690E-09	0.1477E-05	11.5661	580708.7
6228.00	0.5493E-05	0.7966E-07	489.00	420.54	0.5377E-11	0.3357E-09	0.1344E-05	11.6661	583989.5
6229.00	0.5044E-05	0.7314E-07	493.04	427.80	0.4895E-11	0.3056E-09	0.1223E-05	11.7661	587270.3
6230.00	0.4635E-05	0.6720E-07	497.07	435.05	0.4460E-11	0.2784E-09	0.1114E-05	11.8661	590551.2
6231.00	0.4261E-05	0.6179E-07	501.09	442.30	0.4067E-11	0.2539E-09	0.1016E-05	11.9661	593832.1
6232.00	0.3921E-05	0.5686E-07	505.12	449.55	0.3711E-11	0.2317E-09	0.9276E-06	12.0661	597112.8
6233.00	0.3610E-05	0.5235E-07	509.14	456.79	0.3389E-11	0.2115E-09	0.8471E-06	12.1661	600393.7
6234.00	0.3327E-05	0.4824E-07	513.16	464.03	0.3097E-11	0.1933E-09	0.7741E-06	12.2661	603674.6
6235.00	0.3067E-05	0.4448E-07	517.18	471.26	0.2832E-11	0.1768E-09	0.7080E-06	12.3661	606955.3
6236.00	0.2830E-05	0.4103E-07	521.20	478.49	0.2592E-11	0.1618E-09	0.6479E-06	12.4661	610236.2
6237.00	0.2612E-05	0.3788E-07	525.21	485.71	0.2374E-11	0.1482E-09	0.5934E-06	12.5661	613517.1
6238.00	0.2413E-05	0.3500E-07	529.22	492.93	0.2176E-11	0.1358E-09	0.5439E-06	12.6661	616798.0
6239.00	0.2231E-05	0.3235E-07	533.23	500.14	0.1995E-11	0.1246E-09	0.4988E-06	12.7661	620078.7
6240.00	0.2063E-05	0.2992E-07	537.23	507.35	0.1831E-11	0.1143E-09	0.4578E-06	12.8661	623359.6
6241.00	0.1910E-05	0.2769E-07	541.23	514.55	0.1682E-11	0.1059E-09	0.4204E-06	12.9661	626640.5
6242.00	0.1768E-05	0.2564E-07	545.23	521.75	0.1545E-11	0.9650E-10	0.3863E-06	13.0661	629921.3
6243.00	0.1638E-05	0.2376E-07	549.23	528.94	0.1421E-11	0.8674E-10	0.3552E-06	13.1661	633202.1
6244.00	0.1519E-05	0.2203E-07	553.22	536.13	0.1307E-11	0.8165E-10	0.3269E-06	13.2661	636483.0
6245.00	0.1409E-05	0.2043E-07	557.21	543.32	0.1204E-11	0.7518E-10	0.3009E-06	13.3661	639763.8
6246.00	0.1308E-05	0.1897E-07	561.20	550.50	0.1109E-11	0.6928E-10	0.2772E-06	13.4661	643044.6
6247.00	0.1215E-05	0.1761E-07	565.19	557.68	0.1022E-11	0.6385E-10	0.2556E-06	13.5661	646325.5
6248.00	0.1128E-05	0.1637E-07	569.17	564.85	0.9433E-12	0.5889E-10	0.2357E-06	13.6661	649606.3
6249.00	0.1049E-05	0.1521E-07	573.16	572.01	0.8706E-12	0.5433E-10	0.2176E-06	13.7661	652887.2
6250.00	0.9763E-06	0.1415E-07	577.13	579.18	0.8040E-12	0.5019E-10	0.2009E-06	13.8661	656168.0
6250.00	0.9763E-06	0.1415E-07	577.13	579.18	0.8040E-12	0.5019E-10	0.2009E-06	13.8661	656168.0

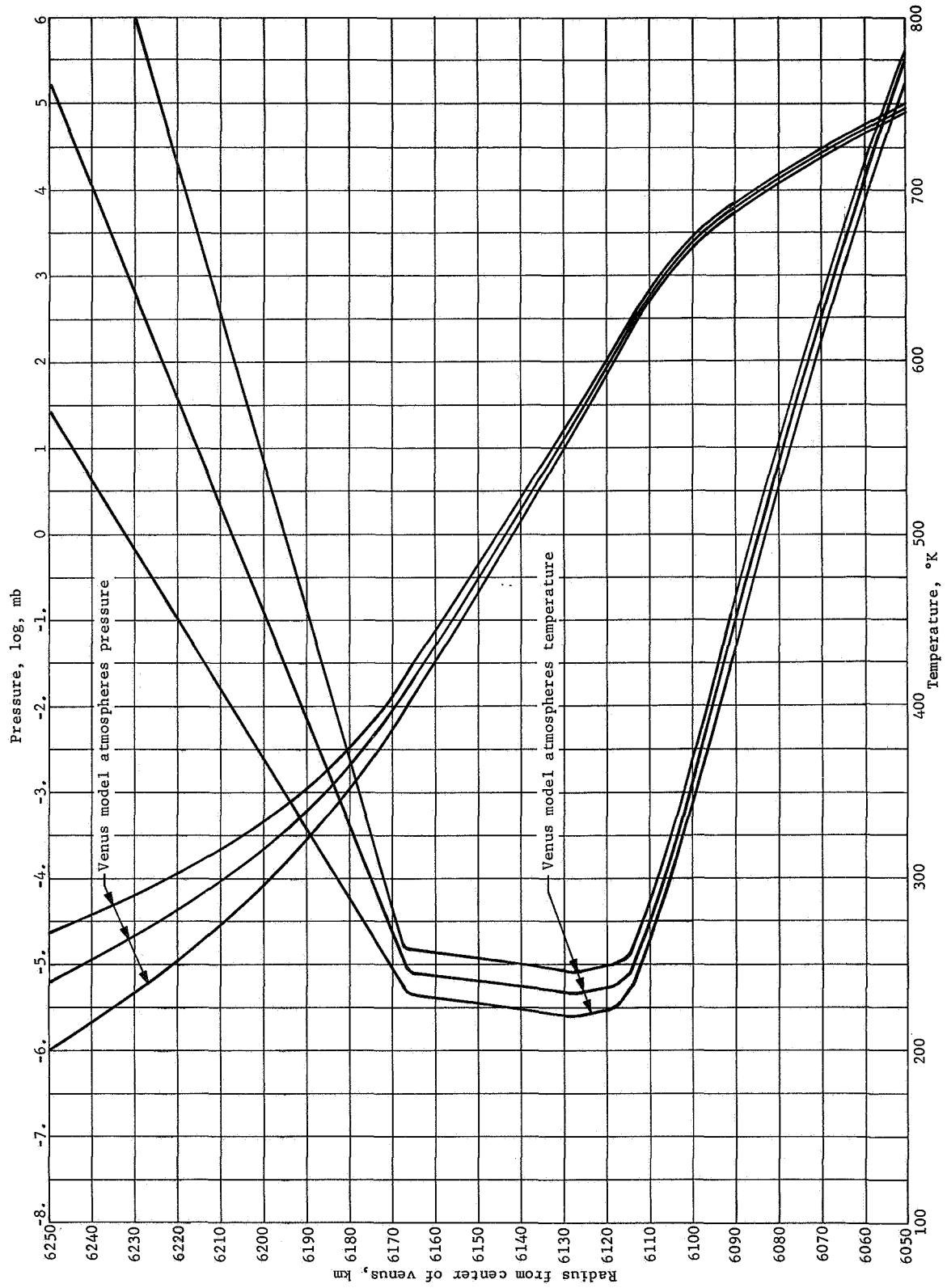


Figure A1.- Venus Pressure and Temperature Profile Models Used in Study

APPENDIX A

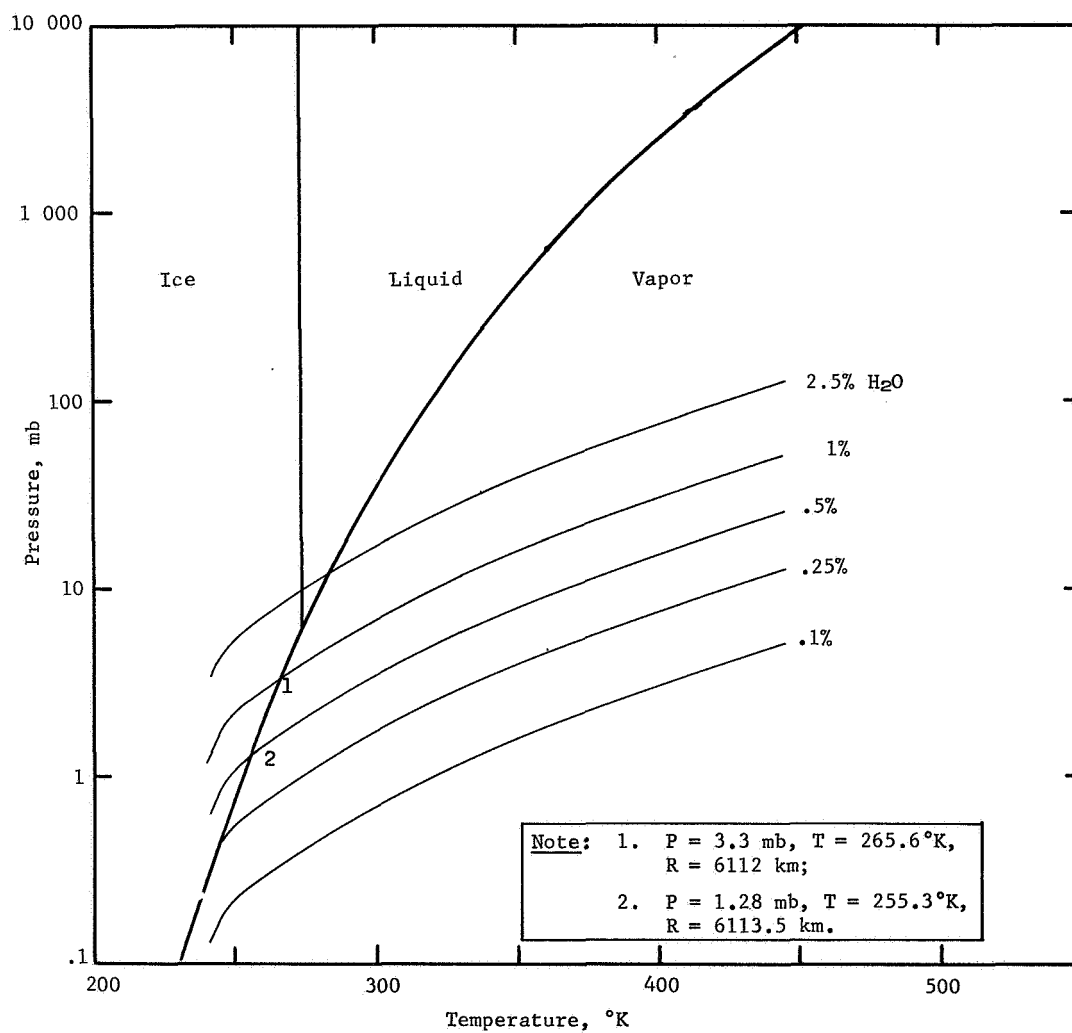


Figure A2.- Venus Pressure vs Temperature on H₂O Phase Diagram

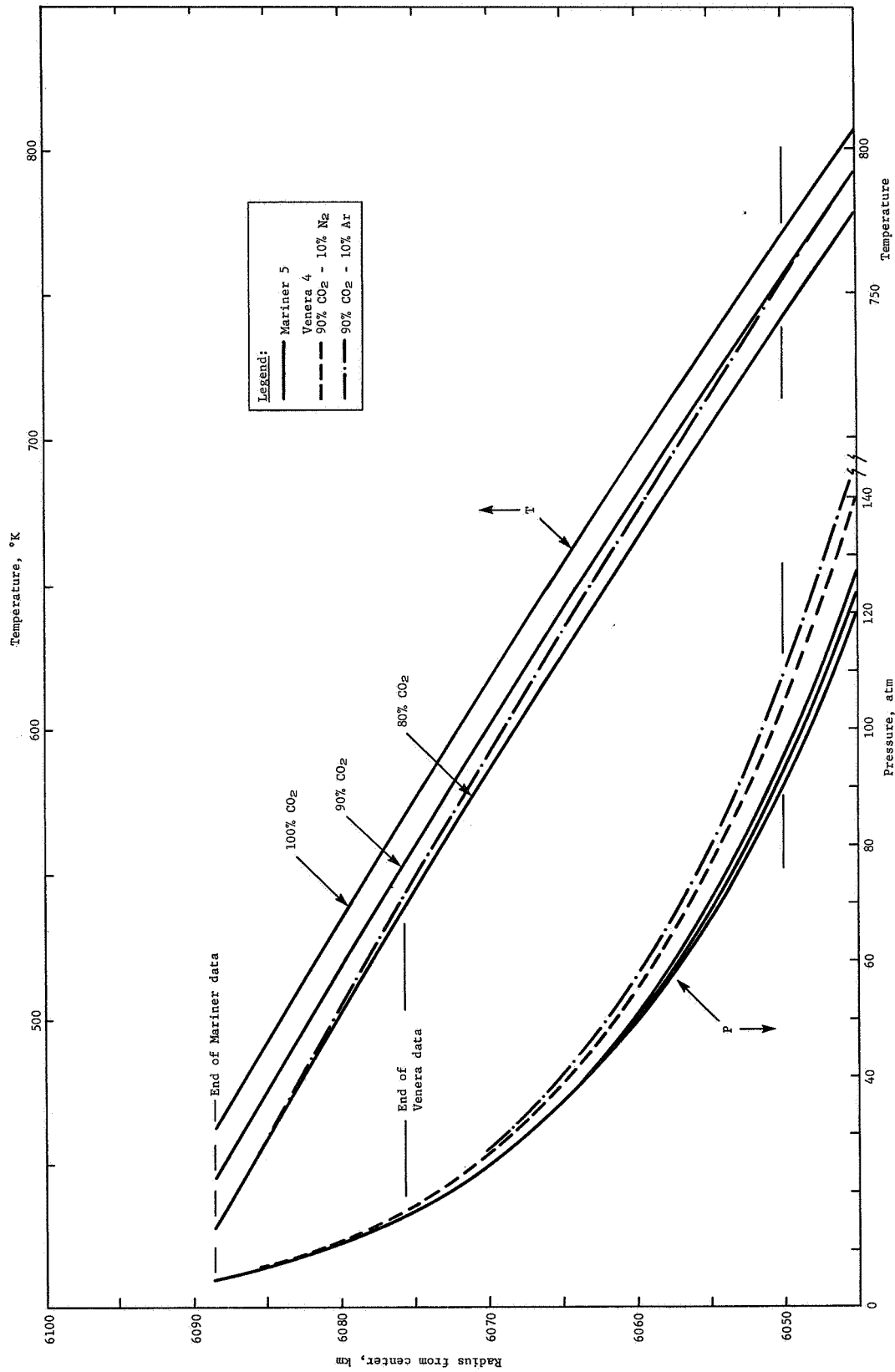


Figure A3.- Venus Lower Atmosphere

APPENDIX A

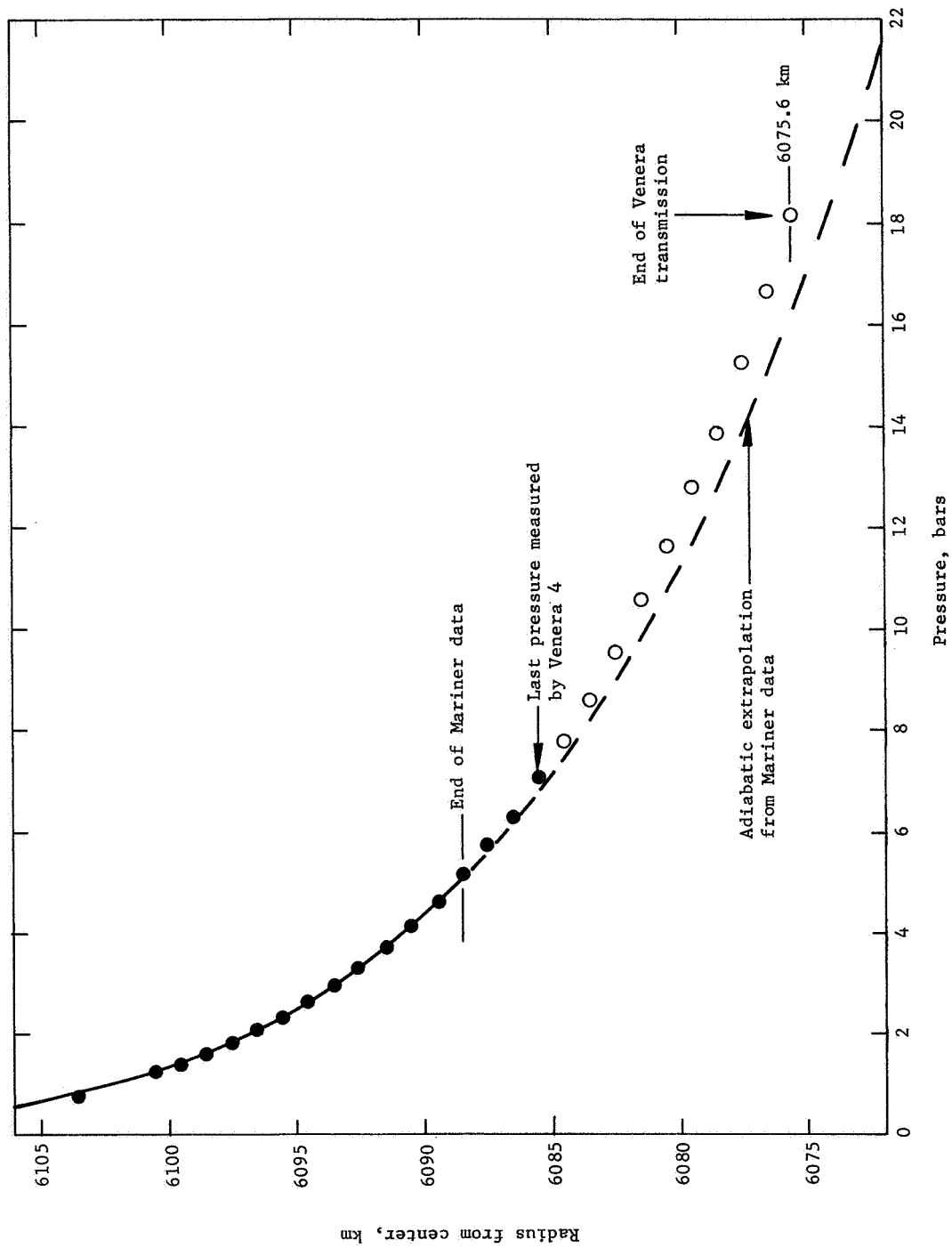
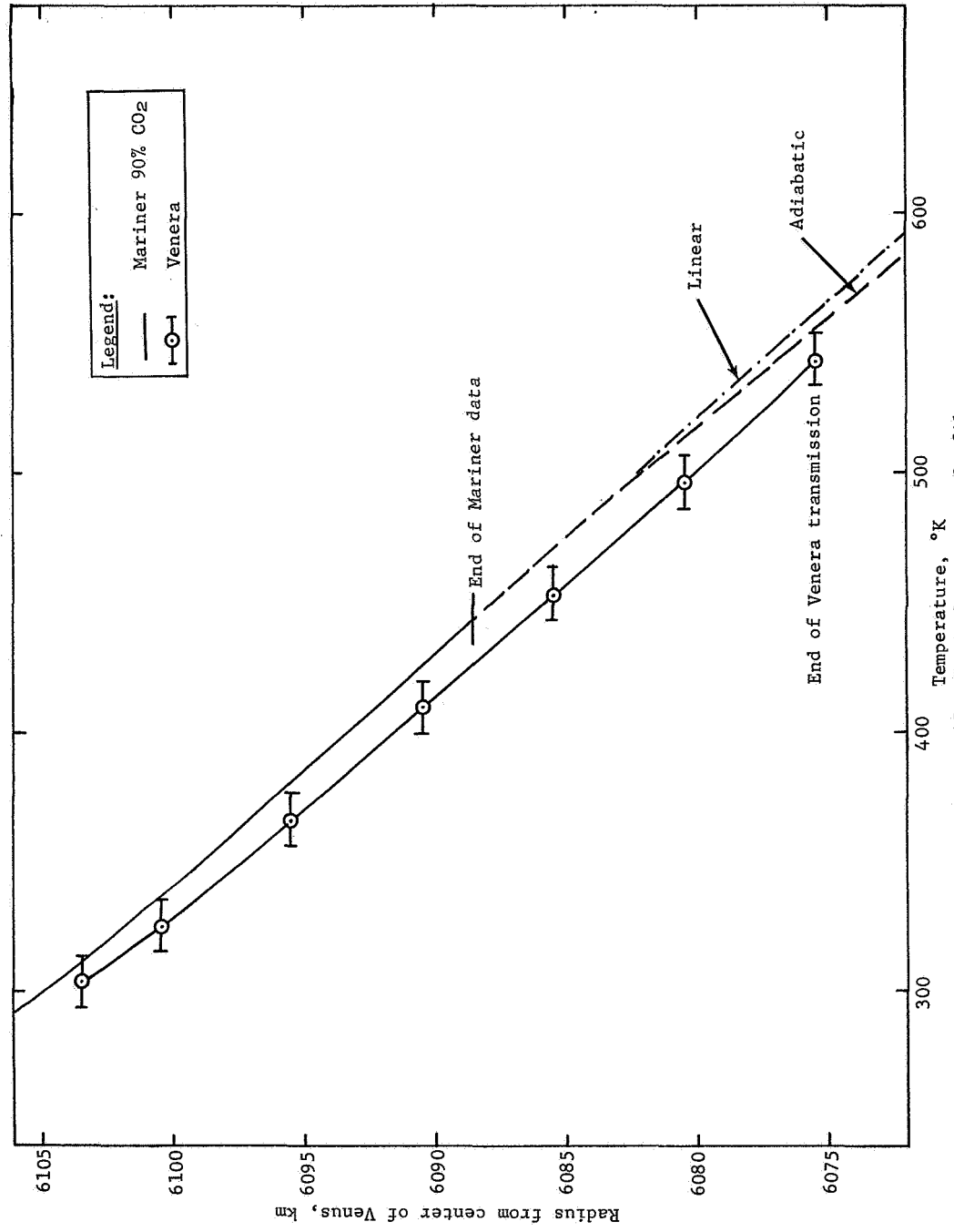


Figure A4.- Mariner and Venera Pressure Profiles

APPENDIX A



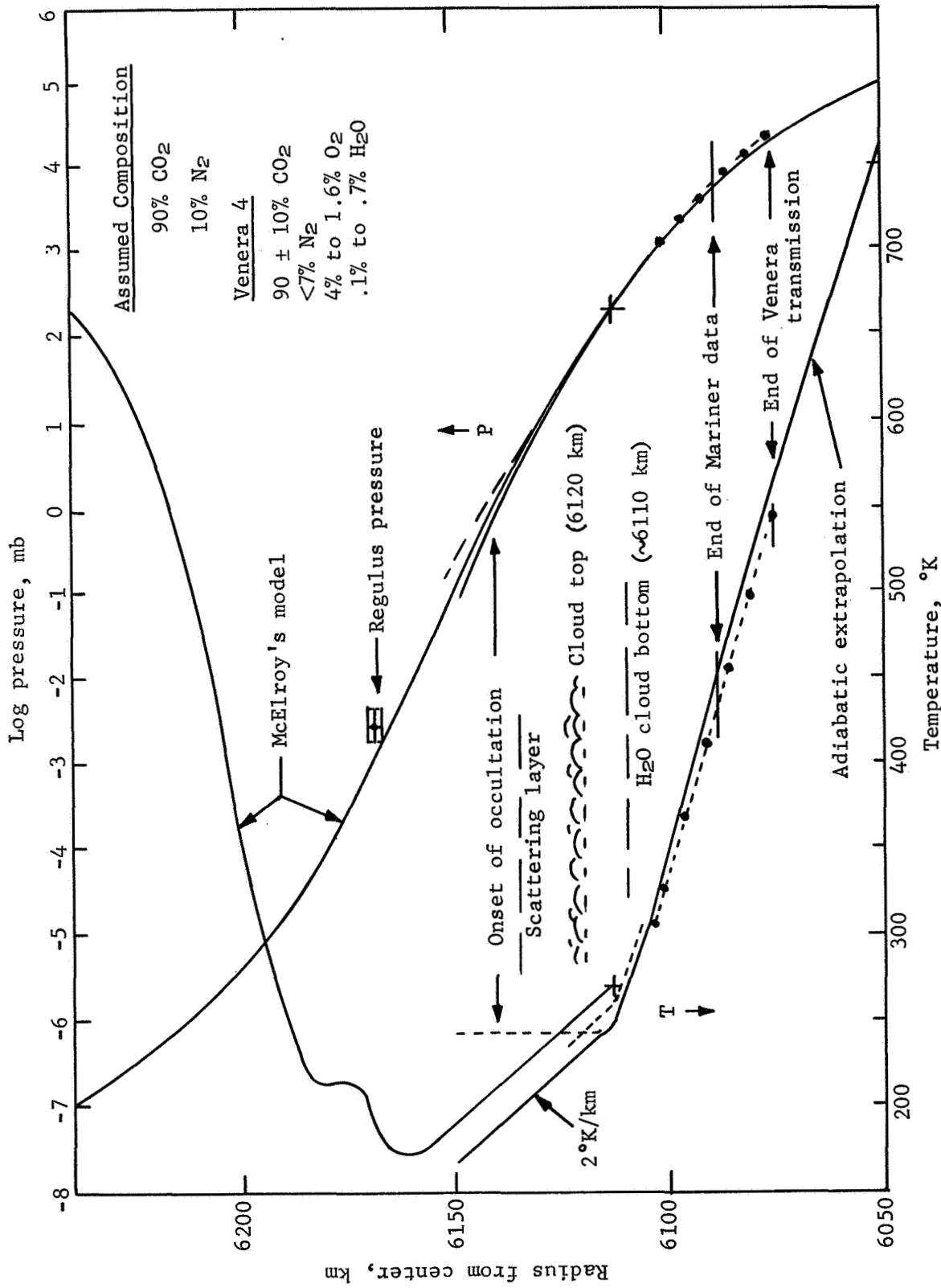


Figure A6.- Venus Atmosphere

APPENDIX A

REFERENCES

- A1. Kliore, A.; Levy, G. S.; Fjeldbo, G.; and Rasool, S. I.: Atmosphere and Ionosphere of Venus from the Mariner V S-Band Radio Occultation Measurement. Science, vol. 158, Dec. 29, 1967, pp. 1683 - 1688.
- A2. Anduevskiy, V. S., et al.: The Model of the Atmosphere of the Planet Venus on the Results of Measurements made by the Soviet Automatic Interplanetary Station "Venera 4." Paper Presented at 2nd Arizona Conference on Planetary Atmospheres, Tucson, Ariz., Mar. 11-13, 1968.
- A3. Kliore, A., et al.: Structure of the Atmosphere of Venus Derived from Mariner V S-Band Measurements, Paper no. f.13 Presented to the Session on the Moon and Planets, 11th COSPAR Meeting, Tokyo, Japan, May 9-21, 1968.
- A4. Maryott, A. A.; and Buckley F.: Table of Dielectric Constants and Electric Dipole Moments of Substances in the Gaseous State. NBS Circular 537, U.S. Government Printing Office, Washington, DC, June 23, 1953.
- A5. McElroy, M. B.: The Upper Atmosphere of Venus. J. Geophys. Res., vol. 73, no. 5, 1968, pp. 1513 - 1521.

APPENDIX B

HEAT SHIELD ANALYSIS

by H. Edward Sparhawk and John R. Mellin
Martin Marietta Corporation

APPENDIX B

The heat shield design requirements for a Venus entry vehicle have been studied for three entry modes: (1) entry from Venus orbit, (2) entry from Venus approach trajectory, and (3) entry from an approach trajectory that allows the spacecraft to swing by Venus and continue on a course to Mercury. The requirement for this study relative to the heat shield has been defined as:

- 1) Determination of the thickness and weight of ablative material required for the missions studied;
- 2) A definition of heat shield development requirements.

HEAT SHIELD REQUIREMENTS

The baseline aeroshell configuration for the three missions considered in the BVS study was selected as a spherically blunted, 55° half-angle cone. The approach taken to define the heat shield requirements for this vehicle was as follows:

- 1) Ablative materials were selected for analysis, which are consistent with the present state of the art in this technology;
- 2) The heat shield thicknesses and unit weights (fig. B1) were determined using nominal material properties, but using heating inputs that have been increased by appropriate uncertainty factors;
- 3) The sensitivity of the predicted backface temperature to uncertainties in both the aerothermal environment and to material performance unknowns were evaluated.

Ablative Material Consideration

The ablative heat shield thicknesses and weights determined for the three BVS missions were based on the properties of ablative materials that have been extensively ground tested and whose performance has been verified during Earth reentry flight test. The materials selected for this study are: Martin Marietta ESA-5500, a carbon filled elastomeric silicone ablator that was used on high heating rate leading edges of the PRIME vehicle; Avcoat 5026-39 HC-G Apollo material, which is a filled epoxy; and laminated carbon phenolic, which has been flight tested in numerous forms on ballistic entry systems. These materials, which represent the three basic types of charring ablation materials, each have specific advantages and disadvantages that must be weighed in terms of specific mission requirements. These are summarized in Table B1.

APPENDIX B

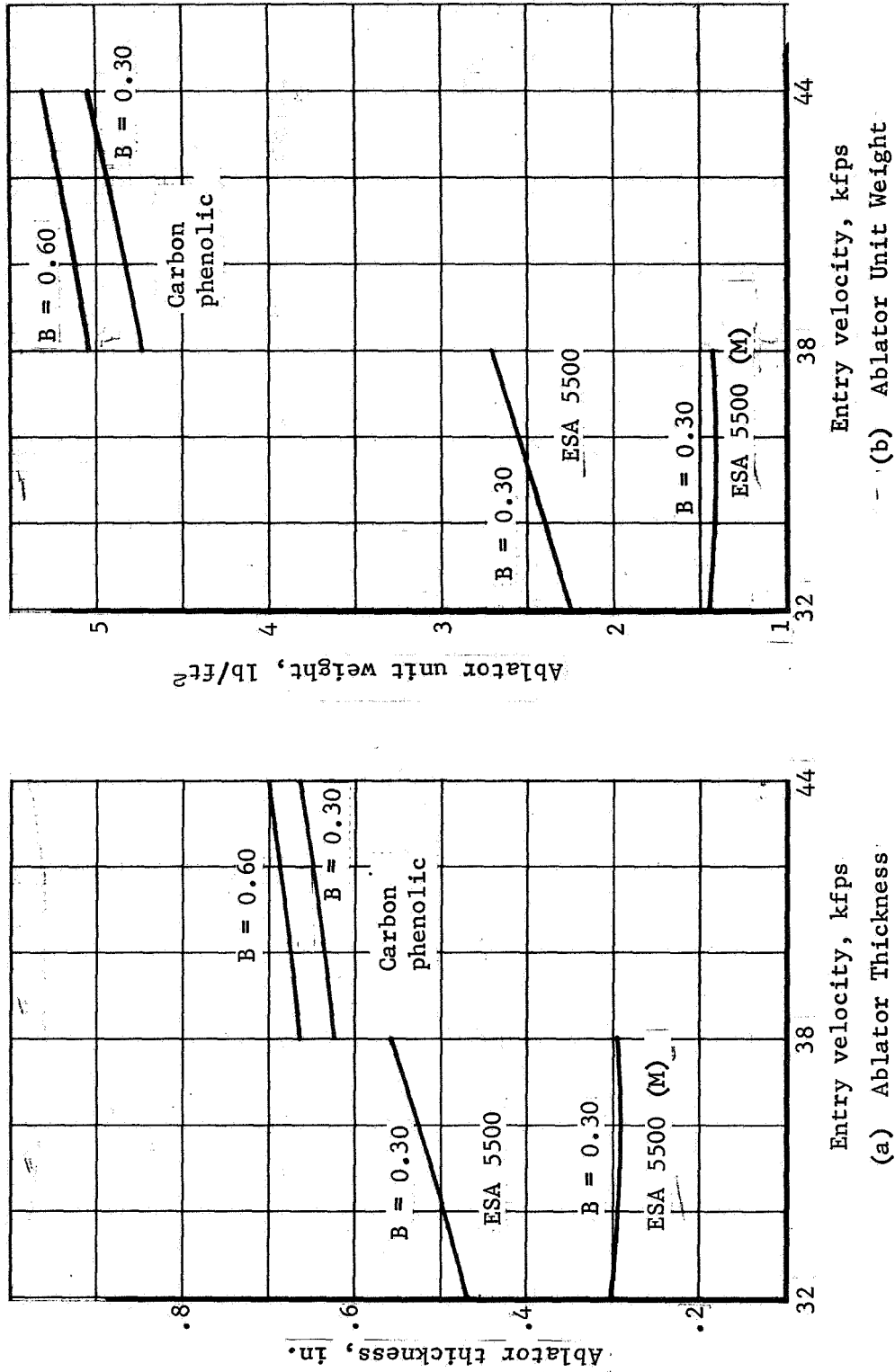


Figure B1.- Ablation Material Required vs Velocity

APPENDIX B

TABLE B1. - HEAT SHIELD MATERIAL ENVIRONMENTAL SENSITIVITY

	Fabrication	Sterilization	Launch loads	Vacuum effects	Low-temperature strain	Entry environment		
						Shear resistance	Insulation efficiency	Thermo structural
Carbon phenolic laminate	Tape winding or shingle; flexible bond and/or mechanical attach	No problem cure temperature 300°F	No problem	No apparent problem	No apparent problem; thermal expansion coefficient compatible with most structural materials	High (~100 psf for high-pressure moldings)	Poor	Thermal stresses will be significant consideration
ESA-5500	Vacuum bagging into H/C reinforcement for thickness ≤0.5 in.; single cell injection for thickness >0.5 in.; H/C rigidly bonded to structure	No apparent problem	No problem	Vacuum offgassing problem; cure process and/or resin modification required	Flexible to -100°F; no problem	Low (mechanical erosion at shears of 15 psf)	Good	No problem
Avcoat 5026-39HCG	Single cell injection into H/C reinforcement; H/C rigidly bonded to structure; casting possible	Possible problem area	No problem	No apparent problem	Rigid material; effects of surface cracking not available	Low (mechanical erosion at shears of 15 psf)	Best of materials being considered	Possible problem area

APPENDIX B

Developmental effort that is common to any material is the detail material processing required before application to the structural substrate and the actual fabrication and curing procedures to be followed. The effects of sterilization on the thermal and mechanical properties must be understood for any material ultimately selected.

After launch and before entry, the response of the heat shield to vacuum and space temperatures must be considered. Of the three materials being considered, carbon phenolic will be the least affected by these environments. Vacuum effects will be minimal because of the highly cross-linked nature of the phenolic resin system. Low temperature soak, although a consideration, is not expected to be a significant problem because the thermal expansion of carbon phenolic approximates that of most commonly used structural materials. Similarly, the ESA-5500 material will present no particular problem at low temperatures because it was specifically formulated with potential low temperature applications in mind. Offgassing of condensable volatiles is a definite problem with this type of material, which will require either resin modification and/or cure cycle changes. In either case, the final product must be reevaluated with respect to its low temperature strain capability. Epoxy-based materials, such as the Avcoat 5026-39HCG, become rigid at low temperatures and crack. For missions in which the heat shield is turned away from the sun, i.e., targeting for sunlight side of the planet, this could be a definite deterrent to the use of this material.

During entry, the heat shield must survive a short (≈ 15 sec) thermal pulse composed of high convective and radiative heating rates and viscous shear levels. After the heat pulse, the heat shield must provide insulation between the hot surface and the structure for approximately 1 minute. Char retention is of paramount importance because reradiation from the high temperature surface is, considering the entire heat pulse, the most important heat-rejection mode. Mechanical erosion of the char drastically reduces the efficiency of a material because of a reduction in surface temperature and, hence, reradiation. When char is eroded, the majority of the heat input must be absorbed by the material. The char strength of carbon phenolic is vastly superior to that of either ESA-5500 or Avcoat 5026-39 HCG when high-pressure molding techniques are used. It is anticipated that this advantage will be retained for the fabrication procedure, which is developed for a Venus entry probe. However, because the strength of graphitic materials, in general, undergoes a sharp drop at temperatures above 6000°F, the char strength at the extreme temperatures predicted for Venus must be investigated.

APPENDIX B

The insulation efficiency of the heat shield is of great importance because the temperature rise of the structure must be limited during a thermal soakout period, which is approximately three times as long (45 vs 15 sec) as the heat pulse itself. In this respect, the Apollo material ranks first by virtue of its low density (33 lb/ft^3) and low thermal conductivity ($1.6 \times 10^{-6} \text{ Btu/in.-sec-}^\circ\text{R}$). Use of ESA-5500 does not result in a large penalty because its density is not high (58 lb/ft^3), and it also has a low thermal conductivity ($3.0 \times 10^{-6} \text{ Btu/in.-sec-}^\circ\text{R}$). The use of carbon phenolic would impose a large weight penalty because its density (91 lb/ft^3) and thermal conductivity ($9 \times 10^{-6} \text{ Btu/in.-sec-}^\circ\text{R}$) are both high.

The third major characteristic to be considered is the thermo-structural capability of the ablative material, i.e., its ability to generate thermal stresses in the ablative layer and bondline during the entry phase. Carbon phenolic laminates retain their high strength at temperatures as high as 5000°F (ref. B1) and, therefore, thermal stress analysis, material thermomechanical property determination, and large-scale verification testing will be a required part of any program in which this type of ablative material is used. Elastomeric materials characteristically have a low modulus and strength so that thermal stresses are relatively insignificant. Elastomeric materials possess many other desirable features, including high insulation efficiency, minimum susceptibility to cold-soak failures, and simplicity of fabrication, inspection, and repair. The major detrimental characteristics of this class of materials, however, is a generally low resistance to aeromechanical forces, i.e., viscous shear stress and pressure gradient. Although shear forces are a consideration in any heat shield design and, in many cases, additional material must be provided to account for mechanical erosion, analytical prediction of mechanical erosion rates is uncertain, and extremely conservative design practices must be used. Because analysis indicates that mechanical erosion increases the thickness of ESA-5500 required by a factor of two over that required if shear is not considered, a series of material tests was initiated to demonstrate the feasibility of formulating an elastomeric material that would not erode mechanically at the moderate shear levels ($<100 \text{ psf}$) predicted for entry from flyby and orbit.

The first step taken was to conduct a screening program in the Martin Marietta Corporation 1.5 MW plasma arc, in which 10 modified versions of ESA-5500 were tested and compared with the original formulation and with carbon phenolic. The models tested were $1\frac{1}{4}$ in. flat-ended cylinders. The two test conditions were as tabulated.

APPENDIX B

Test condition	Heating rate, Btu/ft ² -sec	Enthalpy, Btu/lb	Pressure, atm	Test time, sec
1	1140	7240	1.0	15
2	600	4000	1.0	15

The degree of improvement that can be anticipated is illustrated by comparing the recession rates of the basic ESA-5500 and ESA-5500 (M-10) in Table B2.

TABLE B2.- ESA-5500 AND ESA-5500 (M) RECESSION RATES

Material	Test condition	T _w , °F	\dot{r} , ips	$\frac{\dot{m}^*}{\dot{m}_T}^a$
ESA-5500	1	4600	0.0204	1.73
ESA-5500 (M-10)	1	5020	0.0099	1.025
ESA-5500	2	4050	0.0132	1.02
ESA-5500 (M-10)	2	4200	0.00527	.59

^a $\frac{\dot{m}^*}{\dot{m}_T}$ is the ratio of the measured mass loss rate to the theoretical mass loss rate assuming recession is controlled by diffusion limited combustion of the carbon in the char.

At test condition 1, the recession of (M-10) modification was approximately thermochemical, whereas ESA-5500 was eroded at a rate 70% greater due to pressure forces on the model face.

At this point in time, it appears that, of the group of existing materials, carbon phenolic would be the best material selection on the basis of the factors listed in table B1 and discussed above. The two major negative factors associated with the use of this material are weight and thermal stresses. Both the ESA-5500 and Avcoat 5026-HCG have good insulation characteristics but low char strength and low resistance to aeromechanical forces. The ESA-5500-type material possesses excellent thermostructural characteristics at both low and high temperatures. In view of the overall theoretical and experimental effort that will be required to obtain a high degree of confidence in any Venus heat shield design, it cannot be stated at this time that any of the state-of-the-art materials is a clear cut choice. Thus, ESA-5500 and carbon phenolic have been selected for this study, because Martin Marietta has had the most experience with these materials and can, therefore, predict performance and sensitivity with the highest confidence level. ESA 5500M shows such promise that it has been included in the analysis of heat shield requirements for the various missions.

APPENDIX B

Heat Shield Thickness and Weight Requirements

The thickness and weight per unit area of ablative material required is summarized in figure B2 as a function of initial entry angle and ballistic coefficient for entry velocities of 32 000, 38 000, and 44 000 fps. Because the structural substrate is aluminum, the maximum allowable ablator backface temperature was conservatively selected as 300 °F.

In the design of the heat shield for the three missions, carbon phenolic and ESA-5500M are assumed to recede due to thermochemical reactions as described in reference B2. For ESA-5500, mechanical erosion is assumed to occur at the pyrolysis zone/char interface at a rate limited by the degradation kinetics of the plastic material (ref. B2). Thus, the difference in performance between the two versions of ESA-5500 is due to the mechanical erosion of the unreinforced material.

The ablation predicted for these materials is summarized in figure B3. ESA-5500 ablates a significant fraction of its original thickness, whereas for carbon phenolic and ESA-5500 (M), the material loss is nominal. As shown in this figure, however, predicted surface temperatures are extreme for both of the materials for which erosion is not considered. The possible effects of these high temperatures is discussed later in terms of material resistance to aeromechanical forces.

Structure temperature histories for the design ablator thicknesses are shown in figure B4 for ESA-5500 (M) for the entry from approach trajectory and for carbon phenolic for the V/M flyby mission. The significant point to note from these curves is that there is no structure temperature rise predicted during the entry heating pulse. The entire temperature increase occurs as a result of the thermal soak while the probe is decelerating from Mach 2 (approximately the end of heating) to Mach 0.5, at which the aeroshell is jettisoned.

The aerothermal entry environment and the uncertainty factors applied to the theoretically determined heating components are given in table 93 of this report. Factored heating has been used to determine the design ablator requirements summarized above.

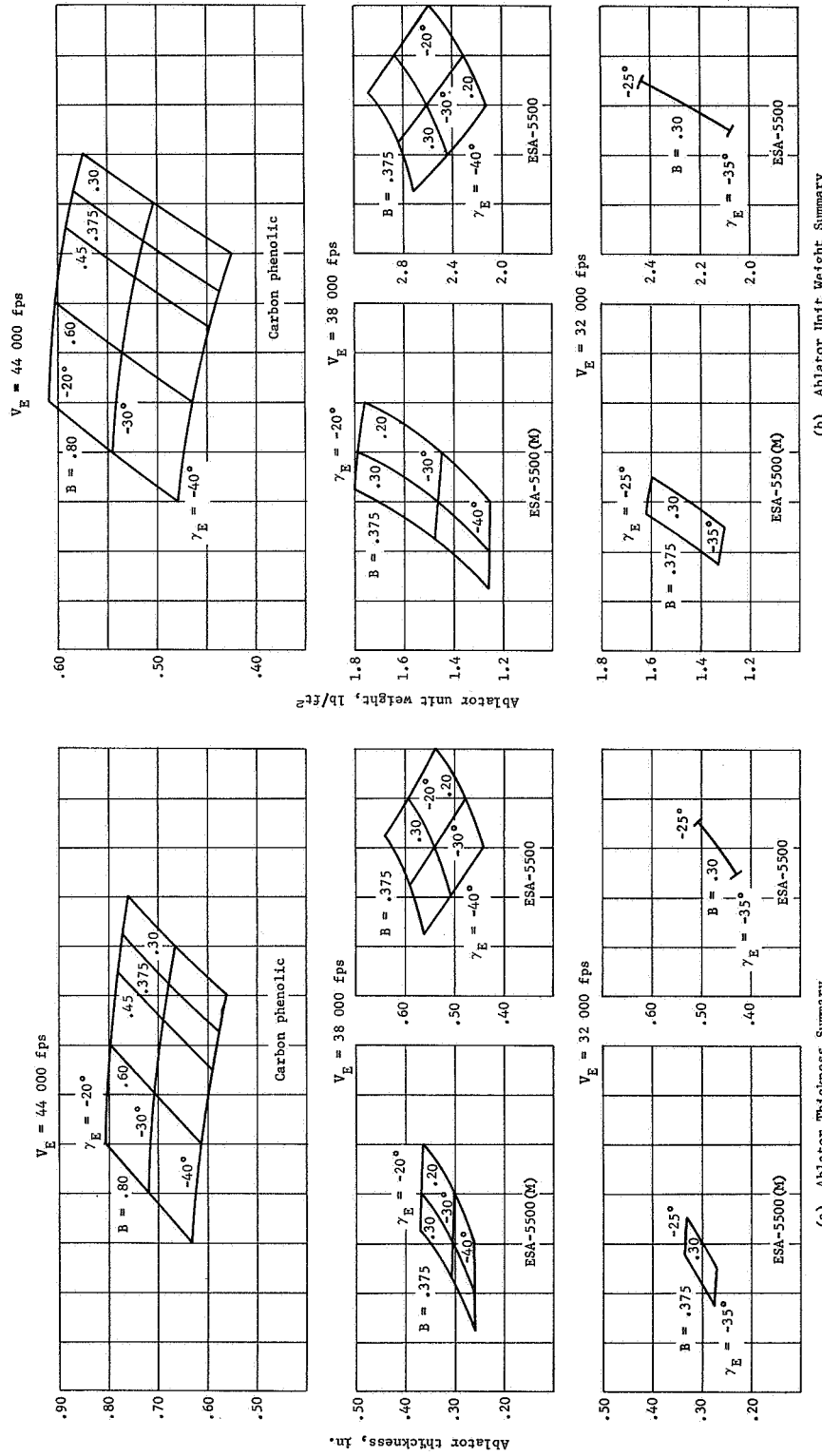


Figure B2.- BYS Heat Shield Requirement Summary

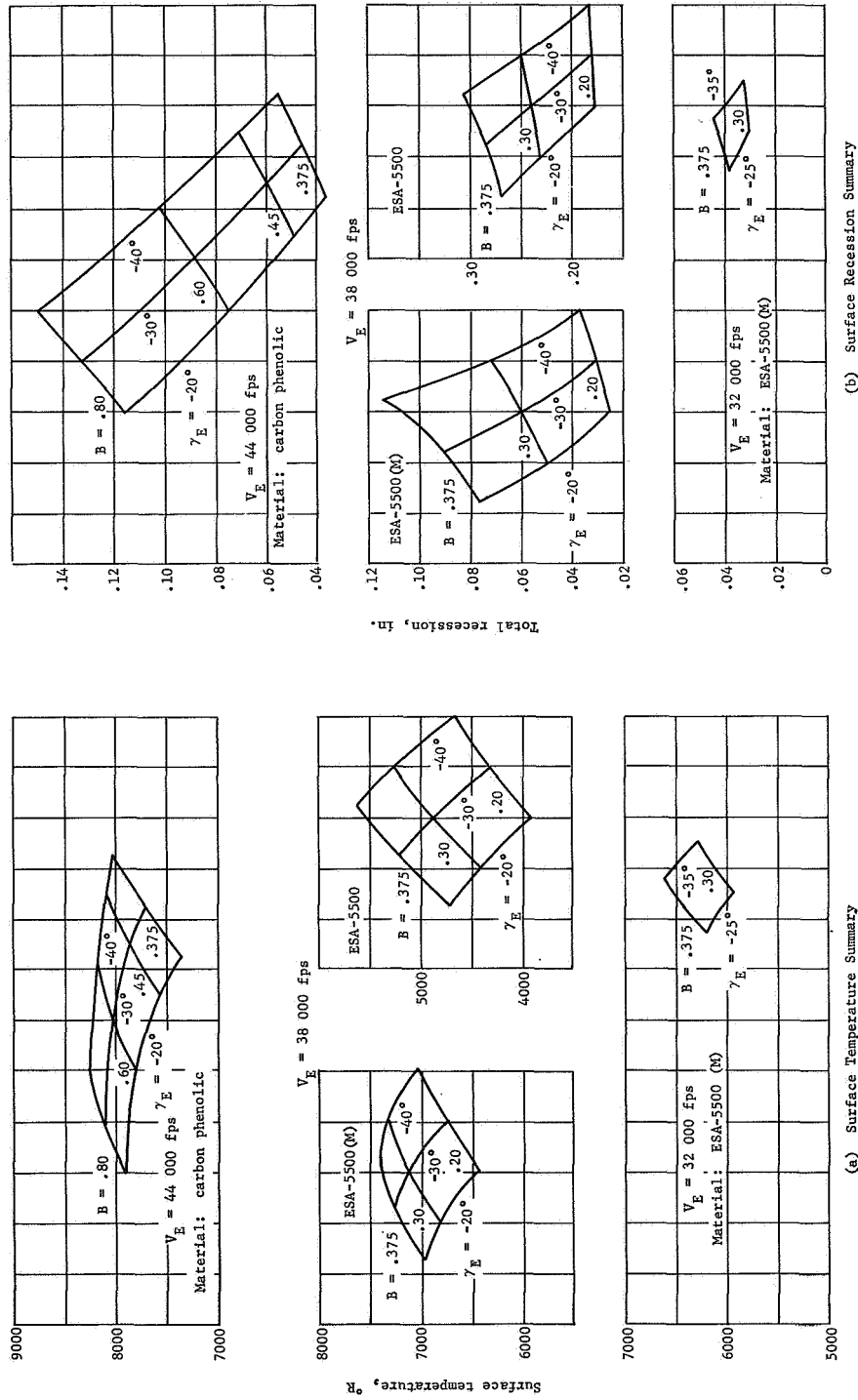


Figure B3.- Heat Shield Ablation Summary

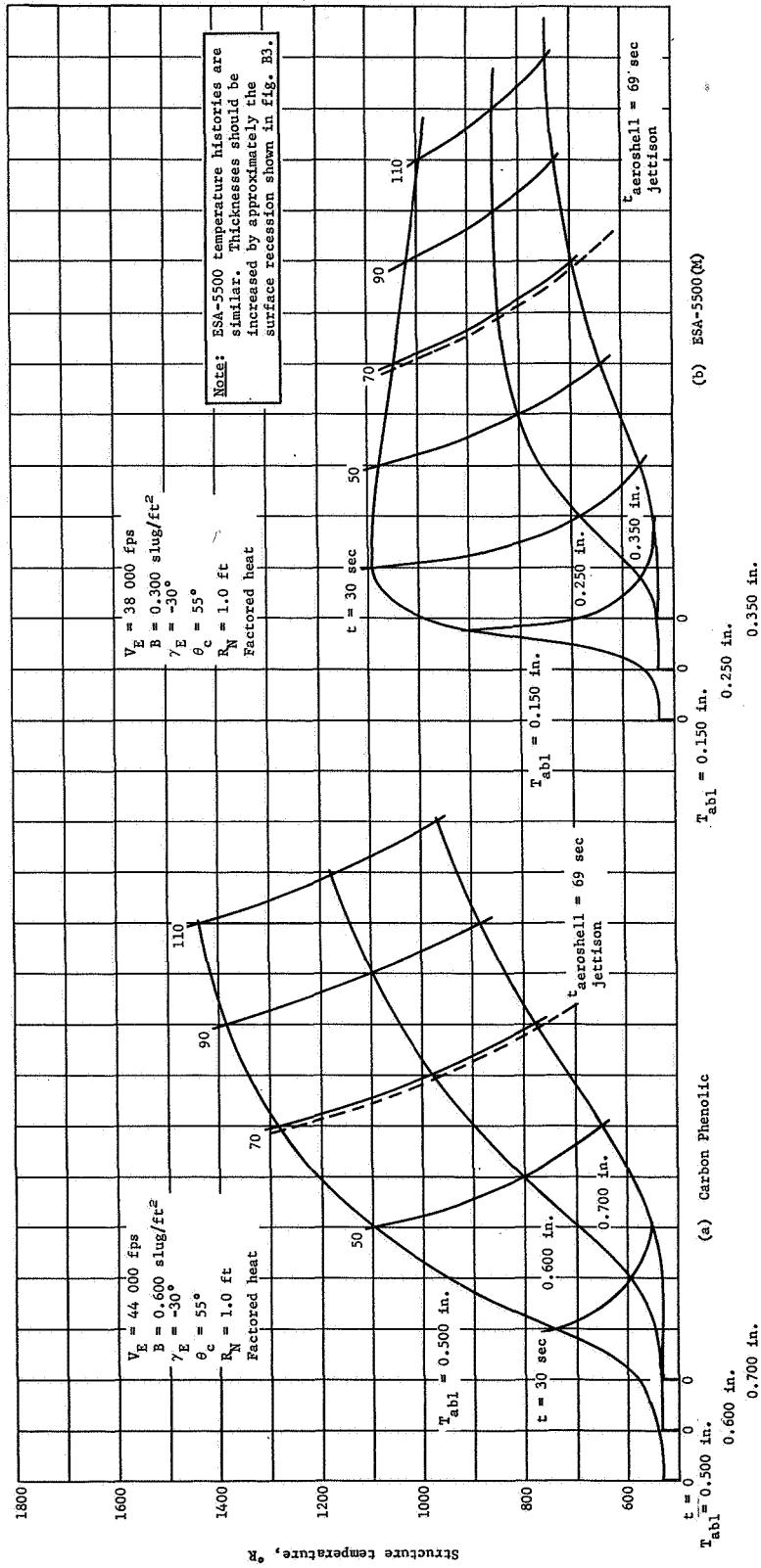


Figure E4.- Structure Temperature Histories

APPENDIX B

Heat Shield Sensitivity Studies

In view of the large uncertainties that are associated with the radiation heating rates and the extreme surface temperatures predicted for Venus entry, evaluation of the effects of unknowns in both the environment and ablation material performance is particularly pertinent to this type of study. Although the sensitivity studies conducted during the BVS study are by no means all-encompassing, they do deal with some of the more important unknowns. Specific problem areas examined were:

- 1) The sensitivity of heat shield thickness requirements to entry environment uncertainties has been examined;
- 2) The sensitivity of carbon phenolic and ESA-5500 (M) ablation have been evaluated in light of high-temperature strength data for graphite and carbon phenolic;
- 3) The effects of uncertainties in the thermodynamic properties of carbon vapor have been examined.

Thermal environment sensitivity. - The following cases were analyzed to determine the variation of the thickness of carbon phenolic required at the stagnation point as a function of variations in the factor applied to the nominal radiative heating rates. The study was made for the direct entry design case, $V_E = 38\ 000$ fps at $\gamma_E = 30^\circ$:

Case	F_c convection	Radiation		
		F_{NEQ} nonequilibrium	F_{EQ} equilibrium and CO_4+	F_{UV} carbon continuum
1	1.0	1.0	1.0	1.0
2	1.0	3.0	1.5	3.0
3	1.0	5.0	1.0	1.0
4	1.5	1.0	1.0	1.0
5	1.5	3.0	1.5	^a 3.0
6	1.5	5.0	1.5	3.0
7	1.5	3.0	1.5	1.5
^a Baseline design criteria.				

APPENDIX B

As can be seen from the results shown in figure B5, the sensitivity of thickness required is relatively insensitive to large uncertainties in the radiative heating of both items of the individual components and the total. For example, comparing the thickness required for the baseline criteria (case 5) with case 4, in which the nominal levels of all components were used, we see that decreasing the total radiant heat by 60% decreases the required thickness by only 7% from 0.624 to 0.585 in. The effect of increasing the nonequilibrium component by a factor of 5 (case 1 vs case 3), which increases the total radiative load by 220% increases the thickness requirement by again only 7%. In addition to the low sensitivity of thickness required to radiant heat, the fact that the curve is smooth indicates an insensitivity to variation in the shape of the radiant pulse because the changes in factors significantly change the pulse shape.

Char strength sensitivity.- In all of the foregoing analyses, with the exception of the analysis of unmodified ESA-5500, it has been assumed that surface recession results from heterogeneous reaction between the boundary layer species and the char and sublimation of the char. However, the char formed by the degradation of a composite ablator, such as those considered in this study, is at best a porous form of graphite and, as such, cannot be expected to possess strength characteristics exceeding those of a good grade of graphite. The variation of ultimate tensile strength with temperature of POCO AXF-5Q graphite (fig. B6 from ref. B3) shows a sharp decrease in the temperature range from 5000 to 6500°F. The comparison between tensile properties of laminates of CCA-1 carbon and G-1550 graphite fabric impregnated with EC-201 phenolic resin and ATJ graphite in data presented in reference B1 at temperatures up to 5000°F indicates a similarity in mechanical properties. Thus, it would not be surprising if 6000°F represented a maximum temperature for carbonaceous composite ablators, beyond which their capability to resist aerodynamic forces was negligible.

Proceeding on the premise that 6000°F represents an upper limit surface temperature, analyses were conducted for carbon phenolic and ESA-5500 (M), in which the surface temperature was not allowed to exceed this value and the maximum char thickness was limited to 0.01 in. during the period when the temperature is so limited. This allowable char thickness is based on the results of tests conducted in the high shear environment of the CAL wave superheater. Thus, it is assumed that for temperatures greater than 6000°F, the char strength is essentially zero, and even small shearing forces result in mechanical erosion of the surface.

APPENDIX B

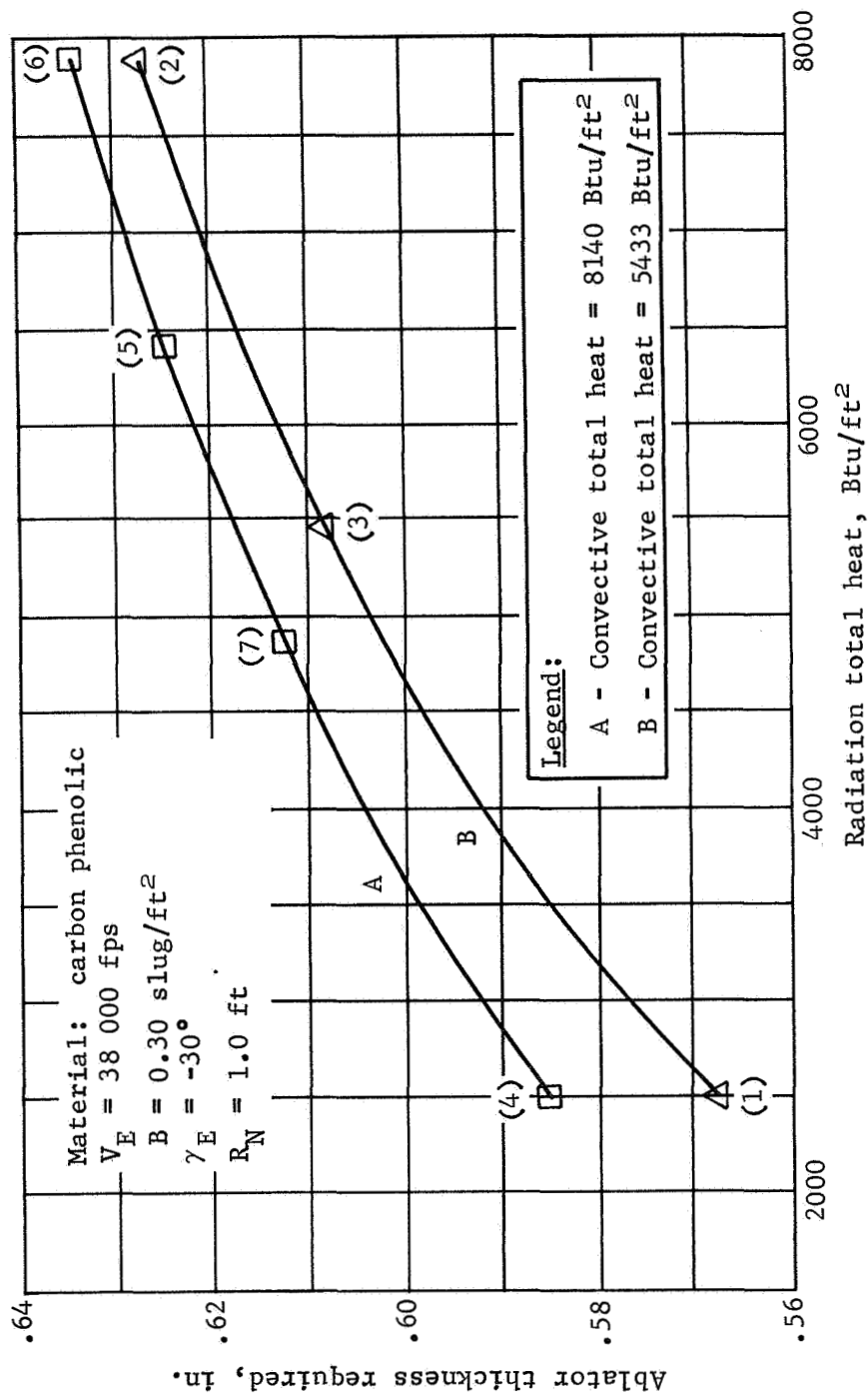


Figure B5.- Stagnation Point Ablator Sensitivity to Radiation Heating

APPENDIX B

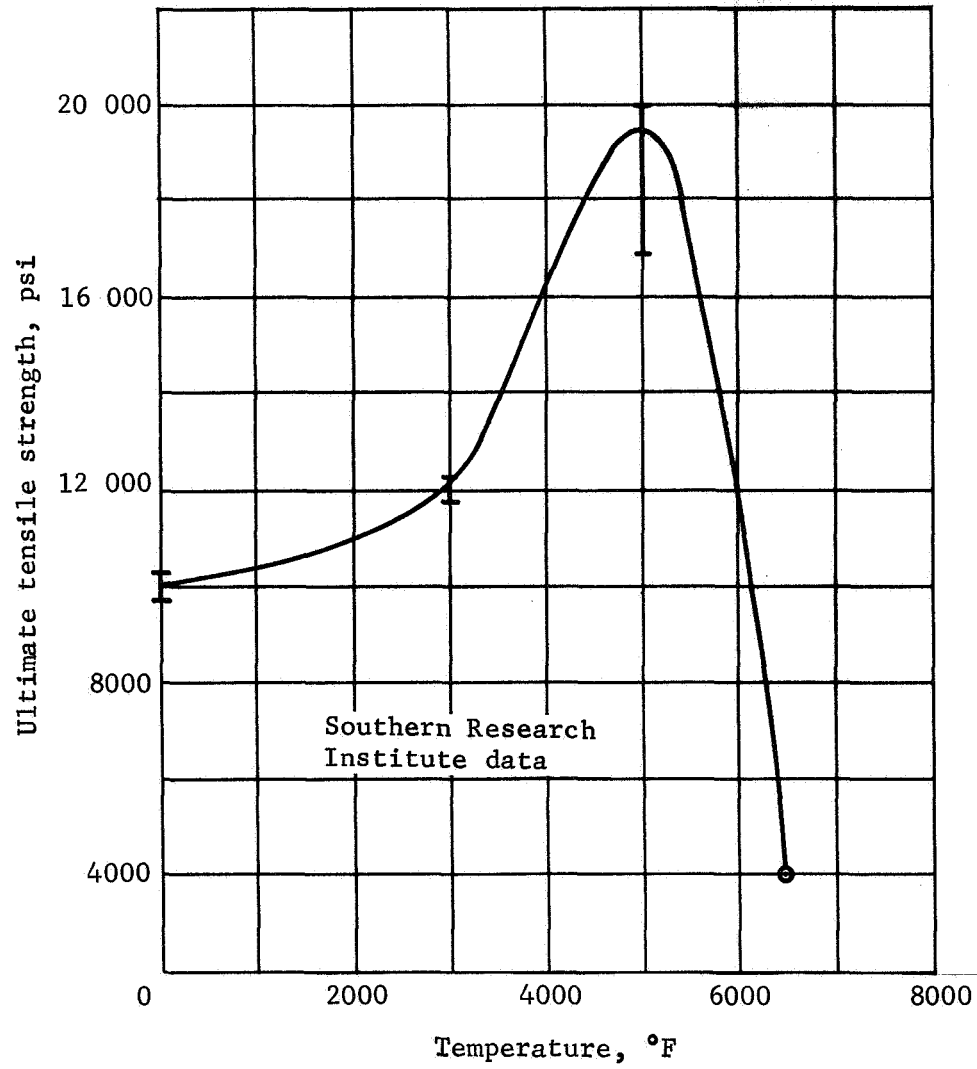


Figure B6.- Ultimate Tensile Strength of AXF-5Q POCO Graphite (ref. B3)

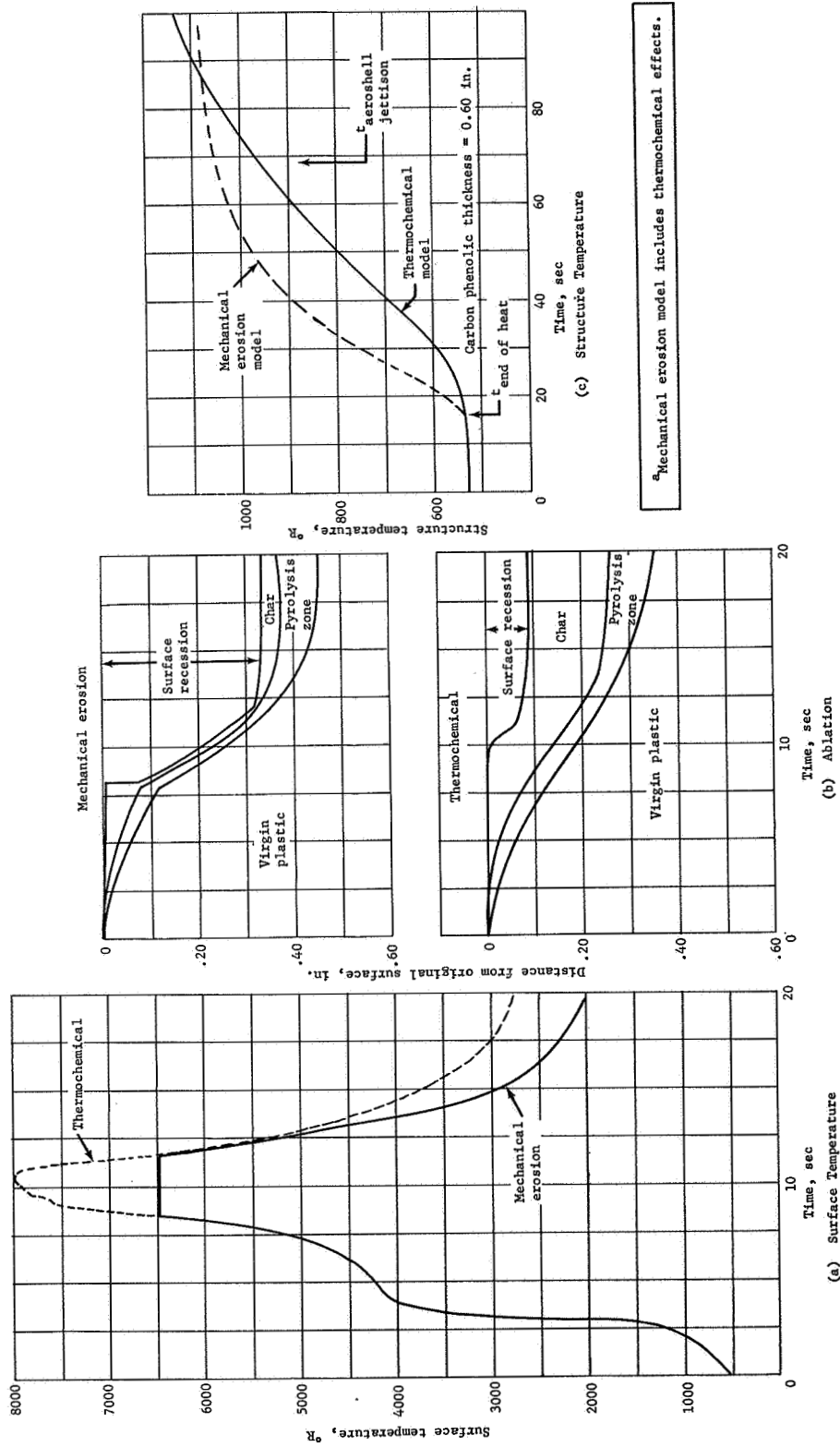
APPENDIX B

The nominal ablation of carbon phenolic compared to the above shear model is shown in figure B7 for the V/M flyby design trajectory. The surface temperature reaches 6000°F at approximately 9 sec. At this time, the char that has been built up is assumed to spall. The surface erosion rate subsequent to this time is controlled by the rate at which heat can be absorbed by the material and rapid recession takes place. At 12 sec, the surface temperature drops below 6000°F because the surface heat flux is decreasing and normal char growth once again takes place. For this case, the mechanical erosion results in a backface temperature increase 90°R above the design value in spite of the fact that the surface recession is increased from 0.085 to 0.34 in. This result is due to the fact that the heat that is stored in the carbon phenolic is reduced by mechanical erosion.

The ablation resulting from the loss of char strength on ESA-5500(M) material is compared to the thermomechanical ablation and the ablation of ESA-5500 in figure B8 the direct entry mission. For the ESA-5500(M) material, the loss of char strength at 6000°F will result in an increase in surface recession from 0.058 in., resulting from chemical erosion to 0.187 in. The structure temperature rise is 140°R greater when mechanical erosion is considered. This in itself is not catastrophic; however, the fact that the remaining thickness is only 0.063 in. and the rapid structure temperature rise indicates that additional thickness will be required to provide a reliable design. Even with the additional thickness requirement, however, the lower density ESA-5500 material will still retain a definite weight advantage over the carbon phenolic for the direct and orbital entries.

Carbon vapor property sensitivity.— The thermodynamic performance of graphitic materials has been the subject of considerable controversy for sometime. Various estimates of the heats of formation of the carbon vapor species evolved at high temperatures have been put forward. An excellent summary of these is presented in reference B4. To evaluate the effect of this uncertainty, analyses were conducted using the two different carbon-vapor pressure curves (fig. B9) that represent the two extremes presented in reference B4. The JANAF data have been used in the design analysis for this study.

The results of analysis conducted for the direct BVS mission are shown in figure B10 (refs. B5 and B6). These data show that although relatively large differences in surface temperature and surface recession result from using the different carbon-vapor properties, the structure temperature is only slightly affected. The properties used in the design analyses (JANAF) are conservative.



^aMechanical erosion model includes thermochemical effects.

Figure B7.- Carbon Phenolic Ablation Sensitivity, V/M Swingby
($V_E = 44,000$ fps, $\gamma_E = -30^\circ$, $B = 0.60$ slug/ft²)

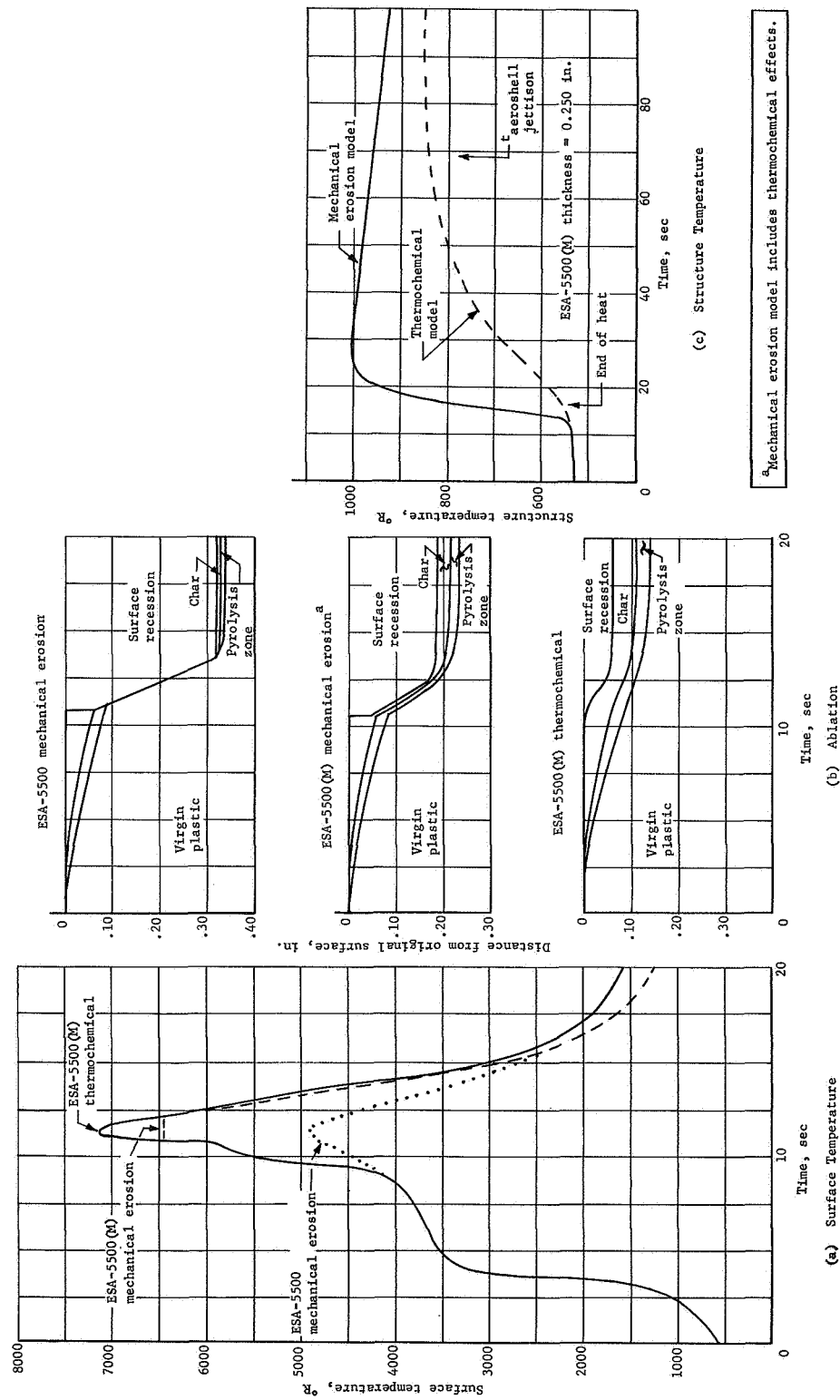


Figure B8.- ESA-5500 and ESA-5500(M) Ablation Sensitivity, Direct Entry
($V_E = 38,000$ fps, $\gamma_E = -30^\circ$, $B = 0.30$ slug/ ft^2)

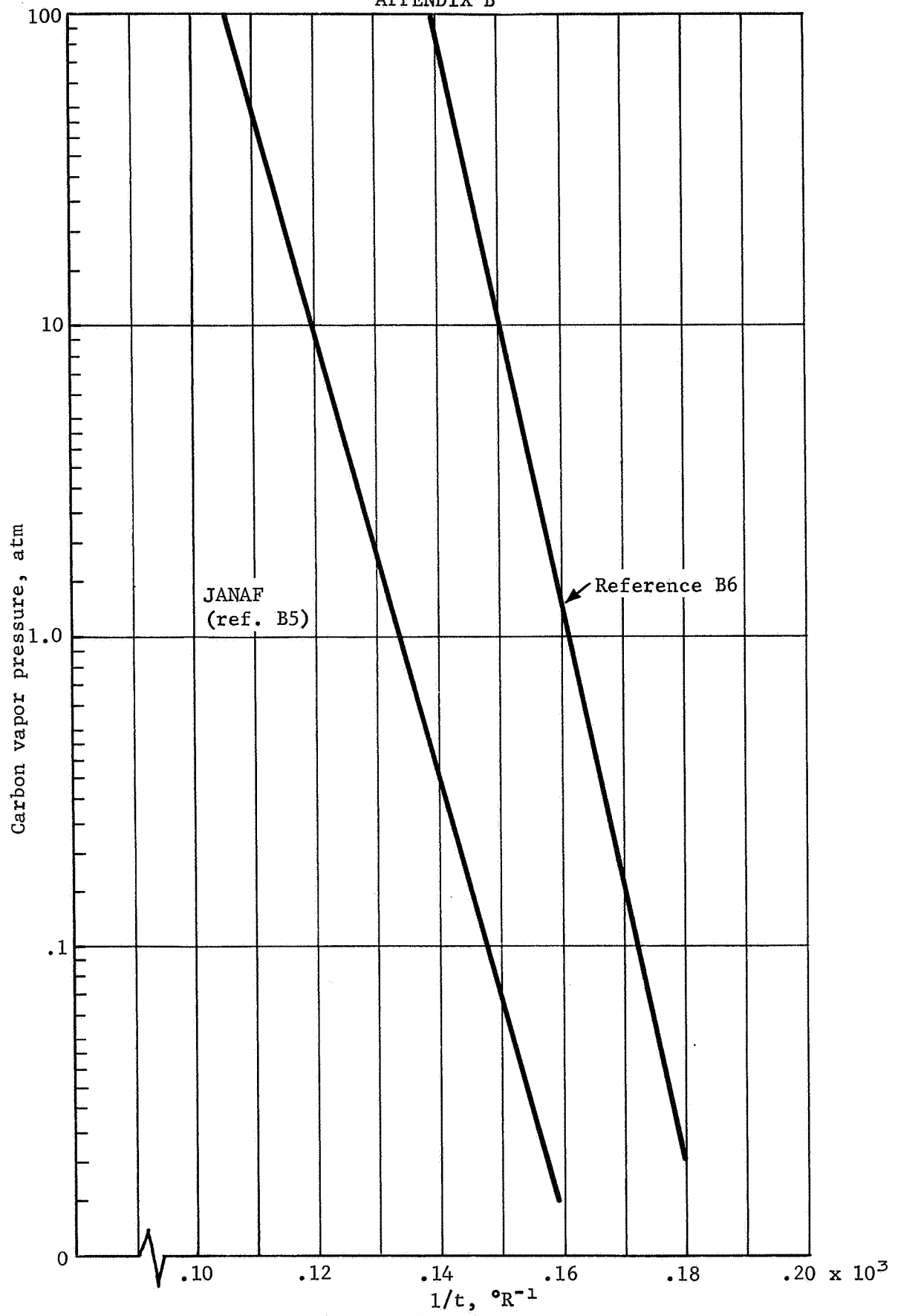


Figure B9.- Carbon Vapor Pressure

APPENDIX B

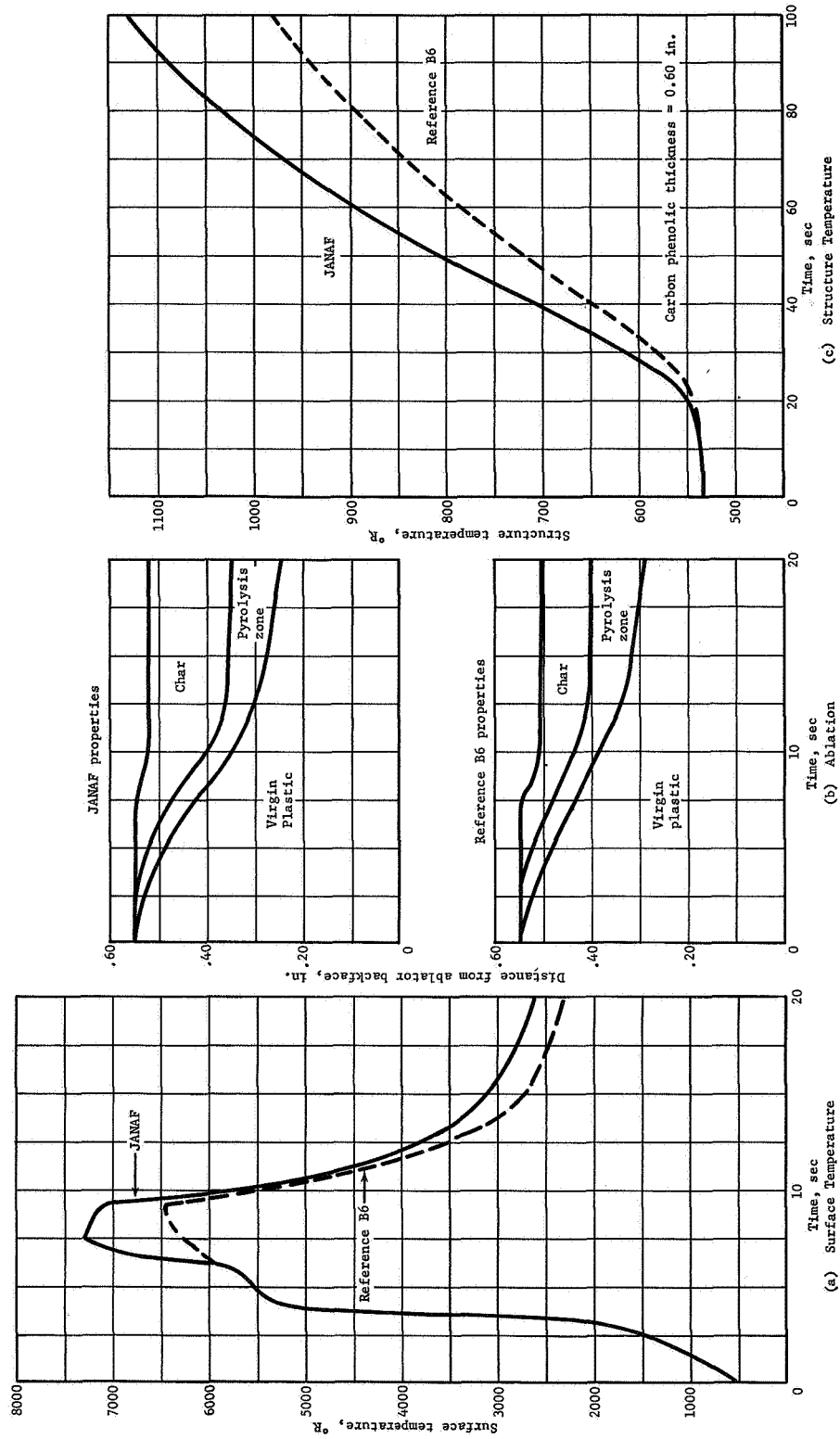


Figure B10.- Effect of Carbon Vapor Properties on Carbon Phenolic Ablation
 $V_E = 38\ 000\ \text{fps}$, $B = 0.30\ \text{slug/ft}^2$, $\gamma_E = -40^\circ$, Stagnation
 Point $R_N = 1.0\ \text{ft}$

HEAT SHIELD DEVELOPMENT REQUIREMENTS

Entry Simulation Testing

Regardless of the material used for the heat shield, even though it is one with extensive flight and ground test experience, a substantial number of development tests will have to be conducted because:

- 1) The formulation and fabrication processes will be different for this application because of the large diameter shallow cone configuration and the requirements for sterilization at high temperatures (the latter affects cure cycles and fabrication sequence of events). Consequently existing performance data may not be valid;
- 2) The Venus entry environment features several unique characteristics as discussed previously, i.e.,
 - a) Very high levels of radiation heating in addition to convective heating,
 - b) High-intensity ultraviolet radiation,
 - c) A high percentage of CO₂ in the atmosphere,
 - d) High surface shear forces in conjunction with very high surface temperatures occur over large areas of the surface.

Also, in the case of rigid materials such as carbon phenolic, a potential problem exists relative to thermal and load induced stresses because of the large diameter relatively thin shell configuration of the heat shield.

Relative to the degree of simulation required in ground tests, it should be pointed out that in no major heat shield design has a complete simulation of the flight environment been possible. In fact, seldom has it been possible to produce the combination of peak levels simultaneously on even a small sample of the material, although this is always the goal. Consequently, the major objective of entry simulation test is to confirm or to establish an analytical model that is then used in design. If the model is heavily dependent on empirical correlations, it is necessary to constrain the design to the range of test conditions, or to use large margins. If the analytical model is a fairly fundamental expression, designs beyond the range of the test data are practical, but more extensive testing is required and design confidence is necessarily lessened.

APPENDIX B

Simulation Requirements for Venus Entry

Surface shear forces should be simulated through the full range of values anticipated in flight, which means cold wall values of 30, 70, and 120 psf for the 32 000, 38 000, and 44 000 fps entry velocities, respectively. These shear forces must be induced in conjunction with a heat flux capable of producing the peak entry surface temperatures calculated in the absence of mass loss by erosion, 6000, 7000, and 8000°R, respectively. Pressure levels should approach 1 atm or greater. These conditions can be achieved in existing plasma arc and laser-plus-cold flow facilities using pipe flow and/or shear wedge models. Shears should also be imposed on models at intermediate surface temperatures and, in these, it will be important to employ CO₂/N₂ as the test fluid because oxidation and other chemical processes will be the predominant contenders with the shear forces for the surface carbon instead of the sublimation process. This type of test can also be performed in existing plasma arc facilities.

Another critical parameter is combined radiant and convective heating. Here, however, it is believed that achievement of peak combined flux values, though highly desirable, is not mandatory. Test points should achieve at least two things: (1) radiant levels sufficient to generate ablative gas mass injection rates that reach or approach the cutoff point in the mass injection vs convective heat blocked relation, and (2) they should produce surface temperatures up through the chemical reaction and well into the sublimation regime with appropriate pressure levels. Assigning specific values of \dot{q}_c and \dot{q}_R to achieve these criteria is difficult because they will vary with the material being tested. However, the \dot{q}_c of 4000 Btu/ft²sec and \dot{q}_R of 1750 Btu/ft²sec planned for the Ames advanced facility should satisfy the minimum criteria stated above even for the 44 000-fps entry with the materials of interest. The peak conditions for the 38 000-fps entry ($\dot{q}_c = 1600$ Btu/ft²sec and $\dot{q}_R = 1700$ Btu/ft²sec) are seen to fall within the ranges of the Ames facility.

A third aspect of the entry environment, the concentration of more than one-half the shock layer radiant energy in the ultraviolet wavelength region, is also of concern. Because the high energy photons of the vacuum ultraviolet region have an undesirable effect on plastic materials even at moderate flux levels, the question of whether a very high flux level will produce an unusual response in the carbonaceous chars of the ablative heat shield materials should be given some attention. No facilities exist or are

APPENDIX B

planned that produce high ultraviolet flux levels; hence, it appears that an attempt should be made to evaluate this phenomenon on a laboratory scale and then decide whether a materials test facility is required, or whether, in fact, the energy can be treated as being absorbed at the surface and converted to heat as is presently assumed. The final aspect of ground test simulation is that of large-scale verification tests. The case of a 3/4-in. thick, 8.5-ft diameter shell constructed of a dense, high-modulus heat shield material bonded and/or mechanically attached to a thin, shallow-cone metal structure presents an entirely different situation relative to thermal/structural interaction than any heat shield design concept previously considered. With this arrangement, which is the most likely for a 44 000-fps entry, the conduction of a large-scale overall thermal/structural integrity test becomes almost a necessity. Even with less dense and less rigid materials, a demonstration of the absence of warping or bond failure should be considered.

The question is, "To what percentage of peak flight temperatures should such a test be conducted to properly represent a verification test?" The answer lies with the evaluation of thermal gradients or temperature distributions, primarily those through the thickness but also those along the cone's length. It may be that existing quartz lamp facilities can be used for the test even though temperature peaks of only the order of 4000°R could be attained, compared with 8000°R predicted for flight. Other possibilities would be the development of a higher-surface-temperature-producing facility involving resistance heated graphite rods or a graphite shell, the use of large-diameter nozzle plasma arc facilities and, less likely, the use of rocket engine exhaust facilities. Another possibility, not yet adequately evaluated, is that of conducting earth entry flight tests.

Conclusions

Heat shield design analyses have been conducted to determine the amount of ablative material required to protect the BVS/entry vehicle structure, equipment, and scientific payload from the entry thermal environment. The results of this study have shown that it is feasible to provide such protection with ablative materials that are now considered operational. Since the Venus entry thermal environment and the predicted response of ablative materials exceeds in severity the range of experience gained in Earth reentry flight and ground tests, it has been necessary to extrapolate beyond existing data. Examination of sensitivity to unknown factors, indicates, however, that the resulting designs are conservative.

APPENDIX B

Another conclusion, relative to the influence of test facility limitations on mission selection, is that at this stage none of the missions studies should be ruled out for reasons of less than total simulation capability although an awareness of the increased development costs and the somewhat greater design risk of the high velocity entries (44 000 fps) should be accounted for in mission trade studies.

REFERENCES

- B1. Welsh, W. E.; and Ching, A: A New Technique for Mechanical Strength Testing of Rapidly Charred Ablation Materials. AIAA J., vol. 5, no. 10, pp. 1882 - 1885.
- B2. Anon.: Buoyant Venus Station Mission Feasibility Study for 1972-1973 Launch Opportunities, Attachment 1, Appendix A. Martin Marietta Corporation, Denver, Colo. June 1968 (Contract NAS1-7590).
- B3. Anon.: Semiannual Technical Progress Report, RESEP 18 April-18 October 1966 (SRI data). DAC-59143. Douglas Aircraft Co.
- B4. Dolton, D. A.; Maurer, R. E.; and Goldstein, H. E.: Thermodynamic Performance of Caron in Hyperthermal Environments. AIAA Paper no. 68-754, Presented at AIAA 3rd Thermophysics Conference, Los Angeles, Cal., June 24-26, 1968.
- B5. Anon.: JANAF, Interim Thermochemical Property Tables. The Dow Chemical Company, Midland, Mich.
- B6. White, H. M.: Estimation of Some Carbon Properties at the Triple Point. TOR-669(S681-20)-12. Aerospace Corporation, June 1966.

APPENDIX C
SPACECRAFT MODIFICATIONS

by Ronald E. Frank and Jack Pettus
Martin Marietta Corporation

APPENDIX C

LUNAR ORBITER

The modified Lunar Orbiter as defined in NASA CR-66302, Study of Applicability of Lunar Orbiter Subsystems to Planetary Orbiters, was specified as the spacecraft for the orbital mission. (The report describes modifications of the Lunar Orbiter for the Mars and Venus missions.) Both versions include -- in addition to the basic spacecraft -- an entry probe system of 115 lb.

No major problems of compatibility between the Lunar Orbiter and the BVS have been identified. However, the assessment was performed only to the detail that could be supported by the referenced report and should be considered as a general survey only.

Of greatest concern was the weight that must be put into orbit, consisting of both the spacecraft and the capsule system. This resulted in a highly eccentric orbit ($e = 0.8$) for the mission. No attempt was made to assess the reasonableness of the Boeing weights; however, it should be noted that a stated guideline of their orbiter study was to use existing proven systems, and no emphasis was placed on reducing weight.

The required modifications to the Lunar Orbiter are summarized in table C1.

Figure C1 shows the orbiter spacecraft with the BVS capsule attached. The major modifications indicated are the larger orbit insertion propulsion module, a scan platform and relay antenna. In addition, the solar panels are shown extended to prevent shading by the 8.5 ft entry vehicle.

The baseline orbiter weights as specified in NASA CR-66302 are restated in table C2. The total orbiting weight of this table (925 lb) is reduced by 149 lb (velocity control) and 115 lb (probe) to arrive at a value of 661 lb "useful weight in orbit" for this mission.

Further modifications required for compatibility with the BVS mission are summarized in table C3. The incremental weight change identified was considered to be small enough to be neglected within the scope of this investigation. On this basis, the all up weight (weight on launch vehicle) becomes:

BVS/EV system	1126 lb
Spacecraft	661
Spacecraft propulsion system (burnout)	298
Midcourse and orbit insertion propellant	1339
Spacecraft-to-booster adapter	<u>174</u>
All up weight	3498 lb

APPENDIX C

TABLE C1.- SPACECRAFT MODIFICATIONS

Modification	Purpose	Justification
Structural modification to support capsule	To provide strength to support capsule	Additional mass due to capsule
Modify S/C attitude control system	Planetary vehicle stabilization during cruise and orbit and origination for capsule separation	Increase of mass to be stabilized/oriented
Add separation system for capsule	To separate capsule	Several discretes required to power up and separate capsule
Modification of S/C thermal control	Control of S/C temperature	Presence of capsule will modify heat balance
Modification of solar panels	Provide view of sun	Presence of capsule will shade present panels
Modification of power system	Provide power to capsule and added S/C systems	See capsule power requirement and other S/C modifications
Add receiver	Receive BVS/entry vehicle telemetry data	Orbiter must provide relay link to Earth
Add bit synchronizer	Bit by bit synchronization of BVS data stream before entry into tape memory	See communications section above
Add command transmitter	To transmit commands to the BVS	Several commands are required to perform the BVS mission
Add command tone generator	To key the command transmitter	Allows commands to be generated
Add rf multiplexer	Provide common connection to the antenna for the two receivers	To allow for single antenna
Add tape recorder	Provide storage for BVS/EV data	Approximately one million bits of data must be stored during entry and deployment of BVS
Add relay antenna	Provide TM link for BVS/EV	Relay link is required
Add new propulsion module	To effectively eliminate gravitational losses during orbit insertion burn ($T/W > 0.2$)	Insertion of total planetary vehicle into orbit does not allow for orbit insertion losses using Titan IIIC booster
Add scan platform	Provide planet coverage for S/C science	
Add sequencer discretes	Provide signals for BVS/EV pre-separation and separation	

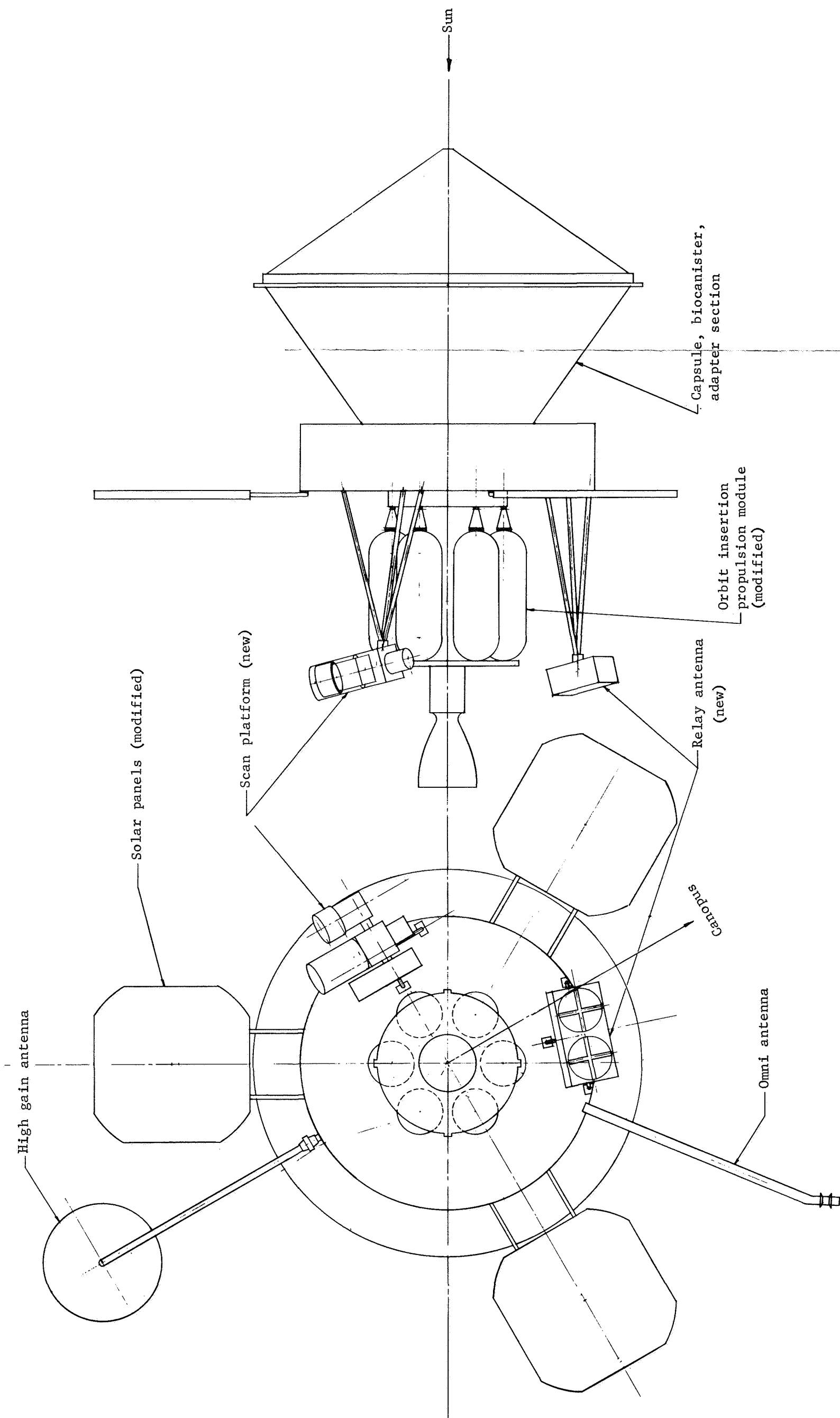


Figure C1.- Orbiter Spacecraft with BVS Capsule

APPENDIX C

TABLE C2.- SUMMARY WEIGHT STATEMENT^a

	Weight, lb	
	Venus	Orbiter
Science payload		
Science	109.0	
Probe (fixed plus separated weight)	^b 115.0	
Subsystems		304.0
Power	138.0	
Telecommunications	72.0	
Programmer CC&S	32.0	
Attitude control	62.0	
Velocity control (included N ₂ gas and fuel reserves)	^b 149.0	
Structures and mechanisms		170.0
Assembly and integration		<u>78.0</u>
Total (useful) orbiting weight		925.0
Propulsion and gas		995.0
Attitude control gas	15.0	
Fuel	377.0	
Oxidizer	603.0	<u> </u>
Total spacecraft weight		1920.0
^a Taken from Boeing Report NASA CR-66302, pp. 4-248, Table 4.6.7.7.		
^b Deleted for BVS study.		

APPENDIX C

TABLE C3.- SPACECRAFT MODIFICATIONS AFFECTING WEIGHT

Item	Weight increment, lb
Structure	Could not be estimated
Telecommunications	
Receiver	+3.0
Bit synchronizer	+1.0
Command transmitter	+4.0
Command tone generator	+2.0
RF multiplexer	+6
Tape recorder	+12.0
Relay antenna	Replaces Boeing added antenna
Power	Minor cabling addition not estimated; sufficient power available
Assembly and integration	
Cabling	Could not be estimated
Science	<u>-11.0</u>
Net weight change	+12

With this payload on a Titan IIIC, which has a total capability of 3850 lb for this mission, the margin is 352 lb.

The orbit-insertion maneuver is a critical factor, especially for the mode of carrying the total planetary vehicle into orbit. Using a 100 lb_f thrust engine, as proposed by Boeing (thrust/initial weight = 0.03), the gravitational losses amount to 26%, approximately 333 lb of propellant.

To reduce the gravitational losses to a negligible amount the propulsion module has been revised to incorporate the Apollo sub-scale engine with a thrust level of 2200 lb. Assuming no losses, the curve of figure C2 indicates the orbit eccentricity that can be achieved as a function of BVS/entry vehicle system weight.

APPENDIX C

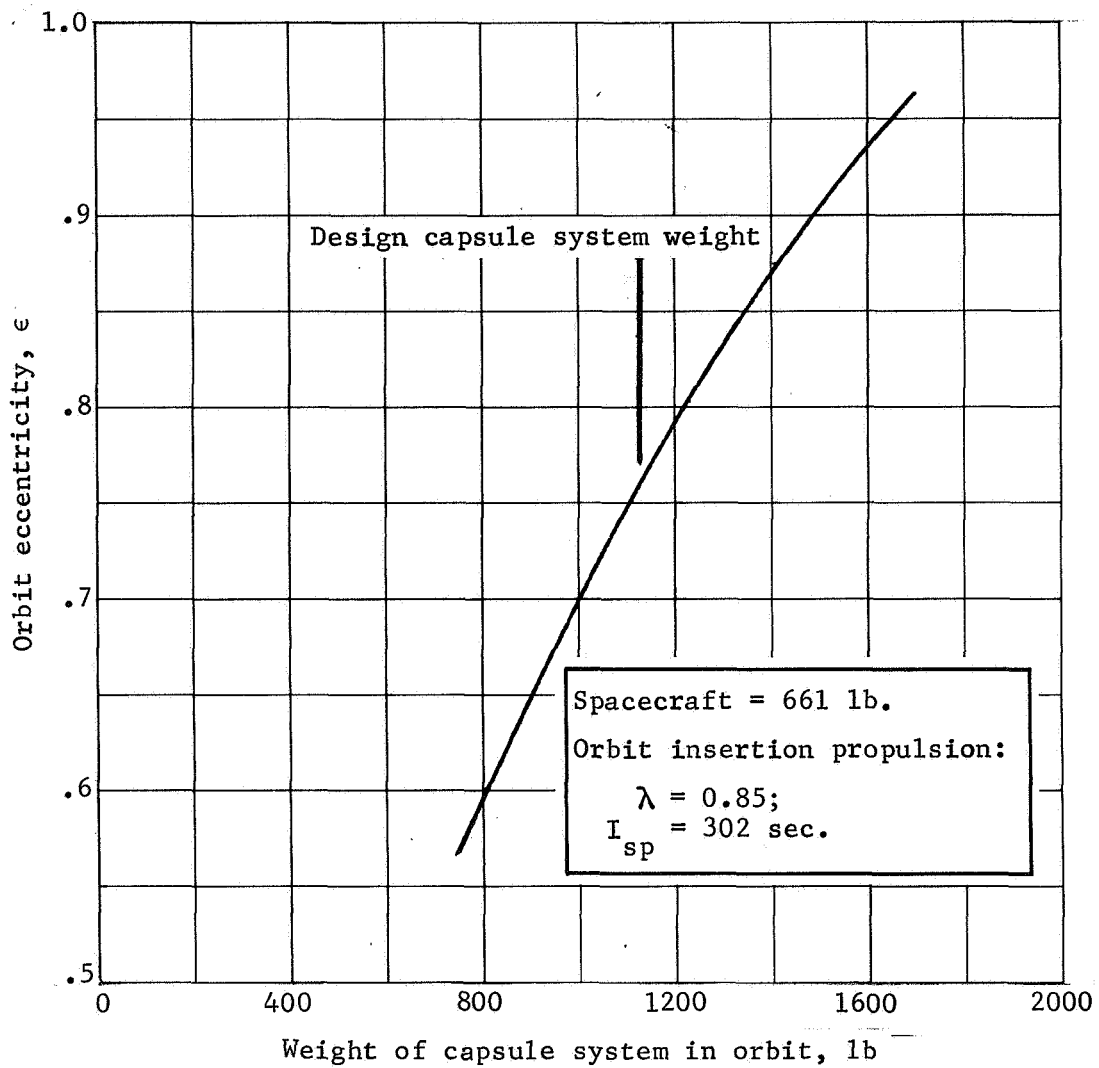


Figure C2.- Performance Capacity, Capsule System Weight in Orbit vs Orbit Eccentricity

APPENDIX C

System Compatibility

Telecommunications.— The major telecommunications support functions that the spacecraft must provide for the subsonic probe and BVS are shown in table C4.

Figure C3, reproduced from the referenced Boeing report, shows the baseline Lunar Orbiter telecommunications systems. (The S-band link to Earth appears to provide the needed bit rates.) The lower portion of this diagram shows a probe antenna, probe receiver, and tape recorder as well as TV and other science (all of which was classified as science in that report). Figure C4 is an expansion of the science equipment block of the Boeing diagram (lower portion of fig. C3) to which additional equipment required to support a subsonic probe and a BVS has been added. The balance of the science block (TV, etc.) is shown unchanged.

Additional equipment required includes a medium-gain antenna, an rf multiplexer, a bit synchronizer, a BVS data receiver, a command transmitter, command tone generator, and a second tape recorder. (It is assumed that characteristics of the probe receiver and antenna shown in the Boeing block diagram -- although not specified -- are such that they would be equivalent in cost to a vhf superheterodyne FSK receiver and vhf antenna meeting the requirements for this mission.)

The equipment required to receive BVS and subsonic probe data is briefly described below.

Receiver: A 390-MHz FSK receiver (identical to the BVS command receiver except for crystal frequency) is required to receive BVS telemetry data. A 400-MHz receiver for subsonic probe data is assumed as existing equipment.

Bit synchronizer: An additional bit synchronizer is required to perform bit-by-bit synchronization of the BVS data stream before entry of data into tape memory. It is assumed that a bit synchronizer for the subsonic probe data is existing equipment in the spacecraft.

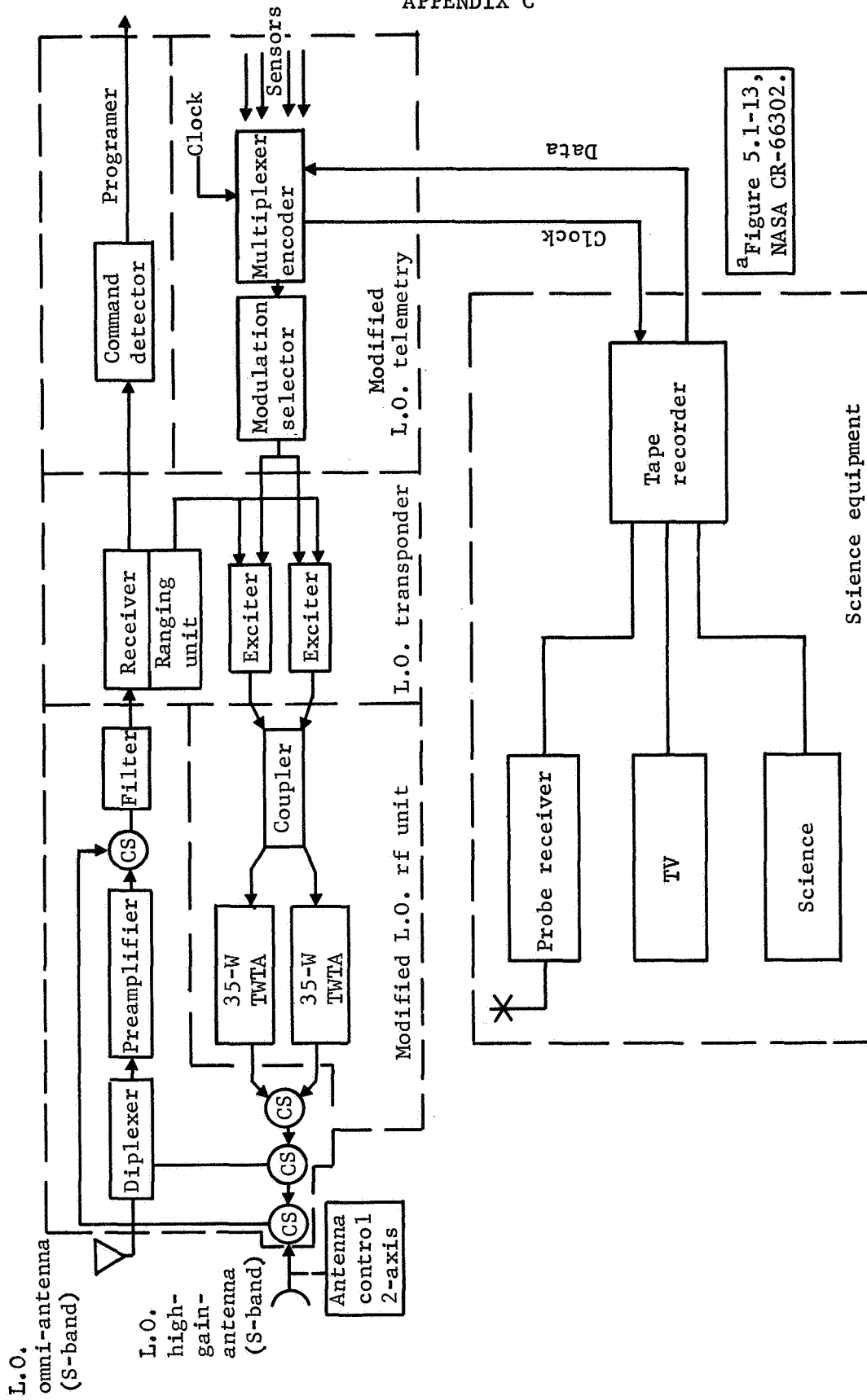
Command transmitter: The command transmitter is a solid-state unit to be frequency shift keyed by command tones from the command tone generator. Keying rates between 500 and 2000 Hz are assumed.

Command tone generator: A command tone generator is required to key the command transmitter using a three-tone sequence for each of six commands. An alert tone and three command tone frequencies are required. The tone sequence and command sequences are controlled by the spacecraft programmer and sequencer in response to Earth-to-spacecraft commands that are stored in the spacecraft.

APPENDIX C

TABLE C4.- BVS AND SUBSONIC PROBE FUNCTIONS TO BE SUPPORTED BY ORBITER SPACECRAFT

Support functions	Requirements	Comments on spacecraft equipment modifications and/or additions
Capsule status monitor functions (preseparation)	Control capsule aeroshell multiplexer and receive hardline telemetry data during cruise mode	Provide required sequencing control, routing and conditioning of aeroshell multiplexer data to S/C engineering multiplexer
Receive entry vehicle data including subsonic probe and BVS deploy data following separation from aeroshell	Receive telemetry data over BVS to S/C link during separation of capsule from S/C and during ΔV burn Receive telemetry data from BVS to S/C link during capsule entry to BVS separation from aeroshell Receive telemetry simultaneously from BVS and from subsonic probe after separation of these from aeroshell Telemetry link modulation and bit rate to be 240 bps FSK both links	Minimum equipment complement to do this: 1) Medium gain antenna array; 2) RF multiplexer; 3) FSK receiver (2 each); 4) Bit synchronizer (2 each).
Receive BVS data during orbital operations	Receive telemetry data from BVS once per orbit Provide margin for a maximum range of 18 000 km BVS transmitter is frequency shift keyed at 240 bps rate	Use same receiver and antenna as above
Beacon and command signals to control transmissions from BVS	Provide a beacon signal to alert BVS to begin transmission when S/C comes within range of BVS Provide tone command modulation to command operating mode of BVS Provide range of at least 18 000 km for command link Transmit carrier unmodulated (after commands are sent) to provide signal for doppler measurement by BVS Provide capacity for 6 discrete commands Store command sequence in S/C; sequence to be received from Earth station	Minimum equipment complement: 1) One frequency shift key modulated transmitter; 2) Tone command generator. Above equipment must be added to S/C; command storage must be provided in S/C programmer and sequencer
Storing and retransmission of data received from subsonic probe and BVS	Provide storage for 1 million bits BVS data and 500 000 bits subsonic probe data to be received simultaneously Once per orbit provide storage for 150 000 bits of data received from the BVS during a period of approximately 10 minutes Transmit data to Earth at least once per orbit	Additional equipment required - tape recorder and control Modifications - provide gating and control of data to NRT buffer of S/C programmer/encoder
Programing of spacecraft power and data transfer to accomplish the functions shown above	The turning on and off of power to receivers, recorder, transmitter, and other S/C equipment used to support the capsule and BVS must be accomplished as well as the control of data flow during receiving and retransmission of the data	The S/C programmer/computer and sequencer must be programed to accomplish these functions

Figure C3.- Unmodified Telecommunication System, Mars/Venus Orbiter^a

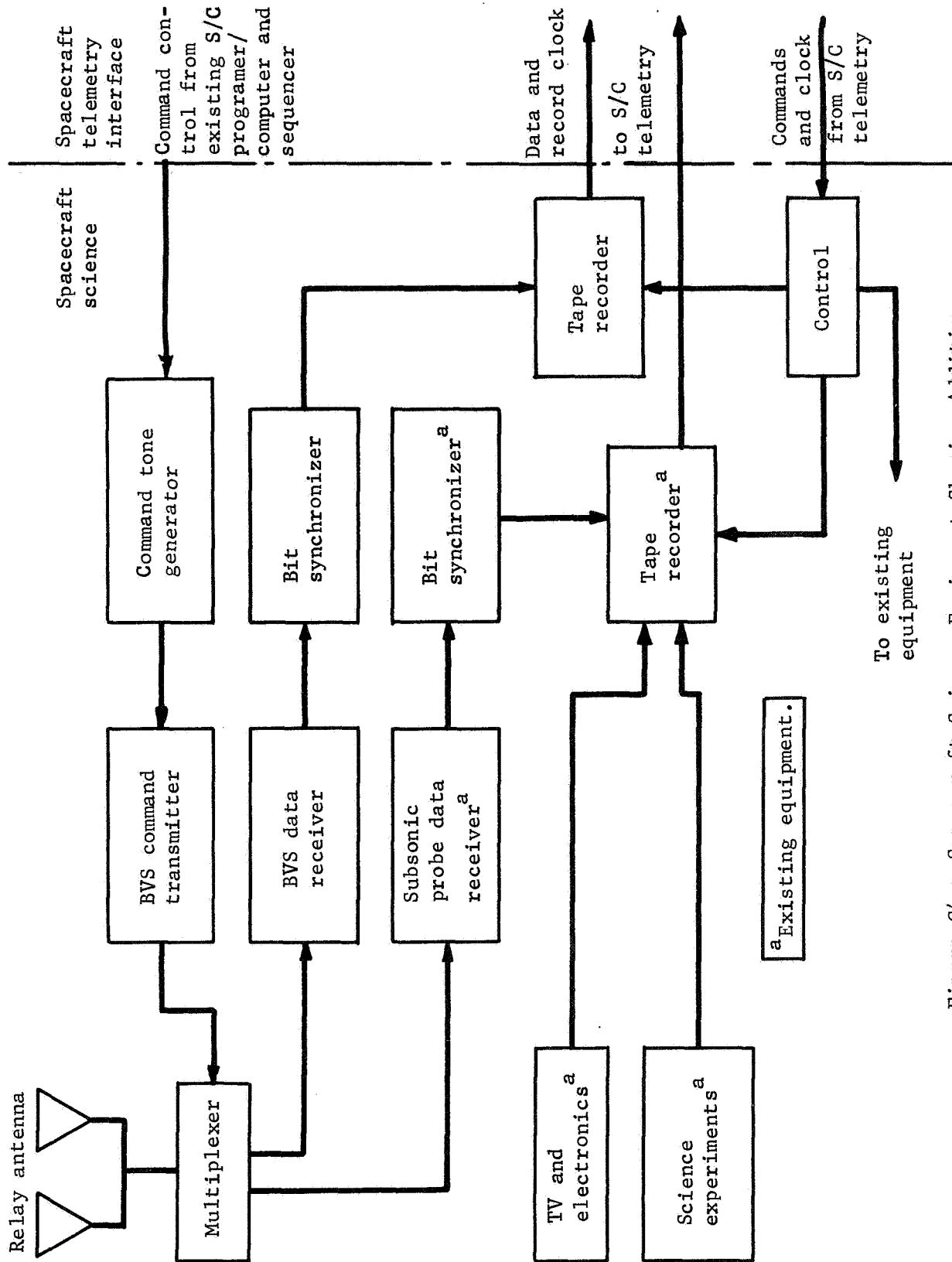


Figure C4.- Spacecraft Science Equipment Showing Additions

APPENDIX C

RF multiplexer: The rf multiplexer isolates the two receivers and transmitter and provides a common connection to the antenna for each of the units.

Tape recorder: A tape recorder for storage and playback of BVS data has been tentatively identified as additional equipment. This recorder can store BVS data during capsule entry and BVS deployment at the same time the existing recorder is storing subsonic probe data. The additional recorder will also allow the storing of TV data at the same time BVS data are being received during orbital operations.

The additional recorder should have a capacity of approximately 1 million bits and must run at playback speeds compatible with the S-band telemetry rates of 200, 400, 800, and 1600 bps (speed will depend on number of real-time words interlaced with the stored data).

Relay antenna: The relay antenna is a dual-element crossed-slot, cavity-backed antenna having an elliptical pattern. Each element is nearly identical to that of the BVS antenna that has been described earlier.

The modification and use of the remaining spacecraft equipment is assumed feasible, although detail information was not available.

Guidance, control, and navigation.- The capsule does not have the capability for maneuvering. Therefore, it is required that the spacecraft maneuver to the required deorbit attitude before capsule separation. To minimize tipoff rates at capsule separation, it is required that the limit cycle rate be limited to $0.1^{\circ}/\text{sec}$.

During the preseparation phase, command update information on deorbit engine burntime will be transmitted from Earth. This information is to be loaded into the aeroshell sequencer burntime update register. In addition, the coast timer initiate and separation sequence initiate commands will be transmitted from Earth. The spacecraft must convert these to discrete signals that will then initiate the aeroshell sequencer functions.

It is assumed that the lunar orbiter system could be modified to perform these functions.

Spacecraft science.- A proposed orbiter science payload is shown in table C5. This payload does not equal the baseline weight allowance; however, it was not feasible to assess the weight significance of the scan platform in this study.

TABLE C5.- ORBITER SPACECRAFT EXPERIMENT CHARACTERISTICS

Experiment	Weight, lb	Power, watts	Data (encounter)	Deployment, mounting	Development status
UV spectrometer	30.0 (25)	12.0	3200 bps	On scan platform	Mariner '69 Instrument
IR spectrometer	17.5	4.5	1330 bps	On scan platform	Similar to Mariner '69 Instrument
IR radiometer	7.5 (35)	3.0 (20)	600 bits/63 sec (9.5 bps)		
TV (3-color)	15.0	20.0	2.5×10^5 bits per picture 10^7 -bit storage	On scan platform	Similar to Mariner '69 Instrument
Three-frequency occultation (receivers and antennas)	8.0	4.0	100 bps	Antennas on end of solar panels	Similar to Mariner '69 Instrument
Magnetometer	5.0	5.0	30 bps	On most of omni antennas	Similar to Mariner '67
Plasma probe	15.0	10.0	50 bps	Facing sun (end of solar panel)	Similar to OGO-E
Totals Allocations	98 (109)	63.5 (72)			

APPENDIX C

Power subsystem.- The baseline Lunar Orbiter solar array (four panels) can supply adequate power for the BVS mission.

Table 5.2-3 of NASA CR-66302 lists the items making up the load demand upon the power subsystem of the Lunar Orbiter. These data form the basis of the report's figure 5.2-3, which has been replotted in figure C5 with the additional loads added for use with the BVS (cross-hatched). Modifications required for use with the BVS include addition of the following equipment:

	<u>Load, W</u>
VHF transmitter	67
VHF receiver	1.5
Bit synchronizer	1
Tape recorder	8

The first three items are in operation from 5 hr before operation of the BVS transmitter to 1½ hr afterward. The tape recorder is in operation when data are being received from the BVS (10 min) and for 20 minutes when the orbiter retransmits these data to Earth.

The modifications cause the maximum demand on the orbiter power subsystem to be increased from 281.2 to 297.8 W. This will have a negligible effect on the power subsystems.

Mechanical interface.- Figure C6 shows the 8.5-ft diameter entry vehicle mounted in the biocanister capsule adapter ring beam attached at eight places. Each of the eight attach points contain a spring to supply separation velocity when the entry vehicle separates from the spacecraft. The aft section of the biocanister is attached to the orbiting spacecraft by V-band clamps. The large diameter ring of the aft biocanister mounts the total system to the Titan III transtage payload ring frame. The forward section of the biocanister is separated pyrotechnically to allow deployment of the entry vehicle.

Electrical interface.- The electrical interface is shown in figure C7. The functions represented include a trickle charge during the cruise mode to the battery chargers mounted in the capsule adapter; status monitor of the BVS subsonic probe and aeroshell mounted equipment and command function as required.

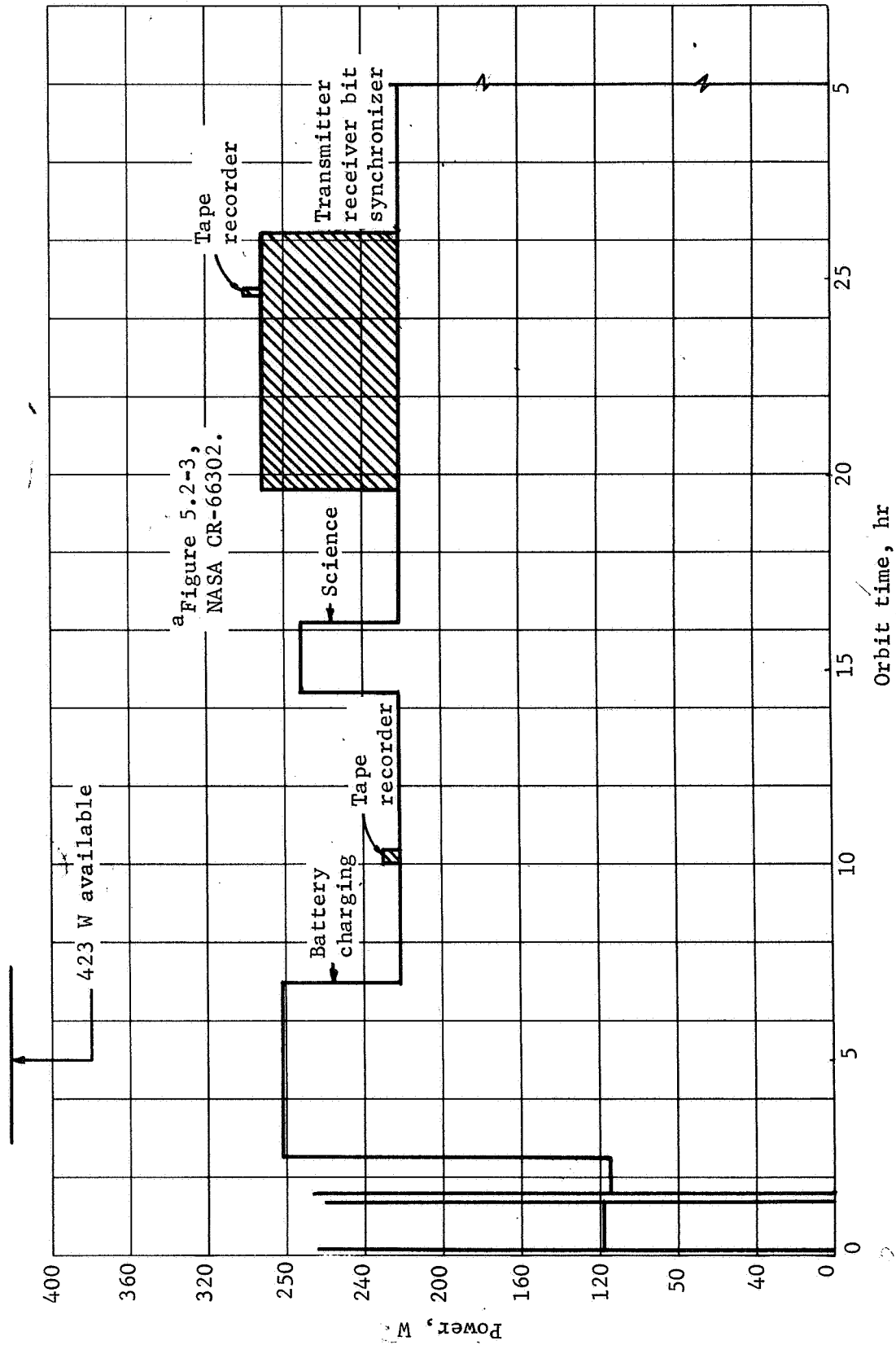
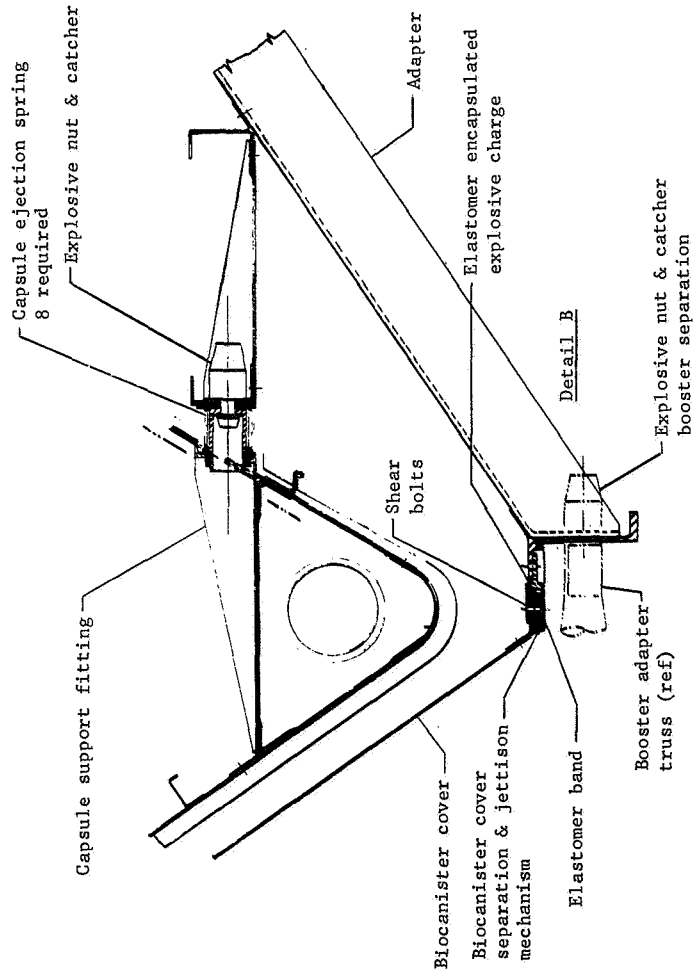
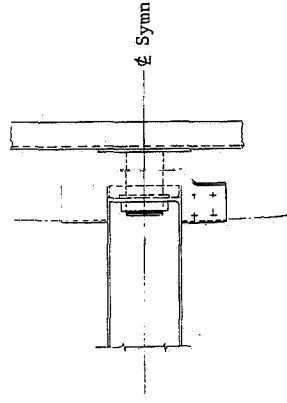
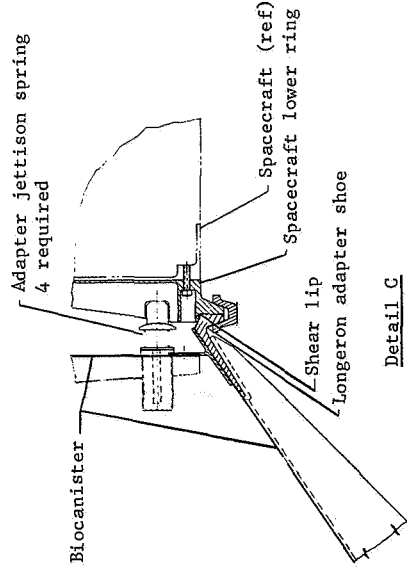
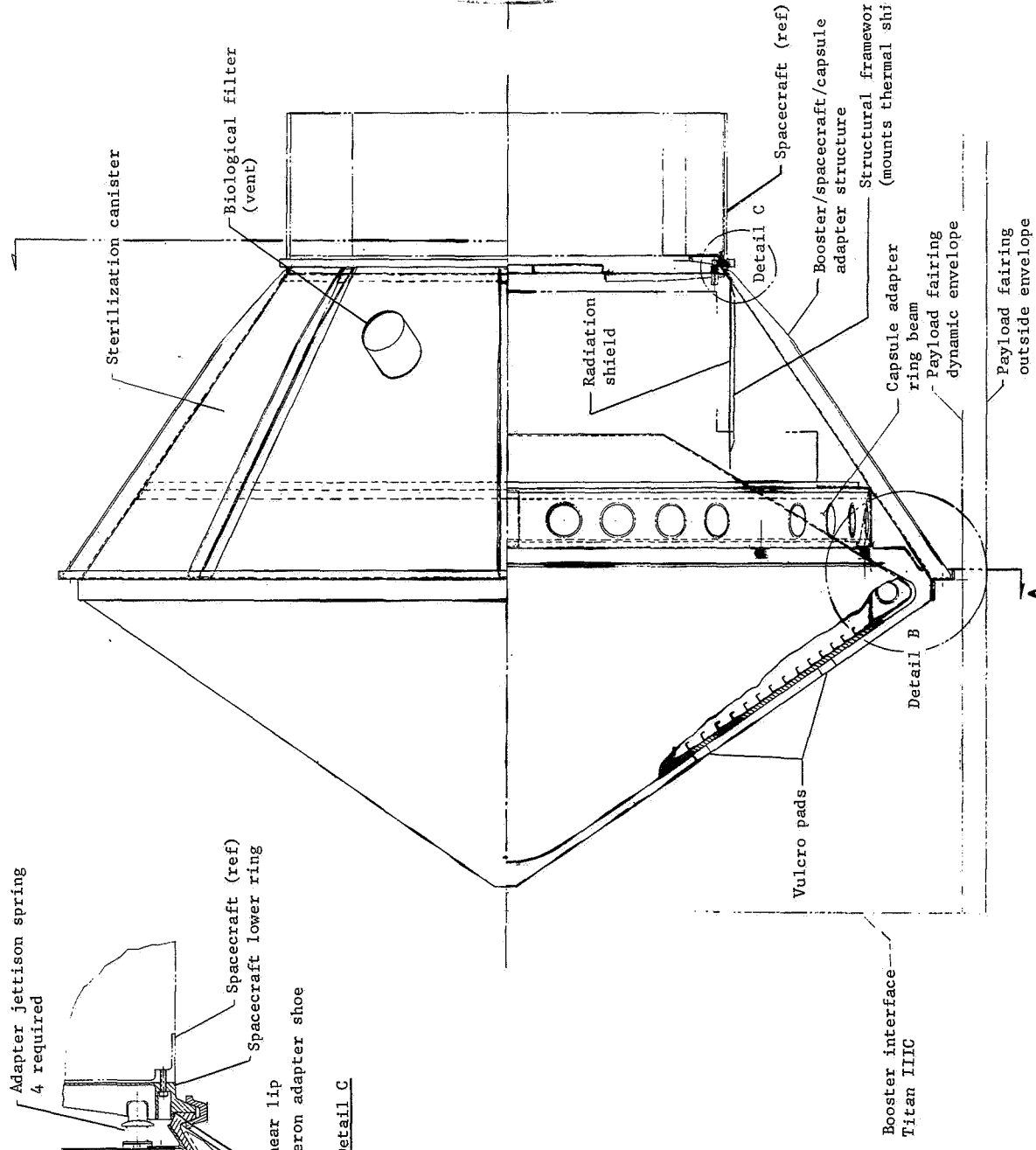


Figure C5.- Orbital Power Requirement for Spacecraft^a



APPENDIX C

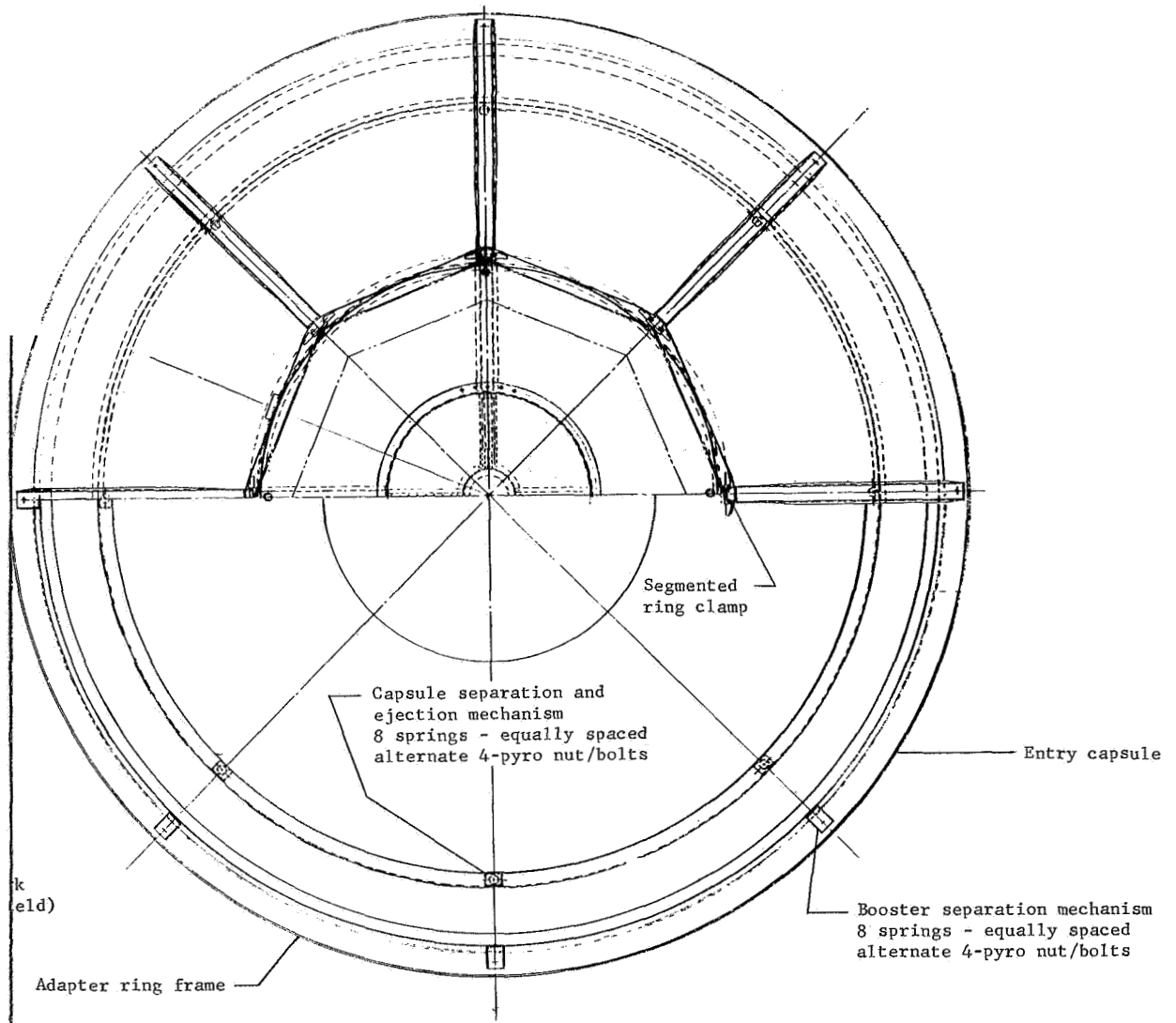


Figure C6.- BVS/Entry Vehicle

APPENDIX C

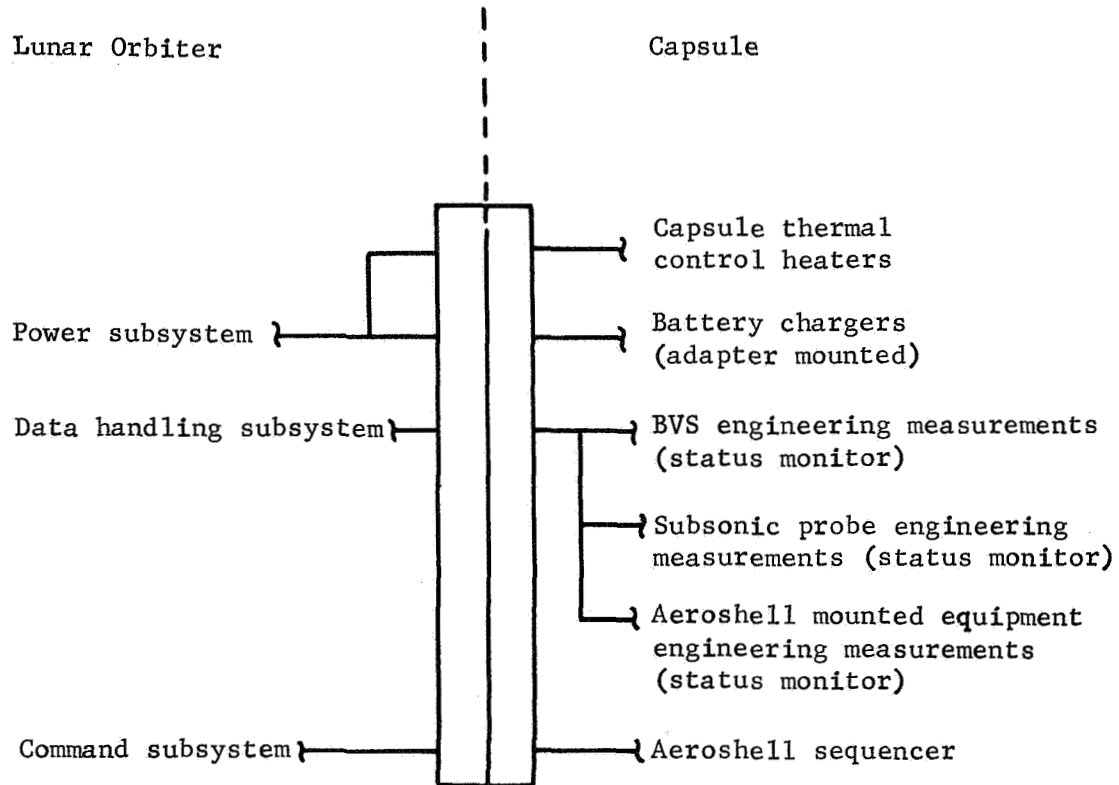


Figure C7.- Lunar Orbiter/Capsule Electrical Interface

APPENDIX C

MARINER '69

The Mariner spacecraft as defined in the Mariner Mars 1969 Functional Requirements Document, with revisions, was specified as the spacecraft for the flyby mission.

No major problems of compatibility between the Mariner '69 and the BVS have been identified. Modifications are required and are identified to support the addition of the BVS/Entry Vehicle during transit, provide status monitor of the BVS, subsonic probe, and aeroshell-mounted equipment, and provide a relay link to Earth for the BVS and subsonic probe during coast, atmospheric entry, and deployment.

The required modifications to the Mariner are summarized in table C6.

Design

Figure C8 shows the integration of the Mariner '69 spacecraft and the BVS/Entry Vehicle in its biocanister. Modifications to the Mariner '69 spacecraft are based on the requirements of a Venus flyby mission and the deployment of an entry vehicle containing the BVS. Because of the sun/Earth/Venus relationship during cruise and encounter, and the fact that the spacecraft must have a communications link with the entry vehicle up to the time of balloon deployment, several modifications to the spacecraft will be necessary. They are as follows:

- 1) The solar panels must be inverted to receive the sun from the capsule side. They must also be lengthened to prevent shading by the capsule;
- 2) The scan platform will be relocated to the opposite side of the octagonal structure, and modified as required to accept the spacecraft science complement;
- 3) The high-gain antenna will be relocated to the new cone and clock angles;
- 4) Two receiving communication systems must be mounted on the spacecraft, one for BVS entry and deployment data, and one for subsonic probe data. A relay antenna plus an additional data storage unit must also be located on the spacecraft;

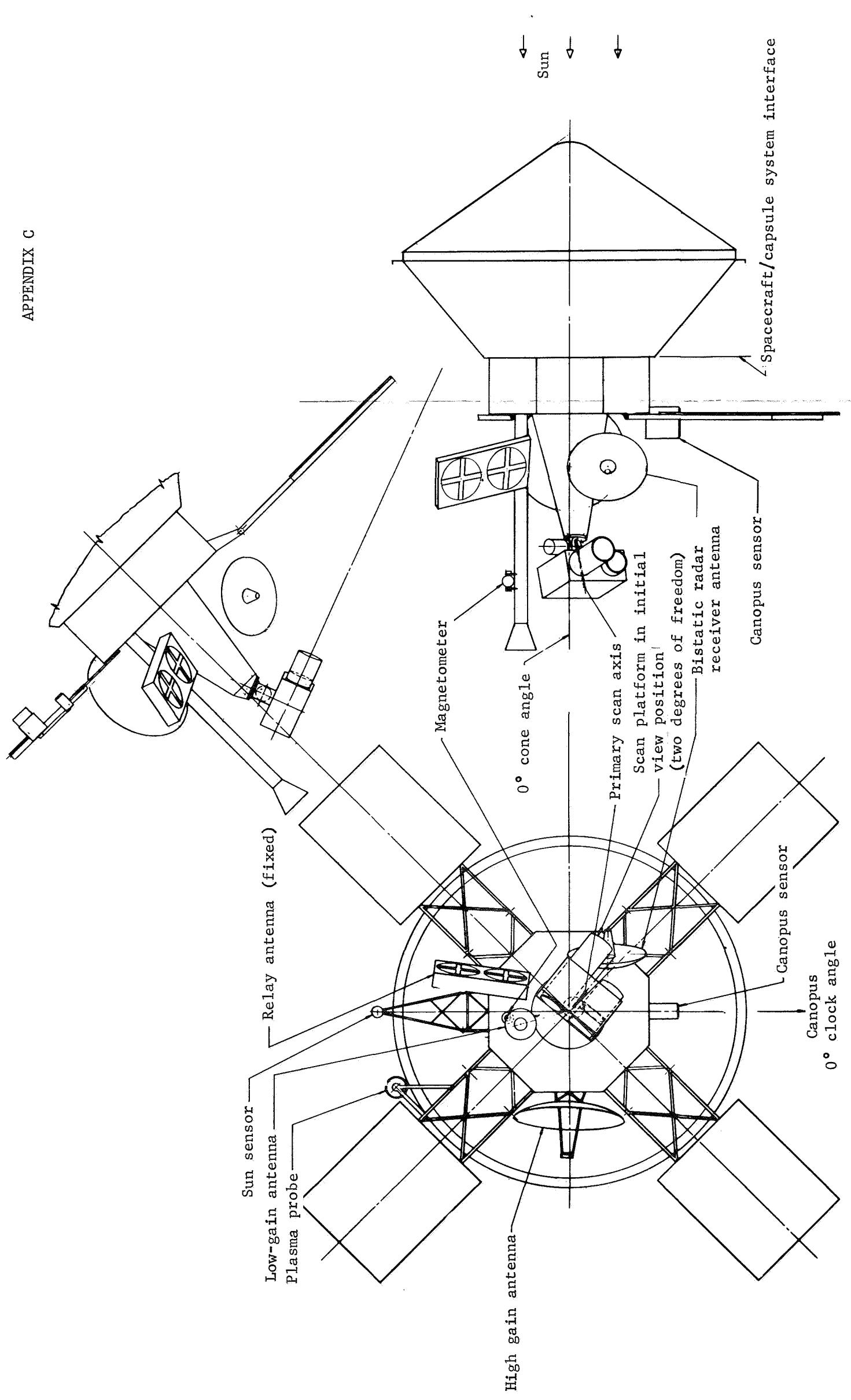


Figure C8.- Flyby Spacecraft Configuration with BVS Capsule

APPENDIX C

TABLE C6.- SPACECRAFT MODIFICATIONS

Modification	Purpose	Justification
Structural modification to attach capsule	To provide interface for capsule adapter	
Modification of S/C thermal control	Control of S/C temperature	Presence of capsule will modify heat balance
Modification of solar panels	Provide view of sun	Presence of capsule will shade panels; also panels must be rotated 180° to view sun
Modification of power system	Provide power to capsule and added S/C systems	See capsule power requirement and other S/C mods
Add receiver (2 each)	Receive BVS/EV telemetry data	S/C must provide relay link to Earth
Add bit synchronizer (2 each)	Bit by bit synchronization of BVS data stream before entry into tape memory	See communications section
Add rf multiplexer	Provide common connection to the antenna for the two receivers	To allow for single antenna
Add tape recorder	Provide storage for BVS/EV data	Approximately one million bits of data must be stored during entry and deployment of BVS
Add relay antenna	Provide TM link for BVS/EV	Relay link is required
Relocate scan platform	Provide planet coverage for S/C science and allow for capsule attachment to S/C	Scan platform mounting on same side as capsule
Add sequencer discretes	Provide signals for BVS/EV preseparation and separation plus receipt of BVS telemetry	
Reorient high-gain antenna	Provide proper orientation to Earth	Cone and clock angles different from Mars mission
Reorient midcourse propulsion engine	Provide proper midcourse maneuver	Engine must provide thrust through planetary vehicle center of gravity
Add bistatic radar antenna	View planet at subearth point during encounter	Required to perform bistatic experiment
Add plasma probe	View sun	Required for plasma experiment
Remove approach guidance subsystem	Experiment for Mars	Not required for Venus mission

APPENDIX C

- 5) The Mariner '69 midcourse propulsion engine will be realigned to act through the new center of gravity;
- 6) A bistatic radar antenna will be added to view the planet at the sub-Earth point during the encounter approach;
- 7) A plasma probe is added to view the sun past the probe canister. It is supported off the solar panel structure and deployed with it;
- 8) A mechanical/electrical interface with the capsule adapter will be required;
- 9) The approach guidance system will not be carried.

The Mariner spacecraft with the modifications made as summarized in table C6 will adequately perform the reference flyby mission.

System Compatibility

Telecommunications.— Spacecraft telecommunications support functions required of the Mariner Mars 1969 spacecraft system to support the 1972 Venus flyby mission are identified in table C7.

Additional equipment required are a relay antenna, rf multiplexer, two receivers (one each for the BVS and subsonic probe), two bit synchronizers, and a digital tape recorder. The spacecraft support equipment is shown in the simplified block diagram of figure C9. The weight and power summary is shown in table C8.

A brief description of the spacecraft equipment required to support the BVS and subsonic probe is provided below.

Relay antenna: The relay antenna is a dual-element cavity-backed crossed-slot having an elliptical pattern. Each element is nearly identical to that of the BVS and subsonic probe antennas described earlier. A gain pattern for the spacecraft relay antenna is shown in the BVS Radio Subsystem Performance section.

RF multiplexer: The rf multiplexer isolates the two receivers and provides a common connection to the spacecraft relay antenna.

APPENDIX C

TABLE C7.- BVS AND SUBSONIC PROBE FUNCTIONS TO BE SUPPORTED
BY MARINER SPACECRAFT

Support function	Requirements	Comments
Capsule status monitor functions (preseparation)	Control capsule aeroshell multiplexer and receive hard-line telemetry data during cruise mode	Provide required sequencing control, routing, and conditioning of aeroshell multiplexer data to S/C engineering multiplexer
Receive entry vehicle data including subsonic probe and BVS deploy data following separation from the aeroshell (until station is completely deployed and subsonic probe has impacted on the planet)	<p>Receive telemetry data over BVS to S/C link during separation of capsule from S/C and during ΔV burn</p> <p>Receive telemetry data from BVS to S/C link during capsule entry to BVS separation from aeroshell</p> <p>Receive telemetry simultaneously from BVS and from subsonic probe after separation of these from the aeroshell</p> <p>Telemetry link modulation and bit rate to be 240 bps FSK both links</p>	<p>Minimum equipment complement to do this:</p> <ol style="list-style-type: none"> 1) Medium gain antenna array; 2) RF multiplexer; 3) FSK receiver (2 each); 4) Bit synchronizer (2 each).
Storage and retransmission of data received from subsonic probe and BVS	Provide storage for 0.86 million bits BVS data and 0.64 million bits subsonic probe data; simultaneous reception will occur during certain mission phases ^a	Minimum equipment complement to to this - digital tape recorder
Programing of spacecraft power, data storage, and transfer to accomplish functions shown above	The turning on and off of power to receivers, recorder, and other S/C equipment used in support of the BVS and subsonic probe must be accomplished as well as the control of data flow during receiving and retransmission of the data	The S/C programmer/computer and sequencer must be programmed to accomplish these functions
^a Data volume is based on BVS transmission from S/C separation for 22 min and from BVS entry - 20 min to BVS entry + 17.5 min at 240 bps. Transmission from entry + 1.5 minutes to entry + 6.5 minutes at 240 bps was assumed for the subsonic probe. This 45-min operating period is compatible with the probe view time for a nominal spacecraft lead time of 45 min.		

APPENDIX C

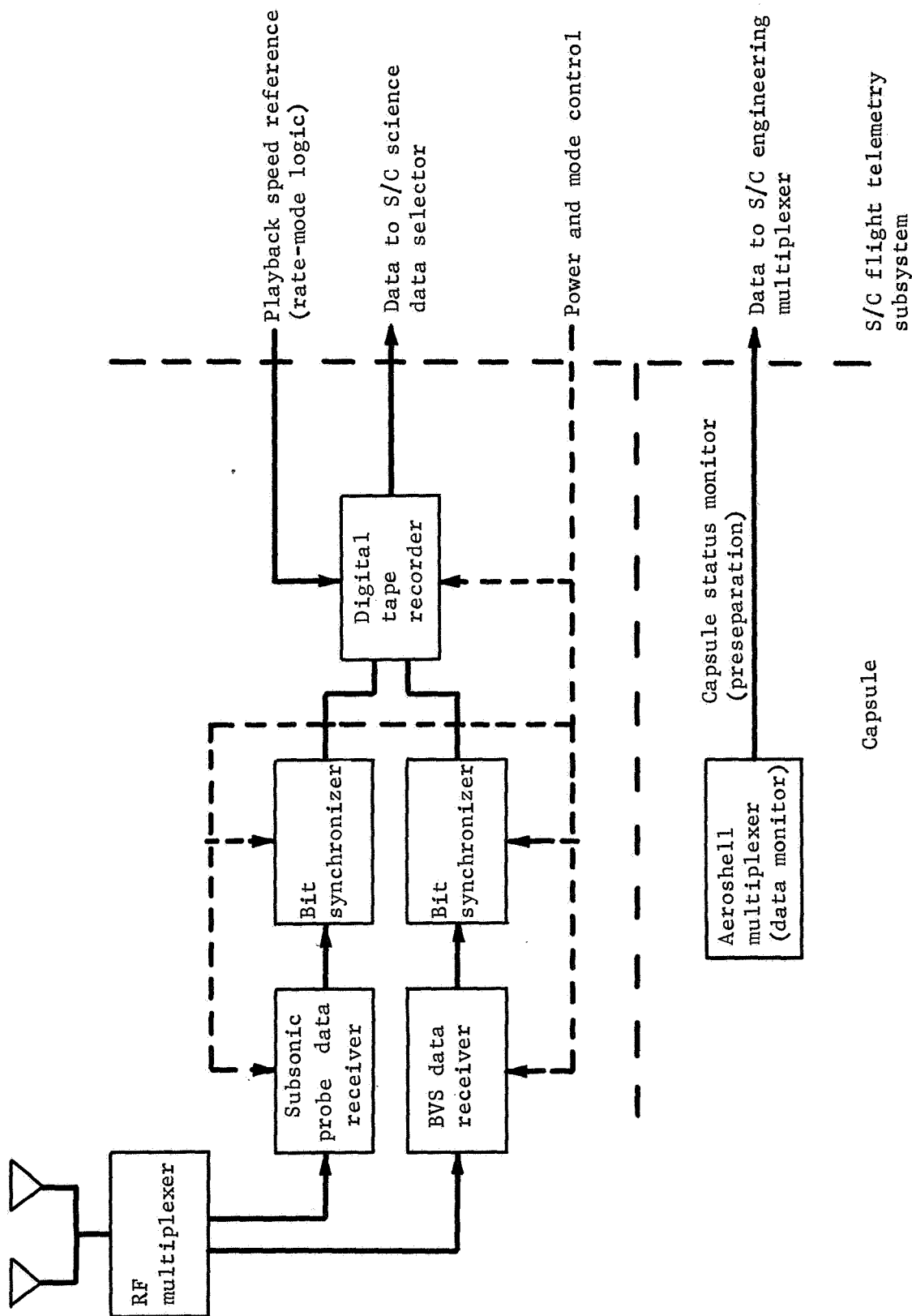


Figure C9.- Spacecraft Support Equipment

APPENDIX C

TABLE C8.- SPACECRAFT SUPPORT EQUIPMENT POWER AND WEIGHT SUMMARY

Equipment	Load, W	Weight, lb
Relay antenna	----	10.0
RF multiplexer	----	.6
FSK receiver (2)	1.5 (each)	3.0 (each)
Bit synchronizer (2)	1.0 (each)	1.0 (each)
Digital tape recorder	<u>8.0</u>	<u>12.0</u>
Totals	13.0	30.6

Receiver: Both the BVS and subsonic probe receivers are double superheterodyne frequency shift key units with mark and space predetection filters followed by square law detectors and a summer. The BVS and probe receiver nominal frequencies are 390 and 400 MHz, respectively. The receivers are of the same design as those required for the orbiter in the BVS orbital mission.

Bit synchronizer: Each bit synchronizer is required to perform bit-by-bit synchronization of the BVS and subsonic probe data streams before entry of data into tape memory. The units are of the same design as required for the orbiter in the BVS orbital mission.

Digital tape recorder: A tape recorder for storage and playback of the BVS and subsonic probe data has been identified as additional equipment. The Mariner Mars 1969 data storage subsystem functional requirements, M69-4-2016A, indicate complete use of present data storage capability is required for existing spacecraft science. The additional recorder will have a minimum storage capability of 1.5 million bits with record and playback speeds compatible with a record data rate of 240 bps and a playback data rate of 270 bps.

The additional equipment will affect several existing spacecraft subsystems, such as structures, power, cabling, flight telemetry, and the programmer. The addition of the tape recorder for example, will require more electric power, control of operating mode (record/playback) and speed, as well as implementing a playback sequence to control the output of the three recorders.

APPENDIX C

Flyby spacecraft experiments.- The spacecraft experiments and their objectives are summarized in table C9.

TABLE C9.- SCIENTIFIC OBJECTIVES AND INSTRUMENTS FOR FLYBY SPACECRAFT

Instrument or experiment	Objectives
Ultraviolet (uv) spectrometer (similar to Mariner '69 instrument)	Obtain high spatial resolution uv spectra of day side, night side, and twilight atmosphere of Venus to determine abundance and altitude distribution of upper atmosphere constituents
Infrared (IR) spectrometer and radiometer (similar to Mariner '69 instruments)	Obtain high spatial resolution IR spectra of atmosphere and clouds to provide information on atmospheric and cloud composition and structure
Photo-imaging (3-color TV)	Obtain images of cloud cover at resolutions of about 0.5 to 1 km/TV line in white, blue, and yellow light providing information on cloud structure, breaks, and circulation pattern
Bistatic radar receiver	Provide information on surface topography, radius of planet, small-scale roughness, and general reflectivity and electrical properties of surface
Magnetometer and plasma probe	Investigate planetary and interplanetary fields, interaction of solar wind with planet, define shock fronts detected by Mariner V
Celestial mechanics	Refine mass of Venus, investigate density distribution within planet

The experiment characteristics are summarized in Table C10. As can be seen, both the total weight and the power are less than that allocated so there is some margin for growth. Most of the experiment characteristics are based on those given in the JPL Mariner '67 and Mariner '69 Functional Requirements Documents.

Power subsystem.- The solar panel area for the Mariner Mars 1969 spacecraft is given as 83 ft². When flown to Venus, this panel area could produce 1050 W, based on a specific output of 12.6 W/ft². Because this power is excessive, as shown below, the area can be reduced considerably.

APPENDIX C

TABLE C10.- FLYBY SPACECRAFT EXPERIMENT CHARACTERISTICS

Experiment	Weight, lb	Power, W	Data (during encounter)	Mounting, deployment	Development status	Viewing
UV spectrometer	30.0	12.0	3200 bps	On scan platform	Mariner '69 instrument	Slit parallel to planet surface, ° within about 40° from subsolar point
IR spectrometer and IR radiometer	17.5 7.5	4.5 3.0	1330 bps 600 bits/63 sec (~9.5 bps)	On scan platform	Mariner '69 instrument	Limb-to-limb scanning, light and dark sides and space
TV (3-color)	15.0	20.0	~2.5 x 10 ⁵ bits/picture 10 ⁷ bit stor- age	On scan platform	Similar to Mariner '69	Limb-to-limb scanning light side and termi- nator
Bistatic radar receiver	15.0	5.0	~200 bps	Body fixed	Unknown, but current technology	Facing sub-Earth point on planet
Magnetometer	5.0	5.0	30 bps	On most of omni-anten- nas	Similar to Mariner V instrument	-----
Plasma probe	15.0	10.0	50 bps	Facing sun	Similar to OGO-E experiment	Facing sun
Totals	105.0	59.5				

APPENDIX C

Power requirements from Table IV of M69-3-250A, dated 15 Nov. 1967, are given below:

<u>Normal flight sequence phases</u>	<u>Mars '69, W</u>
Launch	337
Star acquisition	337
Cruise	315
Maneuver	368
Encounter	389
Playback	331
<u>Abnormal flight sequence phase,</u> <u>gyros on</u>	
Cruise	350
Encounter	428
Playback	366

Contributing to the values shown are the science power requirements listed in Table V of M69-3-250A as:

<u>Item</u>	<u>Power, W</u>
Television power	32.0
Infrared radiometer power	3.0
Infrared spectrometer power	4.0
Ultraviolet spectrometer power	12.0
Data automation subsystem power	<u>20.0</u>
Total science power	71.0

The science items listed will be replaced by those given below:

<u>Item</u>	<u>Power, W</u>
TV (3-color)	20
UV spectrometer	12
Bistatic radar	5
Magnetometer	5
Plasma probe	10
IR spectrometer	<u>20</u>
Total	72

APPENDIX C

The following loads will be added to the spacecraft power subsystem:

<u>Communications</u>	<u>Power, W</u>
FSK receiver (2)	3
Bit synchronizer (2)	2
Digital tape recorder	8
<u>Power</u>	
Chargers (2) for BVS and aeroshell batteries (operating at C/50)	20
<u>Thermal</u>	
Electric heaters for capsule	<u>38</u>
Total	71

Should all of the loads listed be connected simultaneously, the total will be 143 W added, as compared to 71 W replaced or a net gain of 72 W.

Adding the load gain of 72 W due to spacecraft modifications to the value of 428 W shown for "Encounter" (with gyros on) a total of 500 W results. Paragraph 3.4.2.1 of M69-4-2004A, dated 14 Nov. 1967, shows 464 W to be the guaranteed solar panel power capability at encounter. The maximum possible power has been shown to be 70 W over the guaranteed value. Thus, the ratio of maximum possible power to that required is 1.25. Applying this same margin to the new value for the modified spacecraft would give 625 W as the gross output capability of the solar panels. This amount of power would require an area of 49.5 ft² as compared to 83 ft² installed for the Mars mission.

Mechanical interface.- The capsule adapter interface with the spacecraft is shown in figure C2 in the orbital mission section. This interface is essentially identical to that with the orbiting spacecraft. Also, the attachment and separation mechanisms for the capsule from the adapter and the biocanister from the adapter are shown in figure C2.

Electrical interface.- The electrical interface between the spacecraft and capsule system is shown in figure C10. A circuit is required from the spacecraft power subsystem to provide a trickle charge during the cruise mode to the battery chargers mounted in the capsule adapter. This provides charging for the BVS, subsonic probe and aeroshell-mounted batteries.

APPENDIX C

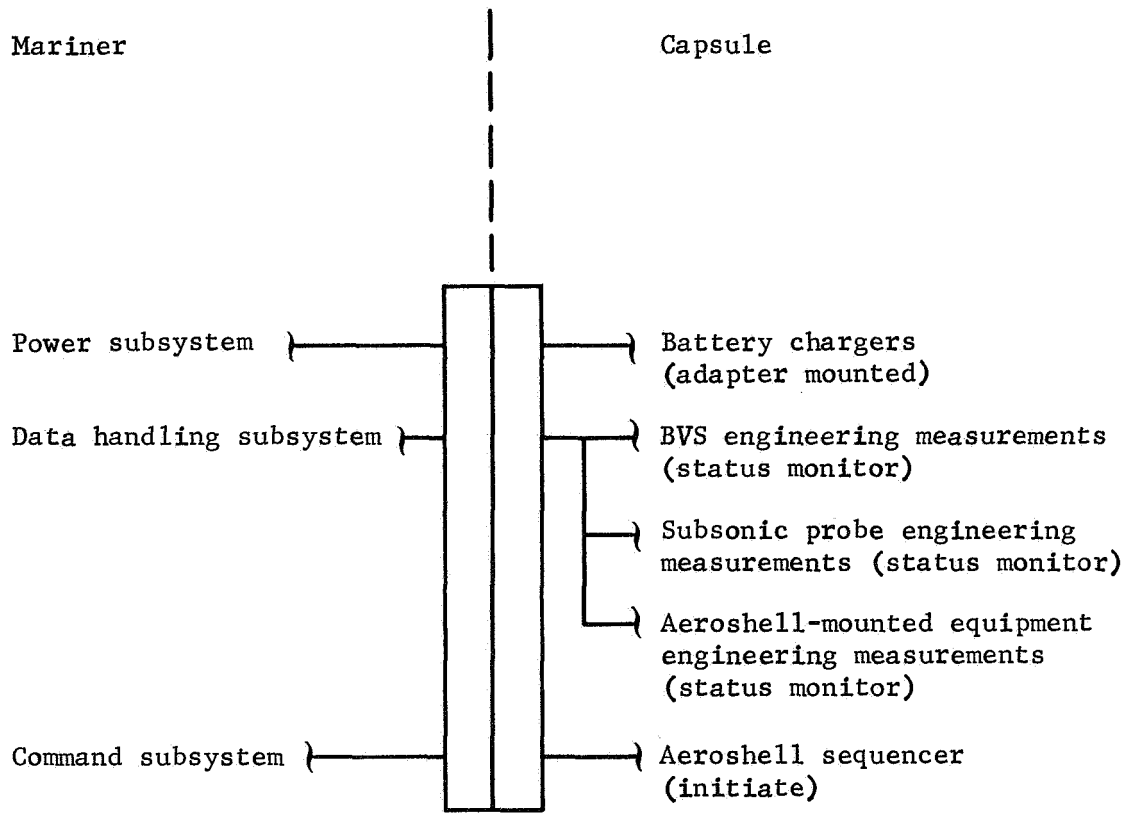


Figure C10.- Mariner/Capsule Electrical Interface

APPENDIX C

A wire bundle of 10 wires is required to provide status monitor of the BVS, subsonic probe, and aeroshell-mounted equipment. This will provide data transmittal and control of status monitor. A circuit is required from the spacecraft command subsystem to the aeroshell sequencer to command the sequencer on and off.

MARINER, VENUS/MERCURY

The Mariner spacecraft as defined in JPL Document 760-1, "Study of a Venus/Mercury Mission with a Venus Entry Probe," was specified as the spacecraft for the Venus/Mercury mission.

No major problems of compatibility between this spacecraft and the BVS/Entry Vehicle have been identified; however, modifications are required to substitute the BVS/Entry Vehicle for the entry probe identified in the JPL document due to the differences in weight and size of the two capsules and use of a direct communications link to Earth instead of a relay link via the spacecraft.

These modifications are summarized in table C11 and are discussed below.

Design Modifications

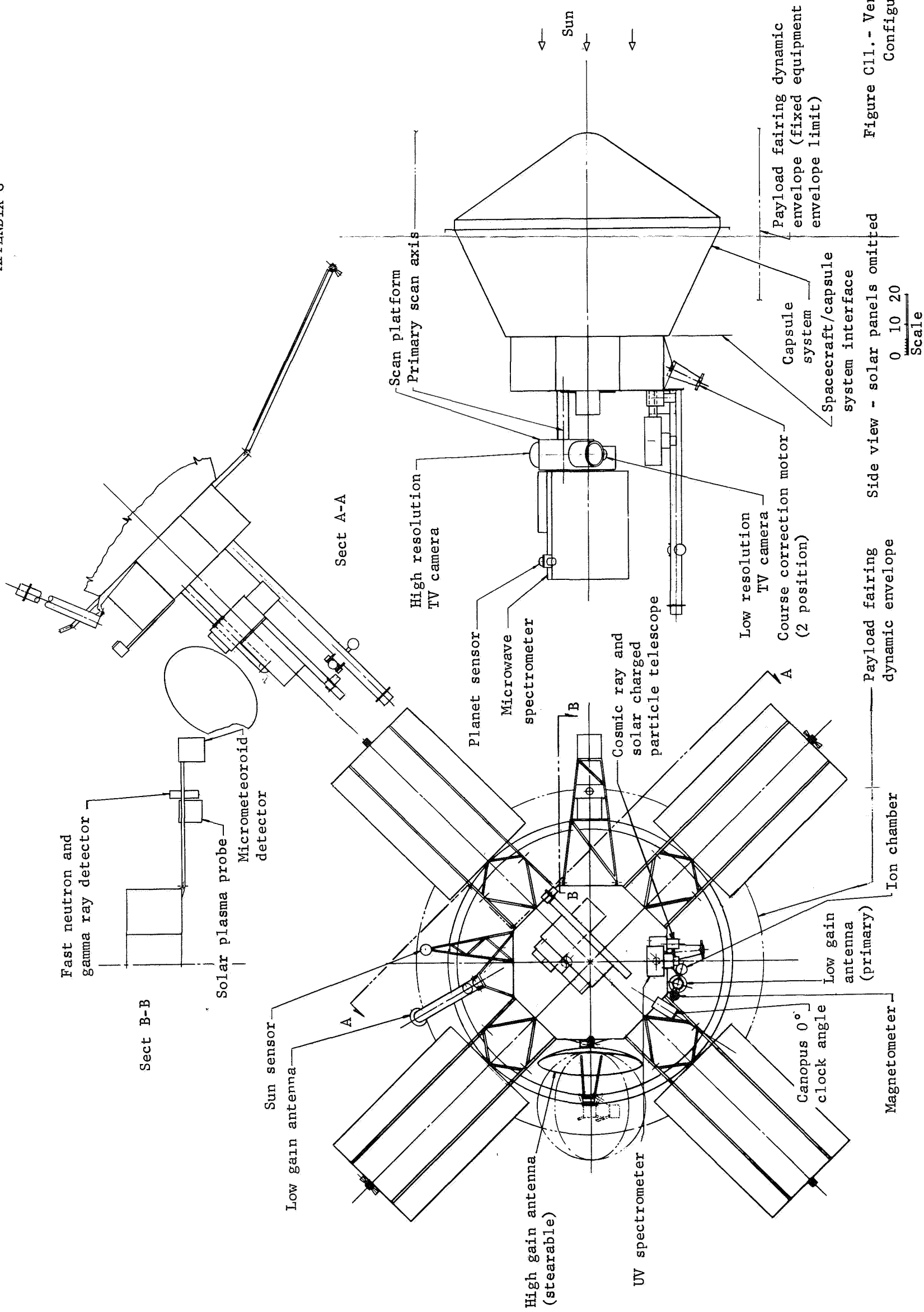
Spacecraft structure.- Figure C11 shows the integration of the spacecraft and the BVS/Entry Vehicle in its biocanister. The diameter of the entry capsule is 7.0 ft and the overall length with propulsion module, is approximately 5.0 ft. It is mounted on the spacecraft in place of the entry probe shown in JPL Document 760-1.

The capsule is adapted to the spacecraft with a cone frustum canister/adaptor that also maintains sterility of the capsule. The biocanister is completed by a closure bulkhead at the spacecraft interface and by a jettisonable canister cover that attaches at the major diameter of the cone frustum. The booster adaptor also attaches at the major diameter of the biocanister.

Modifications to the spacecraft are primarily relocations of science and communications equipment resulting in new mounting and deployment structure. The midcourse engine must be reoriented because of the large difference in Venus capsule system weight. Two position capability will be retained. The basic octagonal body structural configuration will remain the same.

TABLE C11.- SPACECRAFT MODIFICATIONS

Modification	Purpose	Justification
Structural modification to attach capsule	To provide interface for capsule adapter	Presence of capsule will modify heat balance
Modification of S/C thermal control	Control of S/C temperature	Presence of capsule will shade fixed panel area and part of deployed area
Modification of solar panels	Provide view of sun	See capsule power requirements
Modification of power system	Provide power to capsule before power switchover and charge capsule batteries during cruise	Direct link to Earth used for entry and post-entry
Remove S/C-mounted relay link equipment	Relay link not used	Some cruise science deleted (see below)
Modify telemetry format and channel assignments	Compensate for removal of some cruise science	Engine must provide thrust through planetary vehicle center of gravity both before capsule separation and following capsule separation
Reorient midcourse propulsion engine	Provide proper midcourse maneuver both before and following Venus encounter	Increased weight of capsule with BVS requires deleting some cruise science
Remove surplus cruise science	Some cruise science removed to reduce S/C weight	



APPENDIX C

Spacecraft science.- The spacecraft science complement in addition to the BVS/Entry Vehicle is shown in table C12. This reduces the science payload to a total of 180 lb by eliminating some of the cruise science shown in JPL Document 760-1. The encounter science for both Venus and Mercury remains intact and the major science objectives have been retained.

TABLE C12.- SPACECRAFT EXPERIMENTS

Experiment	Weight, lb	Power, W
Television cameras (2 each)	47 (total)	32
Microwave spectrometer/imager	50	40
UV spectrometer .	25	12
Magnetometer	7	5
Plasma probe	15	10
Scan platforms, actuators, etc.	<u>36</u>	<u>20</u>
Totals	180	119

The major effect of the reduced payload on spacecraft subsystems is felt in the spacecraft data automation system that will be required to handle less data in the cruise mode and thus be made compatible with the current science complement.

Spacecraft telecommunications.- No relay communications link between the capsule and the spacecraft is required (the capsule will transmit directly to Earth following its separation from the spacecraft); therefore, the spacecraft relay equipment may be deleted. This eliminates 16.5 lb of equipment consisting of antenna, receiver, and telemetry equipment. The hardlines required for preseparation checkout of the capsule in the JPL configuration can be used for the BVS/Entry Vehicle.

Similarly, the discretes required for powering up the JPL capsule and initiating preseparation and separation sequences can be retained.

Discretes associated with receipt of relay data from the capsule and for transmission of the data to Earth are no longer required and can be deleted.

Spacecraft power subsystem.- Peak power loads for the mission will remain essentially the same because the deletion of the relay equipment results in an insignificant reduction in power.

APPENDIX C

The solar cell configuration, however, must be modified to move both the fixed and deployed panel area further from the roll axis to prevent shading by the larger diameter capsule.

No other modifications to the subsystem have been identified other than removal of power switching for the deleted communications relay equipment.

A photovoltaic array was selected as the baseline power subsystem configuration for the Venus/Mercury mission according to the referenced JPL Document 760-1. Because the mission involves close approach to the sun (0.43 AU at Mercury encounter) the solar panels are exposed to a solar flux several times that at Earth creating severe thermal problems.

The power subsystem is composed of solar cell panels, panel switching circuitry, a battery, and power conditioning equipment. The power source is sized for the continuous power demand (about 270 W), while the battery is sized to supply the launch/preacquisition power requirement and the power peaks, which are beyond the capability of the solar array.

To maintain a solar panel temperature below 140°C to avoid melting the solder connections, a semireflective, semitransparent metal coating was applied at the back of the cover glasses to reflect 61% of the total incoming energy. Seven fixed panels totaling 23 ft² and four extendible panels totaling 34 ft² provide sufficient solar panel area to maintain a minimum of 270 W. To limit the range of voltage input to the power conditioning equipment, sections of the array are electrically reconnected after Venus encounter to increase the number of cells in series by 50%. This compensates for the reduction in cell voltage caused by the increase in temperature. The reconnection will boost the array open-circuit voltage after Venus encounter to about 52 V and will provide at Mercury a minimum array voltage above 28 V.

The power subsystem uses a 1200 W-h battery, identical to that to be used on Mariner 1969. The power conditioning equipment is also based on Mariner 1969 components and design philosophy.

Spacecraft and BVS/Entry Vehicle Interfaces

Mechanical interface.— The capsule adapter interface with the spacecraft is the same as for the orbital and flyby missions discussed previously.

APPENDIX C

Electrical interface.- The electrical interface between the capsule and spacecraft is the same as for the flyby mission consisting of 10 conductors to provide status monitoring data, to provide power to the trickle chargers (to maintain charge on BVS, subsonic probe, and aeroshell batteries), and to provide command control of the capsule subsystems before separation of the capsule.

APPENDIX D

TV DROP SONDE

by Jack D. Pettus, Allan R. Barger
and Paul G. Reznicek
Martin Marietta Corporation

APPENDIX D

This appendix presents a conceptual design of a TV drop sonde concept for use with the BVS. The feasibility of imaging in the clouds or dense atmosphere of Venus depends not only on system design considerations, but also on the question of light levels and degree of diffusion in the atmosphere.

The concept proposed is based on housing a TV camera in a drop sonde to be carried in the BVS. Pictures can be taken from the BVS (at about 60 km altitude) and/or taken during descent. As illustrated in figure D1, the sonde would be about 6-1/2 in. in diameter and 2 ft long, containing a television camera, its electronics, power and data transmission equipment, and atmospheric pressure and temperature sensors. The TV camera looks forward through an optically clear quartz window located symmetrically in the nose section. Three pressure sensors are equally spaced around the body toward the aft end in the region of stable static pressure. A weight allocation is given in table D1.

TABLE D1.- TV SONDE WEIGHT STATEMENT

Item	Weight, lb
TV camera	5.0
TV electronics	10.0
Battery pack	2.2
Transmitter, 2 oscillators	.5
Antenna	.4
Window	.3
Structure (body shell and equipment mounting and thermal control)	<u>12.0</u>
Total	30.4

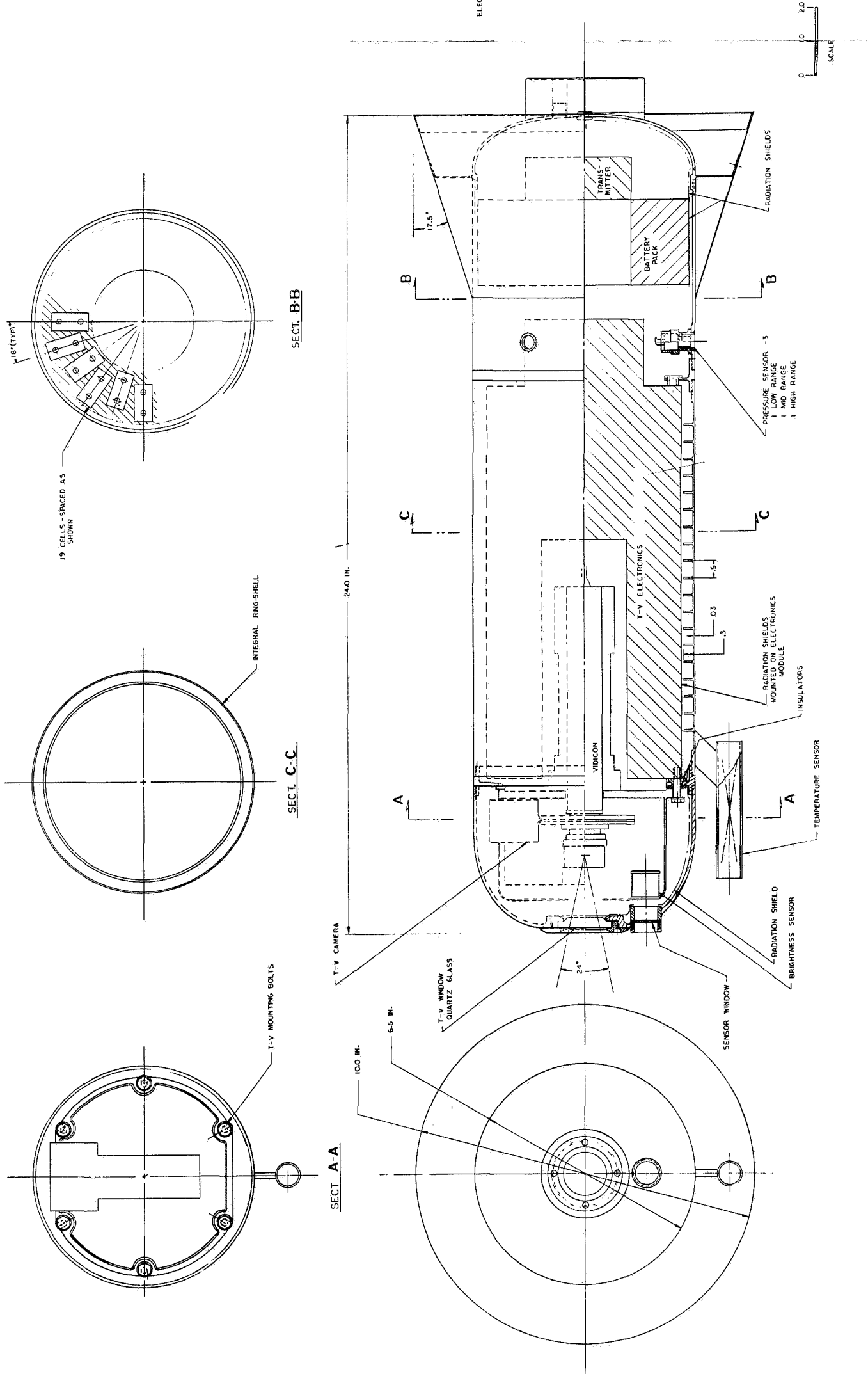


Figure D1.- TV Drop Sonde

APPENDIX D

SYMBOLS

A	visual albedo
B_{\min}	minimum detectable brightness, foot-lamberts
E_o	vidicon tube sensitivity, foot-candle seconds
f/d	relative aperture
F_L	solar constant, lumens/cm ²
f_L	focal length of TV camera lens, cm
I	illumination, foot-lamberts
S	smear rate, degrees/second
t_e	exposure time, seconds
T_T	transmission of the lens
TV	television
α_R	camera angular resolution, radians
θ_f	half-angle of field of view for TV camera, degrees
θ_i	incidence angle of sunlight, degrees

MISSION PROFILE

The altitude/time history of the TV drop sonde is shown in figure D2 from the BVS float altitude to the surface (6050 km radius) for the upper and lower model atmospheres. The sonde, which has a ballistic coefficient of 5.0 slug/ft², is dropped with an initial vertical velocity of zero from the BVS float altitude of 58 km (190 000 ft). The effect on descent time of atmosphere model variation between upper and lower models is seen to be very small. A total of 2000 sec to the surface is required for the upper atmosphere. Mach number remains below 0.3 during the entire drop.

APPENDIX D

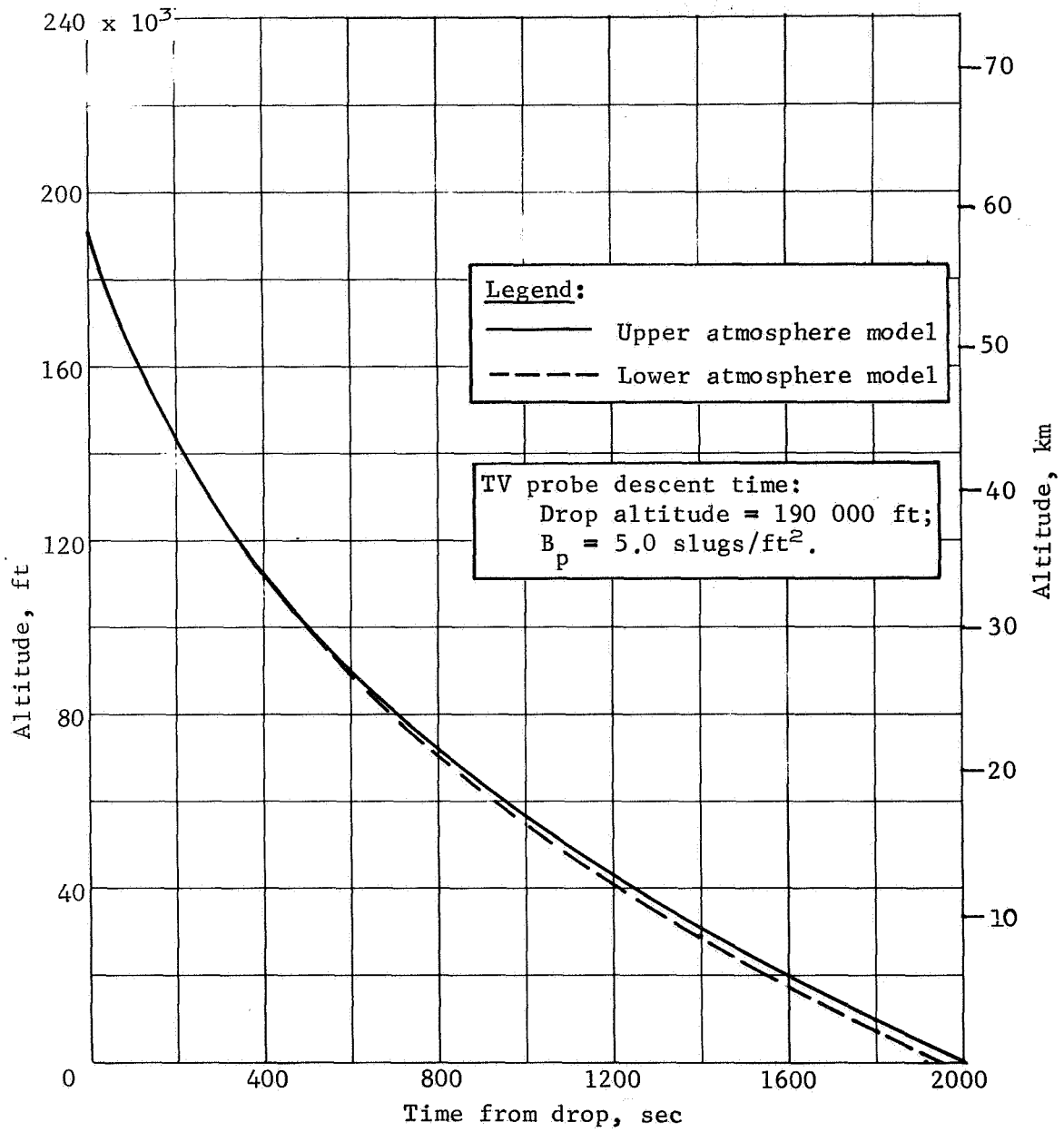


Figure D2.- Altitude/Time History of TV Drop Sonde

APPENDIX D

Imaging begins at an altitude of approximately 20 km with the camera. This is followed by transmission of the image data, then erasure of the image, and exposure for the next image. In all, four images are taken and transmitted with temperature and pressure data injected into the digital data stream.

Temperature and pressure data are stored during the first 18 minutes and transmitted before the first image.

SCIENCE SYBSYSTEM

The science subsystem consists of a TV camera and optics, pressure sensors, and a temperature sensor. The purpose of the TV camera is to obtain visual images of the surface on the near surface environment. At least four pictures are desired starting at about 20 km altitude.

Static pressure sensors and a temperature sensor are included, both to measure the profiles and to provide an altitude reference (barometric) for the TV pictures.

Figure D3 shows a typical arrangement for a TV camera and optics. Some of the mounting structure is superfluous for use on a drop sonde and is estimated to weigh about 5 lb. The associated electronics (not including transmitter) weigh about 8 to 10 lb, for a total of about 15 lb. Power requirements are 2.5 W for the camera and 12.5 W for the electronics.

For purposes of sizing the camera and optics, a resolution of 10 m/TV line in the last picture (taken at about 16 400 ft or 5 km) was selected. The image format on a 1-in. vidicon is 1.12x1.12 cm. The angular resolution (for 10 m at 5 km) is

$$\alpha_R = \frac{10 \text{ m}}{5 \times 10^3 \text{ m}} = 2.0 \times 10^{-3} \text{ rad}$$

and the focal length is

$$f_L = \frac{1.12}{200} = 2.8 \text{ cm}$$

The field of view is then given by

$$\frac{1.12}{2.8} = 2 \tan \frac{\theta_f}{2}$$

or $\theta_f = 22.6^\circ$. The lens diameter, assuming an f-number of 1, is then 2.8 cm.

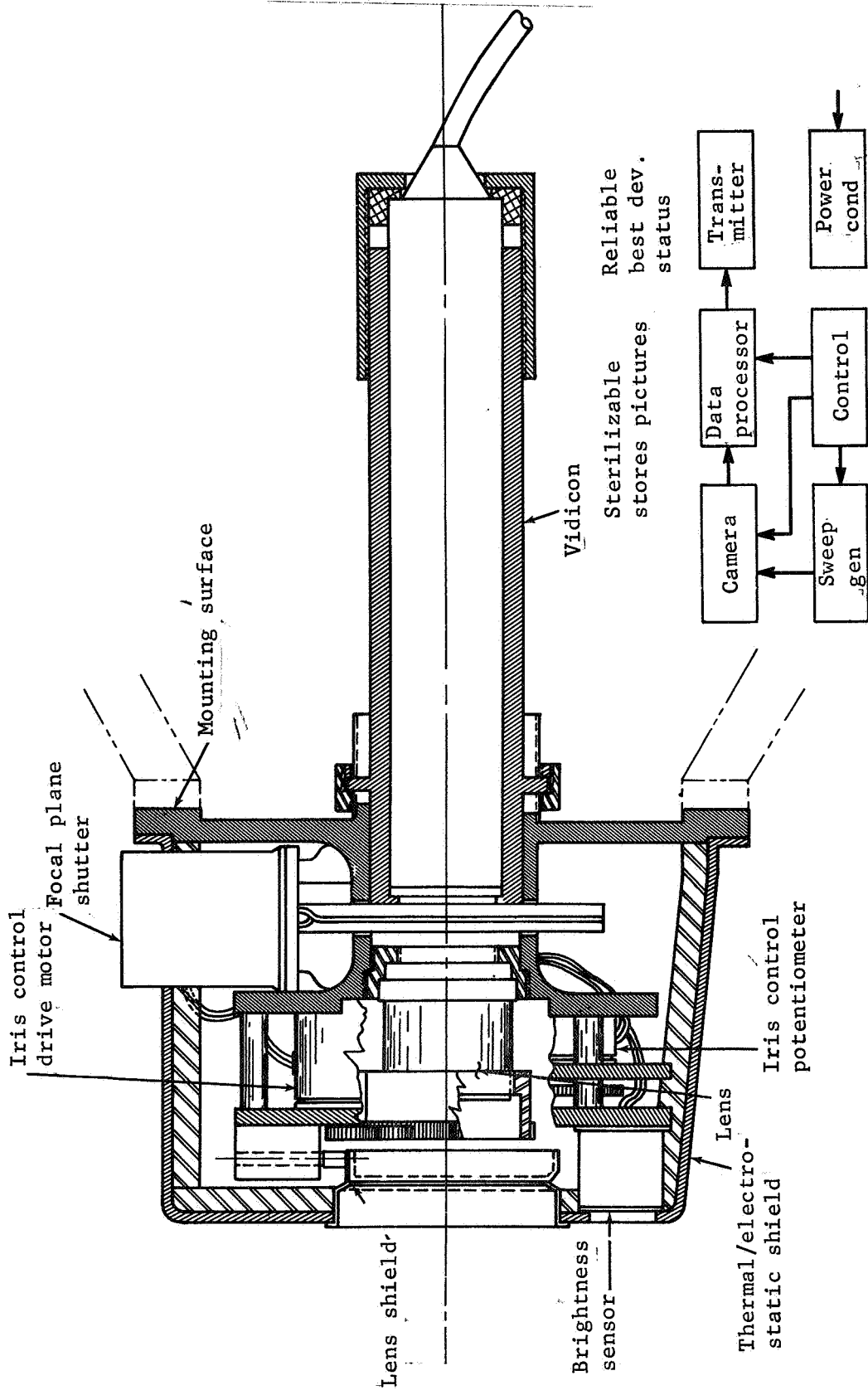


Figure D3.- Surface Imaging

APPENDIX D

With a 5-msec exposure time, the allowable smear rate from all sources (for 1/2 TV line smear) is

$$S = \frac{\alpha_L}{2t_e} = 10^3/5 \times 10^{-3}$$
$$= 1/5 \text{ rad/sec} = 11.5^\circ/\text{sec}$$

The image smear depends on the altitude, horizontal and vertical velocity, and pitch and roll rates. Smear due to horizontal and vertical velocities is negligible ($\lesssim 0.6^\circ/\text{sec}$); smear rates due to pitch and roll are shown in figure D4. Because the pitch rate depends on the wind gusting that is unpredictable, the roll rate should be kept as low as possible, (below $1^\circ/\text{sec}$). This would then leave a comfortable margin of about $5^\circ/\text{sec}$ for the allowable pitch rate before image smear becomes noticeable. -

The major problem in the design of a camera system for this application is the uncertainty in the light levels. For this reason an SEC vidicon tube with a variable iris control is suggested. Iris control from $f/d = 1$ to 20 would give a range of minimum detectable brightnesses from 0.1 to 40 ft-L. A brightness sensor with a large dynamic range (± 3 decades) is required to control the iris.

The probability of obtaining images by using a TV camera depends on the light level, the color of the light, the ratio of the signal to noise (the ratio between the intensity of light reflected or emitted by the objects in the field of view to the intensity of light backscattered by the intervening atmosphere), and the amount of distortion (refraction) of the signal by the media (atmosphere) between the object and camera. Calculations, based upon Rayleigh and Mie scattering in a 100-atm-surface-pressure atmospheric model, of the optical thickness of the Venus molecular (clear) atmosphere and several Venus cloud models indicate that 5 to 1% of the incident light at Venus may penetrate to the surface. These calculations also indicate that the light reaching the surface is completely diffuse (no shadows will exist) and is orange-red in color.

The signal-to-noise ratio has been shown to be sufficiently large over several kilometers of viewing distance to enable imaging. Depending on atmospheric motion, refraction of light by the Venus atmosphere may result in distortion. But, over several kilometers of viewing distance (especially at high altitudes), distortion may be insignificant.

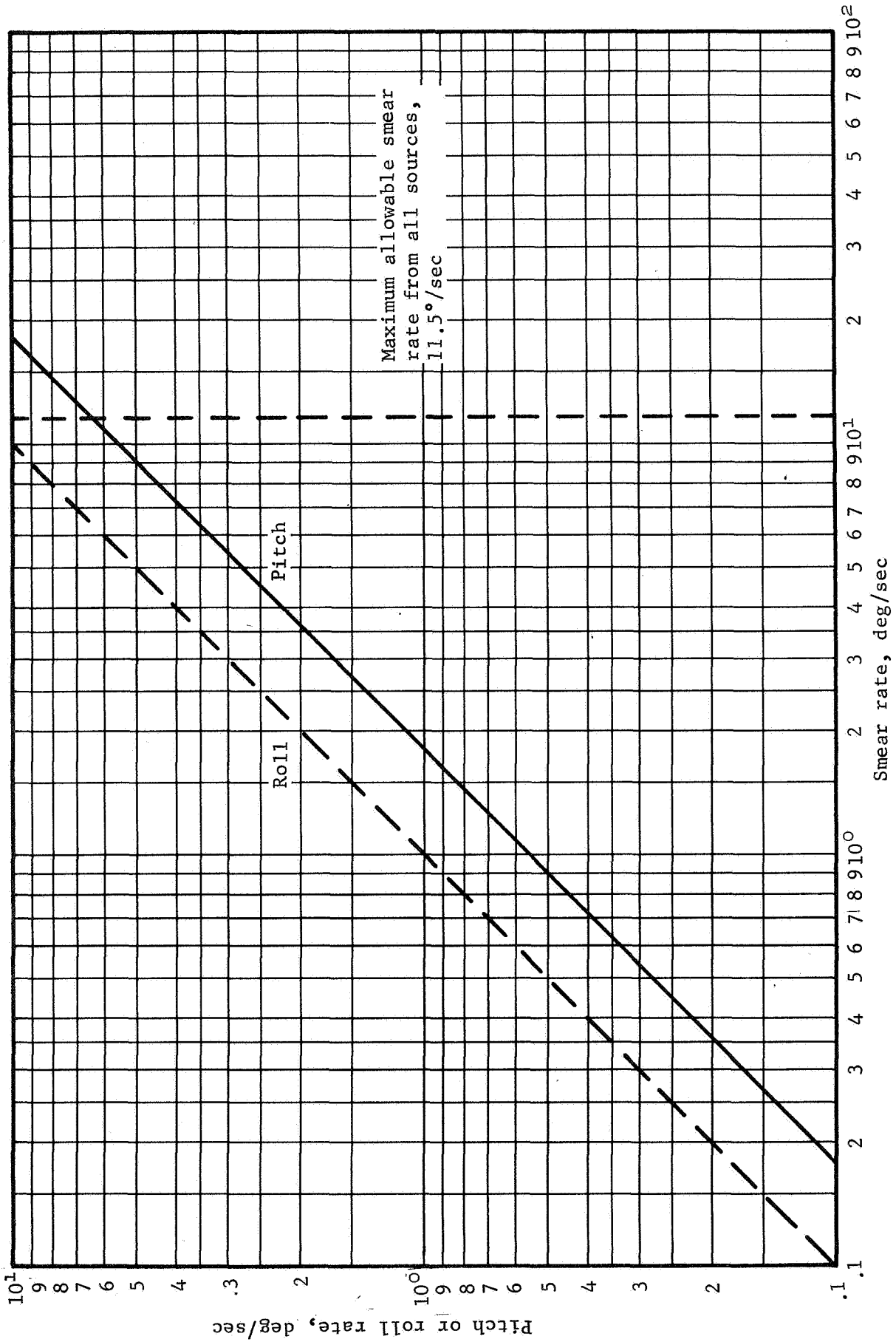


Figure D4.- Smear due to Roll and Pitch

APPENDIX D

TELECOMMUNICATIONS

Telecommunications functions for a TV drop sonde consist of providing a telemetry and data subsystem to interface with science sensors and transmit the accumulated data to the BVS.

The sonde will take four images in the last 18 minutes of fall, at approximately 250 kbits per picture. The TV imaging tube will retain the image so that it may be transmitted directly without storing the picture data in an external store. Pressure and temperature measurement data will be inserted in the data stream at the end of each line of the picture during the minimum data transmission rate, which is approximately 1024 bps for transmitting four images in the last 18 minutes of fall.

A typical block diagram for a sonde telecommunications subsystem is shown in figure D5. The transmitter is of solid-state design and operates continuously at an output of 355 mW and a frequency of 1500 MHz. Modulation is frequency shift key (FSK), with a split phase signal at 1024 bps. The antenna is a circularly polarized curved dipole integral with the aft end of the sonde so that the antenna elements are flush. The antenna half power beam width is 72° , with an "on" axis gain of 8 dB.

The data subsystem consists of a multiverter that interfaces with the camera electronics and with the pressure and temperature instruments. The frame sync generation timing and all picture processing are accomplished by the camera electronics, which is part of the science subsystem.

Performance for the sonde to BVS telemetry link is shown in table D2. Antenna pointing loss of 6 dB for both receive and transmit antenna is shown to allow for drift of the sonde with respect to the station for worst-case range and antenna aspect angle. A maximum frequency uncertainty of 60 kHz including doppler has been assumed requiring a predetection filter bandwidth of 64 kHz.

The 355 mW transmitter power provides a margin allowance for 4 dB multipath and 3.5 dB of adverse tolerances. The 4-dB multipath allowance can be considered extremely conservative because 1 dB is more likely to be the case.

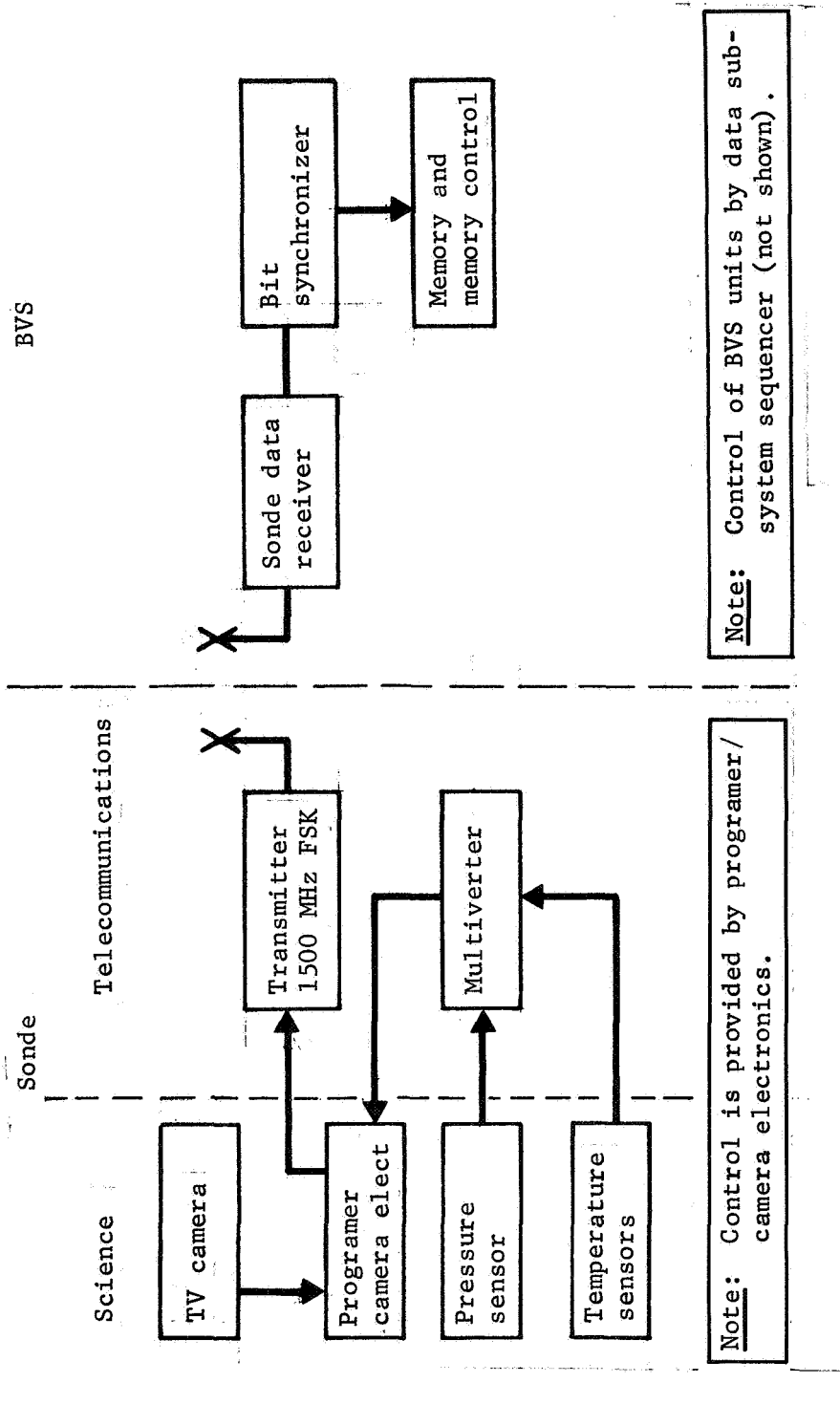


Figure D5.- Sonde Telecommunications

APPENDIX D

TABLE D2.- DROP SONDE LINK CALCULATIONS, FSK
MODULATION (1024 BPS)

Atmospheric attenuation	-1.0
Transmitter circuit loss	-1.0
Transmitter antenna gain	+8.0
Transmitter antenna pointing loss	-6.0
Space loss 1500 MHz, 100 km	-136.3
Receiving antenna gain	+8.0
Receiving antenna pointing loss	-6.0
Receiving circuit loss	<u>-1.0</u>
Net loss	-135.3 dB
Receiver noise spectral density	-165.0 dBm
Channel filter bandwidth (64 kHz)	48.1 dB
Channel noise power	-116.9 dBm
Required input signal to noise for $P_b^e = 10^{-3}$ ($TW = 64\ 000/1024 = 62.4$)	-.4 dB
Multipath margin	+4.0 dB
Adverse tolerance sum	+3.5 dB
Required receive power	-109.8 dBm
Required transmitter power	+25.5 dBm
	355 mW

EFFECT ON BVS AND SPACECRAFT DESIGN FOR ORBITAL MISSION

Presently the data accumulation rates for the baseline (no TV drop sonde) BVS are relatively low, and permit the use of solid-state memories and a data transmission rate of 240 bps for 10 minutes for the BVS-to-spacecraft telemetry link.

The storage capacity required for the BVS to store the 18 minutes of data at a transmission rate of 1024 bps is a minimum of 1 106 000 bits as compared to about 36 000 bits of storage required for the baseline BVS. This can be accomplished with a magnetic tape machine with an estimated weight of 8 lb.

APPENDIX D

The increase in the number of bits of data to be relayed to the spacecraft makes it necessary to increase the BVS-to-spacecraft data transmission rate. Figure D6 shows both the number of bits to be transmitted for a given number of pictures and the data rate required for a given transmission period. For example, at 240 bps (the baseline rate), it requires between 20 and 30 minutes to transmit the station data including one picture. The rate must exceed 450 bps to accomplish the same in 12 minutes. To transmit the basic science data plus four TV pictures to the spacecraft in 12 minutes, the rate from the top curve of figure D6 is more than 1500 bps.

Figure D7 shows the attainable bit rates for various combinations of communication range and sum, in dBw, of transmitter power and antenna gains less a multipath allowance using non-coherent FSK. The example illustrated is appropriate for many station locations with a maximum range of 15 000 km. Under those conditions, a rate of 480 bps may be the maximum that the baseline system should handle. This would yield one picture in a 12-minute period. As the rate is increased without increasing transmitter power or changing to a more efficient modulation scheme, the possibility of a drastically increased data error rate due to the station drifting to an unfavorable location is increased.

Use of coherent phase shift key modulation with the same 20 W of rf power and the same antennas yield the results shown in figure D8. A 5-dB improvement is realized over that of the non-coherent FSK approach, and, from the 15 000-km curve of figure D8, it can be seen that the rate can be increased to 1500 bps or greater. This rate can accommodate the transmission of four images in 12 minutes or less, which will allow relay of the pictures during the first encounter after station deployment. For subsequent communications passes, the data rate could be reduced if desired to provide communications under more adverse conditions.

The effect on spacecraft design is to require additional data storage capacity to accommodate the TV picture data. Additional time will have to be allotted in the spacecraft-to-Earth transmission schedules for relay of the additional data.

APPENDIX D

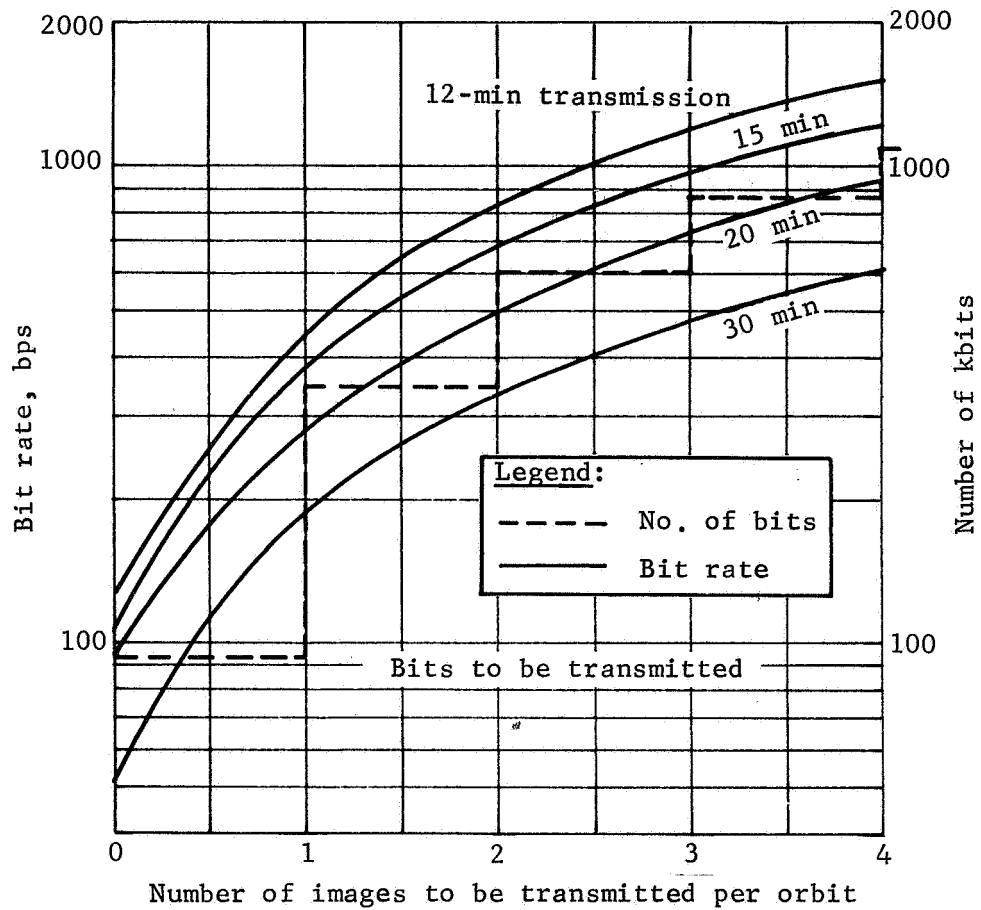
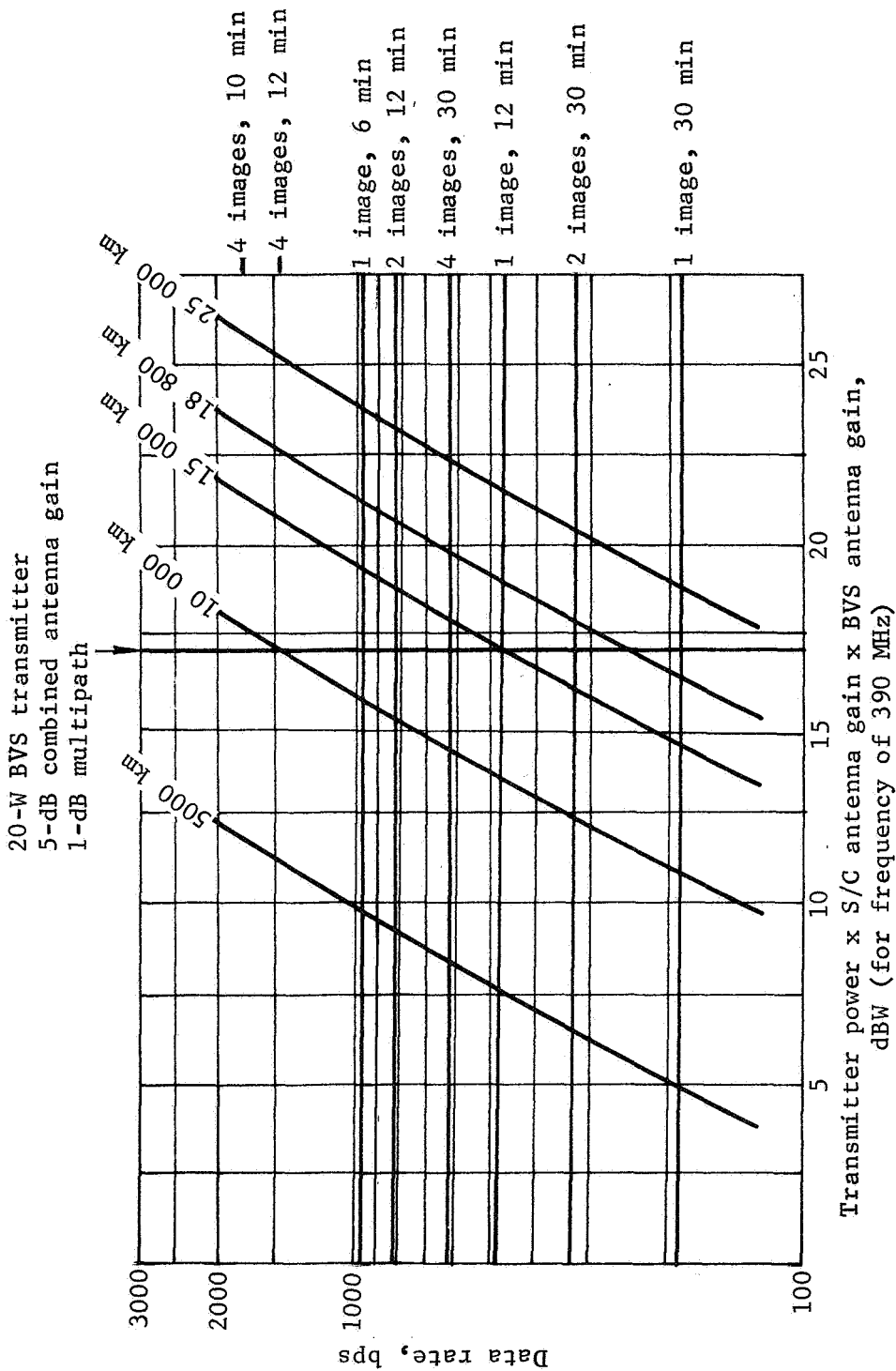


Figure D6.- Bit Rate Required vs Number of Images to be Transmitted for Various Transmission Periods

APPENDIX D

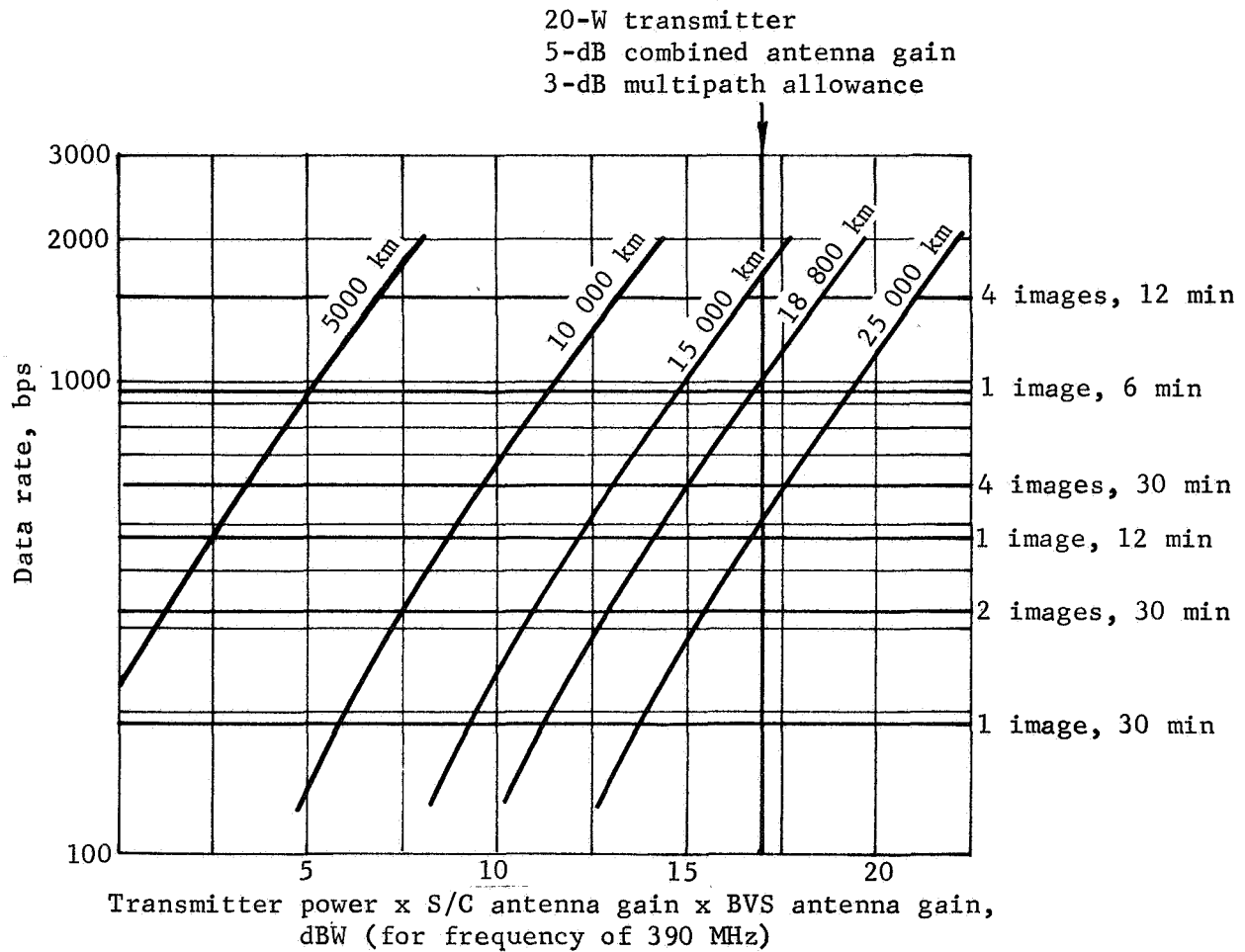


Note:

1. -3.7 dB adverse tolerance has been included.
2. Multipath margin must be accounted for. Example shown reduces gain by 1 dB to account for multipath allowance; i.e., 20-W transmitter and 5-dB antenna gain gives 18 dBW minus 1 dB multipath = 17 dBW.
3. Bit error rate, 1 in 10^5 .

Figure D7.- Transmitter Power Antenna Gain Products vs Bit Rate for Various Communications Ranges Using Frequency Shift Key Modulation

APPENDIX D



Note: 1. -3.7 dB adverse tolerance has been included.
2. Multipath margin must be accounted for. Example shown reduces gain by 3 dB to account for multipath allowance; i.e., 20-W transmitter and 5-dB antenna gain gives 18 dBW minus 1 dB multipath = 17 dBW.

Figure D8.- Transmitter Power Antenna Gain Product vs Bit Rate for Various Communications Ranges Using Coherent Phase Shift Key Modulation

APPENDIX D

EFFECT ON BVS DESIGN WITH A DIRECT EARTH LINK

For direct Earth link transmissions such as used for the Venus flyby and the Venus/Mercury flyby, baseline data rates of 30 and 120 bps, respectively, are used. At these rates it would require 2.3 and 0.75 hr of continuous transmission to send science plus one TV picture to Earth. Use of coding could reduce the required transmission period to about 1.4 and 0.45 hr, respectively, which brings the period for one transmission for the Venus/Mercury mission within range of the present stored electrical energy allocation but the transmission period for the Venus flyby mission would remain a problem.

Increased BVS antenna gain in the form of lightweight switchable arrays integrated into the balloon design may be the answer or dependence on solar energy to provide the additional energy for the flyby mission.

STRUCTURE AND THERMAL CONTROL

The concept selected makes the sonde body a hermetically sealed container that is evacuated. The body structure must therefore withstand the overpressure of 100 atm at the planet surface. The vacuum interior permits use of radiation shields interlining the shell for thermal control as well as mounting the pressure sensors into the body shell and achieving a direct ambient pressure measurement.

A minimum volume body of reasonable length-to-diameter proportions is provided that can package the TV camera and equipment. Because these weight and aerodynamic characteristics do not achieve the desired ballistic coefficient, an aerodynamic flare is provided at the base. The flare also provides good directional stability during descent.

The sonde body structure is made up of a series of integrally machined ring-stiffened cylindrical segments. Threaded joints are employed at the main body assembly joints to facilitate assembly, sealing, and installation of equipment.

APPENDIX D

Two components in the drop sonde have low operating temperature limits; the battery has a desired limit of 90°F, and the TV camera has a limit of 105°F. The maximum temperature of the drop sonde before release is 95°F, because the local atmosphere can be 93°F maximum. Cooling the batteries below local ambient is costly in weight and power, thus it is desirable to take the loss in battery efficiency. To limit the temperature of the battery and TV camera a phase change material that has a melting point above the maximum sonde float temperature of 95°F must be used. Eicosane, a parafin, with a melting point of 98°F and a heat of fusion of 108 Btu/lb, was selected.

Three basic methods of thermal control were considered in limiting the temperature rise of the sonde components during the 33.3-minute descent to a surface atmosphere temperature of 931°F. Temperature of the probe shell was considered to follow the local atmosphere temperature.

One method considered was a vented probe. To cool the hot entering atmosphere, a heat exchanger with phase change material acting as a heat sink is used. The high expected atmosphere pressure eliminates the use of boiling water or ammonia as a heat sink. The optimum thermal control system weight for the vented probe is 8.9 lb. Phase change material with packaging will weigh 7.5 lb and high-temperature fibrous insulation will weigh 1.4 lb. The insulation, 1-in. thick, is on the inside of the container wall.

A second method of control considered a sealed probe but with a gas to eliminate electrical arcing at low pressure. Low pressure could result from outgassing of material with an evacuated probe. This system is similar to the above system except 4.5 lb for heat exchanger and phase change material are not required. The system weight has 1.4 lb of fibrous insulation and 3.0 lb of phase change material with packaging.

A third method (which was selected) has an evacuated sealed container with radiation shields and phase change material. A lightweight radiation shield is attached to the inside of the shell. With 1.3 lb of phase change material, the total thermal control system weight is 1.5 lb.

APPENDIX E

DUAL-ALTITUDE BALLOON

by Patrick C. Carroll and Robert W. Stoffel
Martin Marietta Corporation

APPENDIX E

The statement of work specified that a dual-altitude mission be investigated. The dual-altitude concept implies that some duration of the mission be performed at an initial selected altitude and the remainder of the mission at a different altitude. The 175-lb gondola was used for sizing the various concepts.

Basically, the concept studied consisted of initial deployment at an altitude radius of 6125 km, which is above the clouds, and a second float altitude radius of 6108 km. This change in altitude is accomplished by relieving the hydrogen gas superpressure and pumping atmospheric gas into the balloon maintaining superpressure at the two altitudes. The pumping is accomplished with a small fan-type blower that pumps against the superpressure. The blower power is supplied by either a solar array or batteries; the battery power concept is a significantly heavier system.

A second method studied allowed the balloon to become a zero-pressure balloon by dumping the hydrogen gas superpressure, causing the balloon to descend until a small amount of makeup gas is dumped into the balloon at 6108 km, which allows the balloon to be neutrally buoyant at that altitude.

A third method involves the slow, controlled inflation of the balloon taking place over the altitude range of from 6125 to 6108 km. This produces a descent time of under 1 hr.

A reversed mission, dual-altitude balloon, was analyzed, wherein the balloon (station) is inflated at 6108 km, as in the baseline BVS, but with a larger superpressure balloon enveloping (but collapsed over) the inflated 18-ft diameter balloon. When the gas is released into the larger balloon, it causes the system to rise to 6125 km with the larger, superpressure balloon.

Except for the slow, controlled inflation method, which remains a 400-lb station, all of the above concepts appear feasible, but result in increased station weights of 500 to 900 lb.

APPENDIX E

DUAL-ALTITUDE MISSION DESIGN CRITERIA

The following criteria were used for the dual-altitude concepts:

- 1) Mean atmosphere (90% CO₂);
- 2) Initial float radius of 6125 km,
 $P_a = 30.25 \text{ mb (0.439 psia)},$
 $T_a = -35.7^\circ \text{ F (424}^\circ \text{R)},$
 $\rho_a = 0.004 \text{ lb/ft}^3,$
 $\bar{M}_a = 42.41.$
- 3) Initial superpressure of 6 mb;
- 4) Final float radius for superpressure balloon of 6108 km, except for solar cell power operated pump configuration that will float at radius determined by power limitation of solar cells;
- 5) A 175-lb gondola will be used;
- 6) The following configurations will be analyzed,
 - a) Superpressure throughout mission with battery powered pump,
 - b) Superpressure throughout mission with solar cell powered pump,
 - c) Superpressure initially and then zero pressure for in the clouds mission,
 - d) Superpressure throughout mission with controlled inflation taking place from 6125 to 6108 km. The parachute would be released at 6125 km, and the inflation module released at 6108 km,
 - e) Reversed mission approach, deploying at 6108 km and rising to 6125 km.

APPENDIX E

CONFIGURATION DESCRIPTION AND OPERATION

The baseline single altitude configuration is shown for comparison with the dual-altitude concepts. This configuration is deployed near and stabilizes at a float radius of 6108 km. The baseline concept does not include makeup gas. The baseline concept balloon skin was designed to a film stress of 3600 psi at a superpressure of 6 mb. Although Mylar can be stressed to 10 000 to 12 000 psi, safety margins were selected that resulted in the 3600-psi stress limit. However, for the dual-altitude configurations, the high altitude conditions result in very sensitive weight variations with allowable stress. Results of a parametric trade-off of balloon design vs allowable stress are shown in figures E1 and E2.

Balloon weight is:

$$W_B = A t \rho = \pi D^2 t \rho$$

where

A = balloon area, ft^2 ;

t = balloon skin thickness, ft ;

ρ = balloon material density, lb/ft^3 .

Balloon stress is:

$$\sigma = \frac{PD}{4t} \text{ or } t = \frac{PD}{4\sigma}$$

This produces balloon skin density based on balloon volume:

$$\rho_B = \frac{W_B}{V_B} = \frac{A t \rho}{V_B} = \frac{(\pi D^2) \frac{PD}{4\sigma} \rho}{\frac{\pi}{6} D^3}$$

$$\rho_B = \frac{6}{4} \frac{P \rho}{\sigma}$$

APPENDIX E

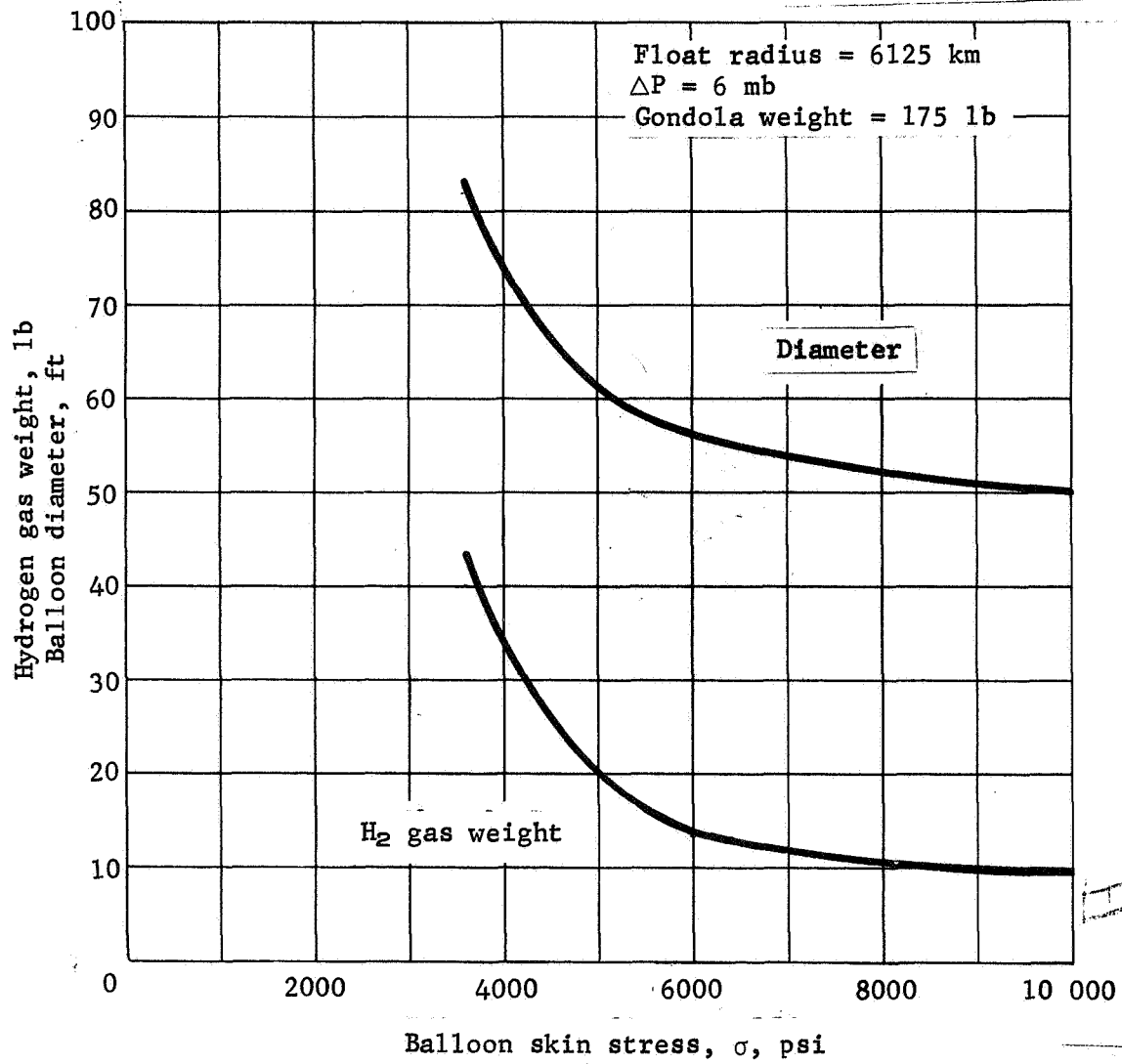


Figure E1.- Effect of Allowable Balloon Stress on Balloon Size

APPENDIX E

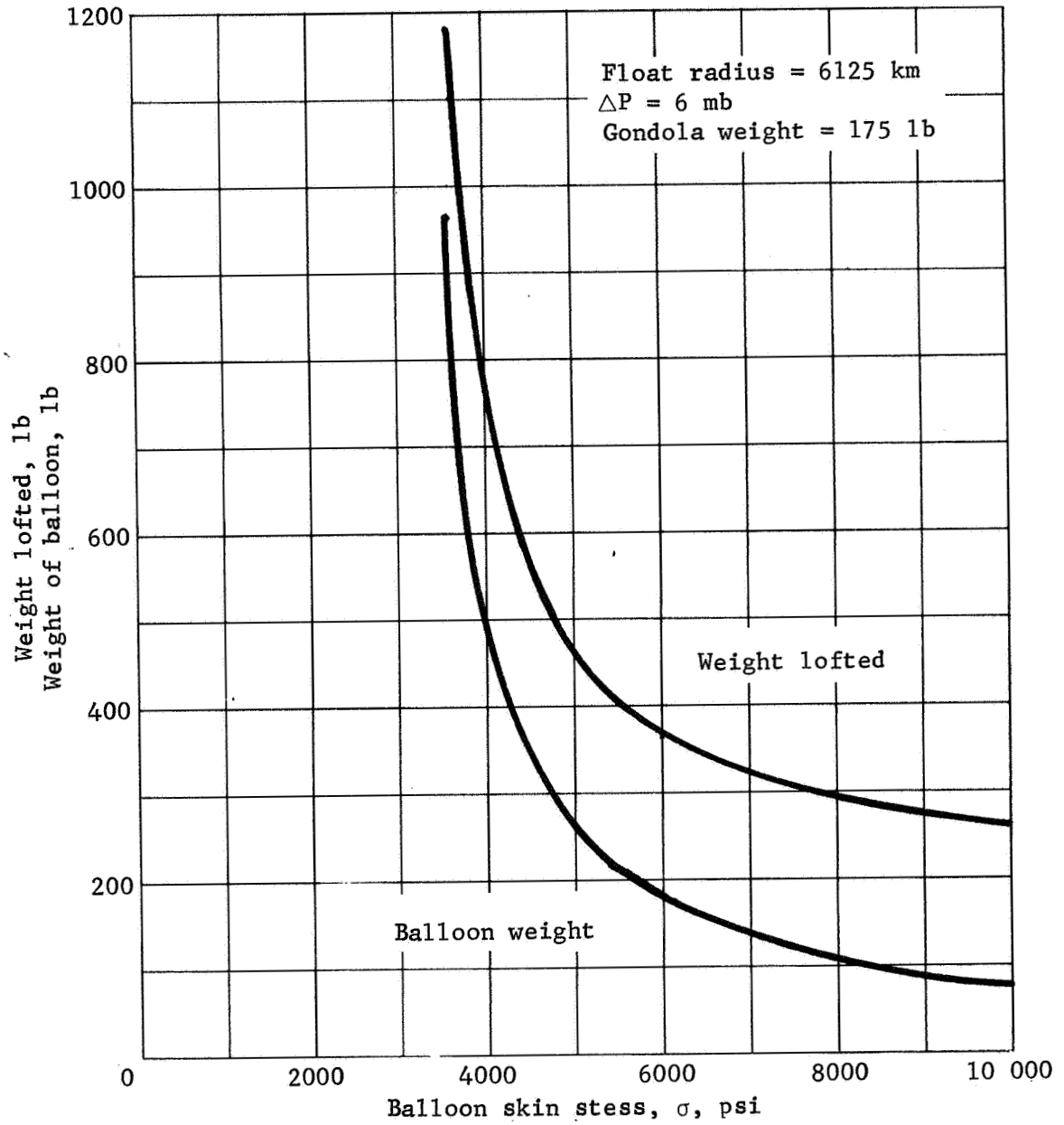


Figure E2.- Effect of Allowable Balloon Stress on Balloon Weight

APPENDIX E

and the required balloon volume is related to the gondola weight densities by:

$$V_B = \frac{W_{\text{gondola}}}{\rho_{\text{Atm}} - \rho_B - \rho_{\text{H}_2}}$$

where

ρ_{Atm} = atmospheric density, lb/ft³,

ρ_{H_2} = buoyant gas density, lb/ft³.

From figures E1 and E2, it can be seen that the system weights, and specifically the balloon weight, are very sensitive to allowable stress, and a value below 6000 psi results in extreme system weights. Therefore, an allowable stress of 6000 psi was selected as the design criterion for the dual-altitude configurations. This stress is still well under the yield stress of 12 000 psi, but results in lower safety factors than that of the baseline design.

A dominant factor in balloon performance is the balloon gas temperature and its relation to the atmospheric temperature. The evaluation of this relationship for the Venus atmosphere is shown in figure E3. The temperatures are for a pure hydrogen gas in the balloon, and the effect of clouds is depicted. Below a radius of 6120 km, the nominal atmosphere assumes clouds exist; however, the temperature was calculated without clouds as well because there is the possibility of breaks in the cloud layer.

For the concepts in which atmosphere is pumped into the balloon to change float altitude, the average balloon gas temperature is shown in figure E3.

APPENDIX E

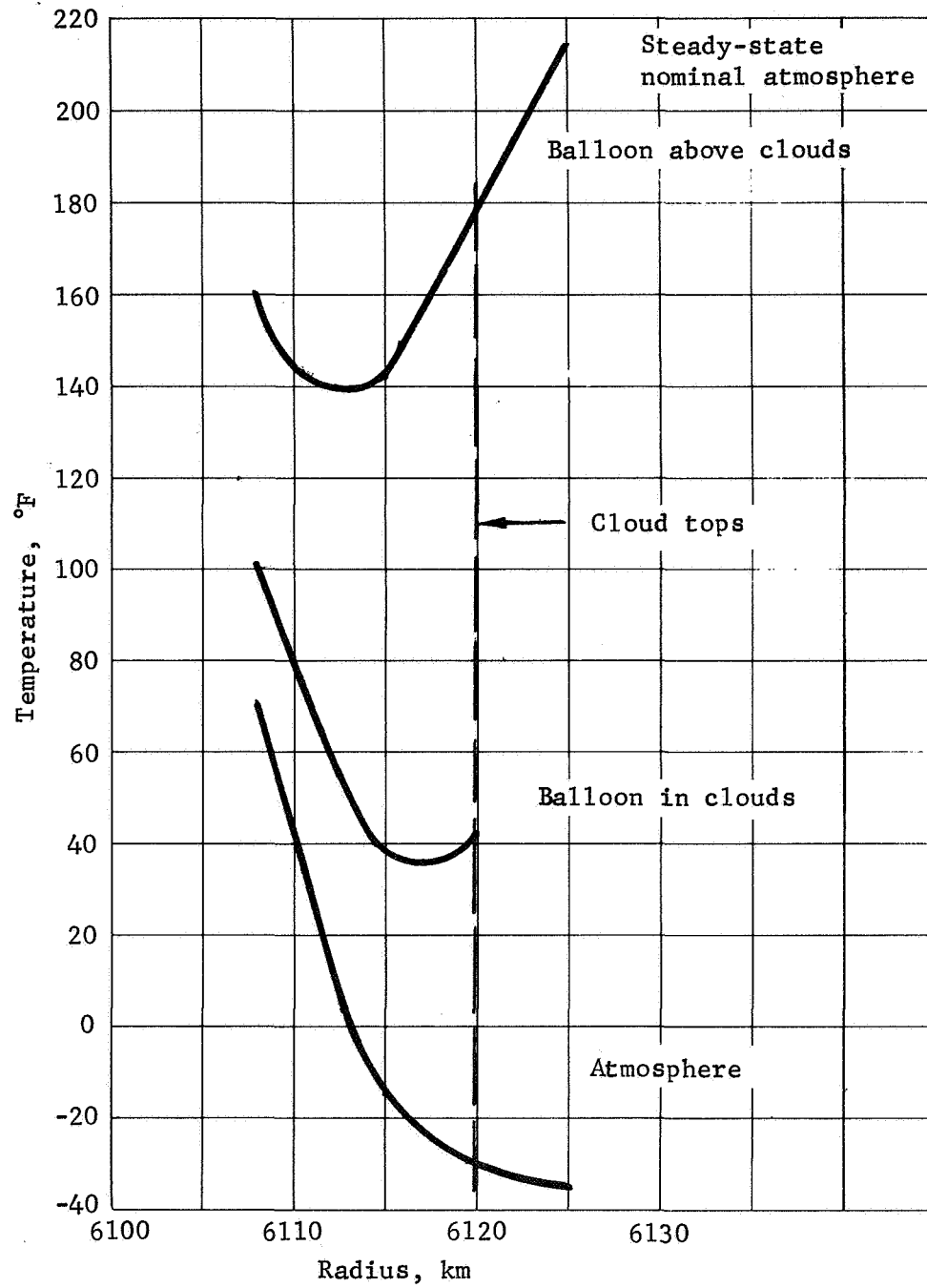


Figure E3.- Balloon Temperature

APPENDIX E

CONCEPT DESCRIPTION AND OPERATION

Configurations A and B are conceptually the same except for the pump power source -- batteries in one case and solar cells in the other. The sequence of events is as follows:

- 1) BVS descends to deployment altitude on parachute;
- 2) Balloon is deployed, inflated, and floats at a radius of 6125 km. A 6-mb superpressure design the balloon at this condition;
- 3) To descend with a constant superpressure of 6 mb, atmosphere is pumped in and H_2 gas is simultaneously vented. Figure E4 shows the H_2 and atmosphere gas mixture required to obtain equilibrium flotation at every altitude during descent. Upon entering the clouds, the temperature drops by about 136°F, thus drastically reducing lift. In actual practice, the balloon would be allowed to descend rapidly through this altitude with no makeup H_2 because, at a lower altitude, less H_2 is required to finally stabilize. At the final altitude, the balloon would have a mixture of atmosphere and hydrogen at a superpressure of 6 mb and a molecular weight slightly lower than the atmosphere, floating in a stable mode. Figure E5 shows a pump installation for the balloon. The blower is mounted to the balloon canister with a shutoff valve.

The significant weight penalty for Configurations A and B (approximately 508 lb) is due to the requirement for 6-mb superpressure, resulting in a significant weight of hydrogen gas and the large balloon (62.5-ft diameter).

The pumping requirement for Configuration A is 85 ft³/min based on a 24-hr period that allows the pumping to be completed within the 25-hr orbital period. A Rotron Manufacturing Company, Inc. PROPIMAX-2 tube axial fan (Model 367JS) will meet the pumping requirement with 80 to 100 ft³/min against a 2.5-mb head at 35 W. This results in 840 W-h or 32.3 A-h for power. The resulting silver-zinc battery weight is 30 lb, and the pump and Rotron Batac power supply (model BC111) weight about 1 lb.

APPENDIX E

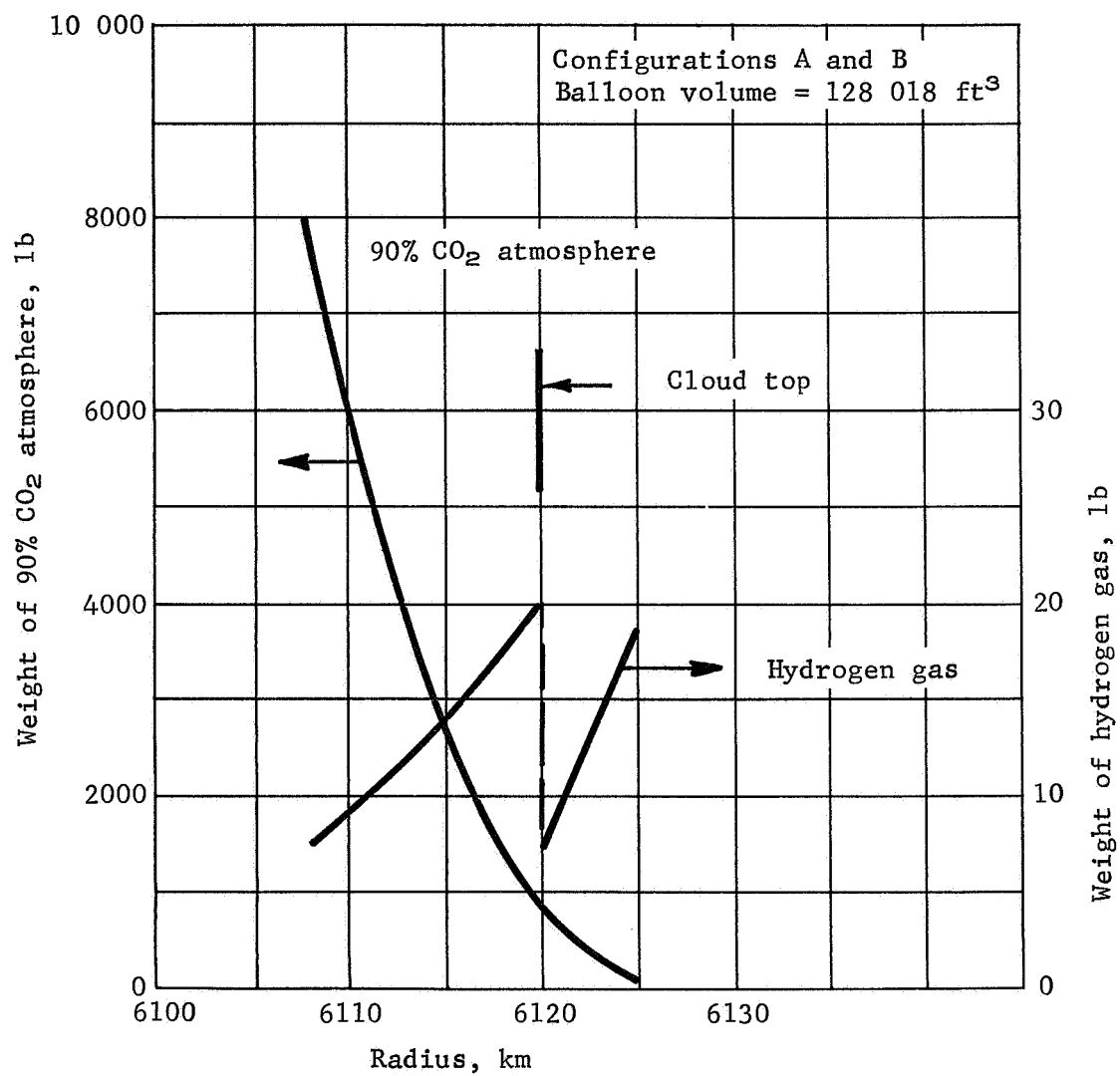


Figure E4.- Gas Mixtures Required for Equilibrium Float

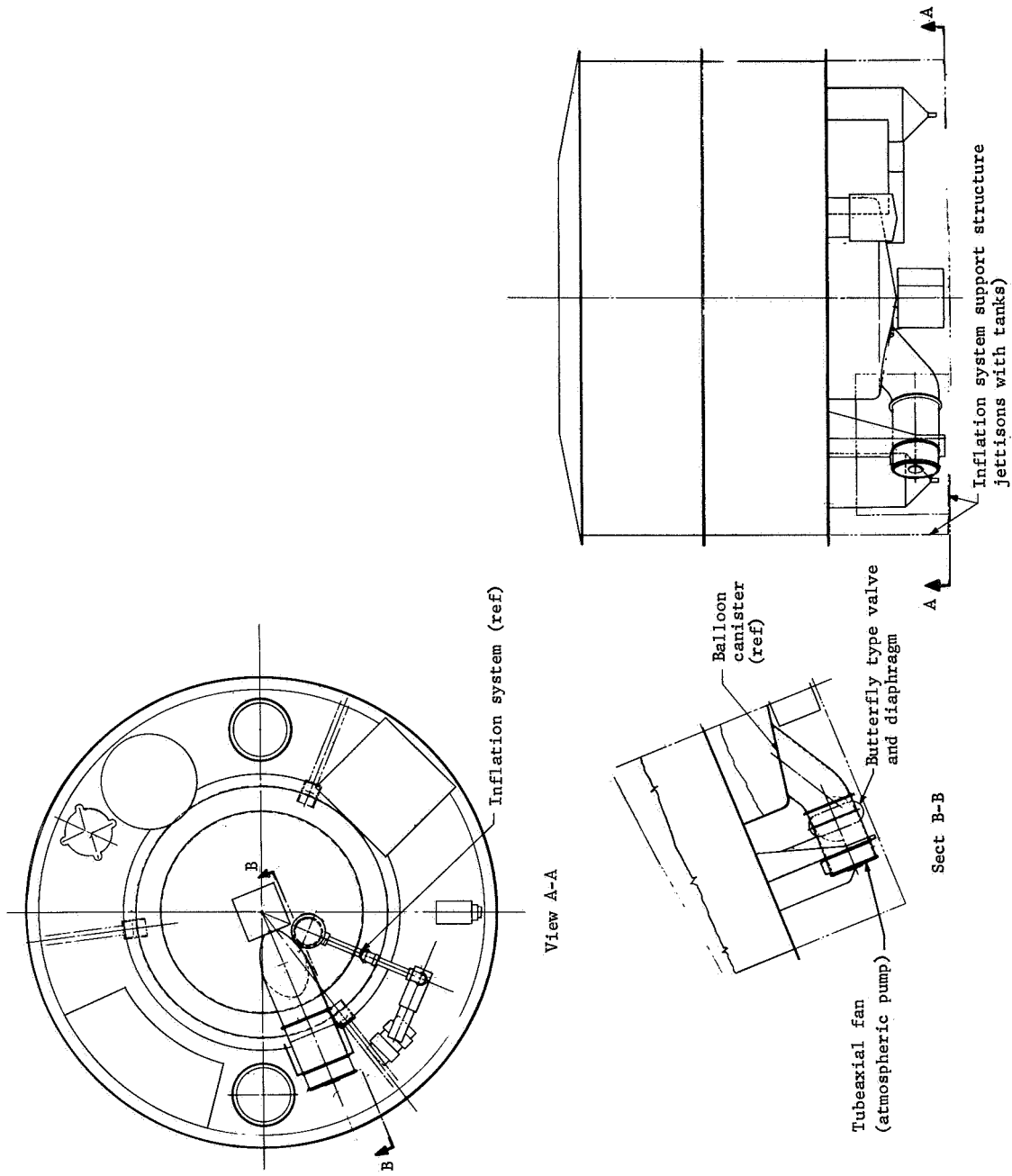


Figure E5.- Gondola Arrangement Showing Pump Installation, Dual-Altitude Mission

APPENDIX E

In Configuration C, rather than pumping atmospheric gases into the balloon to decrease its net lift, balloon gas is vented to start the descent. The balloon is designed to become zero pressure at lower altitudes so it may be designed to a superpressure of only 2 mb at the high altitude providing a margin of 6.7% superpressure at design altitude. The sequence of events is as follows:

- 1) BVS descends to deployment altitude on parachute, is deployed, inflated, and stabilizes at 6125 km. A 2-mb superpressure designs the balloon at this condition;
- 2) The hydrogen gas superpressure is partially vented to start descent;
- 3) Balloon descends to 6108 km, and makeup gas is released into the balloon to provide equilibrium flotation.

This system is neutrally stable because of the zero-pressure condition, but will slowly drift up or down without an active control system to maintain altitude. This concept results in a 665-lb BVS.

Configuration D provides dual-altitude operation by a slow inflation of the balloon. With the baseline balloon, the inflation rate is controlled so that the 6-mb superpressure is not exceeded during the inflation process. The balloon becomes fully extended shortly after passing the radius altitude of 6125 km. Its descent rate is determined by the balance of gravity and aerodynamic drag acting on the balloon. Figure E6 indicates the radius altitude of the balloon as a function of inflation time. The time required for the balloon to sink from 6125 to 6108 km is approximately 30 minutes (1800 sec). These curves were generated from a balloon deployment dynamics program that does not consider solar heating during the inflation process, and therefore, allowed the balloon to be inflated faster than it would be in practice. With a slower inflation, the extra weight of the inflation system must be carried longer, resulting in a slightly faster descent. This method can be accomplished with the 400-lb BVS.

Configuration E represents a natural and simple way to change altitude by reversing the altitude sequence and starting at the low altitude. The concept consists of a balloon inside a larger balloon. The internal balloon is inflated initially at 6108 km and floats with a 6-mb superpressure. When change in altitude is desired, the balloon is vented into the larger collapsed balloon that inflates, and the system rises until the large balloon is fully inflated to a superpressure of 2 mb. In the event of premature failure of the small balloon, the system rises to the upper altitude. This system does not require pumping or makeup gas and is stable at either altitude. This concept results in a 500-lb BVS.

APPENDIX E

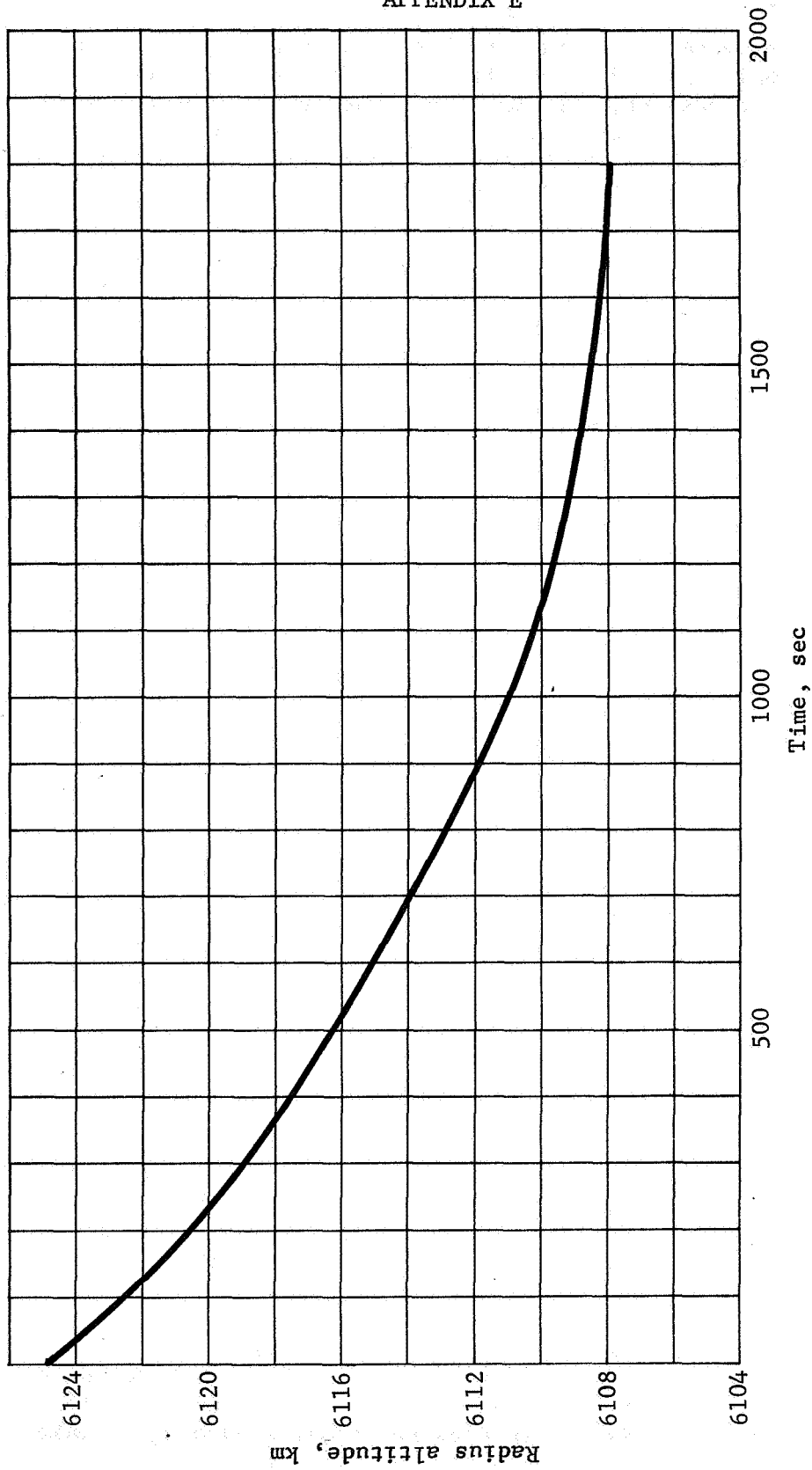


Figure E6.- BVS Altitude with Time for a Slowly Inflated Balloon

APPENDIX E

Comparison

Table E1 displays various weights and parameters for the four dual-altitude concepts under consideration as well as for the baseline single altitude balloon. Of interest is the total system weight, where a minimum increase over the baseline 400-lb is desirable. A second consideration in the comparison of the four concepts is the ability of the particular concept to provide atmospheric measurements at the 6125-km level in addition to the 6108-km level.

Configuration D, in which the balloon does not actually stabilize at a higher altitude, will not provide an appreciable increase in mission success probability because the descent time is only twice that spent descending on a parachute in the baseline configuration. For the orbiter case, this slow descent operation may even inhibit the transmission of atmospheric data during the initial pass of the orbiter because of difficulty in deploying science before dropping the balloon inflation tanks.

Configuration C results in zero-pressure operation at 6108 km and, therefore, will require an active gas makeup or ballasting system to stabilize and maintain that altitude. The extra 265 lb required for this system does not include the weight required for maintenance of altitude. Because the anticipated hazards can be overcome by an active makeup system, in any case, the addition of a gas makeup system or a ballasting system to the baseline design would prove more weight effective.

Configuration E is the lightest of the four dual-altitude schemes and has the added advantage of providing protection against balloon leakage. The operation is in reverse, i.e., the balloon is first deployed at the lower altitude.

Conclusion

The dual-altitude balloon appears feasible. Four of the possible methods have been analyzed and are shown to have various degrees of desirability and mission life at the different altitudes. The dual altitude capability is achieved with some degree of added complexity and weight. The weight increase can amount to slightly more than 500 lb.

APPENDIX E

TABLE E1.- COMPARISON OF DUAL-ALTITUDE CONFIGURATIONS

Parameter	Baseline single altitude mission	Configurations A and B dual-altitude super/super	Configuration C dual-altitude super/zero	Configuration D dual-altitude slow inflation	Configuration E reversed mission super/super
Initial radius, km	6108	6125	6125	6125	6108
Final radius, km	6108	6108	6108	6108	6125
Initial superpressure, mb	6	6	2	6	6
Final superpressure, mb	6	6	0	6	2
Balloon volume, ft ³	3043	128 018	97 361	3043	3844/62459
Balloon diameter, ft	18.0	62.5	57.1	18.0	19.4/49.2
Requires pump	No	Yes	No	No	No
Atmosphere pumped in, lb	None	7933.0	----	----	----
Balloon skin stress, psi	3600	6000	6000	3600	6000
Weight statement					
Balloon weight, lb	14.63	268.3	96.6	14.63	8.1
(Second balloon), lb	----	----	----	----	43.6
Inflation gas, lb	9.14	18.7	12.7	9.14	11.5
Support fabric weight, lb	1.75	10.0	14.0	1.75	15.0
Makeup gas weight, lb	----	----	6.3	----	----
Makeup gas tanks, lb	----	----	87.9	----	----
Pumps and batteries, lb	----	40.0	----	----	----
Gondola weight, lb	175.0	175.0	175.0	175.0	175.0
Initial floated weight	200.52	512.0	389.5	200.52	253.2
10% of initial gas weight, lb	0.92	1.9	1.3	0.92	1.2
Main gas tanks, lb	140.04	288.4	195.6	140.04	177.8
Tank support weight, lb	24.32	50.2	34.0	24.32	30.9
Control weight, lb	16.0	16.0	16.0	16.0	16.0
Parachute weight, lb	18.2	40.0	28.6	18.2	21.6
Total BVS system weight, lb	400.0	908.5	665.0	400.0	500.7

APPENDIX F

STERILIZATION

by James E. Cole and Ted H. Tucker
Martin Marietta Corporation

APPENDIX F

The BVS sterilization study resulted in an interpretation of the planetary quarantine analysis for Venus in terms of engineering criteria. In addition, innovations have been added based on conclusions drawn from corollary sterilization studies and experiments in the general area of bioassay, sterilization/decontamination operations, and sterile-insertion and sterile repair. These techniques permit installation or addition of heat-sensitive items after terminal sterilization as well as replacement of failed hardware without repetition of the terminal sterilization treatment. The only use of the technique in this study is for sterile insertion in the loading of hydrogen gas in the BVS after it has undergone terminal sterilization. R&D studies now in process at Langley and Martin Marietta are expanding the capabilities of these techniques for much wider applications. Significant cost savings can be realized from the recommendation that short exposures to dry heat be substituted for ETO decontamination. This recommendation would classify ETO decontamination as an optional method rather than, as in the beginning of the study, a program requirement -- with no alternative. The alternative method of decontamination is the use of heat as a method for reducing the biological contamination level. In combination, these criteria represent a significant reduction in the impact that sterilization has on the design, development and test of spacecraft for Venus missions without detracting from the basic planetary quarantine requirements.

STERILIZATION CRITERIA

Significant planetary quarantine and sterilization requirements used in this study are as follows:

- 1) Contamination probability level of 10^{-3} for all potential sources of contamination while biological studies of the planet are being carried out;
- 2) The BVS/Entry Vehicle will be heat sterilized so that the probability that a live microorganism remains is 10^{-3} ;
- 3) The probability of impact of the planet Venus by an unsterilized orbiter shall not exceed 3×10^{-5} in an orbit not to decay within 50 yr;

APPENDIX F

- 4) The probability of accidental planetary entry by an unsterilized flyby spacecraft shall not exceed 3×10^{-5} ;
- 5) The BVS/Entry Vehicle shall be biologically sealed in a sterilization canister following terminal sterilization and remain sealed until separation in flight;
- 6) Design of the canister shall be such that no contaminated surface shall be in line-of-sight of a sterile surface during canister separation;
- 7) The trajectory of the separated canister shall be such that it does not violate the planetary quarantine requirement.

STERILIZATION IMPACT ON SYSTEMS AND COMPONENTS

The BVS Sterilization Constraints and Requirements document was developed for use in this study. This document discussed in detail the impact that sterilization requirements have on Venus planetary systems hardware with regard to hardware qualification, and the extent of microbiological contamination control that must necessarily be imposed throughout the assembly and test phase. Itemized below are some of the more pertinent criteria:

- 1) BVS hardware shall be qualified in accordance with the 1973 Voyager Capsule Systems Constraints and Requirements Document, Revision 2, (ref. F1), and supplemented where necessary with JPL Spec VOL-50503-ETS (ref. F2);
- 2) Parts and or materials shall be selected from a NASA-approved sterilizable parts list, or qualified to a Martin Marietta/customer-approved qualification test procedure (a proposed qualification test procedure is shown in the BVS Sterilization Constraints and Requirements Document);
- 3) Qualification of assemblies/subsystems to prove compatibility with sterilization environment shall be by demonstration of structural integrity and normal functioning after exposure to six 64-hr cycles of heat sterilization at 135°C in a nitrogen atmosphere;

APPENDIX F

- 4) Capsule system sterilization qualification shall be performed on the proof test model (PTM) by exposing it to three cycles of heat sterilization at 135°C in a nitrogen atmosphere for periods of 57, 60, and 72 hr, respectively;
- 5) Flight hardware shall be exposed to one sterilization heat cycle in a nitrogen atmosphere at 125°C for a period of 60 hr at assembly/subsystem level;
- 6) Assembly through subsystem level shall be performed in a class 100 000 environment as defined by Fed Std 209a and NASA Std 5340.2;
- 7) Flight capsule system final assembly shall be performed in a class 100 environment as defined by Fed Std 209a and NASA Std 5340.2;
- 8) Biological monitoring shall be performed on all flight and proof test model hardware subsequent to assembly/subsystem assembly until encapsulated in the sterilization canister and terminally sterilized;
- 9) Each flight capsule shall be manufactured, assembled, tested, and encapsulated in such a manner as to enter the terminal sterilization cycle with less than 1×10^5 viable spores;
- 10) The terminal sterilization process shall subject the capsule to a time-temperature cycle equivalent in lethality to 125°C for 24.5 hr.

BVS STERILIZABLE EQUIPMENT SURVEY RESULTS

Table F1 summarizes the results of the BVS sterilizable hardware survey completed near the end of the feasibility study.

The information shown in the table is based, in part, on work done at Martin Marietta with sterilizable electronic hardware and electric power sources. The information came from a variety of reports, but the one most frequently used was a JPL report in which they reported their work with the capsule system advanced development (CSAD) program in their Space Program Summary 37-49, volume III (ref. F3). Martin Marietta report entitled, "Investigation of the Feasibility of Sterile Assembly of Silver-Zinc Batteries" (ref. F4) was another report from which information was obtained.

APPENDIX F

TABLE F1.- BVS STERILIZABLE HARDWARE

BVS equipment list	Sterilization status			Reference/remarks
	Accept- able	Under in- vestiga- tion	To be investi- gated	
Electronic				
Central data multiplexer/ encoder	X			Plated wire memory, CSAD Librascope
Data storage	X	X		
Sonde receiver and data assembly	X			CSAD omni antenna system
Sonde antenna	X			
Data handling S/S prog	X			CSAD (S-band)
Command receiver	X			
Command detector	X			CSAD (S-band)
Command decoder	X			CSAD (S-band)
Transmitter	X			CSAD (S-band)
Diplexer	X			CSAD (S-band)
Main antenna	X			CSAD (S-band)
Radar alt (electronics)	X			
Radar alt (array)				
Sequencer	X			CSAD
Electrical				
Main batteries	X			CSAD
Auxiliary batteries	X			
Instrument power supply	X			CSAD
Power pack	X			
Solar cells	X			
Cable and connectors	X			
Science				
Bioscience			X	
Triax accelerometer	X			CSAD
Pressure exp	X			
Temperature exp	X			CSAD
Light backscatter			X	
Solar aspect	X			1964 Mariner image dissector: CBS Labs
Water vapor detector	X			CSAD
Visual photometer			X	
Mechanical/electromechanical				
Structure	X			
Ordnance valves	X			
Pressure switch	X			
Solenoid valves	X			
Parachute	X			
Balloon		X		

APPENDIX F

The equipment shown as acceptable in the chart indicates that there are acceptable parts available (heat sterilizable) for the general classification of electronic equipment using common parts (integrated circuits, resistors, capacitors, etc.) with the exception of tantalum capacitors for which 125°C is the upper limit.

An investigation is currently in progress at Martin Marietta on sterilization compatibility of balloon materials and processing. Initial test data indicate that the material (singular or composite) can be heat sterilized (ref. F5).

BVS STUDY SUMMARY

The sterilization study has resulted in establishing a feasible plan for selection of sterilizable parts and materials and qualification of parts, assemblies, and subsystems. Manufacturing and test methods developed during the study will assure production of sterilized, flightworthy equipment. Review and evaluation of the BVS equipment list has identified a number of areas requiring additional work to assure sterilizability. Use of short dry heat exposure (in lieu of ETO) is recommended to achieve cost savings and enhanced reliability. This change will permit the use of parts and materials that meet all other program requirements, except for ETO compatibility, and therefore deletes the need for separate qualification tests.

REFERENCES

- F1. Anon.: 1973 Voyager Capsule Systems Constraints and Requirements Document, Revision 2. JPL, June 12, 1967.
- F2. Anon.: Environmental Specification Voyager Capsule Flight Equipment Type Approval and Flight Acceptance Test Procedures for the Heat Sterilization and Ethylene Oxide Decontamination and Environments. Spec VOL-50503 ETS. JPL, Jan. 12, 1966.
- F3. Anon.: Capsule System Advanced Development Program Summary 37-49 vol. III. JPL, Feb. 29, 1968.
- F4. Anon.: Investigation of the Feasibility of Sterile Assembly of Silver-Zinc Batteries. Martin Marietta Corporation, Denver, Colorado, Sept. 1968 (NASA Contract NAS1-7656).
- F5. Anon.: Materials Engineering Test Plan No. 68/50P. Martin Marietta Corporation, Denver, Colorado, July 3, 1968.

APPENDIX G

MULTIPATH ANALYSIS

by James W. Berry
Martin Marietta Corporation

APPENDIX G

The performance, of a relay communications link between a planet descent vehicle and an orbiting or flyby spacecraft may be degraded by scattered signals from the planet surface. The relative magnitude, phase, and time delay between the direct and reflected signals, received at the spacecraft, will determine the degree to which the link will be affected.

The appendix describes the multipath environment considered in the design concept for a relay communication link between the BVS and the spacecraft.

SYMBOLS

c	velocity of light, kilometers/second
E_d	peak direct signal voltage
E_s	peak scattered signal voltage
G_α	ratio of BVS antenna power gain in direction of spacecraft to gain in direction of signal reflected by planet to the spacecraft
M_{rc}	relative permeability
R	surface reflection coefficient
R_{CP}	reflection coefficient for a circular polarized signal
R_d	difference in path length between direct and reflected signal, kilometers
R_V, R_H	reflection coefficient for vertical and horizontal polarized signals, respectively
T	correlation distance
t_D	time delay, seconds
V	velocity, meters/second
Y	normalized admittance
α_p	BVS antenna aspect angle to spacecraft, deg.

APPENDIX G

α_Y	BVS antenna aspect angle of signal reflected from planet, degrees
$(\gamma_{CP})_m$	fading parameter modified for antenna directivity and difference in path length between reflected and direct signal
γ_{FM}	ratio of peak direct signal to rms of scattered signal
ϵ_{rc}	relative complex permittivity
θ_1	local angle of incidence of reflected wave, degrees
λ	wavelength, meters
ρ_R	ratio of reflected signal path length to the direct signal path length
σ_c	conductivity of surface of Venus
σ_d	standard deviation of surface height
τ	correlation time, seconds

SURFACE MODEL

The fading parameter, γ_{FM}^2 , is a measure of the severity of the fading. Turin (ref. G1) defines gamma as

$$\gamma_{FM} \equiv \frac{\text{peak direct signal}}{\text{rms scattered signal}} = E_d / (E_s / \sqrt{2}) \quad (G1)$$

where

$$E_d = \text{peak direct signal}$$

$$E_s = \text{peak scattered signal}$$

Because the surface reflection coefficient, R , is the ratio of the peak scattered signal to peak direct signal, we have from (G1)

$$\gamma_{FM} = \sqrt{2}/R$$

APPENDIX G

Assuming the reflection coefficient for an incident signal of circular polarization can be approximated by

$$R_{CP} = (R_V^2 + R_H^2)^{\frac{1}{2}}$$

where R_V and R_H are the surface reflection coefficients for incident signals of vertical and horizontal polarizations, respectively, then,

$$\gamma_{CP}^2 = \frac{2}{(R_H^2 + R_V^2)} \quad (G2)$$

Equation (G2) was modified to account for the relative magnitudes of the direct signal to the spacecraft and the incident signal to the planet

$$(\gamma_{CP}^2)_m = \gamma_{CP}^2 \rho_R^2 G_\alpha \quad (G3)$$

where ρ_R is the ratio of the reflected signal path length to the direct signal path length and G_α is the BVS antenna gain in the direction of the spacecraft divided by the gain in the direction of the planet.

The surface reflection coefficient is a function of the incidence angle and the electrical properties of the reflecting surface as shown by Beckmann and Spizzichino (ref. G2).

$$R_V = \frac{Y \cos \theta_1 - \sqrt{Y^2 - \sin^2 \theta_1}}{Y \cos \theta_1 + \sqrt{Y^2 - \sin^2 \theta_1}} \quad (G4)$$

$$R_H = \frac{\cos \theta_1 - \sqrt{Y^2 - \sin^2 \theta_1}}{\cos \theta_1 + \sqrt{Y^2 - \sin^2 \theta_1}} \quad (G5)$$

These reflection coefficients are representative of a smooth reflecting surface, where θ_1 is the local angle of incidence (see fig. G1), and Y is the normalized admittance as given by Beckmann (ref. G3).

$$Y = \epsilon_{rc} / M_{rc}$$

APPENDIX G

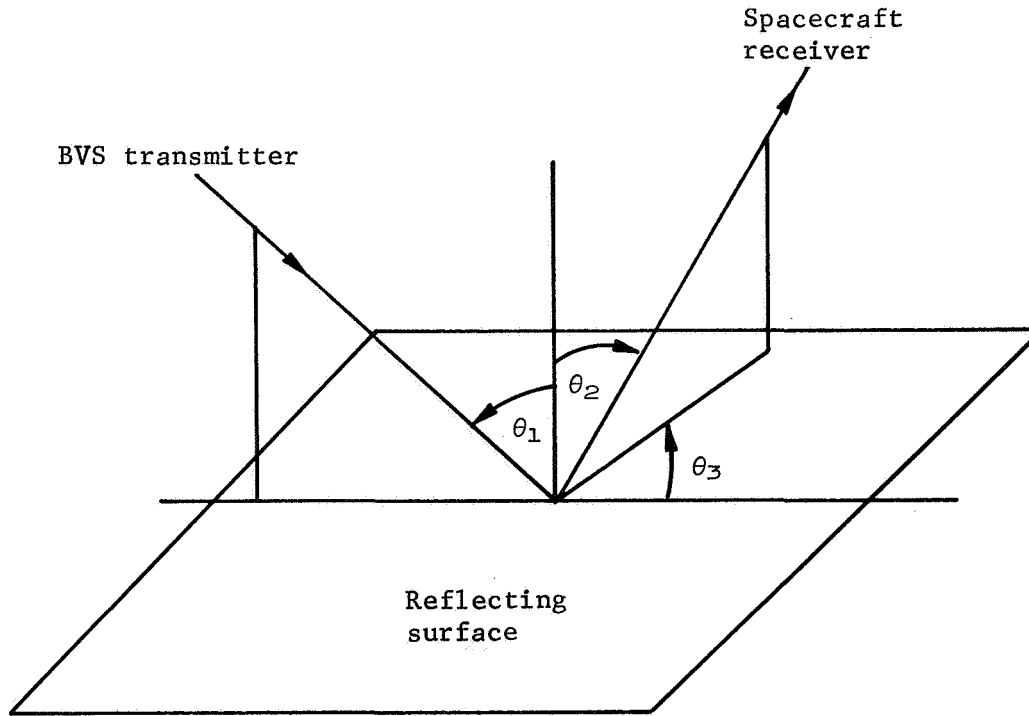


Figure G1.- Angle Convention

where ϵ_{rc} is the relative complex permittivity

$$\epsilon_{rc} = \epsilon/\epsilon_0 + i 60 \lambda \sigma$$

Here, several simplifying assumptions were made: pure specular reflections were considered, i.e., $\theta_1 = \theta_2$ and $\theta_3 = 0^\circ$; the conductivity, σ , of the Venusian surface is sufficiently low at 400 MHz that,

$$\epsilon_{rc} = \epsilon/\epsilon_0$$

and that the relative permeability, M_{rc} of the surface is unity. The surface of Venus is thought to be dry and sandy or rocky with a relative dielectric of permittivity of 3.75, as determined from cw radar measurements (ref. G4). Equations (G4) and (G5), may now be expressed as a function of incidence angle

$$R_V = \frac{3.75 \cos \theta_1 - \sqrt{3.75 - \sin^2 \theta_1}}{3.75 \cos \theta_1 + \sqrt{3.75 - \sin^2 \theta_1}} \quad (G6)$$

APPENDIX G

$$R_H = \frac{\cos \theta_1 - \sqrt{3.75 - \sin^2 \theta_1}}{\cos \theta_1 + \sqrt{3.75 - \sin^2 \theta_1}} \quad (G7)$$

Equations (G3), (G6), and (G7) then define the surface model considered in this analysis. Plots of equations (G6) and (G7) are shown in figure G2.

Fading Margin

The margin in system performance required to overcome effects of the fading environment depends on the selected system modulation, the fading rate, and the time delay between the direct and reflected signals received at the spacecraft.

The BVS attains radial descent shortly after separation from the entry vehicle. Therefore, the correlation time (i.e., time interval between complete correlation of the direct and reflected signals, $\Delta\phi = 0^\circ$, and complete uncorrelation, $\Delta\phi = 180^\circ$), defined in (ref G5) for a falling lander is applicable.

$$\tau = \frac{1}{\sqrt{8K} \nu \sigma_d / T \sin \theta_2}$$

where

ν = radial velocity of descent vehicle

$K = 2\pi/\lambda$

σ_d / T = surface slope (standard deviation/correlation distance)

$\theta_2 = \theta_1$

It has been estimated that the rms slope of the Venus surface is 4 to 7° or

$$0.0345 \leq \sigma_d / T \leq 0.059$$

Because the radial velocity of the BVS is less than 500 m/sec during a majority of the descent profile, the minimum correlation time will be

$$2.5 \leq \tau \leq 7.0 \text{ msec}$$

APPENDIX G

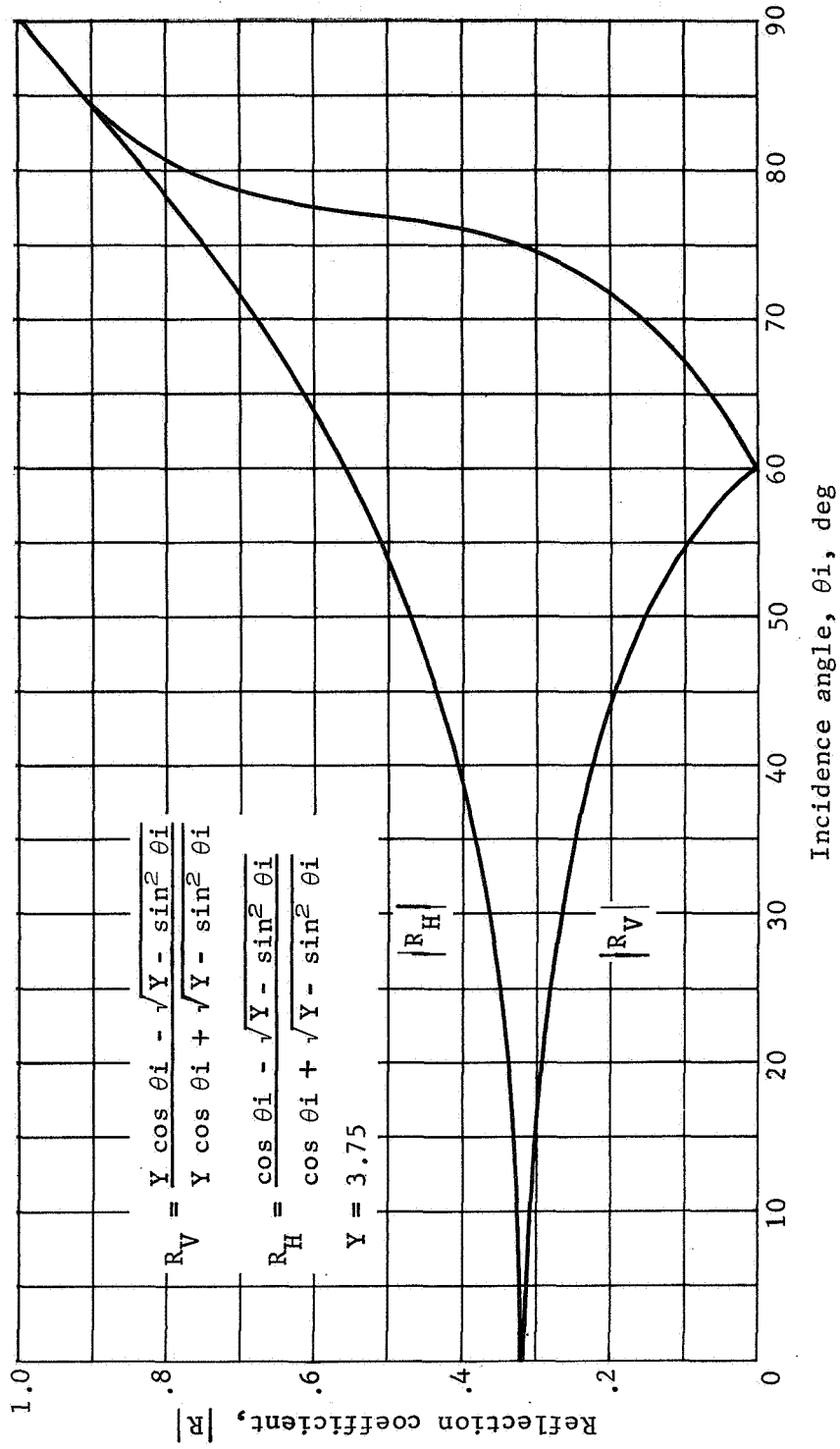


Figure G2.- Reflection Coefficient for Venus Surface

APPENDIX G

The fading rate is considered slow if the received reflected signal is constant over the system information bit period (i.e., correlation time \gg than the system information bit period). The data rate of the reference system is 240 bps or equivalent of a bit period equal to ≈ 4 msec. This would indicate a fast fading rate occurs during a portion of the deorbit trajectory. However, during the terminal phase of the deorbit trajectory, the radial velocity of the BVS is quite low and the correlation time will increase to possibly several seconds. Therefore, the fading rate would go from fast to slow during the descent trajectory and a slow fading condition would have to be considered to ensure a conservative communication link design.

The modulation selected for the reference system was noncoherent FSK. The required fading margin varies with fading parameter as shown in figure G3. These curves were derived from analytical and experimental data (ref. G5) for a system bit error probability of $4 \text{ in } 10^3$, noncoherent FSK modulation and slow fading conditions. The effects of time delay become significant for fading parameters less than 10.

The time delay between the direct and reflected signals received at the spacecraft is

$$t_d = R_d / c$$

where R_d is the difference in path length of the direct and reflected signals and c is the velocity of light. In general, the time delay may be neglected if it is less than 1/10 of the information bit period. For differential path lengths greater than 125 km, the time delay will become significant for the reference system because the bit period is ≈ 4 msec. For the preentry phase (entry - 10 min thru entry) of a typical BVS descent trajectory, differential ranges on the order of 300 km occur. However, during this phase the fading parameter is typically 12 or greater. The differential range has decreased to ≈ 50 km by 30 sec after entry and the fading parameter is approximately 7.5. In general, during periods where the time delay is greater than 1/10 of a bit period, the fading parameter is greater than 12, and the time delay does not become significant. The curve of figure G3, which does not reflect the effect of time delay, was used in the analysis.

APPENDIX G

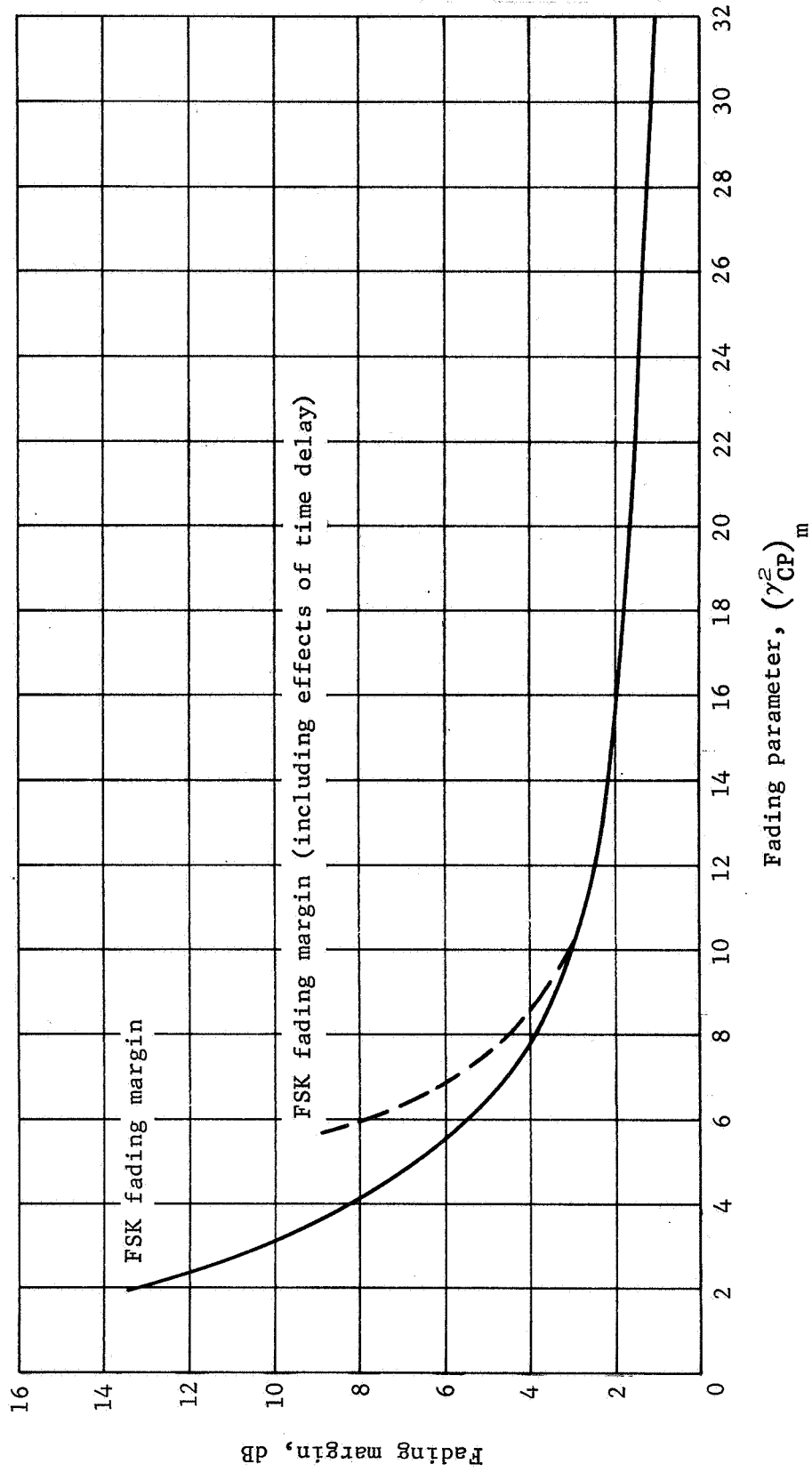


Figure G3.- Fading Margin vs Fading Parameter

APPENDIX G

COMMUNICATIONS GEOMETRY

Typical communications geometry between the spacecraft and BVS is shown in figure G4. Variations in the BVS antenna aspect angles to the spacecraft α_p and to the planet α_y are shown along with the ratio of the BVS antenna direct to reflected signal power gain. Typical variations in incidence angle are shown in figure G5.

SUMMARY

Using this model to simulate the multipath environment, time histories of the required fading margin were calculated. These are shown in figure G5 and on the performance margin profiles (in the telecommunications subsystems section) above the adverse tolerance. The fading margin increases to approximately 4 dB near entry where large incidence angles and small BVS antenna front-to-back gain ratios exist. The fading environment then becomes less severe, due generally to the radial attitude of the BVS, until the spacecraft approaches the terminal link horizon where conditions similar to the entry phase recur.

REFERENCES

- G1. Turin, G. L.: Error Probabilities for Binary Symmetric Ideal Reception through Nonselective Slow Fading and Noise. Proc. IRE, vol. 46, Sept. 1958, pp. 1603 - 1619.
- G2. Beckmann, P.; and Spizzichino, A.: The Scattering of Electromagnetic Waves from Rough Surfaces. Macmillan Company, 1963.
- G3. Beckmann, P.: "The Reflection of Electromagnetic Waves and Synthesis of Media. Acta Thechnica CSAV 1, 1956, pp. 251 - 267.
- G4. Anon.: Final Report - Study of a 1973 Venus-Mercury Mission with a Venus Entry Probe. Document no. 760-1, vol. II, Jet Propulsion Laboratory, June 15, 1967, pp. 5 - 116.
- G5. Anon.: Final Report - Selected Studies of VHF/UHF Communications for Planetary (MARS/VENUS) Relay Links. RCA Astro-Electronics Division, Jan. 15, 1967, p. V-14 (Contract NAS2-3772).

APPENDIX G

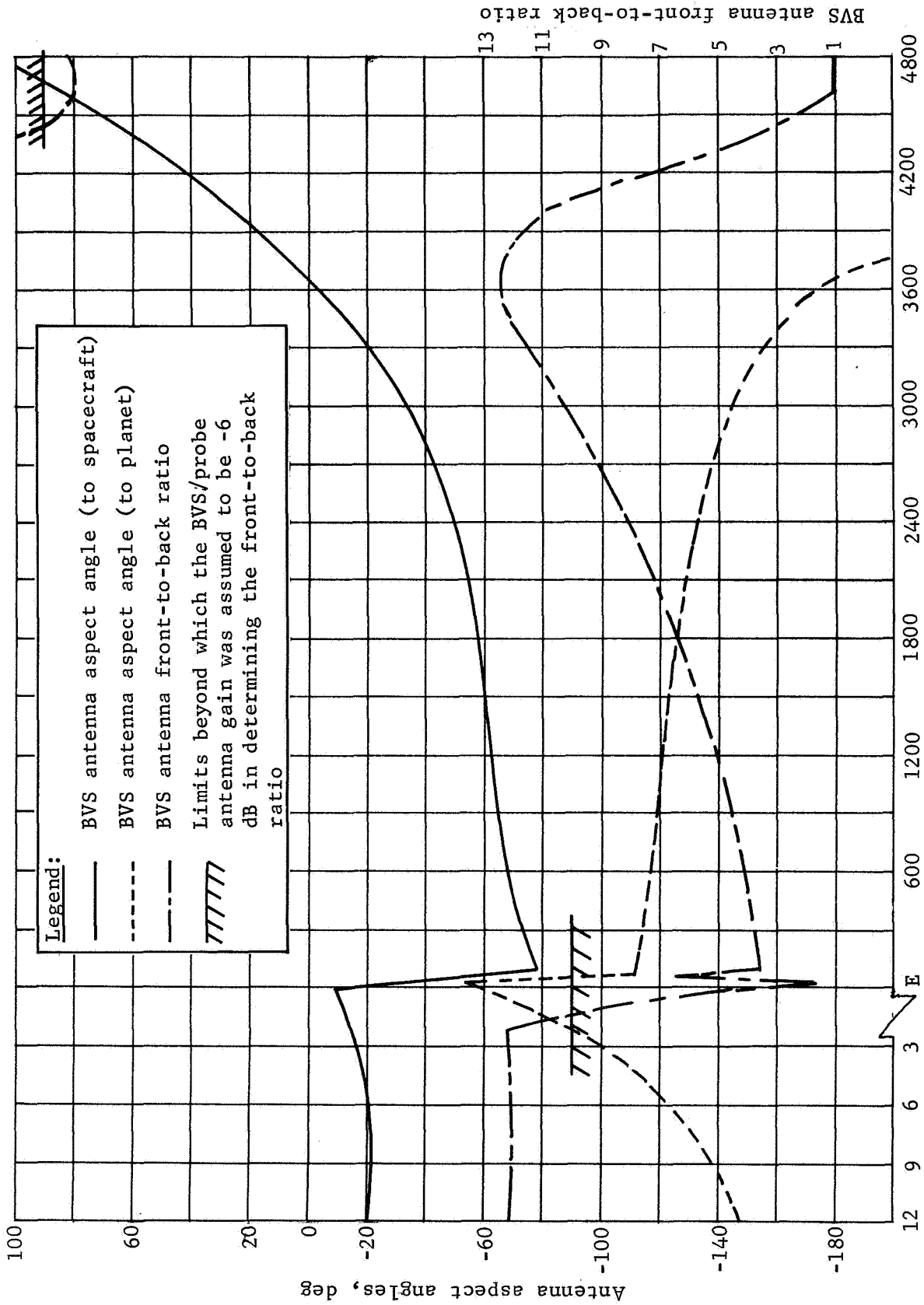


Figure G4.- Communications Geometry

APPENDIX G

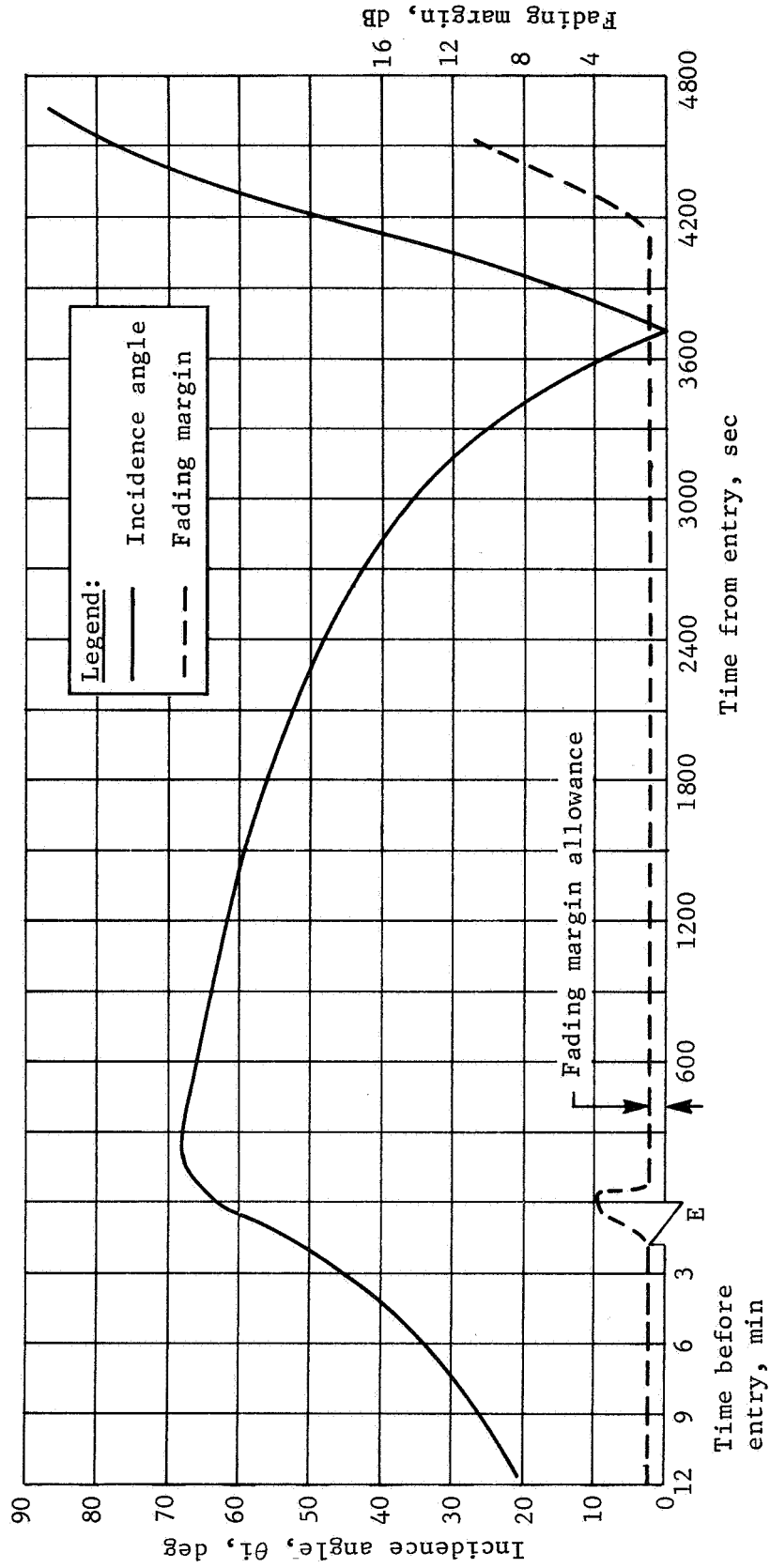


Figure G5.- Incidence Angle Variation and Fading Margin

APPENDIX H

DOPPLER AND RANGING OPTIONS FOR BVS POSITION DETERMINATION

by Walter F. Hane and Jack D. Pettus
Martin Marietta Corporation

APPENDIX H

The baseline communications links between the Buoyant Venus Station (BVS) and the orbiting spacecraft use noncoherent frequency shift keyed (FSK) 400-MHz signals. The link from the spacecraft to the BVS transmits command codes. The link from the BVS transmits telemetry data back to the spacecraft for 10 minutes after the incoming signal from the spacecraft has exceeded a preset level. The spacecraft transmitted frequency is 410 MHz and that from the BVS is 390 MHz. Optional approaches to the baseline were considered, however, for implementing doppler and ranging for the orbital mission without appreciably deteriorating performance of the baseline links. Four approaches were considered, as follows:

- 1) One-way doppler from spacecraft to BVS with doppler data transmitted back to the spacecraft;
- 2) One-way doppler from spacecraft to BVS;
- 3) Two-way doppler from spacecraft to BVS and back to the spacecraft;
- 4) Two-way ranging along with the two-way doppler.

The reference data used as guidelines for the investigation are:

- 1) Two-way range - 50 000 km max., 4000 km min.;
- 2) Two-way propagation time - 0.167 sec max., 0.013 sec min.;
- 3) Desired range resolution - ± 500 m;
- 4) Time for 500-m resolution - 1.67 μ sec;
- 5) Minimum frequency required for 1.67 μ sec, based on $\frac{1}{4}$ -cycle resolution - 150 kHz;
- 6) Range rate resolution - 1 m/sec or less;
- 7) Maximum one-way doppler at 400 MHz - ± 9 kHz;
- 8) Maximum one-way rate of change of doppler - 90 Hz/sec;
- 9) Minimum one-way rate of change of doppler - 5 Hz/sec.

Of primary importance was the criterion that, whatever techniques were selected, they must have minimal detrimental effects on the performance and reliability of the FSK links. It was desired, in the interest of minimum weight, size, and electric power consumption, to include the doppler and ranging function on the FSK command and data rf links. This was accomplished.

Basically, all four approaches use the same carrier generation and recovery techniques. The gated oscillators of the baseline

APPENDIX H

transmitters are replaced by two single-sideband FSK generators that alternately switch from upper sideband to lower sideband single tone modulation for generating the mark and space FSK frequencies. Both of the frequencies transmitted by each transmitter are derived from a common oscillator in the transmitter so that coherent demodulation may be used to recover a FSK modulation exclusive reference signal for doppler measurement and ranging. For doppler measurement, no modulation is required, only frequency measurement of a regenerated reference carrier. For ranging, the FSK signals are phase modulated $\pm 22.5^\circ$ with the ranging code. This reduces the FSK signal strength only 0.7 dB, which, with baseline power, still provides the major portion of the performance margin. The power used for the ranging code is 7.8 dB below that of the FSK signal. The FSK signal level is not reduced when only doppler operation is used without ranging. Operation of the FSK command and data system is unaffected by failure of the doppler and ranging systems to achieve coherent lockup and operation.

Table H1 shows estimates of measurement accuracy for the three doppler and one ranging technique presented. Because the high percentage of error in the one-way doppler measurements use of rate measurements are suggested for a one-way doppler approach. Two-way doppler and ranging, using the technique described, provides a total peak measurement error of less than one doppler cycle from the average over the measurement level and range measurement errors (neglecting relative motion during the ranging interval) of ± 490 m.

SYMBOLS

BPF	bandpass filter
DISCRIM	discriminator
FSK	frequency shift keyed
RCVR	receiver
VXO	voltage controlled crystal oscillator
XMTR	transmitter
XTAL	crystal
ϕ	phase angle, degrees

TABLE H1 .- PERFORMANCE DATA DOPPLER AND RANGING MEASUREMENT SYSTEMS

One-way doppler S/C to BVS	One-way doppler BVS to S/C	Two-way doppler S/C-BVS-S/C	Total range S/C-BVS-S/C
S/C XMTR OSC ± 4100 Hz		Change due to OSC stability = 1×10^{-5} of doppler frequency = ± 0.18 Hz	S/C counter up to 3 μ sec; BVS time delay ± 0.25 μ sec
BVS RCVR OSC ± 410 Hz		Counter error = up to ± 0.5 Hz	Range error peak = 490 m
Total ± 4510 Hz		Total doppler = $\pm 18\ 000$ Hz	Total round trip peak error = 3.25 μ sec
Total doppler ± 9000 Hz		Total peak error = < 1.00 Hz of average over counting period	From ref. H1 the additional rms error due to noise should be < 10 m
Discriminator error 0.5% of measured frequency = 45 Hz			Error due to motion of S/C not included in above
Total peak error = 4555 Hz plus error due to BVS to S/C data system and 40 Hz for digitizing error	Same as one-way S/C to BVS except no additional error due to BVS-S/C data system		

APPENDIX H

CHANGES TO BASELINE SYSTEM

No significant changes to carrier frequencies and none to transmitted power or bit rate are proposed. Therefore, the FSK demodulator design remains basically unchanged. However, the means of generating the FSK output frequencies is changed. The two independent crystal oscillators, in each baseline transmitter, used to generate the FSK signals are replaced by one master oscillator from which the desired output frequencies are generated. This assures an absolute frequency ratio between the output frequencies that aids in the operation of the doppler demodulator. These frequencies are $21 F \pm 0.01 F$ for the spacecraft and $20 F \pm 0.01 F$ for the BVS, where F is 19.5 MHz.

The mark and space frequency difference of ± 195 kc ($\pm 0.01 F$) used in the baseline system is retained. Actually, wide frequency spacing allows simpler less selective input filters. Use of fixed ratio carriers allows use of the total FSK signal power for phase lock loop locking, in a modulation exclusive mode, for operating the doppler and ranging systems.

If it were not required to keep the FSK system operation non-dependent on lockup of the $0.01 F$ carrier oscillator, the FSK predetection filter bandwidths could be reduced to improve performance.

Increase in size, weight, and power for the addition of two-way doppler and ranging (table H2) is slight because common use of the VXO for both receiver and transmitter effects some saving that can be used for the range code detection and regeneration equipment.

ONE-WAY DOPPLER FROM SPACECRAFT TO BVS

A block diagram of the spacecraft transmitter is shown in figure H1. The heart of the transmitter is a single crystal oscillator operating at frequency F (19.5 MHz). This oscillator has a stability of 1×10^{-5} . The output frequency of this oscillator is multiplied by 21 to generate the basic output frequency carrier. The oscillator output is also divided by 100 in a two-stage regenerative divider. The $0.01 F$ (195 kHz) output from this divider is used to tone modulate the $21 F$ output carrier in a balanced modulator, thereby generating a double sideband suppressed carrier signal with sidebands at 21.01 and $19.99 F$.

TABLE H2.- EQUIPMENT WEIGHT, POWER, AND VOLUME SUMMARY

Item	Baseline (one-way doppler)	One-way doppler S/C-BVS	One-way doppler BVS-S/C	Two-way doppler S/C-BVS-S/C	Ranging and two-way doppler
S/C XMTR (1) Weight, lb Power, W Size, in. ³	4 67 96	4.4 72 105	4.4 72 105	4.5 73 107	4.7 74 110
S/C RCVR (1) Weight, lb Power, W Size, in. ³	3 2.5 95	4 2.5 90	5 3.0 100	5 3.5 125	5 3.5 125
S/C range code demod (1) Weight, lb Power, W Size, in. ³	----- ----- -----	----- ----- -----	----- ----- -----	----- ----- -----	2 1.5 30
BVS XMTR (1) Weight, lb Power, W Size, in. ³	4 67 96	4.4 72 105	4.4 72 105	2.5 72 62	2.5 72 62
BVS RCVR (1) Weight, lb Power, W Size, in. ³	3 2.5 95	4 2.5 100	3 2.5 95	4 2.5 100	4 2.5 100
BVS range code demod (1) Weight, lb Power, W Size, in. ³	----- ----- -----	----- ----- -----	----- ----- -----	----- ----- -----	2 1.5 30
Total Weight, lb Power, W Size, in. ³	14 139 382	12.8 149.0 400	16.8 149.5 405.0	16.0 151.0 394.0	20.2 155 457.0

APPENDIX H

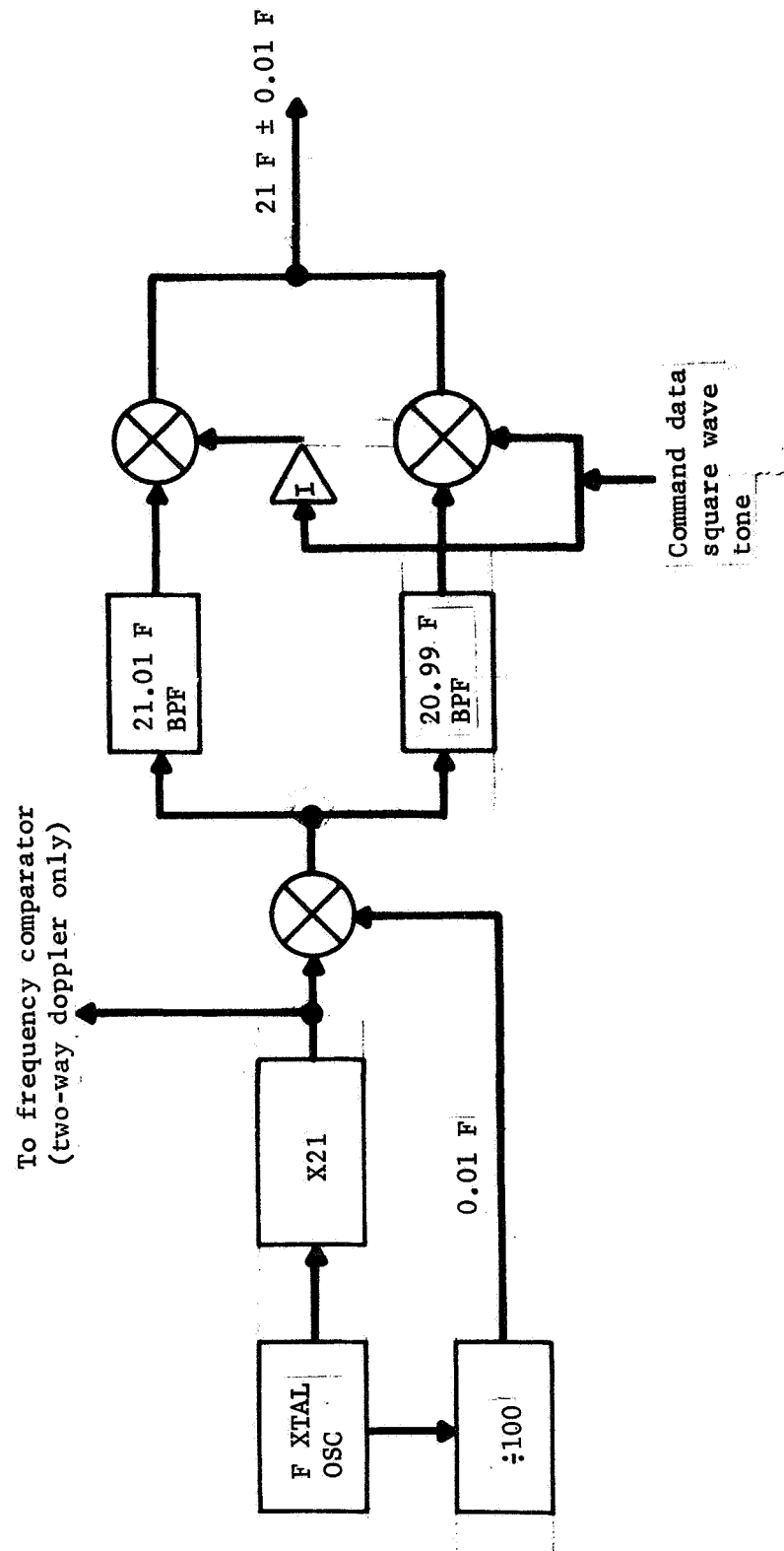


Figure H1.- Spacecraft Transmitter for Doppler and Command

APPENDIX H

These two sidebands are separated by a pair of bandpass filters. The outputs of these bandpass filters are alternately gated to the output power amplifier by the command data; thereby generating an FSK signal. This later operation is the same as that performed in the baseline system. The concern over carrier and sideband suppression usually associated with suppressed carrier modulation systems is minimized in this application because the class C output power amplifier in the transmitter functions similar to a limiter, in that it suppresses the lower level signals in the presence of the single desired high level signal.

Figure H2 is a block diagram of the BVS, FSK, and doppler receiver demodulator. Functional circuitry required for the recovery of the FSK command tones is the same as used in the baseline system except for the fact that the local oscillator is derived by multiplying the voltage controlled crystal oscillator (VXO) frequency by 20. This VXO, when not locked on the signal from the spacecraft, is frequency stabilized by a local crystal with a stability of 1×10^{-6} . The VXO is freed from local crystal frequency control when either the lock start command from FSK tone demodulator is activated by the presence of a command tone of adequate level or by an incoming spacecraft signal at a frequency close to that of the VXO. When released by the lock start command, the VXO will be pulled toward and phase locked to frequency F derived from the spacecraft. (A frequency search capability, not shown, is required due to the frequency uncertainties of the transmitter and receiver and doppler.)

After lock, the local oscillator signal $20 F$ will contain $20/21$ of the incoming doppler shift, and this doppler will be subtracted from the incoming doppler so that the doppler contained in the FSK signal, at the input of the FSK filters, will be reduced by a factor of 21. When the doppler system is locked up, the FSK signals will be centered in the FSK mark and space bandpass filters. A lock indication binary level is provided out of the doppler demodulator to the BVS data system to inhibit the storing of doppler data until the doppler receiver demodulator is locked. The $20 F$ local oscillator signal is mixed with a local crystal oscillator operating at a frequency approximately $20 F + 15 \text{ kHz}$. The output of this mixer is a 15 kHz signal, which may be shifted 13.5 kHz due to doppler, the spacecraft oscillator drift, and the receiver crystal oscillator drift. This signal is used by the frequency modulation discriminator to generate an output analog voltage with a level directly proportional to the input frequency. As shown in table H1, this technique yields a data signal of extremely low accuracy because the combined frequency drift of the oscillators in the spacecraft and BVS appear to the

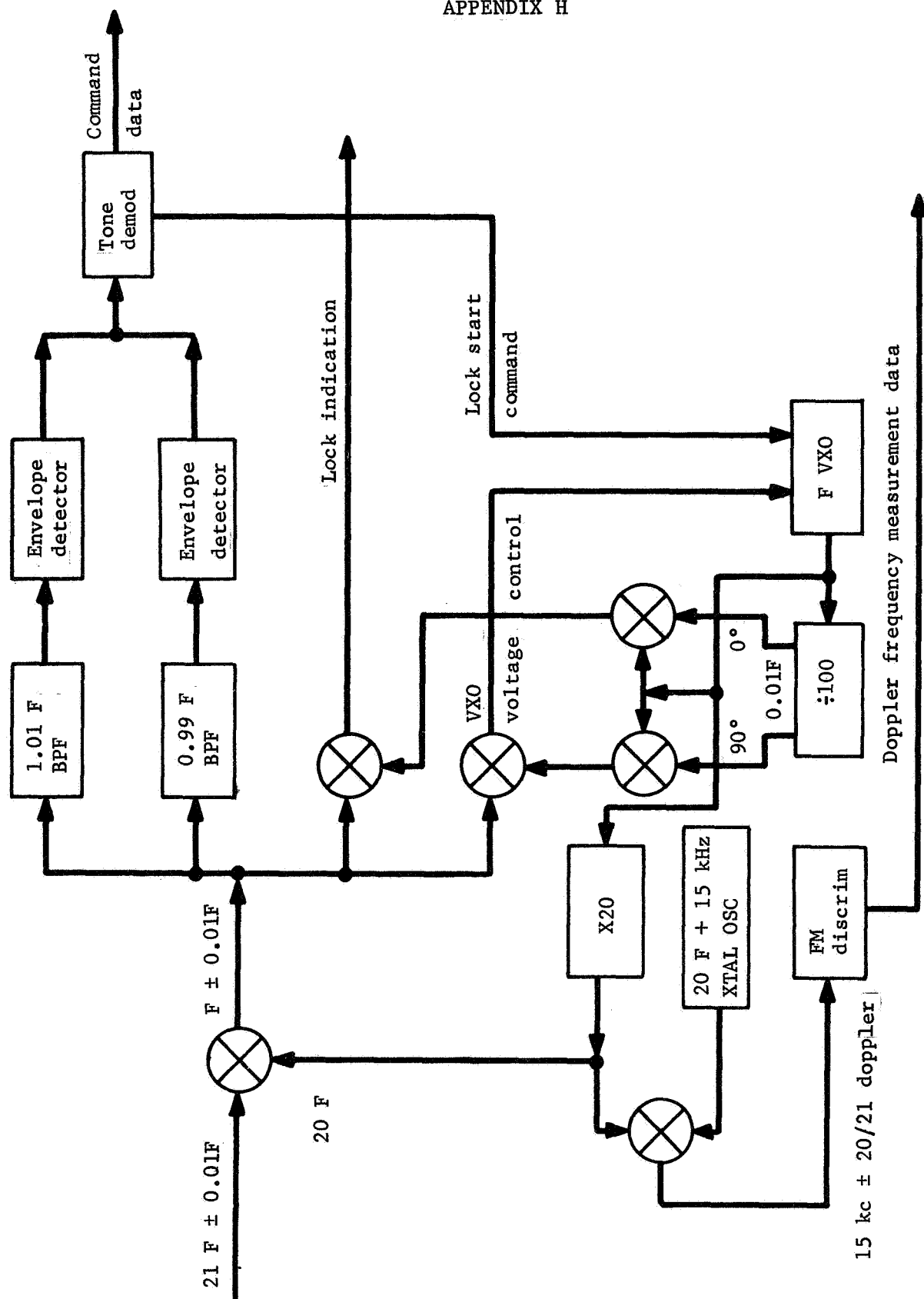


Figure H2.- One-Way Doppler Receiver and Demodulator

APPENDIX H

FM discriminator the same as a doppler signal and can reduce the accuracy of the doppler measurement by 50%. Therefore, this technique is best suited for doppler rate or delta doppler measurements because delta values are based on short-term stability.

ONE-WAY DOPPLER FROM BVS TO SPACECRAFT

The techniques used in this approach are identical to those described in the previous section for the one-way doppler from the spacecraft to BVS. The advantage is that, with this approach, it is not necessary to transmit the resultant doppler data measurement back to the spacecraft from the BVS. Therefore, it does not suffer that additional deterioration in data accuracy. However, this deterioration is extremely small compared to inherent errors associated with oscillator instabilities. A disadvantage for this approach occurs when the BVS transmitter "on" time is limited to a fraction of the total view time for a pass because measurements can be made for only a small portion of the doppler S curve.

TWO-WAY DOPPLER SPACECRAFT TO BVS TO SPACECRAFT

Fundamentally this technique involves the use of two one-way doppler systems operating back to back. The exceptions being that the carrier frequency of the BVS transmitter is derived from the spacecraft transmitter signal by phase locking to it in the BVS receiver and using the local mixer oscillator signal of the BVS receiver as the BVS transmitting carrier. Also, the doppler measurement is made much more accurately. The transmitter block diagram shown in figure H1 is applicable as the two-way doppler spacecraft transmitter with the addition of using the 21 F carrier as shown in the figure. The output of this multiplier is used as the frequency comparator for determining the doppler shift of the incoming BVS signal.

Figure H3 is a block diagram of the BVS receiver and demodulator for two-way doppler operation. It is similar to the one-way doppler system except that it does not use a mixer and FM discriminator for frequency determination at the BVS. The local VXO is phase locked to the incoming signal and, in the process, generates the 20 F signal that is used as the incoming local mixer oscillator. In addition, this 20 F is used as the carrier frequency for the BVS transmitter as shown in figure H4.

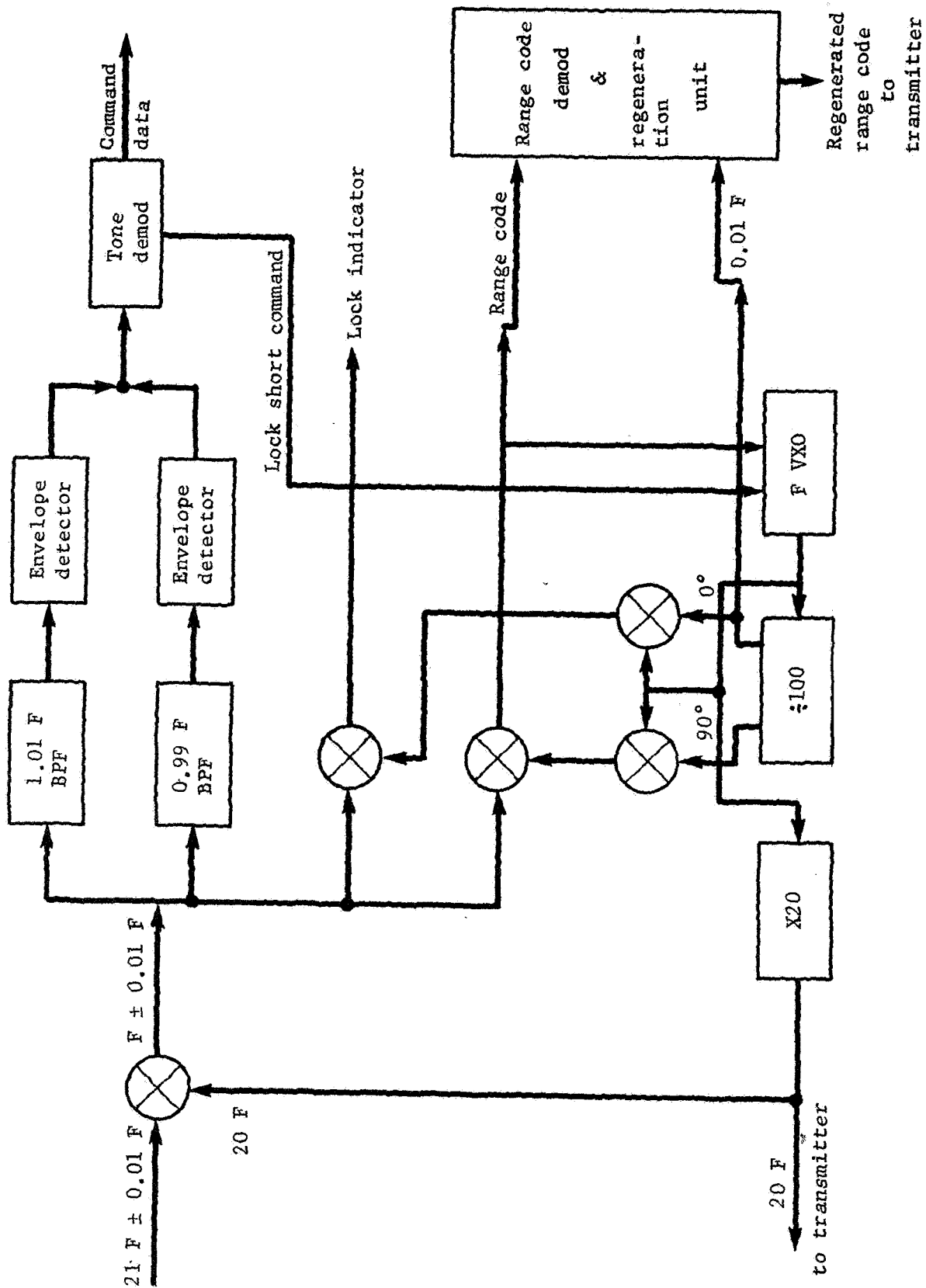


Figure H3.- BVS Receiver and Demodulator for Doppler, Ranging, and Command

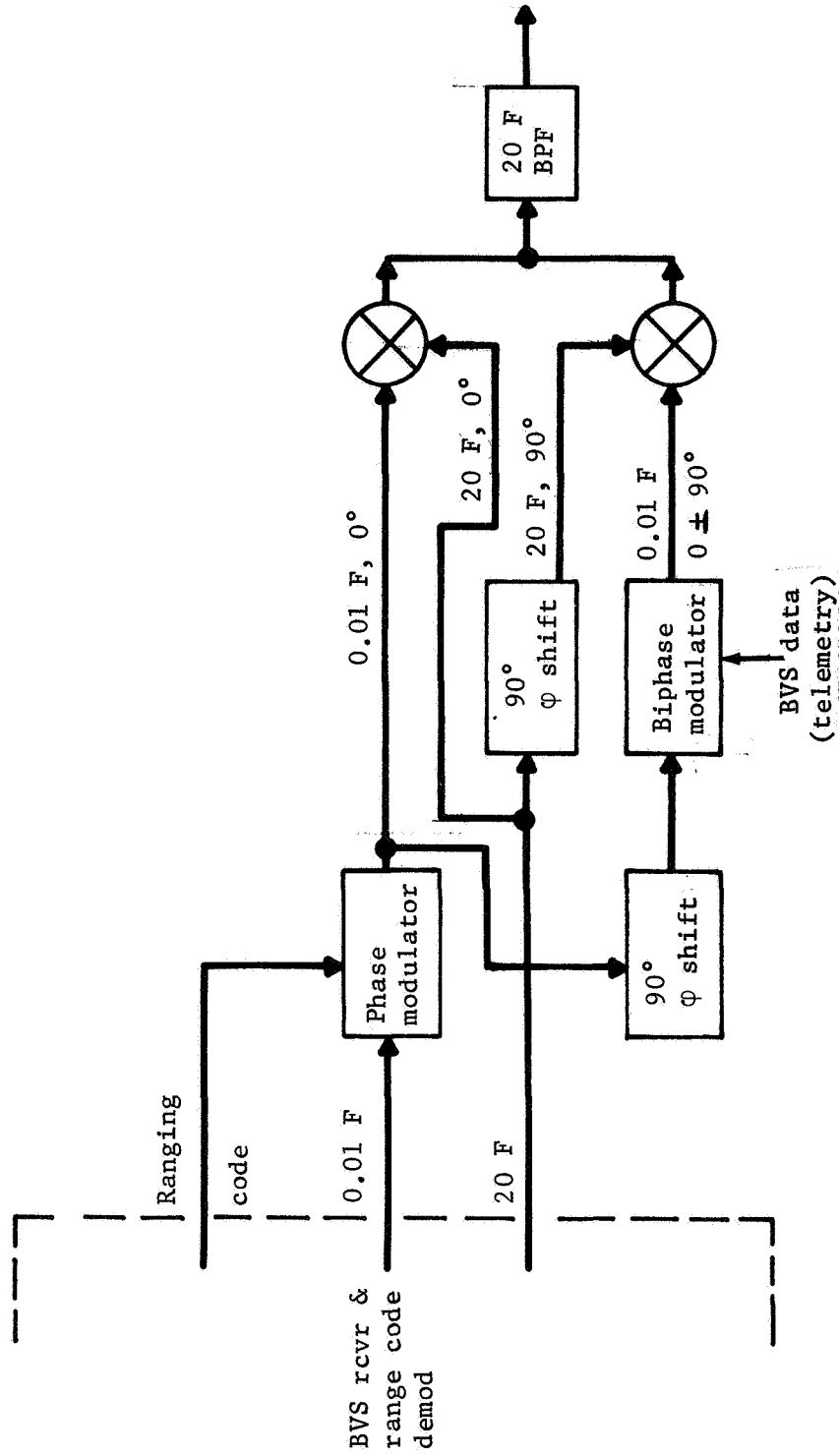


Figure H4.- BVS Transmitter for Ranging, Doppler, and Data

APPENDIX H

This 20 F signal is modulated by the BVS data in the same manner that the spacecraft transmitter operates. The operation of the doppler frequency measurement performed in the spacecraft is shown in figure H5. The received 20 F signal containing doppler from the BVS is multiplied with the local spacecraft 21 F signal and the output of this mixer is used to provide one of the inputs to the quadrature demodulator. The other set of inputs to this demodulator is spacecraft F signal fed to one balanced demodulator 90° out of phase with the input to the other one. The outputs of these two mixers are pulses at twice the doppler rate. The pulses from the two mixers will be either $\pm 90^\circ$ with respect to each other depending on whether the doppler frequency is plus or minus. Thus, doppler polarity is determined by the use of the A and B gates shown in the figure, and the polarity detector. The output of the polarity detector will either be a 1 or a 0 level depending on whether the doppler frequency is plus or minus with respect to the original carrier frequency. The doppler pulses are also fed to an AND gate in the doppler frequency measurement section. Another input to this gate is from a flip-flop that is activated by 1-sec clock pulses after a count ready command is received. After starting count, doppler pulses are fed to the 15-bit register, during the count period, which will be exactly 1-sec increments as determined by the local 1-sec clock. When the count period is complete, a readout ready line is activated, which notifies the spacecraft data system that it can proceed to read out the data stored in the register. Therefore, each measurement is contained in a 16-bit word -- 1 bit for polarity, 15 bits for frequency. The accuracy of this measurement is $\pm \frac{1}{2}$ doppler cycle. In the event that the doppler frequency passes through zero during the period of the count and the polarity data output line changes state, the register is reset and a recount started on receipt of the next 1-sec clock pulse.

TWO-WAY DOPPLER AND RANGING

When ranging capability is provided, it is used in addition to the two-way doppler technique described in the previous section. A PN ranging code is used to phase modulate the FSK signal generated by the spacecraft. The period of the ranging code must be greater in time than the total propagation time from the spacecraft to BVS to spacecraft plus any time delays that occur in the system. In this case, for illustrative purposes, the ranging code period has been selected to be 1.09 sec. The range resolution requirement of ± 500 m dictates the minimum period of 1 bit of the ranging code required to achieve this resolution.

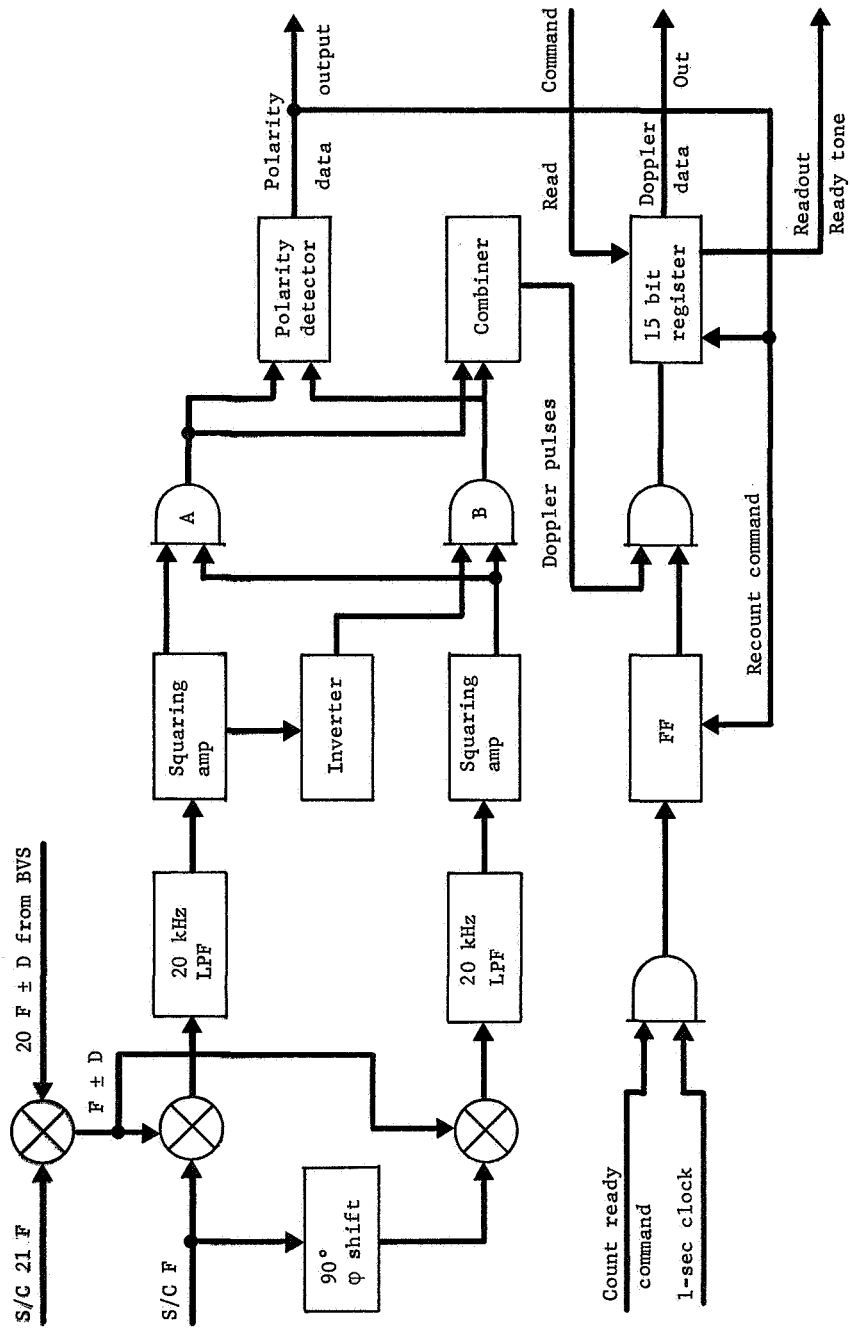


Figure H5.- Spacecraft Doppler Frequency Measurement

APPENDIX H

This resolution is provided by using the $0.01 F$ component for the phase locked loops in the BVS and spacecraft receivers to lock upon.

Figure H6 is a block diagram of the spacecraft transmitter used for the ranging and doppler system. FSK output from this transmitter is the same as that provided in one- and two-way doppler systems. However, due to higher frequency sidebands generated around each of the FSK frequencies by the ranging code it is necessary to delete the relatively narrow bandpass filters used in the previous techniques and replace them by a phasing type of single sideband FSK generation scheme. The F frequency output from the crystal oscillator is divided by 100. This $0.01 F$ signal is phase modulated $\pm 22.5^\circ$ by the ranging code. The phase modulated ranging code is fed directly to one of the balanced modulators and is considered a 0° reference $0.01 F$ signal. The output of the phase modulator is also fed to a 90° phase shifter and then biphase modulated by the command data serial bit stream. This then generates a $0.01 F$ signal that is being changed from $+90^\circ$ to -90° by the data modulation. This signal is used in the other balanced modulator. The output of the crystal oscillator is multiplied by 21, and this signal then used as the other inputs to the two balanced modulators, one of which is shifted 90° as shown in the figure. The outputs of the two balanced modulators are linearly combined and passed through the $21 F$ bandpass filter. The effect of the phase change by the command data is to cause the summing of the outputs of the two balanced modulators to generate an FSK signal with the range code phase modulation impressed on it.

The BVS receiver and demodulator used for ranging and doppler is the same as shown in figure H3. Note, however, that unlike the "doppler only" case, at the output of the phase modulated demodulator, P , the ranging code is present.

The range code demodulator and regeneration unit automatically and sequentially acquires the clock component and each of the three acquirable subsequences of the code assuming a sequence of combined acquirable PN codes having a clock component (ref. H1). This results in the regeneration of the ranging code which is used to modulate the return link to the spacecraft in the same manner that the ranging modulation was applied to the spacecraft transmitter.

The spacecraft range code demodulator and regeneration unit associated with the receiver signal at the spacecraft is identical to the BVS unit except that a counter is added to record time delay in microseconds between identical states of the transmit code generator and the receiver code regenerator.

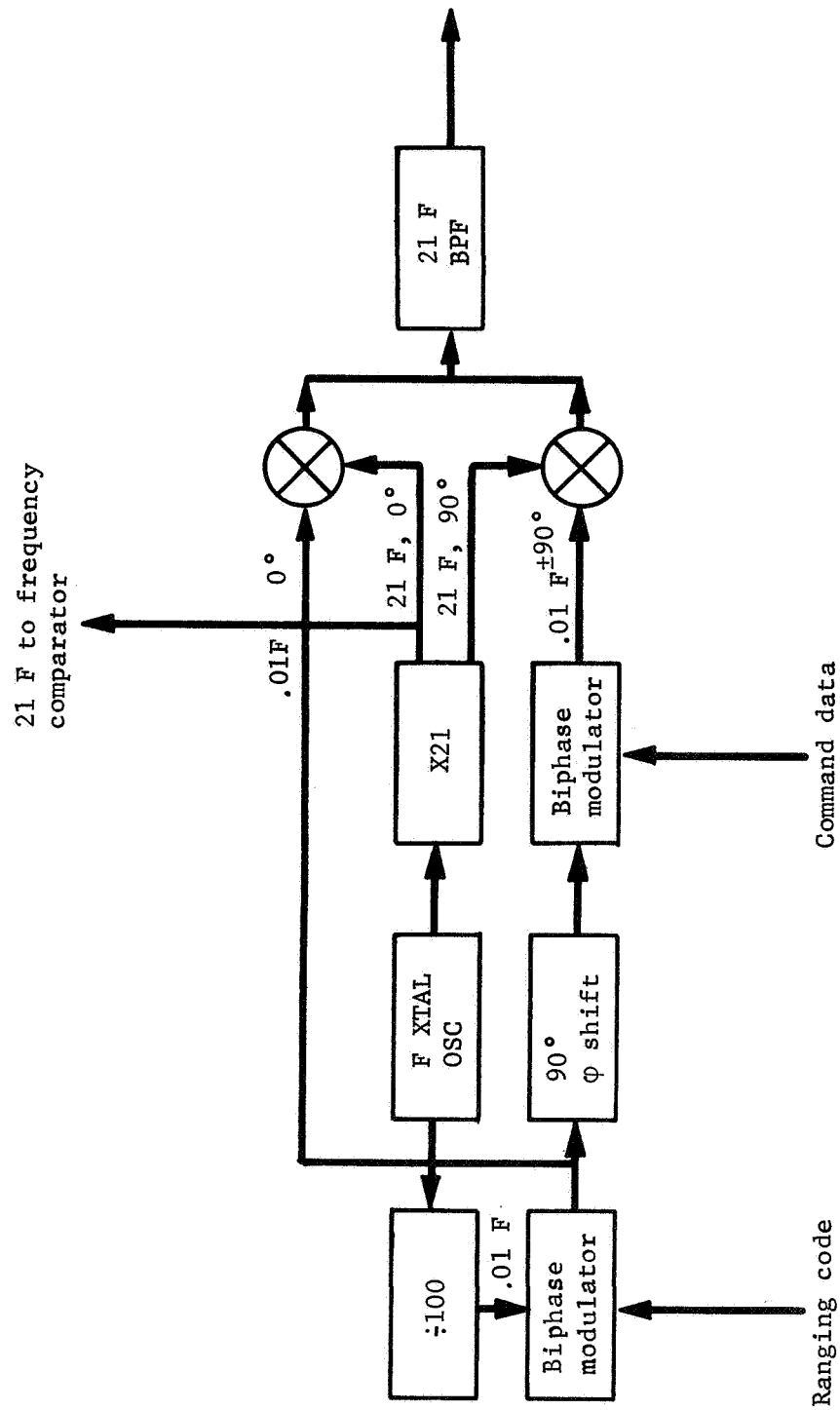


Figure H6.- Spacecraft Transmitters for Ranging, Doppler, and Command

APPENDIX H

Acquisition times associated with the doppler and ranging system along with the code characteristics are shown in table H3. Note that a nominal acquisition period for ranging is approximately 49 sec, including frequency search, carrier lock, clock acquisition, and three-component range code acquisition at both ends of the link.

Because the time is based on the S/N ratio available at threshold for the FSK data link it can be assumed that acquisition of the code and measurement of range can easily be accomplished during the first minute or so of the communications pass.

REFERENCES

- H1. Golomb, S. W. et al.: Digital Communications with Space Applications. Prentice-Hall, Inc., 1964, pp. 91-105.

APPENDIX H

TABLE H3.- ACQUISITION TIME RANGING CODE

<p>Required error probability = 10^{-3} System N/B = -169.5 dBm</p> <p>Signal strength = -132.5 dBm</p> <p>If $ST/(N/B) = X$, then</p> $T = (X) \frac{(N/B)}{S} = \frac{(1.12) 10^{-19}}{(5.62) 10^{-16}} (X) = 1.99(10^{-4}) (X)$ <p>Code characteristics: Each element acquisition time = $P (\log_2 P) T (4)$</p> <p>Maximum range = 328 000 km Code length = 164 000 km Code components = 11,47,103 Cross correlation = 1/2 Clock frequency = 48.8 kHz</p>				
Number of code elements	$\log_2 P$	$St/NB = X$	T	Total time/ component, sec
$P_1 = 11$	3.46	4.0	7.97×10^{-4}	0.121
$P_2 = 47$	5.55	2.8	5.59×10^{-4}	0.583
$P_3 = 103$	6.69	2.6	5.20×10^{-4}	<u>1.43</u>
Total acquisition ^a = 2.134				
<p>^a Does not include two-way carrier and clock acquisition time that is estimated to require an additional 22 sec each way, assuming a search rate of 2.5 kHz for the carrier and 1 sec clock acquisition.</p>				
<p><u>Note:</u> Two-way acquisition ----- 2 (2.134) sec Two-way carrier and clock - <u>2 (22.0) sec</u></p> <p>Total two-way acquisition time (including carrier and clock acquisition) 49 sec</p>				